



UNIL | Université de Lausanne

Unicentre

CH-1015 Lausanne

<http://serval.unil.ch>

Year : 2022

Therapeutic Potential of Hydrogen Sulfide In Peripheral Vascular Diseases

Macabrey Diane

Macabrey Diane, 2022, Therapeutic Potential of Hydrogen Sulfide In Peripheral Vascular Diseases

Originally published at : Thesis, University of Lausanne

Posted at the University of Lausanne Open Archive <http://serval.unil.ch>

Document URN : urn:nbn:ch:serval-BIB_11C6A491BA3F2

Droits d'auteur

L'Université de Lausanne attire expressément l'attention des utilisateurs sur le fait que tous les documents publiés dans l'Archive SERVAL sont protégés par le droit d'auteur, conformément à la loi fédérale sur le droit d'auteur et les droits voisins (LDA). A ce titre, il est indispensable d'obtenir le consentement préalable de l'auteur et/ou de l'éditeur avant toute utilisation d'une oeuvre ou d'une partie d'une oeuvre ne relevant pas d'une utilisation à des fins personnelles au sens de la LDA (art. 19, al. 1 lettre a). A défaut, tout contrevenant s'expose aux sanctions prévues par cette loi. Nous déclinons toute responsabilité en la matière.

Copyright

The University of Lausanne expressly draws the attention of users to the fact that all documents published in the SERVAL Archive are protected by copyright in accordance with federal law on copyright and similar rights (LDA). Accordingly it is indispensable to obtain prior consent from the author and/or publisher before any use of a work or part of a work for purposes other than personal use within the meaning of LDA (art. 19, para. 1 letter a). Failure to do so will expose offenders to the sanctions laid down by this law. We accept no liability in this respect.



UNIL | Université de Lausanne

Faculté de biologie
et de médecine

Service de chirurgie vasculaire, CHUV

Therapeutic Potential of Hydrogen Sulfide In Peripheral Vascular Diseases

Thèse de doctorat ès sciences de la vie (PhD)

Présentée à la faculté de Biologie et de médecine de l'Université de
Lausanne par

Diane MACABREY

Master en Biologie Médicale de l'Université de Lausanne

Jury

Prof. Yasser Khazaal, Président

Dr Florent Allagnat, Directeur de thèse

Dr Sébastien Déglise, Co-directeur de thèse

Prof. Lucia Mazzolai, Experte

Prof. Paul Quax, Expert

Lausanne
(2022)



UNIL | Université de Lausanne

Faculté de biologie
et de médecine

Service de chirurgie vasculaire, CHUV

Therapeutic Potential of Hydrogen Sulfide In Peripheral Vascular Diseases

Thèse de doctorat ès sciences de la vie (PhD)

Présentée à la faculté de Biologie et de médecine de l'Université de
Lausanne par

Diane MACABREY

Master en Biologie Médicale de l'Université de Lausanne

Jury

Prof. Yasser Khazaal, Président

Dr Florent Allagnat, Directeur de thèse

Dr Sébastien Déglise, Co-directeur de thèse

Prof. Lucia Mazzolai, Experte

Prof. Paul Quax, Expert

Lausanne
(2022)



UNIL | Université de Lausanne

Faculté de biologie
et de médecine

Ecole Doctorale

Doctorat ès sciences de la vie

Imprimatur

Vu le rapport présenté par le jury d'examen, composé de

Président·e	Monsieur	Prof.	Yasser	Khazaal
Directeur·trice de thèse	Monsieur	Dr	Florent	Allagnat
Co-directeur·trice	Monsieur	Dr	Sébastien	Déglise
Expert·e·s	Madame	Prof.	Lucia	Mazzolai
	Monsieur	Prof.	Paul	Quax

le Conseil de Faculté autorise l'impression de la thèse de

Diane Macabrey

Maîtrise universitaire ès Sciences en biologie médicale, Université de Lausanne

intitulée

**Therapeutic potential of hydrogen sulfide
in peripheral vascular diseases**

Lausanne, le 17 juin 2022

pour le Doyen
de la Faculté de biologie et de médecine

Dr Yasser KHAZAAL
Médecin chef
Prof. Yasser Khazaal

Table of Content

1	Acknowledgments	ii
2	Abstract	iii
3	Résumé	iv
4	List of abbreviations	v
5	Introduction	1
5.1	Peripheral artery disease	1
5.1.1	Clinical presentation of PAD	1
5.1.2	Current treatment of PAD	3
5.1.3	Intimal hyperplasia	4
5.1.4	Current treatment of intimal hyperplasia	5
5.2	Hydrogen sulfide	7
5.2.1	Endogenous H ₂ S production	7
5.2.2	H ₂ S biological activity	8
5.2.3	H ₂ S in the vascular system	9
5.2.4	H ₂ S inhibits inflammation in the cardiovascular system	13
5.2.5	H ₂ S has anti-oxidant properties	14
6	Aim	16
7	Results	17
7.1	Sodium Thiosulfate acts as a hydrogen sulfide mimetic to prevent intimal hyperplasia via inhibition of tubulin polymerisation	17
7.2	Hydrogen Sulphide Release via the Angiotensin Converting Enzyme Inhibitor Zofenopril Prevents Intimal Hyperplasia in Human Vein Segments and in a Mouse Model of Carotid Artery Stenosis	49
7.3	Sodium thiosulfate, a source of hydrogen sulfide, promotes endothelial cells proliferation, angiogenesis and revascularization following hind-limb ischemia in the mouse	66
8	Conclusion	95
8.1	STS inhibits IH	95
8.2	STS promotes revascularization in a HLI model in mice	96
8.3	Further perspectives: Clinical potential of STS in a mouse model of AAA	100
9	References	103
10	Annex: Clinical use of hydrogen sulfide to protect against intimal hyperplasia	114

1 Acknowledgments

Florent, thank you for helping me grow throughout this PhD. You taught me a lot about science, but also so much about myself. Thank you for your patience and your support.

I would also like to thank Sébastien. Seeing science through the eyes of a medical doctor was always pertinent, helpful and interesting.

I also thank all the members of my Jury, Prof. Jean-Bernard Daeppen, Prof. Lucia Mazzolai, and Prof. Paul Quax for the time invested in my PhD.

Thank you Martine for allowing me to blow some steam during our coffee breaks. And of course, for everything you taught me. Thank you Thomas, Kevin, Arnaud, Séverine and Clémence for all the adventures and laughs we shared. I (almost) always loved coming to the lab and that was in big part thanks to you.

A special thanks to Renzo for your unconditional support and for always believing in me.

Huge thanks to my best friends, Célia, Caroline, Nico, Nico and Jonas. When friends become family, there is nothing more to say.

DrSc Jessica Lavier, I could not have done this without you. Your support during the various existential crisis I had throughout my PhD was instrumental in my success. Thank you.

Finally, I also thank my family. You raised me to think that I could do anything I wanted. You didn't always understand my choices but you never failed to support me, always.

2 Abstract

Atherosclerosis in peripheral arteries leads to peripheral artery disease, where reduced blood flow to the limbs causes ischemia, which may progress to critical limb ischemia and risk of amputation. Vascular surgery is the only option for critical limb ischemia, but it is not always possible or effective. Moreover, surgeries suffer from high failure rates due to re-occlusive vascular wall adaptations, which are largely due to intimal hyperplasia. Intimal hyperplasia develops in response to vessel injury, leading to the formation of a new slowly growing neointima layer, which progressively occludes the lumen of the vessel. It results in costly and complex recurrent end-organ ischemia, and often leads to loss of limb, brain function, or life. Current strategies to limit IH rely on drug eluting stents/balloon, which target cell proliferation, but impair re-endothelialisation. Hydrogen sulfide is a gasotransmitter produced in the vascular system promoting angiogenesis and vasodilation. Hydrogen sulfide also has anti-oxidant and anti-inflammatory properties. Pre-clinical studies using H₂S-releasing molecules showed that it improves revascularization and limits IH formation. In this work, we investigated the therapeutic potential of sodium thiosulfate (STS), a source of sulfur used in the clinic to treat cyanide poisoning and calciphylaxis.

In a first study, we showed that STS reduces the formation of intimal hyperplasia in WT mice and in LDLR^{KO} mice following carotid artery stenosis. STS also rescues CSE^{KO} mice with impaired H₂S production from increased intimal hyperplasia formation. STS interferes with microtubule polymerization, reducing smooth muscle cell proliferation and formation of intimal hyperplasia. In second study, we showed that STS significantly improved reperfusion following hindlimb ischemia in WT and LDLR^{KO} (hypercholesterolemic) mice. Mechanistically, STS inhibited mitochondrial respiration in endothelial cells, thereby inducing a compensatory increase in glycolysis, leading to increase proliferation and migration. Although additional studies are required to insure the safety of long-term STS treatment in humans, the present work underscores the therapeutic potential of STS against vascular diseases.

3 Résumé

L'athérosclérose dans les vaisseaux périphériques entraîne une ischémie des membres pouvant mener à une amputation. A ce jour, la chirurgie vasculaire est le seul traitement pour les cas sévères de maladies artérielles périphériques, mais elle n'est pas sans risques et parfois impossible ou inefficace. De plus, les résultats à moyen-long terme de toute chirurgie vasculaire sont limités par la survenue d'une resténose principalement causées par l'hyperplasie intimale. En effet, la chirurgie déclenche une réaction inflammatoire entraînant la formation de l'HI dans la paroi du vaisseau. La croissance de cette nouvelle couche fibreuse entraîne des ischémies récurrentes qui nécessitent de nouvelles procédures complexes et coûteuses avec des résultats souvent catastrophiques. Les stratégies actuelles limitant l'hyperplasie reposent sur l'utilisation de stents et de ballons actifs limitant la prolifération cellulaire, mais empêchent la ré-endothelialisation. Le H₂S, un gasotransmetteur produit par le système vasculaire, est pro-angiogénique, vasodilatateur, antioxydant et anti-inflammatoire. Des études précliniques montrent que le H₂S améliore la revascularisation et limite le développement de l'HI, mais les molécules utilisées jusqu'à présent ne peuvent pas être utilisées en clinique. Dans ce travail, nous avons examiné le potentiel thérapeutique du sodium thiosulfate (STS), une source de soufre utilisée en clinique pour traiter la calciphylaxie et l'empoisonnement au cyanure.

Premièrement, nous avons montré que le STS limite le développement de l'IH dans des souris WT et hypercholestérolémique (LDLR^{KO}), après une sténose de la carotide. Le STS interfère avec la polymérisation des microtubules, réduisant la prolifération des cellules musculaires lisses et la formation de l'hyperplasie. Deuxièmement, nous avons montré que le STS améliore la reperfusion de la patte après une ligature de la fémorale, dans des souris WT et LDLR^{KO}. Le STS inhibe la respiration mitochondriale des cellules endothéliales, menant à une augmentation de la glycolyse, de la prolifération et de la migration. Même si des études additionnelles sont nécessaires avant d'imaginer un traitement au STS sur le long terme, le présent travail souligne le potentiel thérapeutique du STS dans les maladies vasculaires.

4 List of abbreviations

3-MST: 3-Mercaptopyruvate sulfur transferase	AAA: Abdominal Aortic Aneurysm	ACEi: Angiotensin converting enzyme inhibitor
ALAT: Alanin Amino Transferase	ApoE ^{-/-} : Apolipoprotein E KO	ARBs: Angiotensin Receptor Blocker
ASAT: Aspartate Amino Transferase	ATP: Adenosine triphosphate	ATS: Atherosclerosis
BAPN: β -Aminopropionitrile monofumarate	bFGF: basic Fibroblast Growth Factor	BMS: Bare Metal Stents
CAM: Chick Chorioallantoic Membrane	CAT: Cysteine Amino Transferase	CBS: Cystathionine β -synthase
CK-MB: Creatine Kinase MB	CLI: Critical Limb Ischemia	CML: Cellules Musculaires Lisses
CPT1: Carnitine Palmitoyl Transferase	CRP: C-Reactive Protein	CSE: Cystathionine γ -lyase
CVD: Cardiovascular Diseases	DATS: Diallyl Trisulfite	DCB: Drug Coated Ballons
DES: Drug Eluting Stents	DLL4: Delta Like Canonical Notch Ligand 4	EC: Endothelial Cell
ECM : Extracellular Matrix	EEL : External Elastic Lamina	eNOS : endothelial Nitric Oxide synthase
FASN: Fatty Acid Synthase	FDA: Federal Drug Administration	FOXO1: Forkhead box protein O1
GSH: Gluthation	H ₂ S: Hydrogen Sulfide	HO1: Heme Oxygenase 1
HUVEC: Human Umbilical Vein Endothelial Cells	IC: Intermittent Claudication	ICAM: InterCellular Adhesion Molecule
IEL: Internal Elastic Lamina	IH: Intimal Hyperplasia	IL-1 β : Interleukin 1 beta
Ip: Intraperitoneal	Iv: Intravenous	LC/MS/MS: Liquid Chromatography-Mass Spectrometry
LDL: Low Density Lipoprotein	MAP: Maladie Artérielle Périphérique	MCP-1: Monocyte chemoattractant protein-1
Na ₂ S: Sodium Sulfide	NaHS: Sodium Hydrosulfide	NF- κ B: Nuclear Factor- κ B

NO: Nitric Oxide	OXPHOS: Oxidative Phosphorylation	PAD: Peripheral Artery Disease
PAG: DL-Propargylglycine	PDGF-BB: Platelet-Derived Growth Factor-BB	PFKFB3: 6-Phosphofructo-2-Kinase/Fructose-2,6-Biphosphatase 3
PLP: Pyridoxal 5'-phosphate	POBA: Plain Old Balloon Angioplasty	ROS: Reactive Oxygen Species
SDF-1: Stromal cell-derived factor 1	SQOR: Sulfide Quinone Oxidoreductase	STS: Sodium Thiosulfate
TNF- α : Tumor Necrosis Factor α	TXNIP: Trx-interacting protein	VCAM: Vascular Cell Adhesion Molecule
VEGF: Vascular Endothelial Growth Factor	VEGFR2: Vascular Endothelial Growth Factor Receptor 2	VSMC : Vascular Smooth Muscle Cells
WHO: World Health Organisation	WT : Wild Type	

5 Introduction

Cardiovascular diseases (CVD) are the number one cause of mortality worldwide. An estimated 17.9 million people died from CVDs in 2019, representing 32% of all global deaths (WHO). CVD include coronary heart disease, cerebrovascular disease and peripheral artery disease and their incidence continues to rise worldwide, largely due to the combination of aging, smoking, hypertension, and diabetes mellitus (1-3).

5.1 Peripheral artery disease

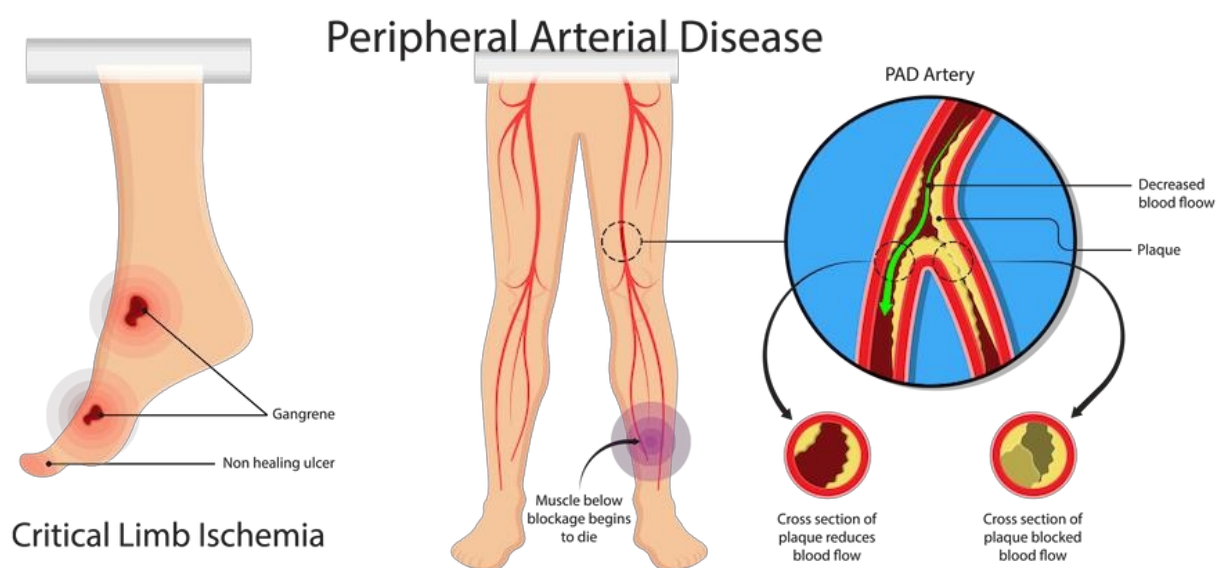
Peripheral artery disease (PAD) affects over 200 million people worldwide and is defined as “all arterial diseases other than coronary arteries and the aorta” (4). Atherosclerosis (ATS) in lower limb arteries accounts for more than 90% of PAD cases (5). The pathophysiology of ATS has been described in details previously (6). Briefly, ATS is a chronic inflammatory disease of the vascular wall, characterized by the formation of lipid- and inflammatory cell-rich plaques. It starts with endothelial cell (EC) dysfunction and vascular inflammation, which leads to entrapment of oxidized low density lipoproteins (LDL) inside the vessel wall. Monocytes attracted to the inflamed vessel wall engulf LDL particles and become foam cells, typical of ATS lesion. Foam cells undergo apoptosis, forming a lipid core inside the vessel wall. Inflammation is further enhanced by pro-inflammatory cytokines, leading to proliferation of VSMC at the injury site, production of extracellular matrix components and development of a fibrous cap overlaying the lipid core. (7).

5.1.1 Clinical presentation of PAD

The plaque grows into the vessel lumen and progressively decreases blood flow. At the beginning, blood flow remains sufficient to provide basal oxygen needs, and patients are accordingly free of symptoms at rest (**scheme 1**). However, during exercise, the muscles' metabolic needs increases cannot be met, which is felt by the patient as cramping pain. Cramping

forces the patient to stop walking, until the pain disappears. Once the cramp is gone, the patient can start walking again, until the pain comes back. Alternating cycles of walking and resting is the typical clinical manifestation of PAD patients, termed intermittent claudication (IC) (8). IC patients have decreased walking capacity, leading to inability to perform daily living activities, and impaired quality of life (4). Although IC is the cardinal symptom of PAD, it is present in only 10 to 35% of patients. Forty to 50% of PAD patients have a broad range of atypical leg symptoms (ex. exertional leg symptoms that begin at rest or exertional leg pain that does not include the calf) and 20 to 50% of patients are asymptomatic (9). IC and atypical leg pain are caused by a moderate ischemia, which does not immediately threaten the limb viability.

Critical limb ischemia (CLI), the most severe manifestation of PAD, is characterized by muscle pain at rest, ulceration and gangrene and 30% of patients with CLI undergo limb amputation.



Scheme 1: Peripheral artery disease

Peripheral artery disease (PAD) is caused by atherosclerosis development in lower limb arteries, leading to ischemia to downstream muscles. Severe cases of ischemia, termed critical limb ischemia (CLI) can cause ulcerations, gangrene, and lead to amputation.

Adapted from <https://ctvstexas.com/about-ctvs/our-services/vascular-services/peripheral-artery-disease/>

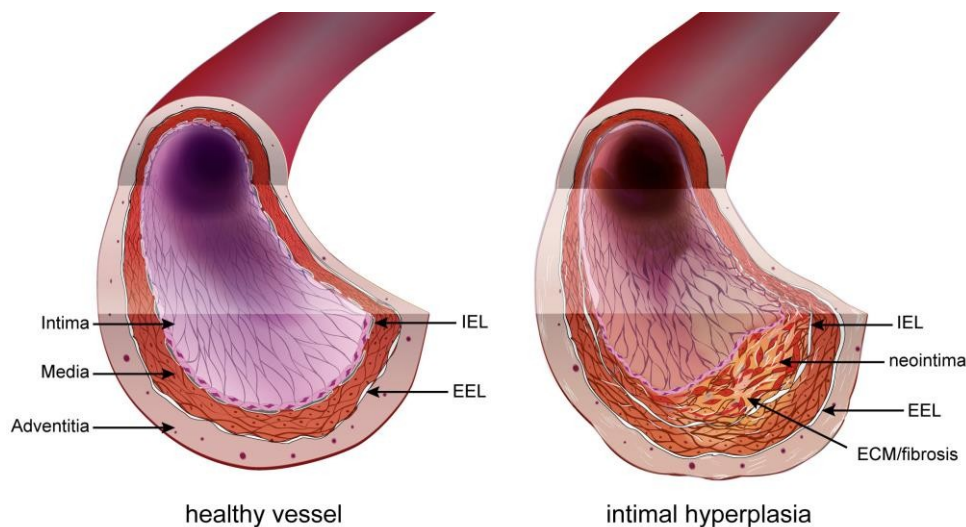
As atherosclerosis is a systemic condition, polyvascular disease is common in patients with PAD. The 1-year incidence of all major cardiovascular events is 30% higher in patients with PAD than in those with coronary or cerebral artery disease (10).

5.1.2 Current treatment of PAD

The management of PAD patients starts by reducing cardiovascular risks through pharmacological therapy (lipid-lowering and antihypertensive drugs), as well as non-pharmacological measures (smoking cessation, healthy diet, etc.). In patients with mild PAD, supervised exercise training (11), statins (12) and ACEi/ARBs (13) improve walking capacity. In severe cases of PAD or CLI, vascular surgery, open or endovascular, remains the only treatment. Unfortunately, surgery may be suboptimal in relieving symptoms and may not be indicated because of disease severity or comorbid conditions. It is estimated that 20 to 40% of CLI patients are not anatomically amenable to revascularization or have failed revascularization (14). Even in the case of a successful surgery, residual microvascular disease may limit its effectiveness. Furthermore, the vascular trauma associated with the intervention eventually leads to secondary occlusion of the injured vessel, a process called restenosis. The overall incidence of restenosis varies greatly depending on the initial clinical presentation and the anatomic pattern of disease (e.g. coronary vs. femoro-popliteal vs. infra popliteal). Overall, for open surgeries such as bypass and endarectomy, the rate of restenosis after 1 year ranges between 20 to 30% (15). For endovascular approaches, the rate of restenosis following plain old balloon angioplasty (POBA) ranges from 30 to 60%, depending on location (16). Restenosis has various origins, such as secondary growth of atherosclerotic lesions or inward remodeling. However, it is due mostly to intimal hyperplasia (IH), a process whereby a “neointima” layer is formed between the internal elastic lamina and the endothelium. This new layer is made of smooth muscle cell (SMC)-like cells and extracellular matrix (ECM) (**scheme 2**).

5.1.3 Intimal hyperplasia

IH is a known complication of all types of vascular reconstructive procedures, including arterial bypass, angioplasty, stenting, and endarterectomy. The progressive thickening of the vessel wall causes both an outward and an inward remodeling, leading to a narrowing of the vessel lumen, and eventually leads to impaired end organ perfusion. IH starts as a physiologic healing response to injury to the blood vessel wall (17).



Scheme 2 Intimal hyperplasia

A healthy vessel (left) is composed of the endothelium (single layer of endothelial cells), an internal elastic lamina (IEL) the media (vascular smooth muscle cells, connective tissue made of collagen, elastin and proteoglycans), the external elastic lamina and the adventitia (collagen and fibroblasts). Intimal hyperplasia develops between the IEL and the endothelium (neointima) and is composed of SMC-like cells of different origin and extracellular matrix.

IH is formed by proliferating VSMC originating from dedifferentiated contractile medial VSMC. Unlike other cells of the myogenic lineage, such as cardiac and skeletal muscle cells, which are terminally differentiated, adult VSMC are highly plastic and capable of profound phenotypic alterations in response to changes in their local environment. Modulation of VSMC from a quiescent 'contractile' phenotype to a proliferative 'synthetic' phenotype is important for vascular injury repair, but is also a key factor in the pathogenesis of vascular proliferative diseases (18). Upon vascular injury, the growth factors (PDGF-BB, bFGF), chemokines (SDF-1 α , MCP-1) and cytokines (TNF- α , IL-1 β) secreted by activated EC, platelets and immune cells, lead to inhibition

of the expression of SMC-specific markers while stimulating the expression of ECM components and matrix metalloproteinases (18, 19).

5.1.4 Current treatment of intimal hyperplasia

The most recent advances in the treatment of IH rely on the use of drug-coated balloons (DCB) and drug-eluting stents (DES), which represent a first line therapy in many endovascular approaches to treat short lesions in coronary or femoral arteries. The most used drug is the anti-tumor chemotherapy Paclitaxel (Taxol™). Several paclitaxel-coated balloons and eluting stents with various formulations and doses of paclitaxel demonstrated superiority to POBA (20-22) or BMS (20, 23). Overall, the arrival of DES and DCB reduced the incidence of restenosis below 10% in coronary arteries (24), although restenosis has been delayed rather than suppressed (25). DES also require prolonged antiplatelet therapy and hinder future surgical revascularization. In peripheral *below the knee* small arteries, the use of DCB is controversial, and stents are not recommended due to the risk of thrombosis (26). In December 2018, Katsanos and colleagues reported, in a systematic review and meta-analysis, an increased risk of all-cause mortality following application of paclitaxel-coated balloons and stents in the femoropopliteal artery (27). Other groups recently confirmed these findings using the same data (28, 29). However, other meta-analyses did not find any association between paclitaxel devices and long-term survival, despite similar target populations and vessel segments (30-34). These reports questioned the widespread use of paclitaxel for the treatment of restenosis (35), and supports the need to develop other approaches or use other molecules. In coronary interventions, Sirolimus is increasingly used (36), and new devices are under evaluation to validate the use of sirolimus-coated devices in *below the knee* peripheral arteries (37). Recent studies even report the safety and efficacy of biodegradable polymer sirolimus-eluting stent (38, 39).

However, all current strategies based on the use of DEB and DES target cell proliferation to reduce IH, but also impair re-endothelisation of the vessel. Endothelium repair is crucial to limit

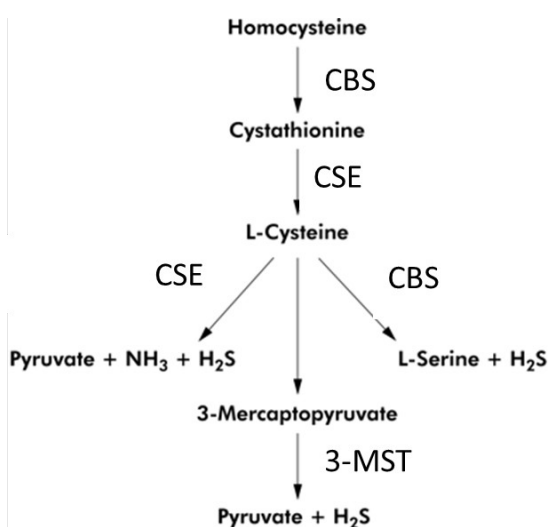
inflammation, remodeling and for vessel healing. Indeed, in normal conditions, EC rapidly produce nitric oxide (NO) via endothelial NO synthase (eNOS) in response to agonists and fluctuations in blood flow. NO rapidly diffuses through the endothelial plasma membrane and leads to inhibition of adhesion and aggregation of platelets and leukocytes and vasorelaxation in VSMC. This ensures that the endothelium remains non-thrombogenic and properly regulates vasomotor tone. In straight segments of arteries, blood flow is laminar and stress is low resulting in eNOS upregulation by EC (7). However, at bifurcations, curvatures, or other regions with complex geometry, blood flow is disturbed and turbulent, leading to reduced NO production. These abnormal patterns of shear stress induce “endothelial dysfunction” or “endothelium activation”. Reduced NO production promotes vasoconstriction, platelet aggregation and recruitment/activation of resident and circulating inflammatory cells mainly through the activation of the pleiotropic transcription factor nuclear factor kappa B (NF- κ B) in EC. This type of lesion serves as a precursor for the development of atherosclerosis (atheroprone endothelium) by facilitating local inflammatory reactions and entrapment of LDL in the vessel wall (40). In addition, any vascular surgery destroys the endothelial layer, furthering endothelium damage on those existing weak spots (41).

In summary, PAD, caused by atherosclerosis development in lower limb muscle, severely affects patient’s quality of life. When life habits changes and medical therapy fail to relieve limb symptoms, vascular surgery remains the only option. Unfortunately, surgery often fails due to IH, an overproliferation of VSMC into the inner layer of the vessel wall. The endothelium, the inner part of the vessel, plays a major role in vessel repair and is dysfunctional in PAD patients. Surgery further increases this dysfunction by damaging the endothelium. So far, therapies to limit IH have focused on inhibiting VSMC proliferation with debating efficacy. Optimal therapy should also promote endothelium recovery. In that regard, the gasotransmitter hydrogen sulfide (H_2S) possesses promising properties.

5.2 Hydrogen sulfide

5.2.1 Endogenous H₂S production

H₂S gas was for long considered only as a toxic byproduct of sulfur mining and sewages (42) until Du Vigneaud found the existence of an endogenous pathway releasing H₂S in mammalian tissues in 1960. He discovered a new pathway involving the inter-conversion of cysteine and homocysteine and termed this pathway “transsulfuration”. Two pyridoxal 5'-phosphate (PLP) dependent enzymes, cystathionine γ -lyase (CSE) and cystathionine β -synthase (CBS) produce H₂S. Two additional PLP-independent enzymes, 3-mercaptopyruvate sulfurtransferase (3-MST) and cysteine aminotransferase (CAT) generate sulfane sulfur that can be further processed into H₂S (**scheme 3**). 3-MST and CAT are expressed ubiquitously, whereas CBS and CSE display more tissue-specific expression. Thus, CBS is the only PLP-dependent enzyme expressed in the brain, while CSE is more prominent in the cardiovascular system. In the kidney and liver, both CSE and CBS are highly expressed. Although the enzymes and pathways responsible for endogenous H₂S production are well defined, little is known about their regulation and their relative contributions to H₂S and sulfane sulfur levels (e.g., polysulfides, persulfides, thiosulfate) in the circulation and in tissues under normal and disease conditions.



Scheme 3: H₂S production in the transsulfuration pathway

H₂S is produced in the transsulfuration pathway during the inter-conversion of cysteine and homocysteine by two pyridoxal 5'-phosphate (PLP) dependent enzymes, cystathionine γ -lyase (CSE) and cystathionine β -synthase (CBS) produce H₂S. 3-mercaptopyruvate sulfurtransferase (3-MST) in combination with cysteine aminotransferase (CAT) generates sulfane sulfur that can be further processed into H₂S.

All H₂S-synthesizing enzymes have been reported to be expressed by cardiovascular cells. The study of CSE^{-/-} mice demonstrated impaired endothelium-dependent vasorelaxation, with no apparent dysfunction at the level of VSMC (43). Furthermore, CSE seems sufficient to observe H₂S-mediated vasodilation (44, 45). These observations strongly promoted the idea that CSE is the main H₂S-producing enzyme in the cardiovascular system at the level of EC. However, other reports suggest a key role of 3-MST and CAT, in H₂S production by the vascular endothelium (46). In contradiction to this early report, studies performed using CSE^{-/-} mice generated on a pure C57BL/6 genetic background by the group of Prof. Isao Ishii failed to show impaired endothelial function and hypertension (47, 48). In addition, most studies of endogenous H₂S inhibition rely of the use of high concentrations of propargylglycine (PAG) to inhibit CSE. At these concentrations, PAG may also inhibit CBS, as well as other nonspecific targets. S. Bibli et al. recently demonstrated that CSE expression is negatively regulated by shear stress, as opposed to eNOS in the mouse aorta (49, 50). This is in line with a previous study showing that only disturbed flow regions show discernable CSE protein expression after carotid artery ligation in the mouse (51).

5.2.2 H₂S biological activity

The chemical nature of the molecules responsible for the biological activity of H₂S remains elusive. HS⁻, polysulfides and sulfates have all been shown to affect a variety of signaling pathways, leading to biological responses. The sulfur atom is a very potent electron acceptor/donor and H₂S can undergo complex oxidation, yielding thiosulfate, sulfenic acids, persulfides, polysulfides and sulfate (52). These oxidative products are likely mediating the principal mechanism through which H₂S exerts its biological actions: post-translational modification of proteins, known as persulfidation. Persulfidation is a chemical reaction whereby a persulfide group (RSSH) is formed on reactive cysteine residues of target proteins (52, 53). Since H₂S has the same oxidation state as cysteine residues, a redox reaction cannot occur. Cysteine residues or H₂S have to be oxidized first (for instance in the form of polysulfides H₂S_n). In 2009, Mustafa et al. performed LC/MS/MS analysis

on liver lysates after NaHS treatment and identified 39 proteins that were persulfidated. Amongst them, they identified GAPDH, β -tubulin, and actin. Interestingly, these proteins were not persulfidated in the liver of mice lacking CSE (CSE KO)(54). Furthermore, new high throughput techniques allowing global assessment of post-translational modification of cysteinyl thiols (-SH) to persulfides (-SSH) demonstrated extensive cysteine residues persulfidation in response to various H₂S donors across various experimental designs (55-57).

5.2.3 H₂S in the vascular system

H₂S participates in the homeostasis of many organs and systems. In the following sections, we will focus on the role of H₂S in the vascular system and H₂S properties relevant to vascular conditions, which are summarized in **scheme 4**.

5.2.3.1 H₂S promotes vasodilation

The first evidence of H₂S being a gasotransmitter comes from the consistent observation across species and vascular beds that H₂S and other derived products induce vasodilation. Pharmacological inhibition of H₂S production using PAG increases blood pressure in rats (58). Myograph studies of CSE knock-out mice (CSE^{-/-}) demonstrated that H₂S-mediated vasorelaxation requires an intact endothelium.

Mechanistically, H₂S triggers vasodilation by interacting with several ion channels in the vascular wall such as K_{ATP} channels in VSMCs and ChTX/apamin-sensitive KCa channels in vascular EC. The activation of these two types of channels by H₂S leads to VSMC hyperpolarization and vasorelaxation (43, 45). H₂S also dilates arteries through activation of EC BKCa channels and Cyp2C with downstream activation of VSMC Ca²⁺ sparks leading to hyperpolarization (59). In addition, H₂S may activate eNOS. H₂S interaction with the NO pathway has been reviewed previously in (60) and in (61).

Interestingly, recent studies performed using lower doses of H₂S donors revealed that H₂S has a biphasic effect on vasomotor tone. Thus, low doses tend to be vasoconstrictors, while higher

doses are generally vasodilators. In addition, accumulating evidence suggest that the contribution of H₂S to vasomotor tone may depend on the vascular beds (e.g., aorta vs. mesenteric artery), vessel size (conduit vs. resistant), and species (for full review see (62)). Overall, H₂S probably contributes to the maintenance of mean arterial blood pressure at physiological levels; however, the importance of CSE, CBS and 3MST-mediated H₂S production remains unclear and probably varies depending on the species and vascular bed.

5.2.3.2 H₂S promotes angiogenesis

Angiogenesis is the physiological process through which new blood vessels form from pre-existing ones. Cells lacking oxygen and nutrient secretes pro-angiogenic factors triggering a remodeling of the vascular network to reperfuse the hypoxic area.

Several *in vivo* studies investigated the effect of H₂S on reperfusion in models of PAD/CLI after skeletal limb ischemia. Rushing et al. showed that SG1002, a H₂S releasing pro-drug, increases leg revascularization and collateral vessel number after occlusion of the external iliac artery in miniswine. Wang et al. showed that NaHS supplementation significantly increased collateral vessel growth in mice after femoral artery ligation (HLI) (63). A study in CBS heterozygous mice showed that GYY4137 supplementation following HLI increased neoangiogenesis in ischemic muscle of treated mice (64). Finally, ZYZ-803, a hybrid NO and H₂S donor, significantly increase limb perfusion after HLI in mice (65). In these studies, H₂S effectively increased angiogenesis and arteriogenesis, 2 processes central for ischemic skeletal muscle repair (66, 67).

On a cellular level, a large amount of studies established that H₂S and polysulfites stimulate EC function to promote angiogenesis. Exogenous H₂S treatment stimulates EC growth, motility and organization into vessel-like structure *in vitro*. On the contrary, inhibition of H₂S biosynthesis, either via pharmacological inhibitors or via silencing of CSE, CBS or 3MST, reduces EC growth, migration and vessel-like structure formation (60, 68). Further *in vivo* studies of chicken

chorioallantoic membranes (CAM) treated with the CSE inhibitor PAG suggest that CSE is important for vessel branching and elongation (69). Matrigel plug angiogenesis assay also confirmed the importance of CSE and H₂S in vascular endothelial growth factor (VEGF)-induced angiogenesis (70, 71).

On a molecular level, several mechanisms have been proposed to explain H₂S-induced angiogenesis. First, H₂S stimulates the VEGF pathway in EC, through persulfidation of the VEGF receptor VEGFR2, increasing its dimerization, autophosphorylation and activation (72). Interestingly, short term exposure of human EC to VEGF increases H₂S production (69), suggesting a positive feedback loop of VEGF signaling through H₂S.

H₂S also promotes angiogenesis by inhibiting mitochondrial electron transport and oxidative phosphorylation, resulting in increased glucose uptake and glycolytic ATP production necessary to provide rapid energy and building blocks for EC proliferation and migration (73). Indeed, despite having access to high circulating levels of oxygen, quiescent ECs produce 80% of their ATP via aerobic glycolysis (74). Glycolysis is critical for ECs, and its complete blockade by using 2-deoxy-glucose leads to decreased proliferation and migration and induces cell death (75). High glycolytic levels in ECs are tightly regulated by several rate limiting enzymes such as 6-phosphofructo-2-kinase/fructose-2,6-biphosphatase 3 (PFKFB3) (76).

Finally, H₂S promotes angiogenesis through its extensive interaction with the NO pathway. In EC, H₂S may induce eNOS persulfidation at Cys433, which increases the phosphorylation of its activator site and stabilizes eNOS in its dimeric form (60, 61). H₂S may also increase intracellular calcium levels, leading to increase eNOS activity and NO production (77, 78). Exogenous H₂S donors have also been shown to stimulate the growth pathways Akt, p38 and ERK1/2, which all promote EC proliferation and migration (69, 71, 79). Interestingly, both H₂S and NO-induced angiogenesis require the other gasotransmitter (60, 61). Thus, the vascular effects of NO and H₂S are interdependent and closely intertwined, with both gasotransmitter having direct and indirect effects on each other (for full review see (80)).

5.2.3.3 H₂S inhibits VSMC proliferation and intimal hyperplasia

Few studies directly assessed the effects of endogenous or exogenous H₂S on IH. CSE expression and activity are reduced after balloon-injury in a rat model of IH (81). CSE expression and activity, as well as free circulating H₂S, are also reduced in human suffering from vascular occlusive diseases (82, 83). We recently demonstrated that, in patient undergoing vascular surgery, circulating H₂S levels were associated with long-term survival (84), suggesting low H₂S production as a risk-factor for cardiovascular diseases. Mice lacking CSE show a significant increase in IH formation as compared to WT mice in a model of carotid artery ligation (85, 86). On the contrary, CSE overexpression decreases IH formation in a murine model of vein graft by carotid-interposition cuff technique (87). Similarly, NaHS administration limits the development of IH in *in vivo* models in rats (81), rabbits (88) and mice (85), and in human great saphenous vein segments *ex-vivo* (89).

The VSMC phenotype switch from quiescent/contractile towards proliferating migrating cells plays important roles in vascular remodeling in IH and in ATS (18). On the cellular level, the effect of H₂S against IH is probably mediated by inhibition of VSMC proliferation and migration. Indeed, it was demonstrated, using BrdU and TUNEL assays, that H₂S supplementation or CSE overexpression decreases VSMCs proliferation and increases VSMCs apoptosis, respectively (88-90). VSMCs isolated from *Cse*^{-/-} mice exhibit more motility than their WT counterpart, and blocking CSE activity using PAG in WT VSMCs increases cell migration (85, 91).

The mechanisms whereby H₂S affect VSMCs are not fully understood. Upon vascular injury, the growth factors (PDGF-BB, bFGF), chemokines (SDF-1 α , MCP-1) and cytokines (TNF- α , IL-1 β) secreted by activated EC, platelets and immune cells trigger pleiotropic signaling pathways, among which the MAPK pathway, including extracellular signal-regulated kinase (ERK), c-Jun-N-terminal kinase (JNK) and p38 mitogen-activated protein kinases, plays a major role in VSMC migration and proliferation (18). Other signals derived from oxidative stress also regulate the p38 MAPK and JNK pathways, thereby influencing VSMC's identity (92). In mouse VSMC, H₂S has been shown to modulate the MAPK pathway, especially ERK1,2 (81), and calcium-sensing receptors

(93, 94). In addition, H₂S may limit MMP2 expression and ECMs degradation, preventing migration of VSMCs from the media to the intima (85, 91). In human VSMC, we recently reported that the H₂S donor Zofenopril decreases the activity of the MAPK and mTOR pathways, which correlates with reduced VSMC proliferation and migration (95). We also showed that the H₂S donor salt NaHS, as well the thiol source sodium thiosulfate, inhibit microtubule polymerization, which results in cell cycle arrest and inhibition of proliferation and migration in primary human VSMC (86) (**Scheme 4**).

Other studies also inform on potential mechanism of action of H₂S on VSMC. As described above, H₂S triggers vasodilation mostly via persulfidation of several ion channels such as K_{ATP}, voltage and Ca²⁺-activated K⁺ channels (44, 45, 59). By reducing extracellular Ca²⁺ entry, H₂S improves VSMC relaxation. Despite the obvious fact that improved vasorelaxation may be beneficial in the context of IH, these channels may also directly regulate cell proliferation in VSMC. For instance, the anti-diabetic and K_{ATP} channel blocker glibenclamide has been shown to reduce VSMC proliferation (96).

5.2.4 H₂S inhibits inflammation in the cardiovascular system

Many studies report anti-inflammatory properties of H₂S, in particular in the context of atherosclerosis and cardiac failure (for full review see(97)). Thus, H₂S reduces adhesion and infiltration of pro-inflammatory cells and circulating levels of pro-inflammatory chemokines and cytokines in the ApoE^{-/-} mouse model of atherosclerosis (98, 99). Similarly, several reports document that H₂S donors (NaHS, DATS, SG1002, STS) or CSE overexpression decrease leukocyte and neutrophil infiltration and cytokine production following ischemic injury in various models of myocardial infarction (100-105).

Mechanistically, evidence from EC and macrophages indicate that Nuclear factor kappa B (NFκB) inhibition seems to be the key to H₂S anti-inflammatory effects (98, 106-108). NF-κB is a transcription factor and a master regulator of pro-inflammatory genes, including cytokines and cell adhesion molecules. NaHS inhibits NF-κB activity probably via persulfidation/stabilization of

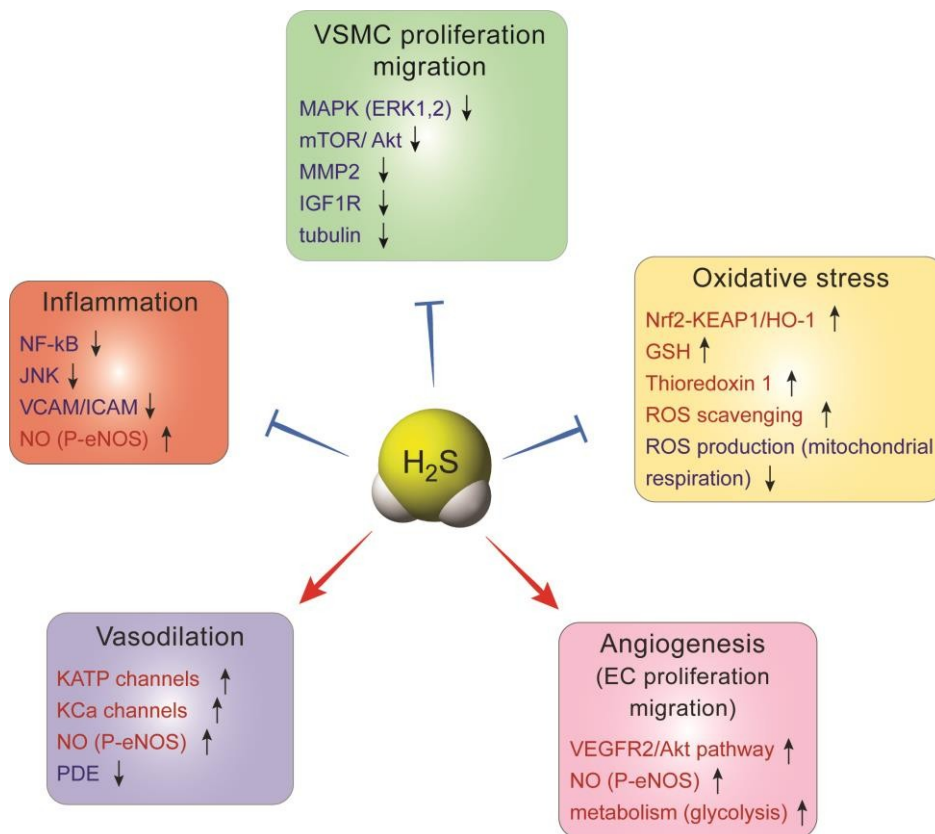
I κ B (109), which controls NF- κ B (p65) translocation to the nucleus. In EC, this leads to decreased expression of adhesion molecule VCAM and ICAM, thereby limiting recruitment of leukocyte to the aortic wall(98, 106, 108). NaHS also promotes a shift in macrophages to the M2, pro-resolution state (110). Moreover, NaHS and GYY increase eNOS phosphorylation, thereby improving NO production, which reduces inflammation (106, 111).

5.2.5 H₂S has anti-oxidant properties

Several studies in various models also consistently showed that H₂S holds anti-oxidant properties. First, H₂S can directly scavenge reactive oxygen species (ROS), such as superoxide anions O₂⁻, at higher rates than other classic antioxidants such as GSH. However, since H₂S physiologic concentration is in the nanomolar range whereas GSH is present in millimolar quantity, it is debatable whether H₂S direct contribution to anti-oxidation is significant (112, 113).

Actually, the effect of H₂S probably arise from stimulation of anti-oxidant pathways, rather than via direct scavenging of ROS. Thus, H₂S has been shown in a number of models to stimulate the anti-oxidant Nrf2 pathway (114-117), or via increase GSH production or thioredoxin 1 expression (118-120). Numerous studies document that H₂S promotes the Nrf2 pathway (reviewed in (117)). H₂S promotes the Nrf2 anti-oxidant response via persulfidation of Kelch-like ECH-associated protein 1 (Keap1), which sequesters Nrf-2 in the cytosol. Keap1 persulfidation prompts dissociation from Nrf2, which induces the expression of several proteins, among which the major antioxidant protein heme oxygenase 1 (HO-1) (116, 121). H₂S interaction with GSH has been studied in details in the central nervous system, where GSH plays a major role in maintaining the homeostasis between anti-oxidant and ROS production (reviewed in details in (122)). In the vascular system, H₂S persulfidated the glutathione peroxidase 1, which promotes glutathione synthesis and results in decreased lipid peroxidation in the aortic wall in the context of atherosclerosis (120). Thioredoxin 1 is instrumental in the cardioprotective effects of H₂S against ischemic-induced heart failure (112). Furthermore, H₂S may suppress the expression of Trx-interacting protein (TXNIP), which inhibit Trx activity in EC (112, 123).

Mitochondrial respiration is a well-established major source of ROS (124, 125). H₂S has a bell-shaped effect on mitochondrial respiration. At low nanomolar concentrations, sulfide quinone oxidoreductase (SQR) transfers electrons from H₂S to the coenzyme Q in the Complex II of the electron transport chain, thereby promoting mitochondrial respiration. At higher concentrations, H₂S binds the copper center of cytochrome c oxidase (complex IV), which inhibits respiration and limits ROS production (126). While these reactions likely occur, the highly unstable and reactive nature of both H₂S and ROS makes it nearly impossible to observe and measure them. These anti-oxidant properties of H₂S may have a beneficial impact on IH, as ROS contribute to endothelial dysfunction and VSMC dedifferentiation (127, 128).



Scheme 4: H₂S actions in the vascular system

In the vascular system, H₂S promotes vasodilation and angiogenesis. It limits oxidative stress, inflammation, as well as VSMC proliferation and migration.

6 Aim

There is currently no clinically approved molecule exploiting the clinical potential of H₂S. Most compounds available for research have poor translational potential due to their pharmacokinetic properties. Other H₂S-releasing molecules extracted from garlic such as DATS (Diallyl trisulfide) is also very short lived and hard to stabilize (129). Against this background, the aim of my thesis was to find new therapeutic options for peripheral vascular diseases by exploiting the beneficial actions of the gasotransmitter Hydrogen sulfide, using already approved drugs.

My work is divided in the following 3 specific aims, which also constitutes the 3 parts of my thesis:

7.1. Sodium Thiosulfate acts as a hydrogen sulfide mimetic to prevent intimal hyperplasia via inhibition of tubulin polymerization.

In this part we describe the benefits of STS, a medically relevant source of sulfur, against intimal hyperplasia using a mouse model and in an *ex vivo* model of IH in human saphenous veins.

7.2 Hydrogen Sulphide Release via the Angiotensin Converting Enzyme Inhibitor Zofenopril Prevents Intimal Hyperplasia in Human Vein Segments and in a Mouse Model of Carotid Artery Stenosis.

Here, we describe the superiority of the sulfhydrated ACE inhibitor Zofenopril over non-sulfhydrated ACE inhibitor such as Enalapril against intimal hyperplasia, using the models described in chapter 7.1.

7.3 Sodium thiosulfate, a source of hydrogen sulfide, promotes endothelial cells proliferation, angiogenesis and reperfusion following hind-limb ischemia in the mouse.

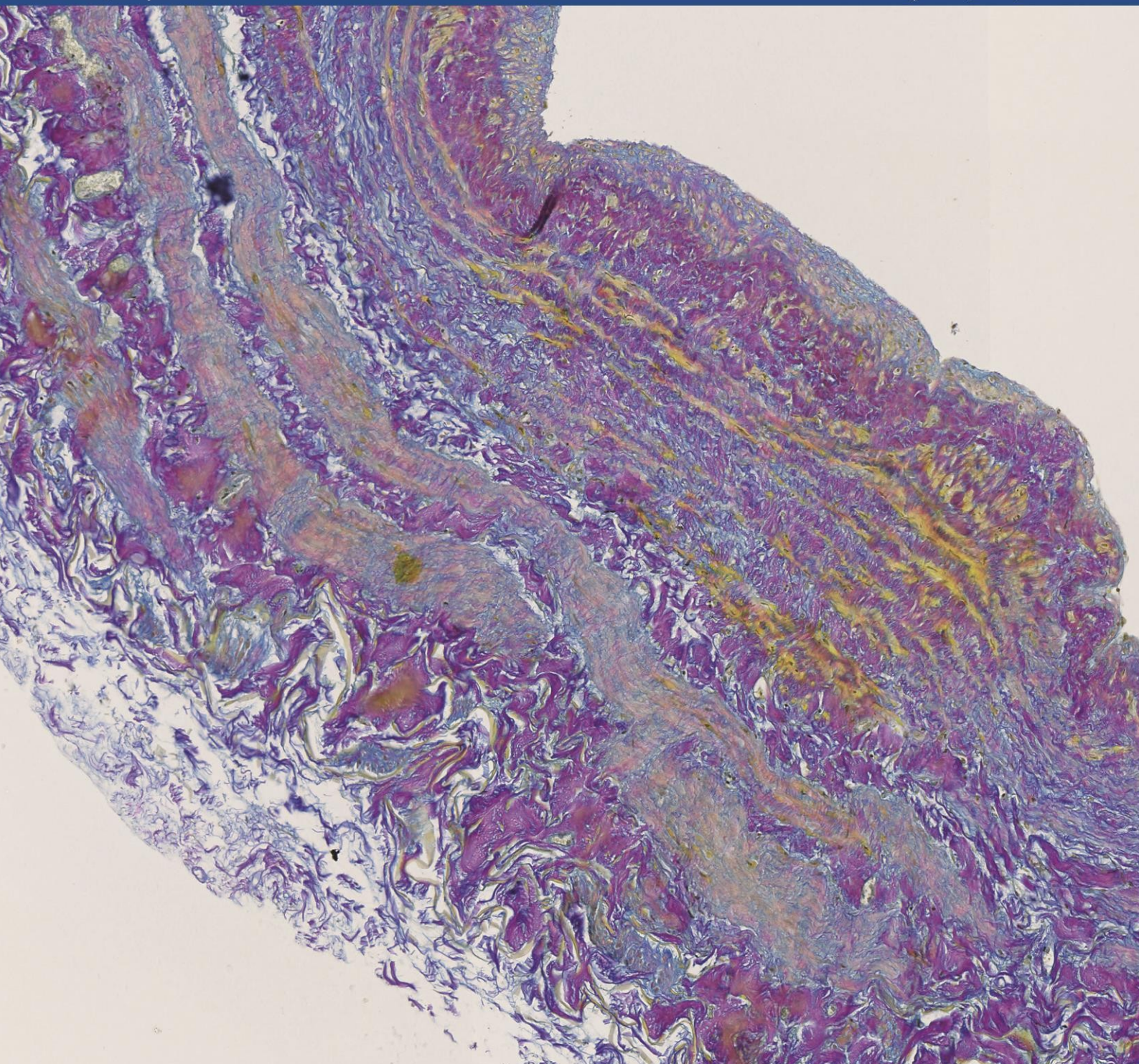
In this study, we tested the therapeutic potential of STS to promote reperfusion and angiogenesis *in vivo* in various models and investigated STS effects on cultured EC. STS stimulated EC proliferation and migration *in vitro* via metabolic reprogramming towards a more glycolytic state.

7 Results

7.1 Sodium Thiosulfate acts as a hydrogen sulfide mimetic to prevent intimal hyperplasia via inhibition of tubulin polymerisation

In this study, we tested the therapeutic potential of STS against intimal hyperplasia. We demonstrated that STS limits IH development *in vivo* in a model of arterial restenosis and in an *ex vivo* model of human veins. STS treatment increased H₂S bioavailability, which inhibited cell apoptosis and fibrosis, as well as VSMC proliferation and migration via microtubules depolymerization.

DOI: <https://doi.org/10.1016/j.ebiom.2022.103954>



Editorial

The science of stress relief

Articles

Sodium thiosulfate inhibits intimal hyperplasia

Review

New diagnostic and therapeutic strategies for myocardial infarction via nanomaterials



Sodium thiosulfate acts as a hydrogen sulfide mimetic to prevent intimal hyperplasia via inhibition of tubulin polymerisation

Diane Macabrey,^{a,b} Alban Longchamp,^{a,b} Michael R. MacArthur,^c Martine Lambelet,^{a,b} Severine Urfer,^{a,b} Sebastien Deglise,^{a,b,1} and Florent Allagnat^{a,b,1*}

^aDepartment of Vascular Surgery, Lausanne University Hospital, Switzerland

^bCHUV-Service de chirurgie vasculaire, Department of Biomedical Sciences, University of Lausanne, Bugnon 7A, Lausanne 1005, Switzerland

^cDepartment of Health Sciences and Technology, Swiss Federal Institute of Technology (ETH) Zurich, Zurich, Switzerland

Summary

Background Intimal hyperplasia (IH) remains a major limitation in the long-term success of any type of revascularisation. IH is due to vascular smooth muscle cell (VSMC) dedifferentiation, proliferation and migration. The gas-transmitter Hydrogen Sulfide (H₂S), mainly produced in blood vessels by the enzyme cystathionine- γ -lyase (CSE), inhibits IH in pre-clinical models. However, there is currently no H₂S donor available to treat patients. Here we used sodium thiosulfate (STS), a clinically-approved source of sulfur, to limit IH.

Methods Low density lipoprotein receptor deleted (LDLR^{-/-}), WT or Cse-deleted (Cse^{-/-}) male mice randomly treated with 4 g/L STS in the water bottle were submitted to focal carotid artery stenosis to induce IH. Human vein segments were maintained in culture for 7 days to induce IH. Further *in vitro* studies were conducted in primary human vascular smooth muscle cells (VSMCs).

Findings STS inhibited IH in WT mice, as well as in LDLR^{-/-} and Cse^{-/-} mice, and in human vein segments. STS inhibited cell proliferation in the carotid artery wall and in human vein segments. STS increased polysulfides *in vivo* and protein persulfidation *in vitro*, which correlated with microtubule depolymerisation, cell cycle arrest and reduced VSMC migration and proliferation.

Interpretation STS, a drug used for the treatment of cyanide poisoning and calciphylaxis, protects against IH in a mouse model of arterial restenosis and in human vein segments. STS acts as an H₂S donor to limit VSMC migration and proliferation via microtubule depolymerisation.

Funding This work was supported by the Swiss National Science Foundation (grant FN-310030_176158 to FA and SD and PZ00P3-185927 to AL); the Novartis Foundation to FA; and the Union des Sociétés Suisses des Maladies Vasculaires to SD, and the Fondation pour la recherche en chirurgie vasculaire et thoracique.

Copyright © 2022 The Author(s). Published by Elsevier B.V. This is an open access article under the CC BY license (<http://creativecommons.org/licenses/by/4.0/>)

Keywords: Intimal hyperplasia; Smooth muscle cells; Proliferation; Hydrogen sulfide; Sodium thiosulfate

Abbreviations: 3-MST/MPST, 3-mercaptopyruvate sulfurtransferase; ALAT, alanine amino-transferase; ASAT, aspartate amino-transferase; BSA, bovine serum albumin; CAS, carotid artery stenosis; Cse/Cth, cystathionine gamma lyase; CBS, cystathionine- β -synthase; CK, creatine kinase; CK-MB, creatine Kinase MB Isoenzyme; CUA, calcific uremic arteriopathy; DAPI, 4',6-diamidino-2-phénylindole; DATS, diallyl trisulfide; DCB, drug-coated balloons; DES, drug-eluting stents; DMF, dimethyl formamide; ECM, extra-cellular matrix (); FBS, foetal bovine serum; H₂S, hydrogen sulfide; IH, intimal hyperplasia; NaHS, sodium hydrogen sulfur; P4HAI, prolyl 4-hydroxylase alpha polypeptide I; PBS, phosphate buffered saline; PCNA, proliferating cell nuclear antigen; SBP, systolic blood pressure; STS, sodium thiosulfate; VSMC, vascular smooth muscle cells; VGEL, Van Gieson elastic lamina; TST, thiosulfate sulfurtransferase; SUOX, sulfite oxidase; LDLR, Low density lipoprotein receptor

*Corresponding author.

E-mail address: Florent.allagnat@chuv.ch (F. Allagnat).

¹ These authors contributed equally to this work.

Research in context

Evidence before this study

Intimal hyperplasia (IH) is a complex process leading to vessel restenosis, a major complication following cardiovascular surgeries and angioplasties. Therapies to limit IH are currently limited. Pre-clinical studies suggest that hydrogen sulfide (H₂S), an endogenous gasotransmitter, limits restenosis. However, despite these potent cardiovascular benefits, H₂S-based therapeutics are not available. Sodium thiosulfate (Na₂S₂O₃) is a FDA-approved drug used for the treatment of cyanide poisoning and calciphylaxis, a rare condition of vascular calcification affecting patients with end-stage renal disease. Evidence suggest that thiosulfate may generate H₂S *in vivo* in pre-clinical studies.

Added value of this study

Here, we demonstrate that STS inhibits IH in a surgical mouse model and in human vein *ex vivo*. We further found that STS increases circulating polysulfide levels *in vivo* and inhibits IH via disruption of the normal cell's cytoskeleton, leading to decreased cell proliferation and migration. Finally, STS rescues *Cse* knockout mice with impaired endogenous H₂S production from accelerated IH formation.

Implications of all the available evidence

These findings suggest that STS holds translational potentials to limit IH following vascular surgeries and should be investigated in clinical trials.

Introduction

Prevalence of peripheral arterial disease continues to rise worldwide, largely due to the combination of aging, smoking, hypertension, and diabetes mellitus.^{1–3} Open or endo-vascular surgery remains the best treatment when daily life activities are compromised despite exercise therapy or in threatened limb.⁴ However, the vascular trauma associated with any vascular surgery eventually lead to secondary occlusion of the injured vessel. Re-occlusive lesions result in costly and complex recurrent end-organ ischemia, and often lead to loss of limb, brain function, or life. Despite the advent of new medical devices such as drug eluting stent (DES) and drug-coated balloons (DCB), restenosis has been delayed rather than suppressed, and stents still suffer from high rates of in-stent restenosis.⁵ Plus, the use of DES and DCB prolongs the need for anti-thrombotic therapies, with their associated risk of haemorrhages. In December 2018, Katsanos and colleagues reported, in a systematic review and meta-analysis, an increased risk of all-cause mortality following application of paclitaxel-coated balloons and stents in the femoropopliteal

artery.⁶ These findings were recently confirmed by other groups using the same data.^{7–8} However, other meta-analyses did not find any association between paclitaxel devices and long-term survival, despite similar target populations and vessel segments.^{9–13} Overall, these reports question the widespread use of paclitaxel for the treatment of restenosis, and supports the development of other approaches or use of other molecules. While the focal nature of restenotic lesions prompts the use of local treatment, systemic approaches for the treatment of restenosis still remains an option.

Restenosis is mainly due to intimal hyperplasia (IH), a process instated by endothelial cell injury and inflammation, which induces vascular smooth muscle cell (VSMC) reprogramming. VSMCs become proliferative and migrating, secrete extra-cellular matrix (ECM) and form a new layer called the neo-intima, which slowly reduces the vessel luminal diameter.¹⁴

Hydrogen sulfide (H₂S) is a gasotransmitter derived from cysteine metabolism, produced endogenously through the transsulfuration pathway by 3 main enzymes, cystathionine-γ-lyase (CSE), cystathionine-β-synthase (CBS) and 3-mercaptopyruvate sulfurtransferase (3-MST).¹⁵ Mice lacking *Cse* develop more IH in after carotid ligation, and are rescued by H₂S supplementation.¹⁶ Circulating H₂S levels are reduced in humans suffering from vascular occlusive disease^{17,18} and pre-clinical studies using water-soluble sulfide salts such as Na₂S and NaHS have shown that H₂S has cardiovascular protective properties,¹⁵ including reduction of IH *in vivo* in rats,¹⁹ rabbits,²⁰ mice,²¹ and *ex-vivo* in human vein segments.²² However, the fast and uncontrolled release, narrow therapeutical range and high salt concentration of these compounds limit their potential. Due to these limitations, H₂S-based therapy are currently not available.

Here, we focused on sodium thiosulfate (Na₂S₂O₃), a FDA-approved drug used in gram-quantity doses for the treatment of cyanide poisoning²³ and calciphylaxis, a rare condition of vascular calcification affecting patients with end-stage renal disease.²⁴ Pharmaceutical-grade sodium thiosulfate (STS) is available and thiosulfate has been suggested to release H₂S through non-enzymatic and enzymatic mechanisms.^{25,26}

We tested whether STS inhibits IH in a surgical mouse model and in an *ex vivo* model of IH in human vein culture. NaHS, a validated H₂S donor, was systematically compared to STS. We observed that STS was at least as potent as NaHS to inhibit IH in our two models. STS increased protein persulfidation and circulating polysulfide levels *in vivo*. STS inhibited apoptosis and matrix deposition associated with the development of IH, as well as VSMC proliferation and migration. We further observed that STS and NaHS induced microtubule depolymerisation in VSMCs, which may explain the anti-proliferative effect of STS in those cells.

Methods

For details on materials and reagents please see the Supplementary Table S1 and 2.

Mouse treatment

WT mice C57BL/6J (RRID:MGI:5752053) mice were purchased from Janvier Labs (Le Genest-Saint-Isle, France). LDL receptor knock out (LDLR^{-/-}) mice (Ldlr^{tm1Her}, JAX stock #002207²⁷; MGI Cat# 3611043, RRID:MGI:3611043), kindly provided by Prof. Caroline Pot (Lausanne university Hospital, Switzerland), were bred and housed in our animal facility and genotyped as previously described.²⁷ All mice were housed at standard housing conditions (22 °C, 12 h light/dark cycle), with ad libitum access to water and regular diet (SAFE[®]150 SP-25 vegetal diet, SAFE diets, Augy, France). LDLR^{-/-} mice were put on a cholesterol rich diet (Western 1635, 0.2% Cholesterol, 21% Butter, U8958 Version 35, SAFE[®] Complete Care Competence) for 3 weeks prior to surgery. 8 to 12 weeks old male WT or LDLR^{-/-} mice were randomly divided into control vs. sodium thiosulfate (STS) or NaHS. Sodium thiosulfate was given in mice via the water bottle at 4 g/L (0.5 g/Kg/day), changed 3 times a week. NaHS was given in mice via the water bottle at 0.5 g/L (125 mg/Kg/day), changed every day. Mice were euthanized after 7 or 28 days of treatment by cervical dislocation under isoflurane anaesthesia (inhalation 2.5% isoflurane under 2.5 L of O₂) followed by PBS perfusion. Aortas, carotid arteries, livers and serum or plasma (via intracardiac blood collection with a 24G needle) were harvested.

Cse^{-/-} mice

Cth knockout (Cse^{-/-}) mice were generated from a novel floxed line generated by embryonic injection of ES cells containing a Cth allele with LoxP sites flanking exon 2 (Cth^{tm1a(EUCOMM)Hmgv}; RRID:IMSR:Cmsu10294). Both ES cells and recipient embryos were on C57BL/6J background. Mice that were homozygous for the floxed allele were crossed with CMV-cre global cre-expressing mice (B6.C-Tg(CMV-cre)1Cgn/J), which have been backcrossed with C57BL/6J for 10 generations to create constitutive whole-body CSE^{-/-} animals on a C57BL/6J background. The line was subsequently maintained by breeding animals heterozygous for the Cth null allele. Mouse ear biopsies were taken and digested in DirectPCR lysis reagent with proteinase K. WT, heterozygous and knockout mice were identified by PCR using the forward primer 5'-AGC ATG CTG AGG AAT TTG TGC-3' and reverse primer 5'-AGT CTG GGG TTG GAG GAA AAA-3' to detect the WT allele and the forward primer 5'-TTC AAC ATC AGC CGC TAC AG-3' to detect knock-out allele using the platinum Taq DNA Polymerase.

Carotid artery stenosis (CAS) surgery

The carotid artery stenosis (CAS) was performed as previously published²⁸ on 8 to 10 weeks old male WT or

LDLR^{-/-} mice. Treatment was initiated 3 days before surgery and continued for 28 days post-surgery until organ collection. The day of the surgery, mice were anaesthetised with an intraperitoneal injection of Ketamine (80 mg/kg) and Xylazine (15 mg/kg). The left carotid artery was exposed and separated from the jugular vein and vague nerve. Then, a 7.0 PERMA silk (Johnson & Johnson AG, Ethicon, Switzerland) thread was looped and tightened around the carotid in presence of a 35-gauge needle. The needle was removed, thereby restoring blood flow, albeit leaving a significant stenosis. The stenosis triggers IH proximal to the site of injury, which was measured 28 days post-surgery.²⁸ Buprenorphine (0.05 mg/kg) was provided subcutaneously as post-operative analgesic every 12 h for 24 h. Mice were euthanized under isoflurane anaesthesia (inhalation 2.5% isoflurane under 2.5 L of O₂) by cervical dislocation and exsanguination, perfused with PBS followed by buffered formalin 4% through the left ventricle. Surgeries were performed in a random order, alternating mice from different cages to minimise potential confounders such as the order of treatments and measurements, or animal/cage location. All series of surgeries included all the groups to be compared to minimise batch effects. Surgeons were blind to the group during surgeries.

Human tissue and VSMC culture

Static vein culture was performed as previously described.^{22,29} Briefly, the vein was cut in 5 mm segments randomly distributed between conditions. One segment (Do) was immediately preserved in formalin or flash frozen in liquid nitrogen and the others were maintained in culture for 7 days in RPMI-1640 Glutamax I supplemented with 10% FBS and 1% antibiotic solution (10,000 U/mL penicillin G, 10,000 U/mL streptomycin sulphate) in cell culture incubator at 37 °C, 5% CO₂ and 21% O₂.

Human VSMCs were also prepared from these human great saphenous vein segments as previously described.^{22,29} Vein explants were plated on the dry surface of a cell culture plate coated with 1% Gelatine type B (Sigma-Aldrich). Explants were maintained in RPMI, 10% FBS medium in a cell culture incubator at 37 °C, 5% CO₂, 5% O₂ environment. 8 different veins/patients were used in this study to generate VSMC.

Carotid and human vein histomorphometry

After 7 days in culture, or immediately upon vein collection (Do), the vein segments were fixed in buffered formalin, embedded in paraffin, cut into 5 µm sections, and stained using Van Gieson Elastic Laminae (VGEL) as previously described.^{22,30} Three photographs per section were taken at 100x magnification and 8 measurements of the intima and media thicknesses were

made, evenly distributed along the length of the vein wall.

Left ligated carotids were isolated and paraffin-embedded. Six- μm sections of the ligated carotid artery were cut from the ligature towards the aortic arch and stained with VGEL for morphometric analysis. Cross sections at every 300 μm and up to 2 mm from the ligature were analysed using the Olympus Stream Start 2.3 software (Olympus, Switzerland). For intimal and medial thickness, 72 (12 measurements/cross section on six cross sections) measurements were performed, as previously described.²²

Two independent researchers blind to the experimental groups did the morphometric measurements, using the Olympus Stream Start 2.3 software (Olympus, Switzerland).²²

H₂S and polysulfide measurement

Free H₂S was measured in cells using the SF₇-AM fluorescent probe³¹ (Sigma-Aldrich). The probe was dissolved in anhydrous DMF at 5 mM and used at 5 μM in serum-free RPMI medium with or without VSMCs. Free polysulfide was measured in cells using the SSP4 fluorescent probe. The probe was dissolved in DMF at 10 mM and diluted at 10 μM in serum-free RPMI medium with or without VSMCs. Fluorescence intensity ($\lambda_{\text{ex}} = 495 \text{ nm}$; $\lambda_{\text{em}} = 520 \text{ nm}$) was measured continuously in a Synergy Mx fluorescent plate reader (BioTek Instruments AG, Switzerland) at 37 °C before and after addition of various donors, as indicated.

Plasma polysulfides were measured using the SSP4 fluorescent probe. Plasma samples were diluted 3 times and incubated for 10 min at 37 °C in presence of 10 μM SSP4. Plasma polysulfides were calculated using a Na₂S₃ standard curve. Liver polysulfides were measured using the SSP4 fluorescent probe. Pulverized frozen liver was resuspended in PBS-0.5% triton X-100, sonicated and adjusted to 0.5 mg/ml protein concentration. Lysates were incubated for 30 min at 37 °C in presence of 10 μM SSP4 and fluorescence intensity ($\lambda_{\text{ex}} = 495 \text{ nm}$; $\lambda_{\text{em}} = 520 \text{ nm}$) was measured in a Synergy Mx fluorescent plate reader (BioTek Instruments AG, Switzerland)

Persulfidation protocol

Persulfidation protocol was performed using a dime-done-based probe as recently described.³² Persulfidation staining was performed on VSMCs grown on glass coverslips. Briefly, 1 mM 4-Chloro-7-nitrobenzofurazan (NBF-Cl, Sigma) was diluted in PBS and added to live cells for 20 min. Cells were washed with PBS then fixed for 10 min in ice-cold methanol. Coverslips were rehydrated in PBS, and incubated with 1 mM NBF-Cl for 1 h at 37 °C. Daz2-Cy5.5 (prepared with 1 mM Daz-2, 1 mM alkyne Cy5.5, 2 mM copper(II)-TBTA, 4 mM ascorbic

acid with overnight incubation at RT, followed by quenching for 1h with 20 mM EDTA) was added to the coverslips and incubated at 37 °C for 1 h. After washing with methanol and PBS, coverslips were mounted in Vectashield mounting medium with DAPI and visualized with a 90i Nikon fluorescence microscope.

BrdU assay

VSMCs were grown at 80% confluence (5-10³ cells per well) on glass coverslips in a 24-well plate and starved overnight in serum-free medium. Then, VSMC were either treated or not (ctrl) with the drug of choice for 24 h in full medium (RPMI 10% FBS) in presence of 10 μM BrdU. All conditions were tested in parallel. All cells were fixed in ice-cold methanol 100% after 24 h of incubation and immunostained for BrdU. Images were acquired using a Nikon Eclipse 90i microscope. BrdU-positive nuclei and total DAPI-positive nuclei were automatically detected using the ImageJ software.²²

Flow cytometry

VSMCs were grown at 70% confluence (5-10⁴ cells per well) and treated for 48 h with 15 mM STS or 10 nM Nocodazole. Then, cells were trypsinised, collected and washed in ice-cold PBS before fixation by dropwise addition of ice-cold 70% ethanol while slowly vortexing the cell pellet. Cells were fixed for 1 h at 4 °C, washed 3 times in ice-cold PBS and resuspended in PBS supplemented with 20 $\mu\text{g}/\text{mL}$ RNase A and 10 $\mu\text{g}/\text{mL}$ DAPI. Flow cytometry was performed in a Cytoflex-S apparatus (Beckmann).

Wound healing assay

VSMCs were grown at confluence (10⁴ cells per well) in a 12-well plate and starved overnight in serum-free medium. Then, a scratch wound was created using a sterile p200 pipette tip and medium was changed to full medium (RPMI 10% FBS). Repopulation of the wounded areas was recorded by phase-contrast microscopy over 24 h in a Nikon Ti2-E live cell microscope. All conditions were tested in parallel. The area of the denuded area was measured at $t = 0 \text{ h}$ and $t = 10 \text{ h}$ after the wound using the ImageJ software by two independent observers blind to the conditions. Data were calculated as a percentage of the wound closure.

Immunohistochemistry

Polychrome Herovici staining was performed on paraffin sections as described.³³ Young collagen was stained blue, while mature collagen was pink. Cytoplasm was counterstained yellow. Haematoxylin was used to counterstain nuclei blue to black.

Collagen III staining was performed on frozen sections (OCT embedded) of human vein segments using

mouse anti-Collagen III antibody. Briefly, tissue slides were permeabilised in PBS supplemented with 2 wt. % BSA and 0.1 vol. % Triton X-100 for 30 min, blocked in PBS supplemented with 2 wt. % BSA and 0.1 vol. % Tween-20 for another 30 min, and incubated overnight with the primary antibody diluted in the same buffer. The slides were then washed 3 times for 5 min in PBS supplemented with 0.1 vol. % Tween-20, and incubated for 1 h at room temperature with anti-mouse AlexaFluor 568 (1/1000, ThermoFischer). Slides were visualised using a Nikon 90i fluorescence microscope (Nikon AG). Collagen III immunostaining area was quantified using the ImageJ software and normalised to the total area of the vein segment.

PCNA (proliferating cell nuclear antigen), P4HA, cleaved caspase 3 and α -tubulin immunohistochemistry was performed on paraffin sections.³⁴ After rehydration and antigen retrieval (TRIS-EDTA buffer, pH 9, 17 min in a microwave at 500 W), immunostaining was performed on human vein or carotid sections using the EnVision[®]+ Dual Link System-HRP (DAB+) according to manufacturer's instructions. Slides were further counterstained with haematoxylin. PCNA and haematoxylin positive nuclei were manually counted by two independent observers blinded to the conditions.

α -tubulin immunofluorescent staining in human VSMCs was performed as previously described. Cells were fixed at -20 °C for 10 min in absolute methanol. Then, cells were blocked/permeabilised in PBS- triton 0.2%, BSA 3% for 45 min at room temperature. Cells were incubated overnight at 4 °C in the primary antibody diluted in PBS-0.1% tween, 3% BSA, washed 3 times in PBS and incubated for 1 h at room temperature with the secondary antibody diluted in PBS-0.1% tween, 3% BSA, washed again 3 times in PBS and mounted using Vectashield mounting medium for fluorescence with DAPI. The microtubule staining was quantified automatically using Fiji (ImageJ, 1.53c). Image processing was as follows: Plugin, Tubeness/Process, Make Binary/Analyze, Skeletonize 2D/3D. Data were summarised as filament number and total length, normalised to the number of cells per images. Data were generated from images from 3 independent experiments, 3 to 4 images per experiment per condition.

Reverse transcription and quantitative polymerase chain reaction (RT-qPCR)

VSMCs were homogenised in Tripure Isolation Reagent (Roche, Switzerland), and total RNA was extracted according to the manufacturer's instructions. After RNA reverse transcription (Prime Script RT reagent, Takara), cDNA levels were measured by qPCR Fast SYBR[™] Green Master Mix in a Quant Studio 5 Real-Time PCR System (Applied Biosystems, ThermoFischer Scientific), using the following primers: Homo sapiens thiosulfate sulfurtransferase (*TST*), forward:5'-

GCTGGTGGATTCAAGGTCTCA-3', Reverse: 5'-GACG GCACCACGGATATGG-3'; Homo sapiens sulfite oxidase (*SUOX*), forward: 5'-GGTGCAGTGTGGCC-TATCA-3', Reverse: 5'-ACCCAGATCCCAGTCTCAGG-3'.

Western blotting

Mice aortas or human vein segments were flash-frozen in liquid nitrogen, grinded to powder and resuspended in SDS lysis buffer (62.5 mM TRIS pH6.8, 5% SDS, 10 mM EDTA). Protein concentration was determined by DC protein assay. 10 to 20 μ g of protein were loaded per well. Primary cells were washed once with ice-cold PBS and directly lysed with Laemmli buffer as previously described.^{22,29} Lysates were resolved by SDS-PAGE and transferred to a PVDF membrane Immobilon-P. Immunoblot analyses were performed as previously described²⁹ using the antibodies described in supplementary Table S1. Membranes were revealed using Immobilon Western Chemiluminescent HRP Substrate in an Azure Biosystems 280, and analysed using Image J. Protein abundance was normalised to total protein using Pierce[™] Reversible Protein Stain Kit for PVDF Membranes.

In vitro tubulin polymerization assay

The assay was performed using the *In Vitro* Tubulin Polymerization Assay Kit ($\geq 99\%$ Pure Bovine Tubulin), according to the manufacturer's instruction.

Statistical analyses

All experiments adhered to the ARRIVE guidelines and followed strict randomisation. All experiments and data analysis were conducted in a blind manner using coded tags rather than actual group name. A power analysis was performed prior to the study to estimate sample-size. We hypothesized that STS or NaHS would reduce IH by 50%. Using an SD at +/- 20% for the surgery and considering a power at 0.9, we calculated that $n = 12$ animals/group was necessary to validate a significant effect of the STS or NaHS. Animals with pre-existing conditions (malocclusion, injury, abnormal weight) were not operated or excluded from the experiments upon discovery during dissection (kidney disease). A few animals died during surgery or did not recover from surgery and had to be euthanized before the end of the experiment. All experiments were analysed using GraphPad Prism 9. Normal distribution of the data was assessed using Shapiro-Wilk test and Kolmogorov-Smirnov test. All data had a normal distribution. One or 2-ways ANOVA were performed followed by multiple comparisons using post-hoc t-tests with the appropriate correction for multiple comparisons.

Ethics statement

Human great saphenous veins were obtained from donors who underwent lower limb bypass surgery.³⁵ Written, informed consent was obtained from all vein donors for human vein and VSMC primary cultures. The study protocols for organ collection and use were reviewed and approved by the Centre Hospitalier Universitaire Vaudois (CHUV) and the Cantonal Human Research Ethics Committee (<http://www.cer-vd.ch/>, no IRB number, Protocol Number 170/02), and are in accordance with the principles outlined in the Declaration of Helsinki of 1975, as revised in 1983 for the use of human tissues.

All animal experimentations were conformed to the *National Research Council: Guide for the Care and Use of Laboratory Animals*.³⁶ All animal care, surgery, and euthanasia procedures were approved by the CHUV and the Cantonal Veterinary Office (SCAV-EXPANIM, authorisation number 3114, 3258 and 3504).

Role of funding source

The funding sources had no involvement in study design, data collection, data analyses, interpretation, or writing of report.

Results

STS limits IH development in mice after carotid artery stenosis

We first assessed whether STS protects against IH as measured 28 days after mouse carotid artery stenosis (CAS).²⁸ STS treatment (4 g/L) decreased IH by about 50% in WT mice (Figure 1a), as expressed as the mean intima thickness, the ratio of intima over media thickness (I/M), or the area under the curve of intima thickness calculated over 1 mm. We further tested the safety of systemic STS treatment by looking at several blood

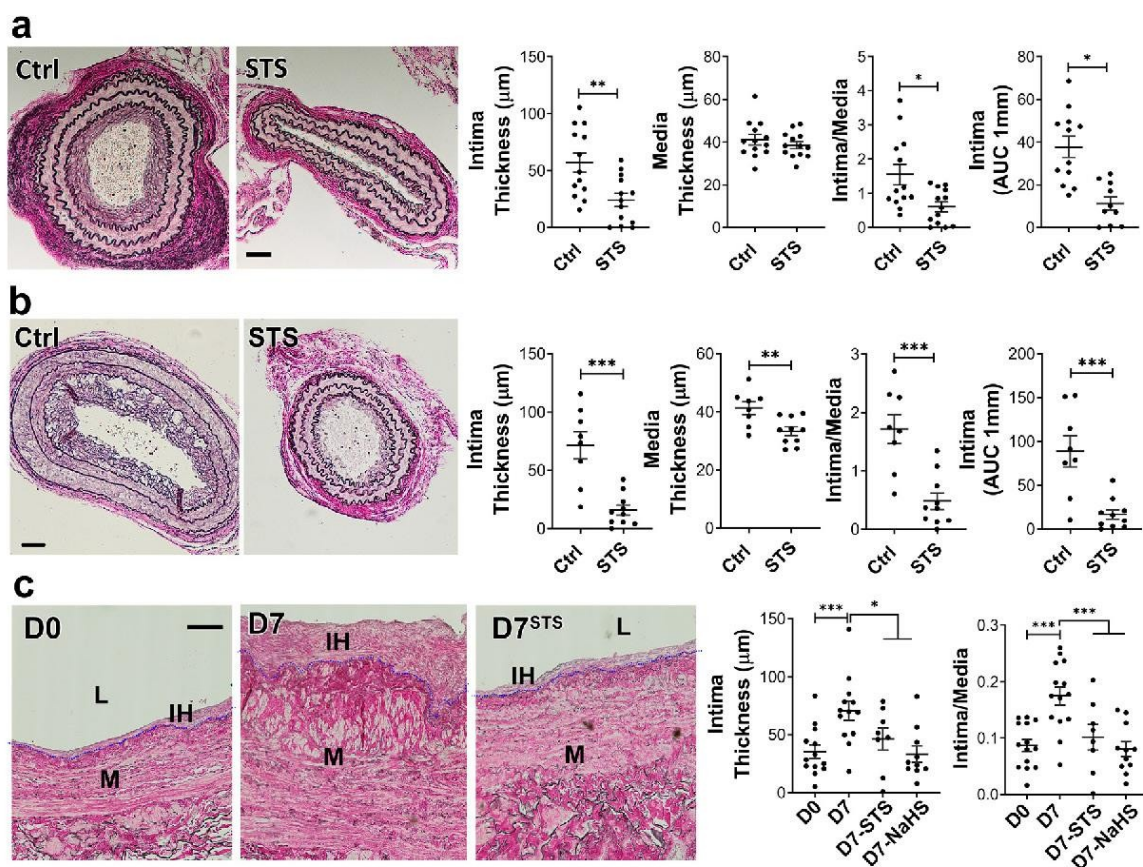


Figure 1. STS decrease IH formation after carotid artery stenosis in mice and in cultured human saphenous veins. a, b) WT (a) or LDLR^{-/-} mice (b) treated or not (ctrl) with 4 g/L STS were subjected to the carotid artery stenosis surgery. VGEL staining of left carotid cross sections and morphometric measurements of intima thickness, media thickness, intima over media ratio and intima thickness AUC. Scale bar 40 μm. Data are mean±SEM of 13 (c) and 8 (b) animals per group. **p* < .05, ***p* < .01, ****p* < .001 as determined by bilateral unpaired t-test. c) Intima thickness, media thickness and intima over media ratio of freshly isolated human vein segments (D0) or after 7 days (D7) in static culture with STS (15 mM) or NaHS (100 μM). Scale bar 60 μm. Data are mean ± SEM of 12 different veins/patients. **p* < .05, ***p* < .01, ****p* < .001, as determined by repeated measures one-way ANOVA with Dunnett's multiple comparisons.

parameters, revealing that STS had no effect on kidney (urea), liver (ASAT, ALAT) and heart (CK, CK-MB) function. STS also had no effect on blood pH and HCO_3^- levels and blood chemistry (Na, Ca, K) levels (supplemental Table S3). To model the hyperlipidemic state of patients with PAD, we also performed the CAS model on hypercholesterolemic LDLR^{-/-} mice fed for 3 weeks with a cholesterol-rich diet. As expected, the LDLR^{-/-} mice developed more IH than WT mice upon CAS, and STS treatment lowered IH by about 70% (Figure 1b). Interestingly, STS did not reduce media thickness in WT mice ($p = 0.39$) but significantly reduced media thickness in LDLR^{-/-} mice ($p = 0.0067$; Figure 1b). STS had no effect on media thickness in native carotids of WT and LDLR^{-/-} mice (Figure S1 in the online supplementary files). Of note, the sodium salt H_2S donor NaHS (0.5 g/L) also significantly decreased IH following carotid stenosis in WT mice (Figure S2).

STS limits IH development in a model of *ex vivo* human vein segment culture

Both STS (15 mM) and NaHS (100 μM) inhibited IH development in our validated model of static *ex vivo* human vein segment culture²² as measured by intima thickness and I/M ratio (Figure 1c). The polysulfide/ H_2S donors diallyl trisulfide (DATS), cysteine-activated H_2S donor 5a and GYY4137 also prevented the development of IH in human vein segments (Figure S3).

STS is a biologically active source of sulfur

Overall, STS and “classical” H_2S donors similarly inhibit IH. To measure whether STS releases detectable amounts of H_2S or polysulfides, we used the SF₇-AM³¹ and SSP4 probes,³⁷ respectively. We could not detect any increase in SF₇-AM or SSP4 fluorescence in presence of STS with or without VSMCs. Na_2S_3 was used as a positive control for the SSP4 probe and NaHS as a positive control for the SF₇-AM probe (Figure S4). The biological activity of H_2S is mediated by post-translational modifications of reactive cysteine residues by persulfidation, which influence protein activity.^{32,38} As a proxy for H_2S release, we assessed global protein persulfidation by DAZ-2-Cys5.5 labelling of persulfide residues in VSMCs treated for 4 h with NaHS or STS. Both STS and NaHS similarly increased persulfidation in VSMCs (Figure 2a). STS, but not NaHS, also increased the mRNA expression of *TST* and *SUOX* (Figure 2b, c), which are key enzymes of the H_2S biosynthetic pathway and sulfide oxidizing unit involved in thiosulfate metabolism.^{39,40} Using the SSP4 probe, we further observed higher polysulfides levels *in vivo* in the plasma of mice treated for 1 week with 4 g/L STS (Figure 2d). Similarly, we observed a non-significant increase in polysulfides in the liver of mice treated with STS ($p = 0.15$). As a positive control, mice treated with 0.5 g/L NaHS

had significantly higher polysulfides levels in the liver (Figure 2e). CSE is the main enzyme responsible for endogenous H_2S production in the vasculature and Cse^{-/-} mice have been shown to develop more IH.^{16,21,41} To study the impact of STS on restenosis independently of endogenous H_2S production, we generated a new Cse^{-/-} mouse line. As expected, these mice did not express Cse (Figure 2f), nor produced H_2S in the liver (Figure 2g), which is the main CSE-expressing tissue. These mice did not display any growth defect (Figure S5a), had normal systolic blood pressure (Figure S5b) and carotid and aortic arteries were similar to Cse^{+/-} littermates (Figure S5c). Consistent with a role as an H_2S donor, STS fully rescued Cse^{-/-} mice from increased IH in the model of carotid artery stenosis (Figure 2h).

STS limits IH-associated matrix deposition and apoptosis in human vein segments

We further assessed matrix deposition and apoptosis in human vein segments. Concomitant with IH formation, *ex vivo* vein culture (D7) resulted in *de novo* collagen deposition compared to D0, as assessed by polychrome Herovici staining (Figure 3a). Analysis of immature collagen III levels confirmed that vein culture (D7) resulted in collagen deposition compared to D0, as assessed by immunostaining (Figure S6a) and Western blotting (Figure S6b). Furthermore, vein culture (D7) resulted in overexpression of the prolyl 4-hydroxylase alpha polypeptide I (P4HA1), which catalyses folding of collagen polypeptide chains into stable triple-helical molecules.⁴² Overall, STS and NaHS treatments reduced collagen deposition as assessed by Herovici staining, Collagen III and P4HA1 analyses (Figures 3 and S6). TUNEL assay revealed that STS, and to a lesser degree NaHS, decreased apoptosis observed after 7 days in culture (D7) (Figure 3c). STS also attenuated pro-apoptotic protein Bax overexpression observed after 7 days in culture, while NaHS decreased Bax level ($p = .11$; Figure 3d). STS and NaHS also increased the protein level of anti-apoptotic protein Bcl-2 ($p = .06$ and $p = .04$; Figure 3d). Of note, cleaved caspase 3 immunostaining in CAS-operated carotids in WT mice revealed that there is no detectable apoptosis in the carotid wall in this model 28 days after surgery (Figure S7).

STS blocks VSMC proliferation and migration

IH is driven by VSMC reprogramming towards a proliferating, migrating and ECM-secreting phenotype.¹⁴ Both STS and NaHS significantly reduced the percentage of proliferating cells (defined as PCNA positive nuclei over total nuclei) *in vivo* in CAS-operated carotids in WT mice (Figure 4a) and *ex vivo* in human vein segments (Figure 4b).

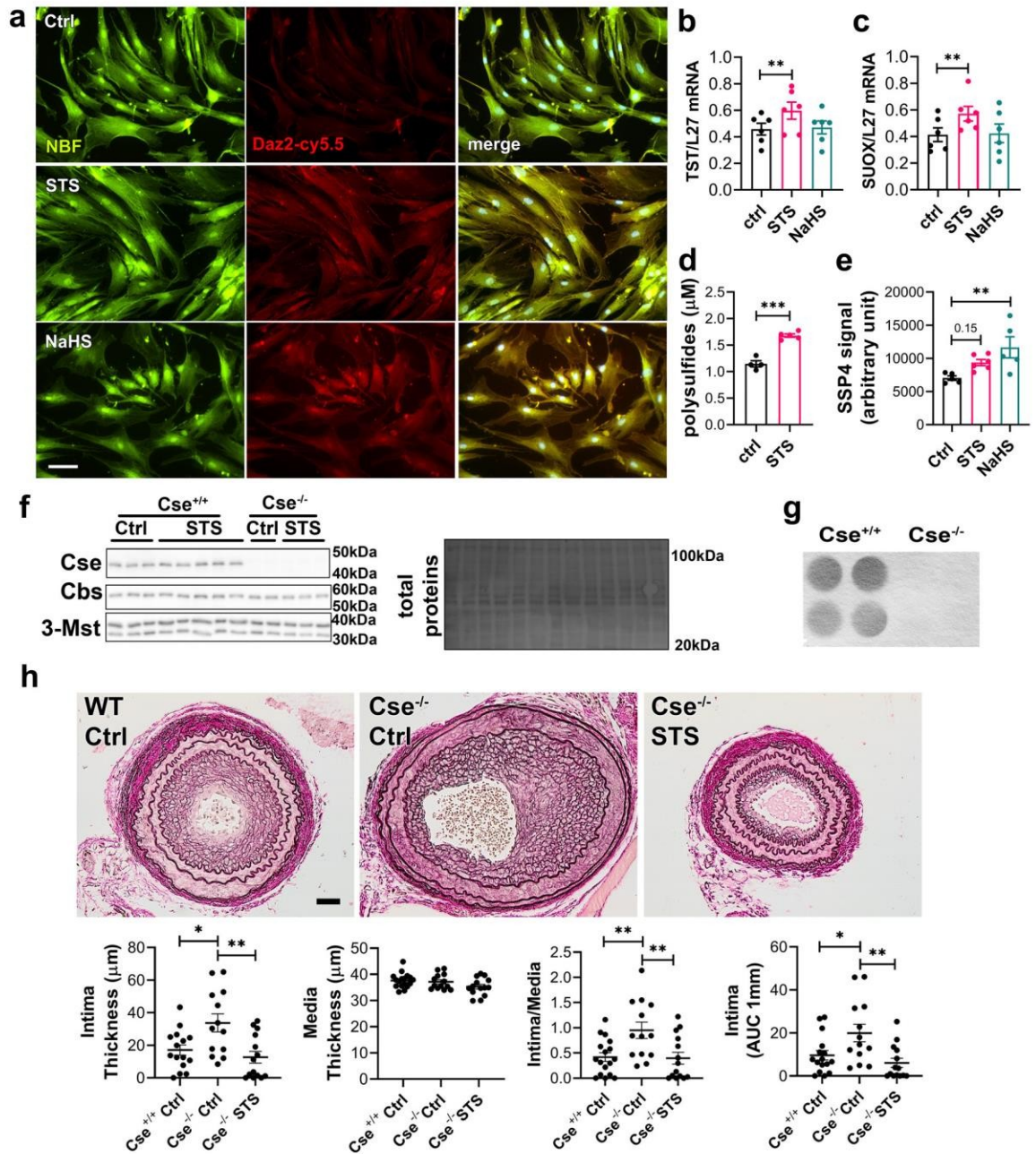


Figure 2. STS increases protein persulfidation. (a) *In situ* labelling of intracellular protein persulfidation assessed by Daz-2:Cy5.5 (red), normalized to NBF-adducts fluorescence (green), in VSMCs exposed for 4 h to NaHS (100 μM) or STS (15 mM). Representative images of 5 independent experiments. Scale bar 20 μM . (b, c) Human *TST* and *SUOX* mRNA levels in VSMCs treated or not (Ctrl) for 24 h with NaHS (100 μM) or STS (15 mM). (d) Plasma polysulfides levels, as measured by the SSP4 probe, in mice treated 7 days with STS 4 g/L. Data are scatter plots with mean \pm SEM of 4 animals per group. $***p < .001$ as determined by bilateral unpaired t-test. (e) Polysulfides levels, as measured by the SSP4 probe in liver extracts of mice treated 7 days with STS 4 g/L or NaHS 0.5 g/L. Data are scatter plots with mean \pm SEM of 5 animals per group. $**p < .01$ as determined by One-way ANOVA with post-hoc t-tests with Tukey's correction for multiple comparisons. (f) Western blot analysis of Cse, Cbs and 3-Mst in Cse^{-/-} and Cse^{+/+} mice, treated or not with STS 4 g/L for 4 weeks (3 to 5 animals per group). (g) Led acetate assay to measure Cse-mediated H₂S production in Cse^{-/-} and Cse^{+/+} mice. Data are representative of 4 animals per group. (h) Intima thickness, media thickness, intima over media ratio and intima thickness AUC of CAS operated mice measured 28 days after surgery in Cse^{+/+} versus Cse^{-/-} mice treated or not (Cse^{-/-} Ctrl) with 4 g/L STS (Cse^{-/-} STS). Scale bar 50 μm . Data are scatter plots with mean \pm SEM of 8 to 10 animals per group. $*p < .05$, $**p < .01$, as determined by one-way ANOVA with post-hoc t-tests with Tukey's correction for multiple comparisons.

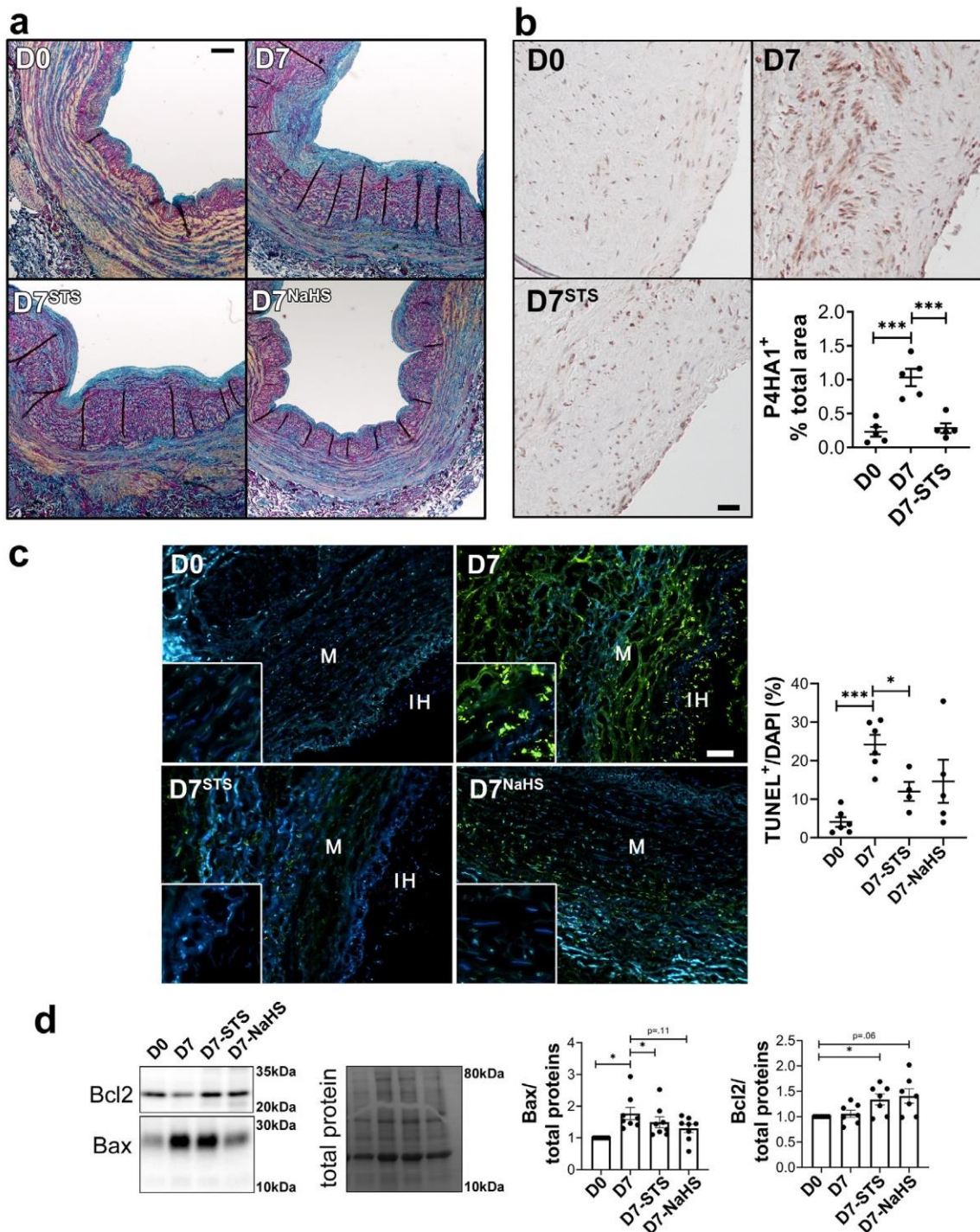


Figure 3. STS decreases apoptosis and matrix deposition in human vein segments. Human vein segment at day 0 (D0) or after 7 days of static culture with or without (D7) 15 mM STS or 100 μ M NaHS. (a) Representative Herovici staining of 5 different human vein segments. Mature collagen I is stained pink; new collagen III is stained blue; cytoplasm is counterstained yellow; nuclei are stained blue to black. Scale bar=80 μ m (b) *Left panels*: Representative P4HA1 staining. Scale bar=50 μ m. *Right panel*: Quantitative assessment of P4HA1 staining. Data are scatter plots of 5 different veins with mean \pm SEM. *** $p < .01$ as determined by paired repeated measures one-way ANOVA with Dunnett's multiple comparisons. (c) *Left panels*: Representative TUNEL staining in human vein segments. *Right panel*: Apoptosis is expressed as TUNEL positive (green) over DAPI positive nuclei. Scale bar= 50 μ m. Data are

In vitro, STS dose-dependently decreased primary human VSMC proliferation as assessed by BrdU incorporation assay (Figure 5a). Of Note, NaHS as well as DATS, H₂S donor 5A and GYY4137, also decreased VSMC proliferation (Figure S8). STS and NaHS also decreased VSMC migration in a wound healing assay, in absence (Figure 5b), or in presence of the mitosis inhibitor mitomycin C (Figure S9). Further evaluation of cell morphology during the wound healing revealed that STS and NaHS-treated cells lost the typical elongated shape of VSMCs, as measured through the area, Feret diameter and circularity of the cells (Figure 5c). Of note, 15 mM STS did not induce VSMC apoptosis after 48 h, while 40 mM STS increased apoptosis levels to 5%. 80 mM STS for 48 h raised apoptosis levels to 10% (Figure S10).

STS does not significantly impact VSMC metabolism

We previously showed that H₂S inhibits the mitochondrial metabolism while increasing glycolysis in endothelial cells.⁴³ To assess the impact of STS on VSMC metabolism, Seahorse experiments were performed on VSMCs treated for 4 or 24 h with STS. Surprisingly, STS did not inhibit mitochondrial respiration in a mitochondrial stress test after 4 h of pre-treatment, while NaHS had a slight effect on basal respiration and ATP production (Figure S11a). After 24 h of treatment, both STS and NaHS increased respiration mildly (Figure S11b). We also performed a glycolysis stress test to evaluate the metabolic flexibility of VSMCs (Figure S11c). After 24 h of pre-treatment, neither STS nor NaHS impacted glycolysis. Of note, VSMCs had a null glycolytic reserve, i.e. glycolysis did not increase upon inhibition of mitochondrial respiration with oligomycin. Further analysis of oxphos proteins by western blot showed no effect of a 24 h STS treatment on key mitochondrial enzymes (Figure S12). Overall, STS effect on mitochondrial respiration and glycolysis cannot explain the reduced proliferation and migration observed.

STS interferes with microtubules organization

Given the impact of STS on cell morphology, we examined the effect of STS on the cytoskeleton. α -tubulin levels were increased in the carotid wall of CAS-operated mice, which were reduced by STS, as demonstrated by immunohistochemistry (Figure 6a). α -tubulin levels were also decreased in the native aorta of mice treated with STS for 7 days (Figure 6b). On the other hand, STS did not impact tubulin staining in native carotids

of WT and LDLR^{-/-} mice (Figure S13a). STS treatment also had no effect on tubulin levels in the liver and kidney (Figure S13b). In *ex vivo* vein segments, total α -tubulin levels were decreased after 7 days of STS or NaHS treatment (Figure 6c, d). Looking further at α -tubulin by immunofluorescent staining showed a loss in microtubule in VSMCs treated with STS or NaHS for 8 h (Figure 6e, f). To study the effect of H₂S on microtubule formation, an *in vitro* tubulin polymerization assay was performed in presence of 15 mM STS, 100 μ M NaHS or 10 μ M Nocodazole, an inhibitor of microtubule assembly. As expected, Nocodazole slowed down microtubule assembly as compared to the control. Surprisingly, both NaHS and STS fully blocked microtubule assembly in this assay (Figure 6g). Further studies of the cell cycle in VSMCs revealed that 48 h of treatment with STS or Nocodazole resulted in accumulation of cells in G₂/M phase (Figure 6h).

Discussion

Despite decades of research and the advent of drug-eluting stents (DES) and drug-coated balloons (DCB), intimal hyperplasia (IH) remains one of the major limitations in the long-term success of revascularization. All current strategies based on the use of DES and DCB limit VSMC proliferation and IH, but they also affect re-endothelisation, limiting their long-term efficacy and prolonging the need for anti-thrombotic. Moreover, recent controversies regarding the long-term safety of paclitaxel-releasing devices^{6–13} advocate for the development of new therapies to limit IH. These new strategies should focus on inhibiting VSMC proliferation while promoting endothelium recovery. In that regard, the gasotransmitter H₂S possesses interesting properties. Here, we demonstrate that exogenous sulfur supplementation in the form of STS limits IH development *in vivo* following mouse carotid artery stenosis. Furthermore, STS reduced apoptosis, vessel remodelling and collagen deposition, along with IH development in our *ex vivo* model of IH in human vein segments. We propose that STS limits IH by interfering with the microtubule dynamics, thus VSMC proliferation and migration.

An ever increasing number of studies document the protective effects of H₂S against cardiovascular diseases,⁴⁴ including studies showing that H₂S reduces IH in preclinical models.^{19–21,45} The administration of H₂S in those studies relies on soluble sulfide salts such as NaHS with narrow therapeutic range due to fast and uncontrolled release. Thiosulfate is an intermediate of

scatter plots of 5 to 6 different veins with mean \pm SEM. * p < .05, *** p < .001 as determined by mixed model analysis with Dunnett's multiple comparisons. (d) Representative western blot of Bax and Bcl2 over total protein and quantitative assessment of 7 different human veins. Data are scatter plots with mean \pm SEM. * p < .05 as determined by repeated measures one-way ANOVA with Dunnett's multiple comparisons (For interpretation of the references to color in this figure legend, the reader is referred to the web version of this article.).

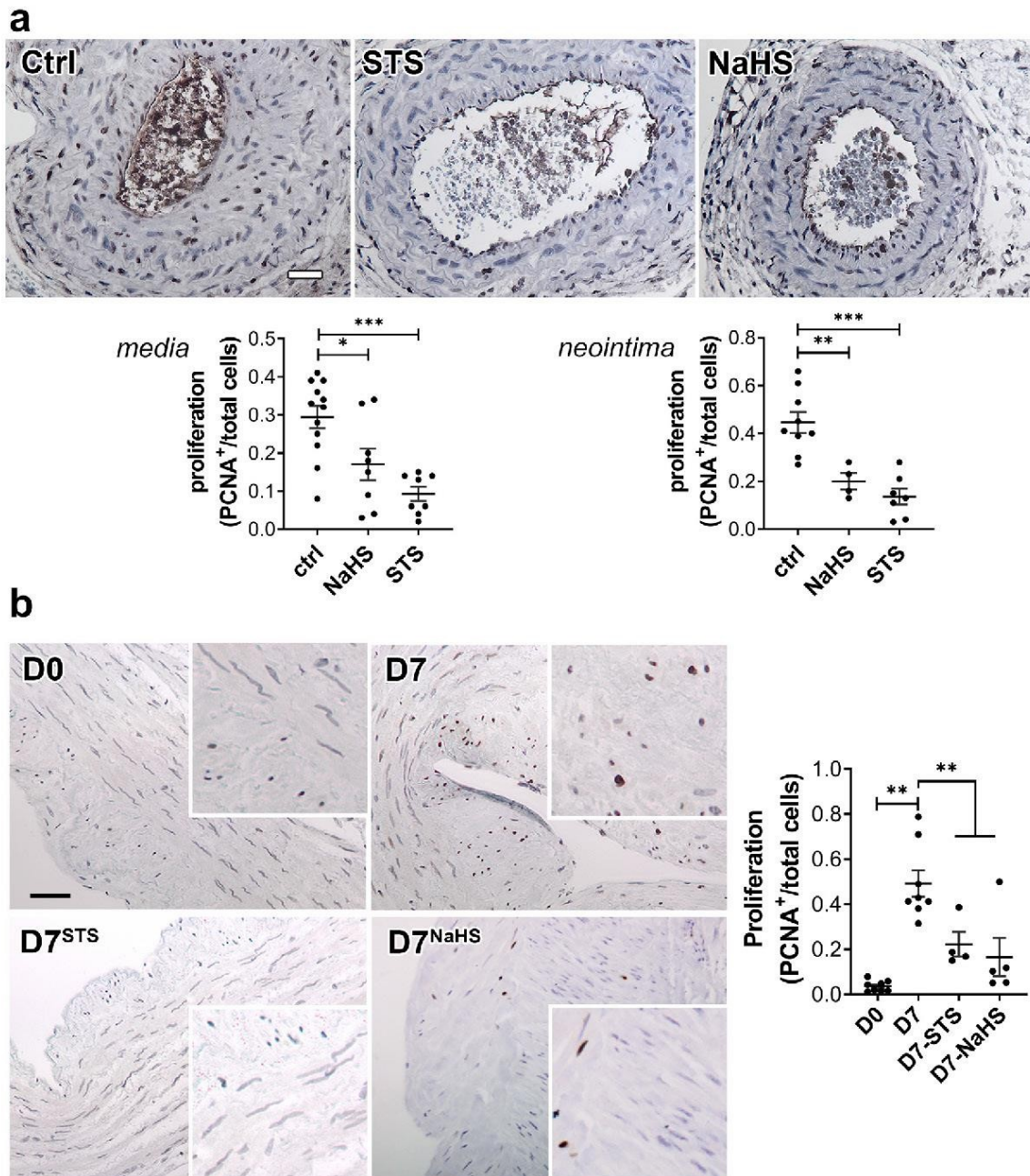


Figure 4. STS inhibits cell proliferation *in vivo* in mouse carotids and *ex-vivo* in human vein segments. PCNA immunostaining on CAS operated carotids in WT mice (a) treated or not (Ctrl) with STS 4 g/L or NaHS 0.5g/L for 28 days, and human vein segments (b) incubated or not (Ctrl) with 15 mM STS or 100 μ M NaHS for 7 days. Proliferation is expressed as the ratio of PCNA positive (brown) nuclei over total number of nuclei. Data are scatter plots with mean \pm SEM. (a) Scale bar 20 μ m. * p < .05, ** p < .01, *** p < .001 as determined from 8 to 12 animals per group by one-way ANOVA with Dunnett's multiple comparisons. (b) Scale bar 50 μ m ** p < .01, as determined from 5 to 7 different veins by mixed model analysis and Dunnett's multiple comparisons.

sulfur metabolism shown to release H_2S *in vivo* through non-enzymatic and enzymatic mechanisms.^{25,26,46,47} Importantly, STS is clinically approved and safe in gram quantities in humans. Although STS yields no detectable H_2S or polysulfide *in vitro*, we observed

increased circulating and liver levels of polysulfides in mice, as well as increased protein persulfidation in VSMCs. We further showed that STS treatment rescues Cse^{-/-} with impaired endogenous H_2S production from increased IH. This is in line with a previous study

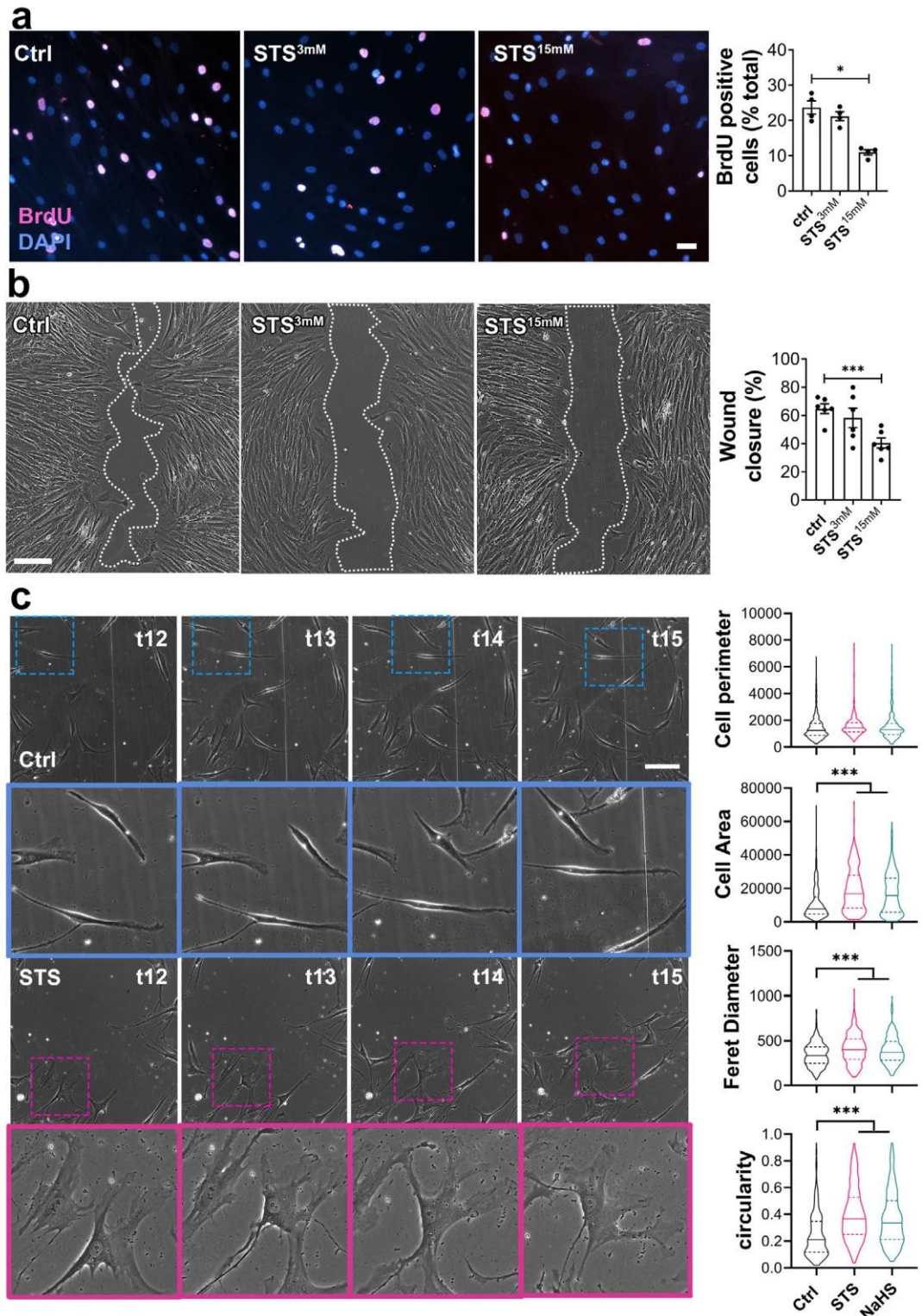


Figure 5. STS inhibits VSMC proliferation and migration *in vitro*. (a) VSMC proliferation (BrdU incorporation) in cells treated or not (Ctrl) for 24 h with 3 or 15 mM STS. Data are % of BrdU positive nuclei (pink) over DAPI positive nuclei (blue). Scale bar: 25 μ m. Data shown as mean \pm SEM of 6 different experiments. * $p < .05$ as determined by repeated measures one-way ANOVA with Dunnett's multiple comparisons tests. (b) VSMC migration in cells treated or not (Ctrl) with 3 or 15 mM STS, as assessed by wound healing

showing that NaHS rescues increased IH in a model of carotid ligation in another *Cse*^{-/-} mouse line.²¹ Overall, STS has protective effects against IH similar to the H₂S salt NaHS and several other “classical” H₂S donors, but holds much higher translational potential.

Mechanistically, we first observed that STS reduces cell apoptosis and matrix deposition in our *ex vivo* model of human vein segments. This anti-apoptotic effect of STS and NaHS is in line with known anti-apoptotic effects of H₂S.⁴⁴ STS also reduces IH *in vivo* following carotid artery stenosis. In this model, matrix deposition plays little role in the formation of IH, which relies mostly on VSMC proliferation.¹⁴ Therefore, although ECM and especially collagen deposition are major features of IH in humans,^{48,49} reduced apoptosis and matrix deposition is not sufficient to fully explain the protection afforded by STS in carotids *in vivo*.

STS, similarly to the H₂S donor NaHS, inhibits VSMC proliferation in the context of IH *in vivo* in mouse stenotic carotids, *ex vivo* in human vein segments, and *in vitro* in primary human VSMCs. These findings are in line with previous studies demonstrating that “classical” H₂S donors decrease VSMCs proliferation in pre-clinical models.^{20,22,50} In mouse VSMC, exogenous H₂S has been proposed to promote cell cycle arrest,¹⁶ and regulate the Mitogen-activated protein kinases (MAPK) pathway¹⁹ and Insulin-like Growth Factor (IGF-1) response.⁵¹ Regarding mouse VSMC migration, H₂S may limit $\alpha_5\beta_1$ -integrin and matrix metalloproteinase-2 (MMP2) expression, preventing migration and ECMs degradation.^{16,21} In this study, we further document that STS and NaHS disrupt the formation of microtubules in human VSMCs *in vitro*. Our findings are in line with previous studies showing that Diallyl trisulfide, a polysulfide donor, inhibits microtubule polymerization to block human colon cancer cell proliferation.⁵² NaHS also depolymerizes microtubules within *Aspergillus nidulans* biofilms.⁵³ The α/β tubulin dimer has 20 highly conserved cysteine residues, which have been shown to regulate microtubule formation and dynamics.⁵⁴ In particular, thiol–disulfide exchanges in intra-chain disulfide bonds have been proposed to play a key role in microtubule assembly.⁵⁵ Several high throughput studies of post-translational modification of protein cysteinyl thiols (-SH) to persulfides (-SSH) demonstrated that cysteine residues in α - and β -tubulin are persulfidated in response to H₂S donors in various cell types.^{56,57} Given the prominent role of cytoskeleton dynamics and remodelling during

mitosis and cell migration, we propose that STS/H₂S-driven microtubule depolymerisation, secondary to cysteine persulfidation, contributes to cell cycle arrest and reduces migration in VSMC.

Our findings suggest that STS holds strong translational potential to limit restenosis following vascular surgeries. The dosage of STS used in this study is comparable to previous experimental studies using oral administration at 0.5 to 2 g/Kg/day,^{25,26,46,47} and we did not observe any adverse effect of the 30-days treatment with STS on blood chemistry and plasmatic markers of kidney, liver and heart function. In humans, 12.5 and 25 g of STS have been infused without adverse effects⁵⁸ and short-term treatment with i.v. STS is safely used in patients for the treatment of calciphylaxis.²⁴ Of note, the pathophysiology of calciphylaxis, also known as calcific uremic arteriopathy (CUA), is caused by oxidative stress and inflammation, which promote endothelial dysfunction, leading to medial remodelling, inflammation, fibrosis and VSMC apoptosis and differentiation into bone forming osteoblast-like cells. Although the main effect of STS on CUA is via formation of highly soluble calcium thiosulfate complexes, our data supports the use of STS in the treatment of calciphylaxis. Plus, STS infusions have been shown to increase distal cutaneous blood flow, which could be beneficial in the context of vascular occlusive disease.

Here, we propose that STS treatment results in persulfidation of cysteine residues in the tubulin proteins, which lead to microtubule depolymerisation. However, further studies are required to test this hypothesis and demonstrate the STS-induced persulfidation of tubulin cysteine residues. In addition, although we show *in vitro* that H₂S directly affect microtubule formation in a cell-free environment, other proteins involved in the microtubules dynamics *in vivo* may also be modified by H₂S, and contribute to the effect of STS on microtubule polymerisation and cell proliferation. This effect on microtubules could lead to side effects similar to microtubule targeting agents such as nocodazole or colchicine and paclitaxel, which are widely used in the treatment of various cancers. However, unlike chemotherapeutic agents, the effect of STS/H₂S should be reversible, which should reduce side effects. That said, additional experiments in larger animals are required to better assess haematological, gastrointestinal and neurological toxicities of long-term treatment with STS. In this study, STS was administered in the water bottle. However, given the low and variable bioavailability of oral STS,

assay, expressed as the percentage of wound closure after 10 h. Scale bar: 100 μ m. Data are scatter plots with mean \pm SEM of 5 independent experiments in duplicates. ****p* < .001 as determined by repeated measures one-way ANOVA with Dunnett's multiple comparisons. (c) Bright field images of VSMC morphology in cells exposed or not (Ctrl) to 15 mM STS or 100 μ m NaHS, as measured as cell perimeter, cell area, Feret diameter and circularity index assessed during wound healing assay. Data are violin plots with median and quartiles (dotted lines) of 5 independent experiments. ****p* < .001 as determined by one-way ANOVA with Dunnett's post-hoc test. Scale bar: 80 μ m. Pink and blue insets are 3-fold magnifications of outlined areas.

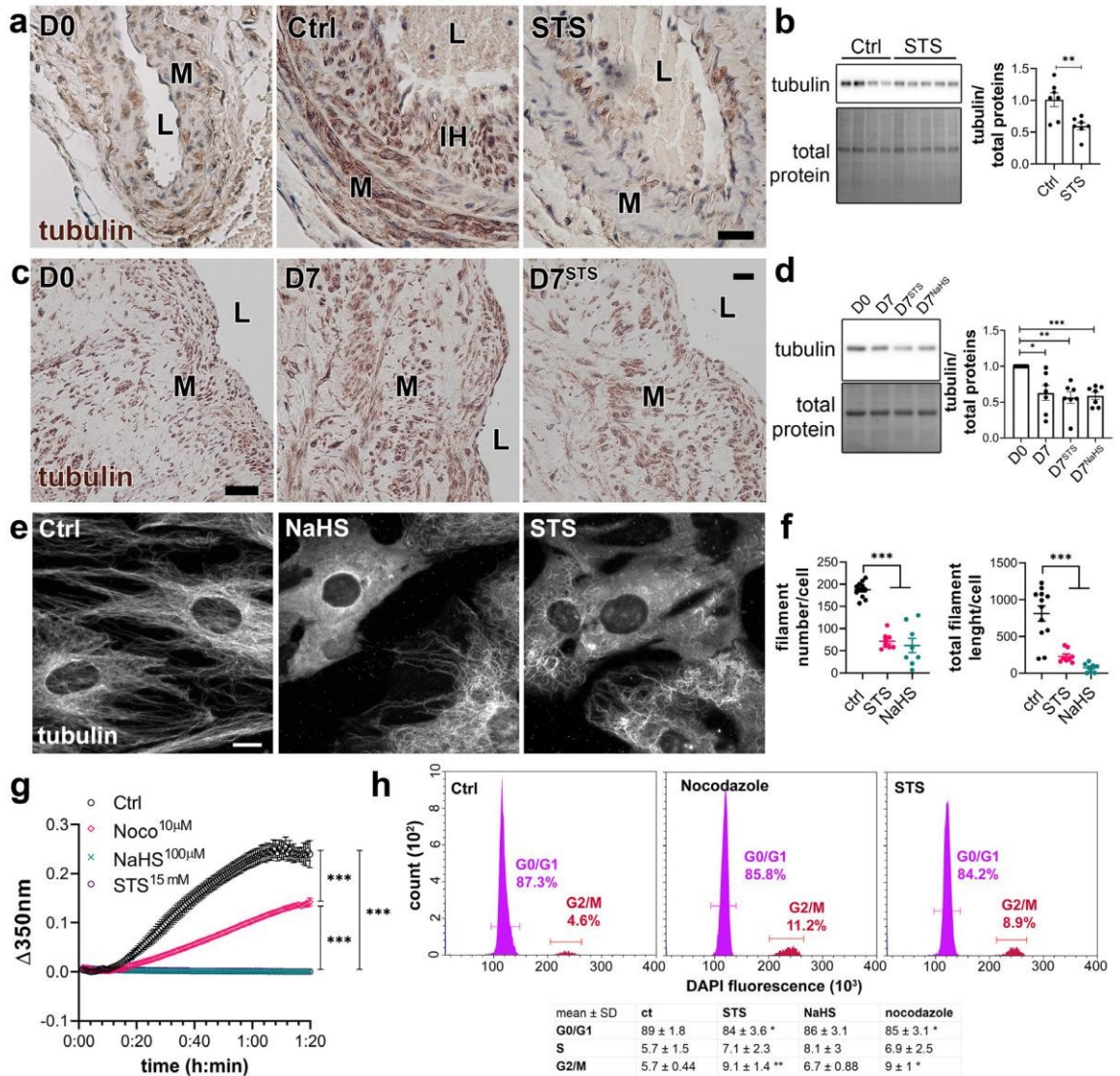


Figure 6. STS inhibits microtubule polymerization in VSMC. (a) α -tubulin immunolabelling in carotids of native (D0) or CAS-operated mice treated or not (Ctrl) with STS 4 g/L. L=Lumen; M= Media; IH= Intimal Hyperplasia. Images are representative of 5 to 8 mice per group. Scale bar 20 μ m (b) WB analysis of α -tubulin over total protein in aortas of mice treated or not (Ctrl) with STS 4 g/L for 7 days. Data are scatter plots of 7 mice per groups with mean \pm SEM with $**p < .01$, as determined by one-way ANOVA with Tukey's multiple comparisons tests. (c) α -tubulin immunolabelling in human vein segments kept or not (D0) in culture in presence or not (Ctrl) of 15 mM STS for 7 days. Scale bar 40 μ m. L=Lumen; M=Media. Images are representative of 5 different veins. (d) WB analysis of tubulin over total protein in human vein segments kept or not (D0) in culture in presence or not (Ctrl) of 15 mM STS or 100 μ M NaHS for 7 days. $*p < .05$, $**p < .01$, $***p < .001$, as determined by repeated measures one-way ANOVA from 7 different veins with Dunnett's multiple comparisons tests. (e) α -tubulin immunofluorescent staining in VSMC exposed or not to 15 mM STS or 100 μ M NaHS for 8 h. Images are representative of 5 independent experiments. Bar scale 10 μ m. (f) Quantitative assessment of microtubule filaments immunostaining per cell. Data are representative of 3 independent experiments, 3 to 4 images per experiment per condition. $***p < .001$ as determined by one-way ANOVA with Tukey's multiple comparisons tests. (g) *In vitro* tubulin polymerization assay in presence or not (Ctrl) of 15 mM STS, 100 μ M NaHS or 10 μ M Nocodazole. Data are mean \pm SEM of 3 independent experiments. (h) Flow cytometry analysis of cell cycle (DNA content) using DAPI-stained VSMC treated or not (Ctrl) for 48 h with 15 mM STS or 10 nM Nocodazole. Upper panel: representative histograms; lower panel: table with mean \pm SD of 5 independent experiments. $*p < .05$, $**p < .01$ as determined by one-way ANOVA with Dunnett's multiple comparisons tests.

only intravenous STS should be prescribed.⁵⁸ Moving forward, further studies in large animals are required to validate the therapeutical potential and setup the i.v. dose of STS required in a model of restenosis. Case reports and case series suggest that i.v. STS administration is safe, even for relatively long periods of time.^{59,60} However, randomised controlled trials testing long-term administration of STS are lacking,⁶⁰ and the long-term safety and effects of STS administration should be further explored.

In summary, under the conditions of these experiments, STS, a FDA-approved compound, limits IH development *in vivo* in a model of arterial restenosis and *ex vivo* model in human veins. STS most likely acts by increasing H₂S bioavailability, which inhibits cell apoptosis and matrix deposition, as well as VSMC proliferation and migration via microtubules depolymerisation.

Contributors

FA, AL and SD designed the study. FA, DM, MMA, ML and SU performed the experiments. FA, DM, MMA, ML and SD analysed the data. FA, DM, MMA, AL and SD wrote the manuscript. FA, AL, SD and DM revised the manuscript.

Data sharing statement

The data that support the findings of this study are available from the corresponding author, Florent Allagnat, upon request.

Declaration of interests

The authors declare no competing interests.

Acknowledgments

We thank the mouse pathology facility for their services in histology (<https://www.unil.ch/mpf>).

Supplementary materials

Supplementary material associated with this article can be found in the online version at doi:10.1016/j.ebiom.2022.103954.

References

- Eraso LH, Fukaya E, Mohler ER, Xie D, Sha D, Berger JS. Peripheral arterial disease, prevalence and cumulative risk factor profile analysis. *Eur J Prev Cardiol.* 2014;21(6):704–711.
- Fowkes FG, Rudan D, Rudan I, et al. Comparison of global estimates of prevalence and risk factors for peripheral artery disease in 2000 and 2010: a systematic review and analysis. *Lancet.* 2013;382(9901):1329–1340.
- Song P, Rudan D, Zhu Y, et al. Global, regional, and national prevalence and risk factors for peripheral artery disease in 2015: an updated systematic review and analysis. *Lancet Glob Health.* 2019;7(8):e1020–e1030.
- Bjorck M, Earnshaw JJ, Acosta S, et al. Editor's choice - European Society for Vascular Surgery (ESVS) 2020 clinical practice guidelines on the management of acute limb ischaemia. *Eur J Vasc Endovasc Surg.* 2020;59(2):173–218.
- Jukema JW, Verschuren JJ, Ahmed TA, Quax PH. Restenosis after PCI. Part 1: pathophysiology and risk factors. *Nat Rev Cardiol.* 2011;9(1):53–62.
- Katsanos K, Spiliopoulos S, Kitrou P, Krokidis M, Karnabatidis D. Risk of death following application of paclitaxel-coated balloons and stents in the femoropopliteal artery of the leg: a systematic review and meta-analysis of randomized controlled trials. *J Am Heart Assoc.* 2018;7(24):e01245.
- Rocha-Singh KJ, Duval S, Jaff MR, et al. Mortality and paclitaxel-coated devices: an individual patient data meta-analysis. *Circulation.* 2020;141(23):1859–1869.
- Royce S, Chakraborty A, Zhao Y. US Food and Drug Administration perspective on "mortality and paclitaxel-coated devices: an individual patient data meta-analysis". *Circulation.* 2020;141(23):1870–1871.
- Dinh K, Gomes ML, Thomas SD, et al. Mortality after paclitaxel-coated device use in patients with chronic limb-threatening ischemia: a systematic review and meta-analysis of randomized controlled trials. *J Endovasc Ther.* 2020;27(2):175–185.
- Ipema J, Huizing E, Schreve MA, de Vries JPM, Unlu C. Editor's choice - drug coated balloon angioplasty vs. standard percutaneous transluminal angioplasty in below the knee peripheral arterial disease: a systematic review and meta-analysis. *Eur J Vasc Endovasc Surg.* 2020;59(2):265–275.
- Katsanos K, Spiliopoulos S, Kitrou P, Krokidis M, Paraskevopoulos I, Karnabatidis D. Risk of death and amputation with use of paclitaxel-coated balloons in the infrapopliteal arteries for treatment of critical limb ischemia: a systematic review and meta-analysis of randomized controlled trials. *J Vasc Interv Radiol.* 2020;31(2):202–212.
- Nordanstig J, James S, Andersson M, et al. Mortality with paclitaxel-coated devices in peripheral artery disease. *N Engl J Med.* 2020;383(26):2538–2546.
- Secemsky EA, Kundi H, Weinberg I, et al. Association of survival with femoropopliteal artery revascularization with drug-coated devices. *JAMA Cardiol.* 2019;4(4):332–340.
- Davies MG, Hagen PO. Reprinted article "pathophysiology of vein graft failure: a review". *Eur J Vasc Endovasc Surg.* 2011;42 Suppl 1: S19–S29.
- Zhang L, Wang Y, Li Y, et al. Hydrogen sulfide (H₂S)-releasing compounds: therapeutic potential in cardiovascular diseases. *Front Pharmacol.* 2018;9:1066.
- Yang G, Wu L, Bryan S, Khaper N, Mani S, Wang R. Cystathionine gamma-lyase deficiency and overproliferation of smooth muscle cells. *Cardiovasc Res.* 2010;86(3):487–495.
- Islam KN, Polhemus DJ, Donnarumma E, Brewster LP, Lefer DJ. Hydrogen sulfide levels and nuclear factor-erythroid 2-related factor 2 (NRF2) activity are attenuated in the setting of critical limb ischemia (CLI). *J Am Heart Assoc.* 2015;4(5).
- Longchamp A, MacArthur MR, Trocha K, et al. Plasma hydrogen sulfide production capacity is positively associated with post-operative survival in patients undergoing surgical. *Revascularization.* 2021. 2021.02.16.21251804.
- Meng QH, Yang G, Yang W, Jiang B, Wu L, Wang R. Protective effect of hydrogen sulfide on balloon injury-induced neointima hyperplasia in rat carotid arteries. *Am J Pathol.* 2007;170(4):1406–1414.
- Ma B, Liang G, Zhang F, Chen Y, Zhang H. Effect of hydrogen sulfide on restenosis of peripheral arteries after angioplasty. *Mol Med Rep.* 2012;5(6):1497–1502.
- Yang G, Li H, Tang G, et al. Increased neointimal formation in cystathionine gamma-lyase deficient mice: role of hydrogen sulfide in alpha5beta1-integrin and matrix metalloproteinase-2 expression in smooth muscle cells. *J Mol Cell Cardiol.* 2012;52(3):677–688.
- Longchamp A, Kaur K, Macabrey D, et al. Hydrogen sulfide-releasing peptide hydrogel limits the development of intimal hyperplasia in human vein segments. *Acta Biomater.* 2019.
- Bebarta VS, Brittain M, Chan A, et al. Sodium nitrite and sodium thiosulfate are effective against acute cyanide poisoning when administered by intramuscular injection. *Ann Emerg Med.* 2017;69(6):718–725. e4.
- Nigwekar SU, Thadhani R, Brandenburg VM. Calciphylaxis. *N Engl J Med.* 2018;378(18):1704–1714.
- Olson KR, Deleon ER, Gao Y, et al. Thiosulfate: a readily accessible source of hydrogen sulfide in oxygen sensing. *Am J Physiol Regul Integr Comp Physiol.* 2013;305(6):R592–R603.

- 26 Snijder PM, Frenay AR, de Boer RA, et al. Exogenous administration of thiosulfate, a donor of hydrogen sulfide, attenuates angiotensin II-induced hypertensive heart disease in rats. *Br J Pharmacol*. 2015;172(6):1494–1504.
- 27 Ishibashi S, Brown MS, Goldstein JL, Gerard RD, Hammer RE, Herz J. Hypercholesterolemia in low density lipoprotein receptor knockout mice and its reversal by adenovirus-mediated gene delivery. *J Clin Invest*. 1993;92(2):883–893.
- 28 Tao M, Mauro CR, Yu P, et al. A simplified murine intimal hyperplasia model founded on a focal carotid stenosis. *Am J Pathol*. 2013;182(1):277–287.
- 29 Allagnat F, Dubuis C, Lambelet M, et al. Connexin37 reduces smooth muscle cell proliferation and intimal hyperplasia in a mouse model of carotid artery ligation. *Cardiovasc Res*. 2017;113(7):805–816.
- 30 Longchamp A, Alonso F, Dubuis C, et al. The use of external mesh reinforcement to reduce intimal hyperplasia and preserve the structure of human saphenous veins. *Biomaterials*. 2014;35(9):2588–2599.
- 31 Lin VS, Lippert AR, Chang CJ. Cell-trappable fluorescent probes for endogenous hydrogen sulfide signaling and imaging H₂O₂-dependent H₂S production. *Proc Natl Acad Sci U S A*. 2013;110(18):7131–7135.
- 32 Zivanovic J, Kouroussis E, Kohl JB, et al. Selective persulfide detection reveals evolutionarily conserved antiaging effects of S-sulphydration. *Cell Metab*. 2019;30(6):1152–1170. e13.
- 33 Teuscher AC, Statzer C, Pantasis S, Bordoli MR, Ewald CY. Assessing collagen deposition during aging in mammalian tissue and in *Caenorhabditis elegans*. *Methods Mol Biol*. 2019;1944:169–188.
- 34 Allagnat F, Haefliger JA, Lambelet M, et al. Nitric oxide deficit drives intimal hyperplasia in mouse models of hypertension. *Eur J Vasc Endovasc Surg*. 2016;51(5):733–742.
- 35 Dubuis C, May L, Alonso F, et al. Atorvastatin-loaded hydrogel affects the smooth muscle cells of human veins. *J Pharmacol Exp Ther*. 2013;347(3):574–581.
- 36 National Research Council (U.S.). Committee for the Update of the Guide for the Care and Use of Laboratory Animals, Institute for Laboratory Animal Research (U.S.), National Academies Press (U.S.). *Guide for the Care and Use of Laboratory Animals*. 8th ed. Washington, D.C.: National Academies Press; 2011. xxv, 220 p. p.
- 37 Bibli SI, Luck B, Zukunft S, et al. A selective and sensitive method for quantification of endogenous polysulfide production in biological samples. *Redox Biol*. 2018;18:295–304.
- 38 Li Z, Polhemus DJ, Lefer DJ. Evolution of hydrogen sulfide therapeutics to treat cardiovascular disease. *Circ Res*. 2018;123(5):590–600.
- 39 Paul BD, Snyder SH, Kashfi K. Effects of hydrogen sulfide on mitochondrial function and cellular bioenergetics. *Redox Biol*. 2021;38:101772.
- 40 Olson KR. H₂S and polysulfide metabolism: conventional and unconventional pathways. *Biochem Pharmacol*. 2018;149:77–90.
- 41 Yuan S, Yurdagul A, Peretik JM, et al. Cystathionine gamma-lyase modulates flow-dependent vascular remodeling. *Arterioscler Thromb Vasc Biol*. 2018;38(9):2126–2136.
- 42 Myllyharju J. Prolyl 4-hydroxylases, the key enzymes of collagen biosynthesis. *Matrix Biol*. 2003;22(1):15–24.
- 43 Longchamp A, Mirabella T, Arduini A, et al. Amino acid restriction triggers angiogenesis via GCN2/ATF4 regulation of VEGF and H₂S production. *Cell*. 2018;173(1):117–129. e14.
- 44 Szabo C. A timeline of hydrogen sulfide (H₂S) research: from environmental toxin to biological mediator. *Biochem Pharmacol*. 2018;149:5–19.
- 45 Kip P, Tao M, Trocha KM, et al. Periprocedural hydrogen sulfide therapy improves vascular remodeling and attenuates vein graft disease. *J Am Heart Assoc*. 2020;9(22):e016391.
- 46 Marutani E, Yamada M, Ida T, et al. Thiosulfate mediates cytoprotective effects of hydrogen sulfide against neuronal ischemia. *J Am Heart Assoc*. 2015;4(11).
- 47 Lee M, McGeer EG, McGeer PL. Sodium thiosulfate attenuates glial-mediated neuroinflammation in degenerative neurological diseases. *J Neuroinflammation*. 2016;13:32.
- 48 Farb A, Kolodgie FD, Hwang JY, et al. Extracellular matrix changes in stented human coronary arteries. *Circulation*. 2004;110(8):940–947.
- 49 Suna G, Wojakowski W, Lynch M, et al. Extracellular matrix proteomics reveals interplay of aggrecan and aggrecanases in vascular remodeling of stented coronary arteries. *Circulation*. 2018;137(2):166–183.
- 50 Yang G, Wu L, Wang R. Pro-apoptotic effect of endogenous H₂S on human aorta smooth muscle cells. *FASEB J*. 2006;20(3):553–555.
- 51 Shuang T, Fu M, Yang G, Wu L, Wang R. The interaction of IGF-1/IGF-1R and hydrogen sulfide on the proliferation of mouse primary vascular smooth muscle cells. *Biochem Pharmacol*. 2018;149:143–152.
- 52 Hosono T, Hosono-Fukao T, Inada K, et al. Alkenyl group is responsible for the disruption of microtubule network formation in human colon cancer cell line HT-29 cells. *Carcinogenesis*. 2008;29(7):1400–1406.
- 53 Shukla N, Osmani AH, Osmani SA. Microtubules are reversibly depolymerized in response to changing gaseous microenvironment within *Aspergillus nidulans* biofilms. *Mol Biol Cell*. 2017;28(5):634–644.
- 54 Britto PJ, Knippling L, McPhie P, Wolff J. Thiol-disulphide interchange in tubulin: kinetics and the effect on polymerization. *Biochem J*. 2005;389(Pt 2):549–558.
- 55 Chaudhuri AR, Khan IA, Luduena RF. Detection of disulfide bonds in bovine brain tubulin and their role in protein folding and microtubule assembly *in vitro*: a novel disulfide detection approach. *Biochemistry*. 2001;40(30):8834–8841.
- 56 Bibli SI, Hu J, Looso M, et al. Mapping the endothelial cell S-sulphydrome highlights the crucial role of integrin sulphydration in vascular function. *Circulation*. 2021;143(9):935–948.
- 57 Fu L, Liu K, He J, Tian C, Yu X, Yang J. Direct proteomic mapping of cysteine persulfidation. *Antioxid Redox Signal*. 2020;33(15):1061–1076.
- 58 Farese S, Stauffer E, Kalicki R, et al. Sodium thiosulfate pharmacokinetics in hemodialysis patients and healthy volunteers. *Clin J Am Soc Nephrol*. 2011;6(6):1447–1455.
- 59 Bruculeri M, Cheigh J, Bauer G, Serur D. Long-term intravenous sodium thiosulfate in the treatment of a patient with calciphylaxis. *Semin Dial*. 2005;18(5):431–434.
- 60 Schlieper G, Brandenburg V, Ketteler M, Floege J. Sodium thiosulfate in the treatment of calcific uremic arteriolopathy. *Nat Rev Nephrol*. 2009;5(9):539–543.

Supplementary Methods

Apoptosis assay

Apoptosis TUNEL assay was performed using the DeadEnd™ Fluorometric TUNEL system kit on frozen sections of human vein segments. Immunofluorescent staining was performed according to the manufacturer's instruction. Apoptotic nuclei were automatically detected using the ImageJ software and normalized to the total number of DAPI-positive nuclei. *In vitro* VSMC apoptosis was determined by Hoechst/Propidium Iodide staining of live VSMCs and manually counted by two independent blinded experimenters (1).

Seahorse

Glycolysis and Mitochondrial stress tests were performed on confluent VSMCs according to the manufacturer's kits (Seahorse XF Glycolysis Stress Test Kit and Seahorse XF Cell Mito Stress Test Kit) and protocol (Agilent Technologies). Cells were treated for 4 or 24 hours with NaHS or STS before the seahorse experiments. Data were analysed using the Seahorse Wave Desktop Software (Agilent Technologies).

Blood analyses

Analyses were performed on blood from mice treated for 3 weeks with 0.5g/Kg/day sodium thiosulfate. Blood chemistry (pH, HCO₃, Na, K and Ca) analyses were performed on whole blood (95µL) immediately upon cardiac puncture using an i-STAT apparatus equipped with CG8⁺ cartridges. Levels of Urea, CK, CK-MB, ASAT and ALAT were measured in heparinised plasma in a Cobas 8000 (Roche Diagnostics; Lausanne University Hospital).

Systolic blood pressure measurement

Systolic blood pressure (SBP) was monitored daily by non-invasive plethysmography tail cuff method (BP-2000, Visitech Systems Inc.) on conscious mice (2).

Supplementary Table S1: Antibodies

Target antigen	Vendor	Catalog #	Working concentration	RRID
Collagen III	Abcam	ab7778	1/100 (IHC-Fz)	AB_306066
Bax	Santa Cruz	Sc-526	1/500 (WB)	AB_2064668
Bcl2	Santa Cruz	Sc-492	1/500 (WB)	AB_2064290
Goat anti-Rabbit IgG Secondary Antibody, Alexa Fluor 680	Thermo Fisher Scientific	A21109	1/250 (ICC)	AB_2535758
α-Tubulin	Sigma-Aldrich	T6074	1/10000 (WB) 1/1000 (IHC-P)	AB_477582
Anti-Rabbit HRPO	Thermo Fisher Scientific	31460	1/20000 (WB)	AB_228341
Anti-mouse HRPO	Jackson ImmunoResearch Labs	115-035-146	1/15000 (WB)	AB_2307392

BrdU	BD Biosciences	555627	1/200 (ICC)	AB_10015222
P4HA1	Proteintech	12658-1-AP	1/1000 (IHC-P)	AB_2283162
PCNA	Dako (Now Agilent)	M0879	1/100 (IHC-P)	AB_2160651
Cleaved Caspase 3	Cell Signaling Technology	9661	1/200 (IHC-P)	AB_2341188
Total OXPHOS Human WB Antibody Cocktail	Abcam	ab110411	1/5000 (WB)	AB_2756818
CSE	Proteintech	12217-1-AP	1/1000 (WB)	AB_2087497
CBS	Santa Cruz	sc-133154	1/1000 (WB)	AB_2244094
3-MST	Novus	NBP1-82617	1/2000 (WB)	AB_11014969

Supplementary Table S2: Reagents

Kit/product	Vendor	Catalog #	link
Sodium Thiosulfate	Hänseler AG	06-6688-01	https://www.reactolab.ch/boutique/hanseler/sodium-thiosulfate-500-gr/
NaHS	Sigma-Aldrich	161527	https://www.sigmaaldrich.com/catalog/product/sigald/161527?lang=fr&region=CH&cm_sp=Insite-_-caSrpResults_srpRecs_srpModel_16721-80-5--srpRecs3-1
GY4137	Sigma-Aldrich	SML0100	https://www.sigmaaldrich.com/CH/en/product/sigma/sml0100
Diallyl Trisulfide (DATS)	Cayman Chemical	10012577	https://www.caymanchem.com/product/10012577/diallyl-trisulfide
H ₂ S Donor 5a.	Cayman Chemical	11238	https://www.caymanchem.com/product/11238/h2s-donor-5a
Sodium trisulfide (Na ₂ S ₃)	SulfoBiotics	SB03-10	https://www.dojindo.eu.com/store/p/859-SulfoBiotics-Sodium-trisulfide-Na2S3.aspx
Nocodazole	Sigma-Aldrich	M1404	https://www.sigmaaldrich.com/CH/en/product/sigma/m1404
<i>In Vitro</i> Tubulin Polymerization Assay Kit	Sigma-Aldrich	17-10194	
DeadEnd Fluorometric TUNEL system	Promega	G3250	https://ch.promega.com/products/cell-health-assays/apoptosis-assays/deadend-fluorometric-tunel-system/?catNum=G3250
Immobilon Western Chemiluminescent HRP Substate	Millipore	WBKLS0050	https://www.merckmillipore.com/CH/de/product/Immobilon-Western-Chemiluminescent-HRP-Substrate,MM_NF-WBKLS0050

Immobilon-P transfer membrane	Millipore	IPVH00010	https://www.merckmillipore.com/CH/de/product/Immobilon-P-PVDF-Membrane.MM_NF-IPVH00010
EnVision® + Dual Link System-HRP (DAB+)	DAKO (now Agilent)	K4065	https://www.agilent.com/cs/library/packageinsert/public/PD04048EFG_01.pdf
Antifade Mounting Medium with DAPI	Vectashield	H-1200	https://vectorlabs.com/products/mounting/vectashield-with-dapi
Pierce reversible protein Stain Kit for PDGF membranes	Thermo Fisher Scientific	24585	https://www.thermofisher.com/order/catalog/product/24585#/24585
Seahorse XF Glycolysis Stress Test Kit	Agilent	103020-100	https://www.agilent.com/store/productDetail.jsp?catalogId=103020-100&catId=SubCat2ECS_897073
Seahorse XF Cell Mito Stress Test Kit	Agilent	103015-100	https://www.agilent.com/store/en_US/Product/103015-100/103015-100
DirectPCR Lysis Reagent (Ear)	Viagen	402-E	http://www.viagenbiotech.com/index.php/directpcr-lysis-reagents/tail/500-mouse-tails-100-ml.html
Proteinase K	Qiagen,	1122470	https://www.qiagen.com/us/products/discovery-and-translational-research/lab-essentials/enzymes/qiagen-protease-and-proteinase-k/?catno=19131
Platinum™ Taq DNA Polymerase	Invitrogen	10966-026	https://www.thermofisher.com/order/catalog/product/10966026
RPMI-1640 Glutamax I	Gibco	61870-010	https://www.thermofisher.com/RPMI
Gelatin type B	Sigma-Aldrich	G9391	G9391 Sigma
Tripure	Roche	11667157001	Roche tripure
DAz-2	Cayman Chemicals	13382	www.caymanchem.com/product/13382
Cyanine 5.5 alkyne	Lumiprobe	C70B0	https://www.lumiprobe.com/p/cy55-alkyne
4-Chloro-7-Nitrobenzofurazan	Sigma Aldrich	163260	https://www.sigmaaldrich.com/catalog/product/aldrich/163260?lang=fr&region=CH
SF7-AM fluorescent probe	Sigma-Aldrich	748110	Sigmaaldrich 748110
SSP4 fluorescent probe	Dojindo Molecular Technologies	SB10	https://www.dojindo.com/product/sulfobiotics-ssp4-sb10/
Ketamin (Ketasol-	Gräub E.Dr.AG, Bern	NA	https://www.graeb.com/fr/products/product/k

100)	Switzerland		etasol-100/2054
Xylasin (Rompun®),	Provet AG, Lyssach, Switzerland	NA	http://www.provet.gr/en/animal-health/products/pharmaceuticals/veterinary-pharmaceuticals/rompun-inj.-sol./7-489
Buprenorphine (Temgesic)	Reckitt Benckiser AG, Switzerland	NA	Temgesic
Resorcine-Fuchsine Weigert	Waldeck	2E-030	https://www.reactolab.ch/boutique/chroma/resorcine-fuchsine-weigert-solution-500-ml/
Hematoxylin crist.	Merck	1.04302.0025	Hematoxylin-cryst
Acid Fuchsin	Sigma-Aldrich	F8129	https://www.sigmaaldrich.com/catalog/product/sigma/f8129?lang=fr&region=CH
Picric acid	Sigma-Aldrich	197378	https://www.sigmaaldrich.com/catalog/product/aldrich/197378?lang=fr&region=CH
Neo-Clear	Merck	1.09843.5000	Neo-Clear
Ethanol absolu	Merck	1.00983.2500	Ethanol
Phosphate Buffered Saline (PBS)	Bichsel:	100 0324	https://www.bichsel.ch/
i-STAT CG8+ CARTRIDGE	Abbot	03P88-25	https://www.globalpointofcare.abbott/en/product-details/apoc/istat-cg8plus-test-cartridge.html
Sodium dodecyl sulfate (SDS)	Promega	H5114	https://ch.promega.com/products/biochemical/ssodium-dodecyl-sulfate
Tween-20	Applichem	A1389	https://www.applichem.com/tween
Triton x-100	Sigma-Aldrich	T8787	https://www.sigmaaldrich.com/catalog/product/sigma/t8787?lang=fr&region=CH
Bovine Serum albumin (BSA)	Applichem	A1391	https://www.applichem.com/albumin-fraktion-v
Recombinant Human PDGF-BB	PeproTech House	100-14B	recombinant-human-pdgf-bb
DC™ Protein Assay Kit I	Bio-Rad Laboratories	5000111	Bio-rad dc-protein-assay
Fast SYBR™ Green Master Mix	Applied Biosystems	4385618	
PrimeScript RT Reagent Kit (Perfect Real Time)	Takara Bio	RR037B	https://www.takarabio.com/products/real-time-pcr/reverse-transcription-prior-to-qpcr/primescript-rt-reagent-kit

Supplementary Table S3: Blood panel

Mean (SD)	Ctrl (n=8)	STS (n=8)	p
pH	6.99 (0.07)	7.03 (0.05)	0.23
HCO ₃ (mM)	21.52 (2.48)	21.85 (1.24)	0.74
Na (mM)	150.1 (2.85)	147.5 (3.30)	0.11
K (mM)	5.6 (0.63)	4.8 (0.66)	0.02
Ca (mM)	1.39 (0.06)	1.35 (0.1)	0.33
Urea (mg/dL)	68 (8.4)	56 (10)	0.04
CK (U/L)	177.4 (47)	202.8 (50)	0.71
CK-MB (U/L)	73.8 (8.5)	86.6 (14.4)	0.39
ASAT (U/L)	75.6 (8.8)	82.4 (10.7)	0.64
ALAT (U/L)	43.9 (8.1)	39.5 (6.3)	0.69

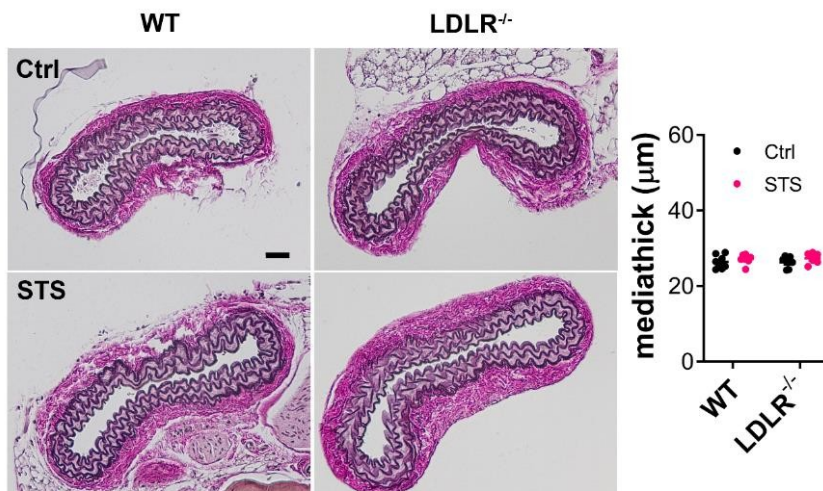


Figure S1. STS does not impact media thickness in native carotids of WT and LDLR^{-/-} mice.

WT and LDLR^{-/-} mice were treated for 28 days with 4 gr/L STS in the water bottle. Representative VGEL staining of carotid cross sections and morphometric measurements of media thickness. Data are mean±SEM of 6-8 animals per group.

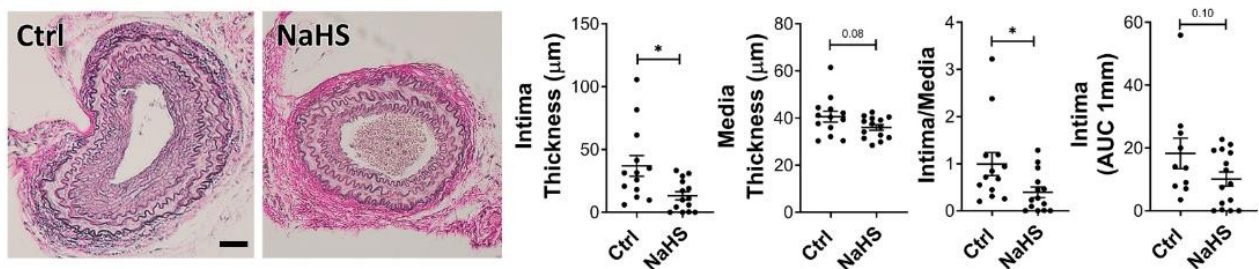


Figure S2. NaHS decreases IH formation after carotid artery stenosis in mice

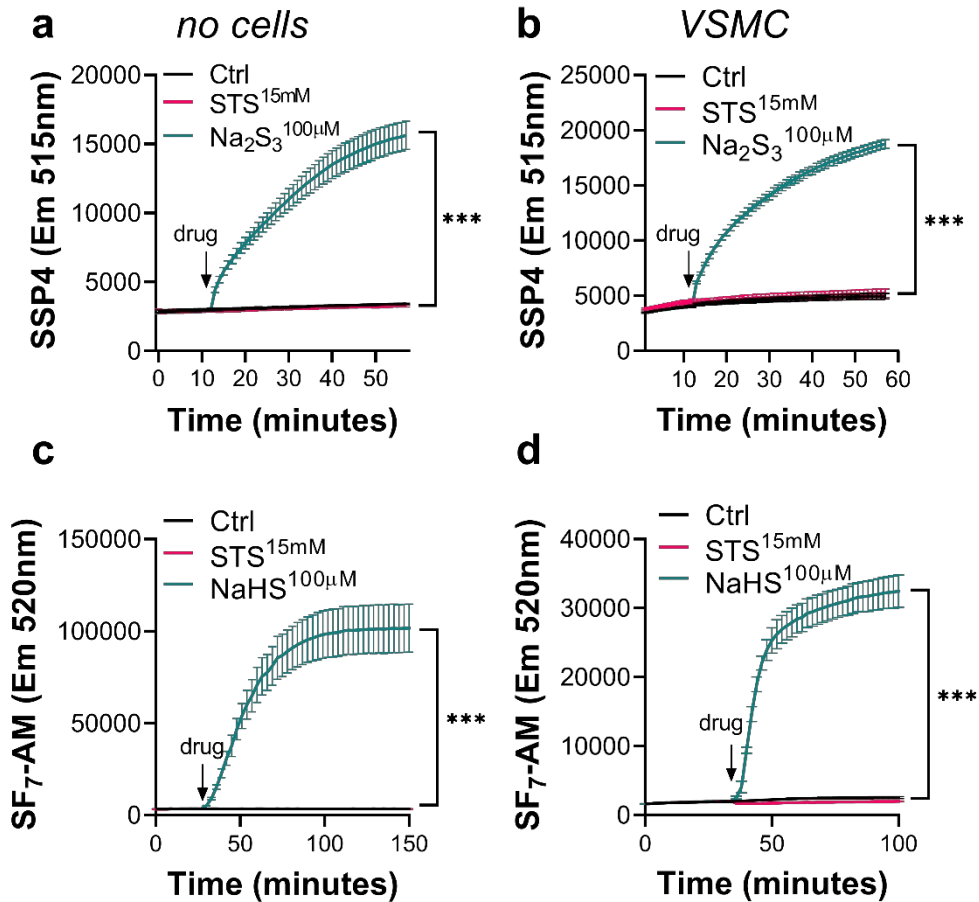


Figure S4. STS does not release detectable amounts of H₂S or polysulfides *in vitro*

a-b) Polysulfides release measured by the SSP4 probe in RPMI media without cells (**a**) or in presence of VSMC (**b**). **c-d)** H₂S release measured by the SF₇-AM probe in RPMI media without cells (**c**) or in presence of VSMC (**d**). Data are mean±SEM of 4 independent experiments. ***p<.0001 as determined by repeated measure 2 way ANOVA with Tukey's multiple comparisons.

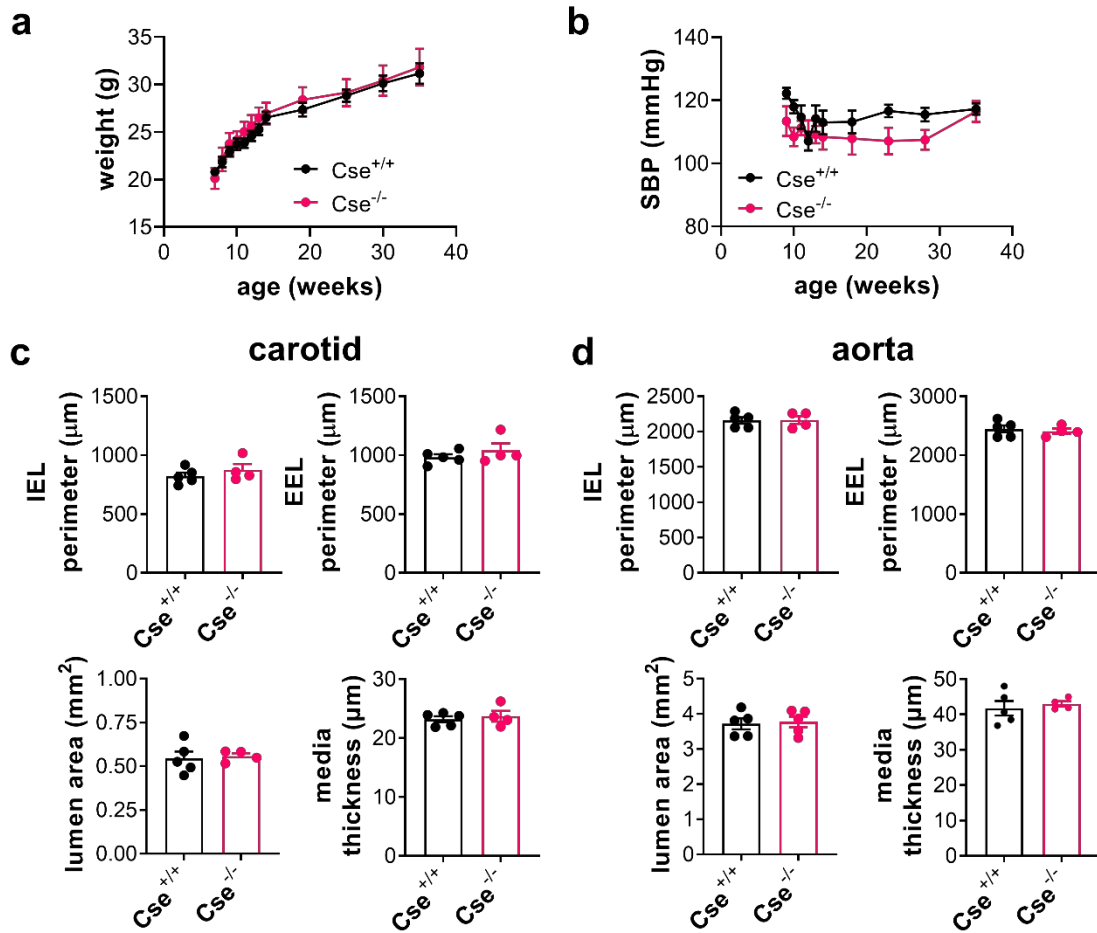


Figure S5. *Cse*^{-/-} mice display no evident vascular phenotype

a) Weight curves of *Cse*^{-/-} and WT (*Cse*^{+/+}) littermates. **b)** Systolic Blood pressure (SBP) in *Cse*^{-/-} and WT (*Cse*^{+/+}) littermates. **c-d)** Carotid and aorta histomorphometry in *Cse*^{-/-} and WT (*Cse*^{+/+}), as measured on VGEL-stained cross section of carotid or aorta. Data are mean±SEM of 4 to 6 animals per group. IEL:internal elastic lamina; EEL:external elastic lamina.

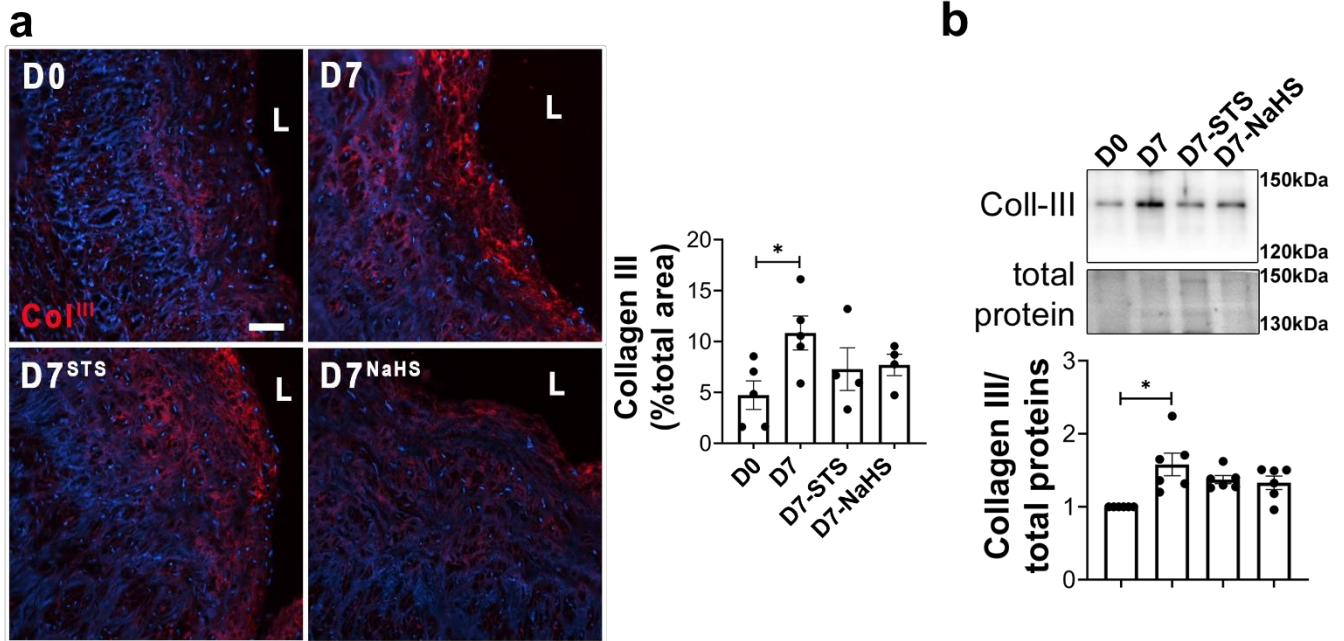


Figure S6. STS and NaHS reduce collagen III accumulation in ex vivo vein segments

A) Left panel: Representative collagen III immunofluorescent staining. Scale bar=50 μ m. **Right panel:** Quantitative assessment of Collagen III immunofluorescent staining. Data are scatter plots of 5 different veins with mean \pm SEM. * p <.05 as determined by paired repeated measures one-way ANOVA with Dunnett's multiple comparisons. **B)** Representative western blot of collagen III over total protein and quantitative assessment of 6 different human vein segments. Data are scatter plots with mean \pm SEM. * p <.05 as determined by paired repeated measures one-way ANOVA with Dunnett's multiple comparisons.

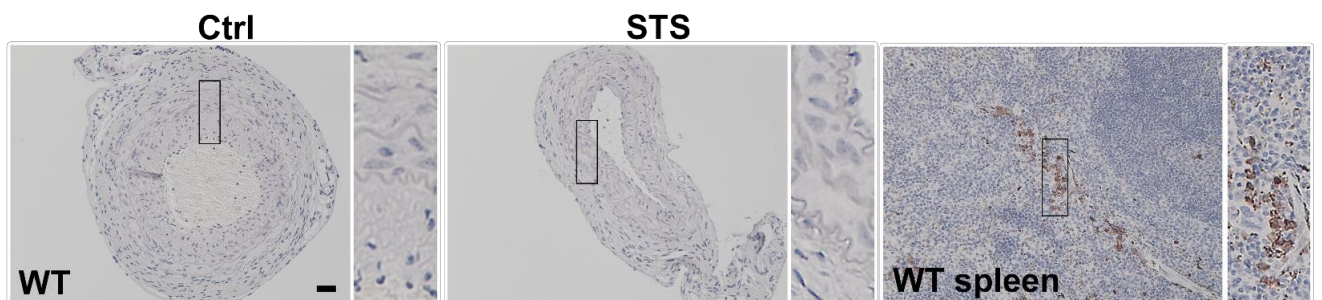


Figure S7. STS does not induce cell apoptosis in vivo in mouse carotids

Cleaved caspase 3 immunostaining (in brown) on CAS operated carotids in WT mice treated or not (Ctrl) with STS 4g/L for 28 days. Tissue was counterstained with hematoxylin to label nuclei (in blue). Spleen from a WT mouse was used as a positive control for Cleaved caspase 3 immunostaining. Scale bar 40 μ m. Insets are 4 fold magnification of main images.

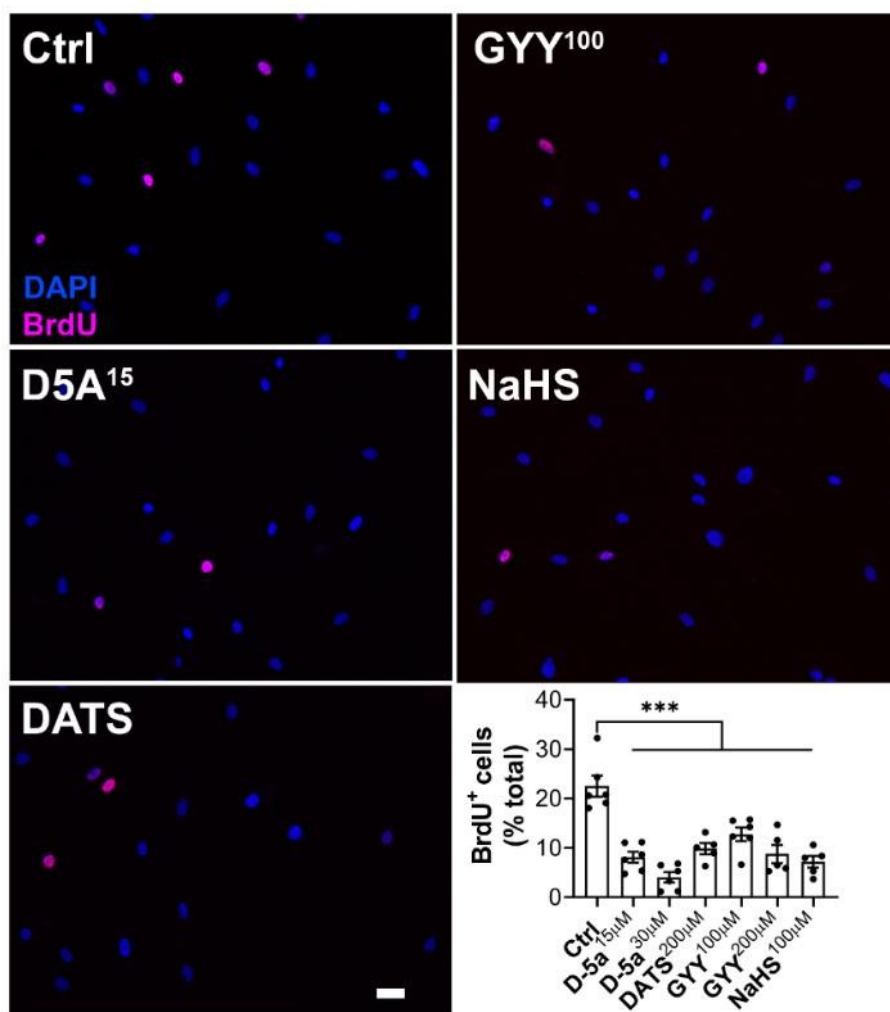


Figure S8. H₂S donors inhibit VSMC proliferation *in vitro*

VSMC proliferation as assessed by BrdU incorporation (pink) over total nuclei (blue) for 24 hours in presence or absence (Ctrl) of Diallyl trisulfide (DATS 200 µM) or GYY4137 (GYY 100 or 200 µM) or Donor 5A (D5A at 15 or 30 µM) and NaHS (100 µM). Scale bar: 25 µm. Data are mean±SEM of 6 independent experiments. ***p<.001 as determined by repeated measures ordinary one-way ANOVA with Dunnett's multiple comparisons.

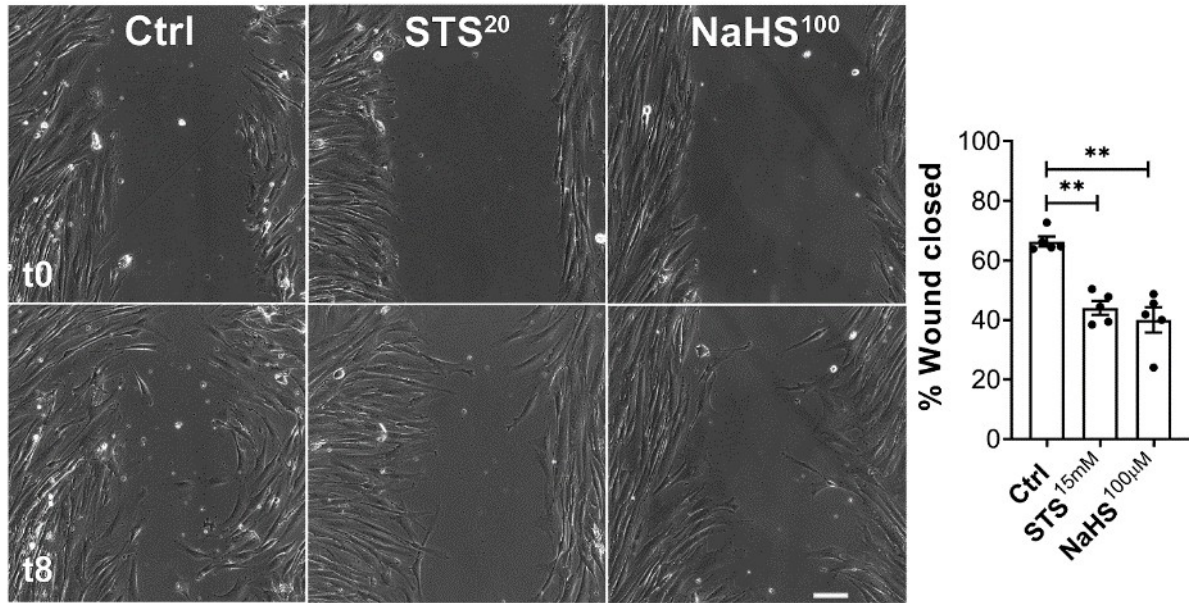


Figure S9. STS and NaHS inhibit VSMC migration

VSMC migration in cells treated or not (Ctrl) with 15 mM STS or 100 µM NaHS in presence of 10 µg/mL Mitomycin C, as assessed by wound healing assay, expressed as the percentage of wound closure after 8 hours. Scale bar: 100 µm. Data are scatter plots with mean±SEM of 5 independent experiments in duplicates. ***p<.001 as determined by repeated measures one-way ANOVA with Dunnett's multiple comparisons.

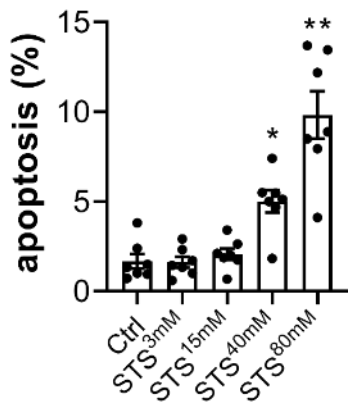


Figure S10. STS is not cytotoxic at 15mM in VSMC

VSMC apoptosis after 48 hours of cell culture in presence of increasing concentration of STS, as indicated. Data shown as mean ± SEM. *p<.05, **p<.01 as determined by repeated measures ordinary one-way ANOVA followed by Dunnett's multiple comparisons tests.

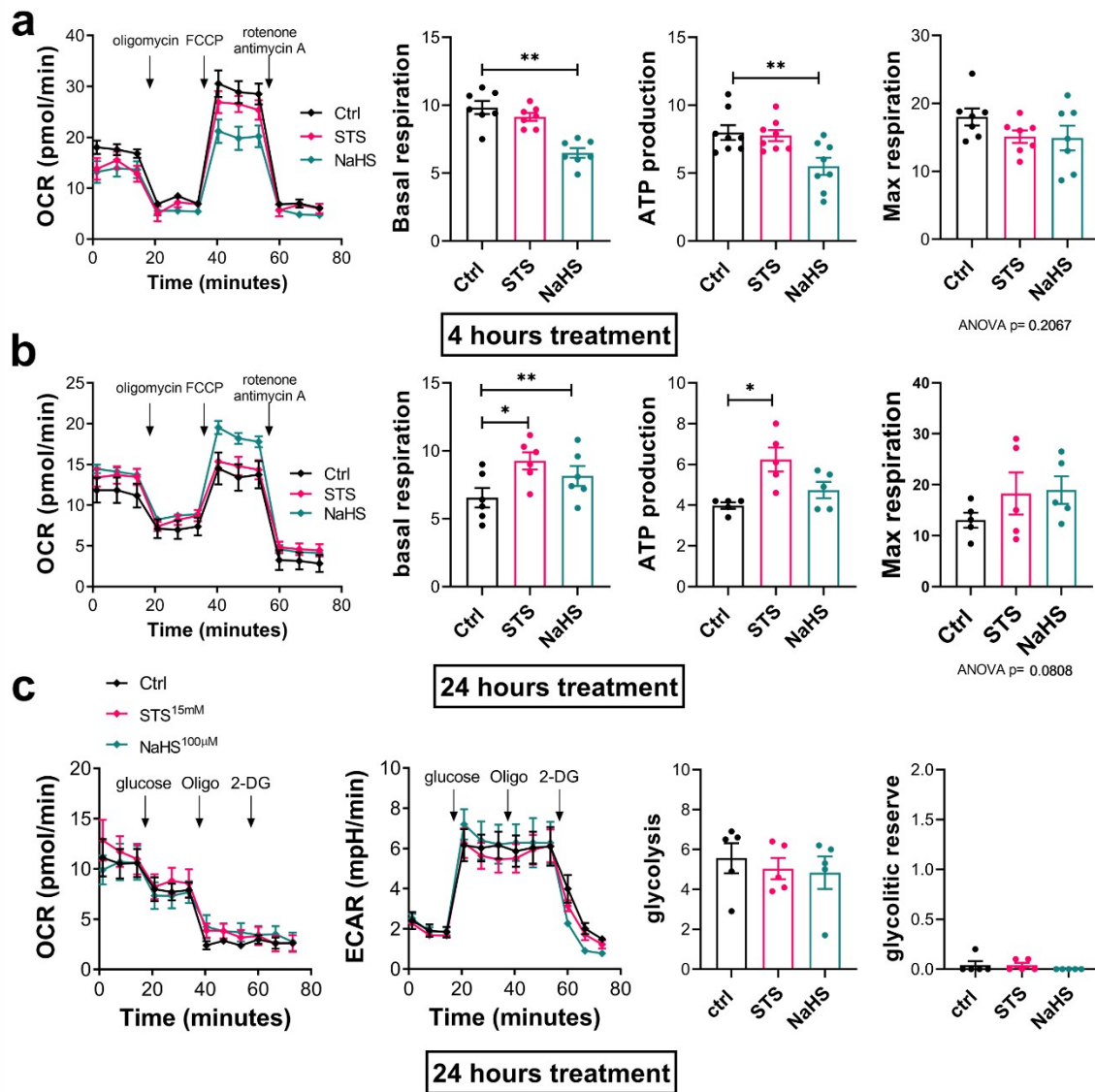


Figure S11. STS does not significantly impact VSMC metabolism *in vitro*

a-b) Mito stress test assay in VSMC pre-treated or not (Ctrl) for 4h (**a**) or 24h (**b**) with 100 μ M NaHS or 15 mM STS. **c)** Glucose stress test assay in VSMC pre-treated or not (Ctrl) 24h with 100 μ M NaHS or 15 mM STS. Data are representative Seahorse traces and mean \pm SEM of 5-6 independent experiments. * $p < .05$, ** $p < .01$ as determined by 2 way ANOVA with Tukey's multiple comparisons.

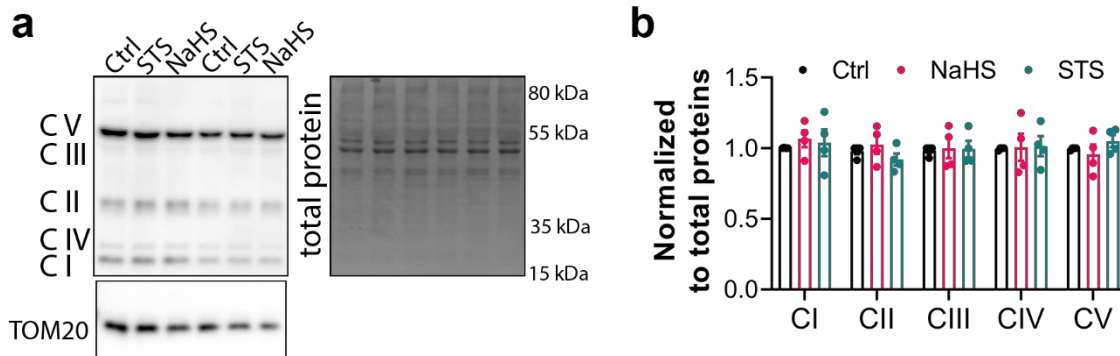


Figure S12. STS does not significantly impact the mitochondrial respiratory chain in VSMC *in vitro*

VSMC were treated for 24 hours with 15 mM STS or 100 μM NaHS. Representative Western blot (A) and quantitative assessment of Oxphos complexes (B), normalized to total protein in 4 independent experiments.

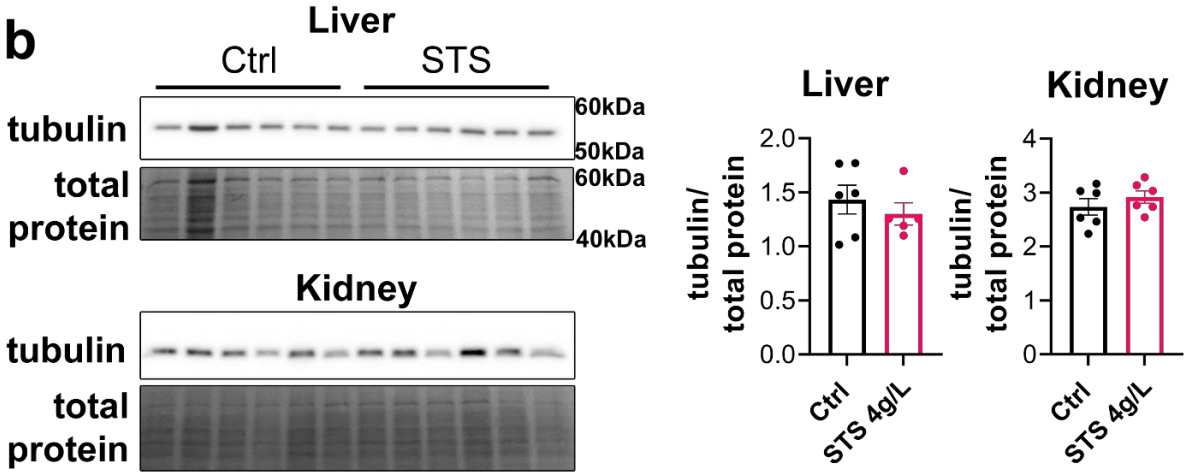
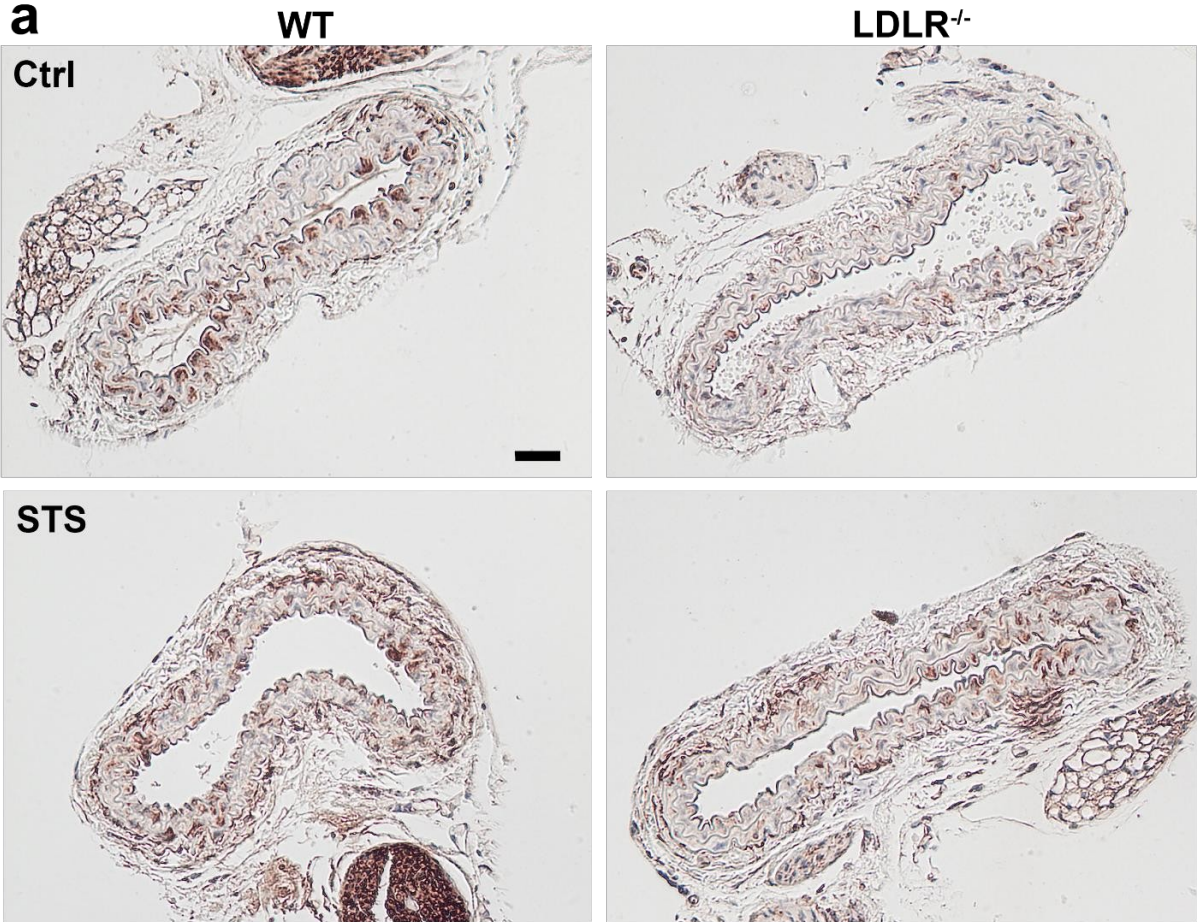


Figure S13. STS treatment does not decrease tubulin in native carotids, liver and kidney of WT mice.

a) WT and LDLR^{-/-} mice were treated for 28 days with 4 gr/L STS in the water bottle. Representative tubulin immunostaining of carotid cross sections. Data are mean±SEM of 4-6 animals per group. b) WT mice were treated for 28 days with 4 gr/L STS in the water bottle. Representative tubulin Western blotting and quantitative assessment of tubulin levels, normalized to total proteins, in the liver and kidney of 5-6 animals per group.

References

1. Allagnat F, Fukaya M, Nogueira TC, Delaroche D, Welsh N, Marselli L, et al. C/EBP homologous protein contributes to cytokine-induced pro-inflammatory responses and apoptosis in beta-cells. *Cell Death Differ.* 2012;19(11):1836-46.
2. Le Gal L, Alonso F, Wagner C, Germain S, Nardelli Haefliger D, Meda P, et al. Restoration of connexin 40 (Cx40) in Renin-producing cells reduces the hypertension of Cx40 null mice. *Hypertension.* 2014;63(6):1198-204.

7.2 Hydrogen Sulphide Release via the Angiotensin Converting Enzyme Inhibitor Zofenopril Prevents Intimal Hyperplasia in Human Vein Segments and in a Mouse Model of Carotid Artery Stenosis

In this study, we demonstrated that Zofenopril is not only more potent than enalapril in reducing IH in hypertensive Cx40^{-/-} mice, but it also suppresses IH in normotensive conditions, where other ACEi have no effect. Furthermore, zofenopril prevents IH in human saphenous vein segments in the absence of blood flow. The effect of zofenopril on IH correlates with reduced VSMC proliferation and migration, and decreased activity of the MAPK and mTOR pathways.

DOI: <https://doi.org/10.1016/j.ejvs.2021.09.032>

Hydrogen Sulphide Release via the Angiotensin Converting Enzyme Inhibitor Zofenopril Prevents Intimal Hyperplasia in Human Vein Segments and in a Mouse Model of Carotid Artery Stenosis

Diane Macabrey^{a,b,†}, Céline Deslarzes-Dubuis^{a,b,†}, Alban Longchamp^{a,b}, Martine Lambelet^{a,b}, Charles K. Ozaki^c, Jean-Marc Corpataux^{a,b}, Florent Allagnat^{a,b,*,§}, Sébastien Déglise^{a,b,§}

^a Department of Vascular Surgery, Lausanne University Hospital, Lausanne, Switzerland

^b Department of Biomedical Sciences, University of Lausanne, Lausanne, Switzerland

^c Department of Surgery and the Heart and Vascular Centre, Brigham and Women's Hospital and Harvard Medical School, Boston, MA, USA

WHAT THIS PAPER ADDS

The current strategies to reduce intimal hyperplasia (IH) rely principally on local drug delivery, in an endovascular approach. The oral angiotensin converting enzyme inhibitor (ACEi) zofenopril has additional effects to other non-sulphydrated ACEi to prevent intimal hyperplasia and re-stenosis. Given the number of patients treated with ACEi worldwide, these findings call for further prospective clinical trials to test the benefits of sulphydrated ACEi over classic ACEi for the prevention of re-stenosis in hypertensive patients.

Objective: Hypertension is a major risk factor for intimal hyperplasia (IH) and re-stenosis following vascular and endovascular interventions. Preclinical studies suggest that hydrogen sulphide (H₂S), an endogenous gasotransmitter, limits re-stenosis. While there is no clinically available pure H₂S releasing compound, the sulphydryl containing angiotensin converting enzyme inhibitor zofenopril is a source of H₂S. Here, it was hypothesised that zofenopril, due to H₂S release, would be superior to other non-sulphydryl containing angiotensin converting enzyme inhibitors (ACEi) in reducing intimal hyperplasia.

Methods: Spontaneously hypertensive male Cx40 deleted mice (Cx40^{-/-}) or wild type (WT) littermates were randomly treated with enalapril 20 mg or zofenopril 30 mg. Discarded human vein segments and primary human smooth muscle cells (SMCs) were treated with the active compound enalaprilat or zofenoprilat. IH was evaluated in mice 28 days after focal carotid artery stenosis surgery and in human vein segments cultured for seven days *ex vivo*. Human primary smooth muscle cell (SMC) proliferation and migration were studied *in vitro*.

Results: Compared with control animals (intima/media thickness 2.3 ± 0.33 μm), enalapril reduced IH in Cx40^{-/-} hypertensive mice by 30% (1.7 ± 0.35 μm; *p* = .037), while zofenopril abrogated IH (0.4 ± 0.16 μm; *p* < .002 vs. control and *p* > .99 vs. sham operated Cx40^{-/-} mice). In WT normotensive mice, enalapril had no effect (0.9665 ± 0.2 μm in control vs. 1.140 ± 0.27 μm; *p* > .99), while zofenopril also abrogated IH (0.1623 ± 0.07 μm; *p* < .008 vs. control and *p* > .99 vs. sham operated WT mice). Zofenoprilat, but not enalaprilat, also prevented IH in human vein segments *ex vivo*. The effect of zofenopril on carotid and SMCs correlated with reduced SMC proliferation and migration. Zofenoprilat inhibited the mitogen activated protein kinase and mammalian target of rapamycin pathways in SMCs and human vein segments.

Conclusion: Zofenopril provides extra beneficial effects compared with non-sulphydryl ACEi in reducing SMC proliferation and re-stenosis, even in normotensive animals. These findings may hold broad clinical implications for patients suffering from vascular occlusive diseases and hypertension.

Keywords: ACE inhibitor, Hydrogen sulphide, Hypertension, Intimal hyperplasia, Proliferation, Smooth muscle cells, Restenosis, Zofenopril

Article history: Received 16 February 2021, Accepted 17 September 2021, Available online 13 December 2021

© 2021 The Author(s). Published by Elsevier B.V. on behalf of European Society for Vascular Surgery. This is an open access article under the CC BY-NC-ND license (<http://creativecommons.org/licenses/by-nc-nd/4.0/>).

[†] These authors contributed equally as first authors.

[§] These authors contributed equally as senior authors.

* Corresponding author. CHUV – Service de Chirurgie Vasculaire, Département des Sciences Biomédicales, Bugnon 7A Lausanne, 1005, Switzerland.

E-mail address: florent.allagnat@chuv.ch (Florent Allagnat).

1078-5884/© 2021 The Author(s). Published by Elsevier B.V. on behalf of European Society for Vascular Surgery. This is an open access article under the CC BY-NC-ND license (<http://creativecommons.org/licenses/by-nc-nd/4.0/>).

<https://doi.org/10.1016/j.ejvs.2021.09.032>

INTRODUCTION

Intimal hyperplasia (IH) remains the major cause of restenosis following vascular surgery, leading to potential limb loss and death. IH develops in response to vessel injury, leading to inflammation, vascular smooth muscle cell (VSMC) dedifferentiation, migration, and proliferation, and secretion of extracellular matrix. Despite decades of research, there is no effective medication to prevent restenosis.¹ The only validated therapy against IH is the local drug delivery strategy, used especially in the endovascular approach. However, this strategy seems to be limited;² other complementary oral treatments target either steps involved in IH, such as SMC proliferation, or risk factors for re-stenosis such as hypertension.

Hydrogen sulphide (H₂S) is an endogenously produced gasotransmitter.³ Preclinical studies have shown that H₂S has cardiovascular protective properties,⁴ including reduction of IH,^{5–7} possibly via decreased VSMC proliferation.^{6,8} However, there is currently no clinically approved H₂S donor.⁹

Hypertension is a known risk factor for re-stenosis and bypass failure.¹⁰ Current guidelines recommend angiotensin converting enzyme inhibitors (ACEi) as the first line therapy for the treatment of essential hypertension.¹¹ Although various ACEi reduce re-stenosis in rodent models,¹² prospective clinical trials failed to prove efficacy of the ACEi quinapril or cilazapril for the prevention of re-stenosis at six months after coronary angioplasty.^{13–15} Several *in vitro* studies suggest that the ACEi zofenopril, owing to a sulfhydryl moiety in its structure, releases H₂S.^{16–18} The therapeutic potential of sulfhydryl ACEi zofenopril has never been tested in the context of re-stenosis.

The purpose of this study was to test whether zofenopril, owing to its H₂S releasing properties, is superior to non-sulfhydryl ACEi in limiting IH in a surgical mouse model of IH *in vivo* and in an *ex vivo* model of IH in human vein culture. Zofenopril was systematically compared with the non-sulfhydrated ACEi enalapril.

MATERIALS AND METHODS

Materials

Drugs and reagents are described in [Supplementary Table S1](#). Datasets are available at <https://doi.org/10.5281/zenodo.5017874>

Experimental group design

All experiments were performed using 8 – 10 week old male Cx40 deleted mice (Cx40^{-/-})¹⁹ and wild type (WT) littermate mice on a C57BL/6J genetic background. Mice randomly assigned to the experimental groups were treated with the various ACEi at 10 mg/kg/day via a water bottle.

Blood pressure experiments. WT ($n = 22$) or Cx40^{-/-} ($n = 18$) mice were randomly divided into three groups: control, enalapril, and zofenopril. Basal systolic blood pressure (SBP)

was measured for four days then treatments were initiated and SBP was measured for 10 more days. WT groups were done in parallel ($n = 22$) with Cx40^{-/-} ($n = 6$) untreated mice. Cx40^{-/-} groups ($n = 18$) were done in parallel with WT untreated mice ($n = 6$).

WT mice ($n = 12$) were randomly divided into three groups: control ($n = 4$), quinapril ($n = 4$), and lisinopril ($n = 4$). Basal SBP was measured for four days and then treatments were initiated and SBP was measured for 10 more days.

SBP was monitored daily by the non-invasive plethysmography tail cuff method (BP-2000; Visitech Systems, Apex, NC, USA) on conscious mice.²⁰

Mouse carotid artery stenosis model. WT mice ($n = 26$) were divided into three groups: control (ctrl; $n = 9$), enalapril ($n = 9$), and zofenopril ($n = 8$). Cx40^{-/-} mice ($n = 24$) were divided into three groups: ctrl ($n = 11$), enalapril ($n = 6$), and zofenopril ($n = 7$). Seven days post-treatment, IH was induced via a carotid stenosis.

Carotid artery stenosis (CAS) was performed as previously published.²¹ For surgery, mice were anaesthetised with ketamine 80 mg/kg and xylazine 15 mg/kg. The left carotid artery was located and separated from the jugular vein and vagus nerve. Then, a 7.0 PERMA silk (Johnson & Johnson AG, Ethicon, Neuchâtel, Switzerland) thread was looped under the artery and tightened around the carotid in the presence of a 35 G needle. The needle was removed, thereby restoring blood flow, albeit leaving a significant stenosis.²¹ Buprenorphine 0.05 mg/kg was provided as post-operative analgesia every 12 hours for 48 hours. Treatment with the ACEi of choice was continued for 28 days post-operatively until organ collection. In another set of procedures, WT mice ($n = 17$) were randomly divided into three groups: control ($n = 6$), quinapril ($n = 6$) and lisinopril ($n = 5$). Seven days post-treatment, IH was induced via a carotid stenosis.

All mice were euthanised 28 days post-operatively under general anaesthesia by cervical dislocation and exsanguination, perfused with phosphate buffered saline (PBS) followed by buffered formalin 4% through the left ventricle, and the carotids were taken for IH measurements.

All animal experimentation conformed to the National Research Council: Guide for the Care and Use of Laboratory Animals.²² All animal care, surgery, and euthanasia procedures were approved by the Centre Hospitalier Universitaire Vaudois (CHUV) and the Cantonal Veterinary Office (Service de la Consommation et des Affaires Vétérinaires SCAV-EXPANIM, authorisation number 3258).

Ex vivo static human vein culture and smooth muscle cell culture

Human vein segments were retrieved from discarded tissue obtained during lower limb bypass surgery. Each native vein was cut into 7 mm segments randomly distributed between conditions (day [D]0; D7, ctrl; D7, enalaprilat; D7, zofenoprilat). One segment (D0) was immediately flash frozen in liquid nitrogen or optimal cutting temperature (OCT)

compound and the others were maintained in culture for seven days in RPMI-1640 Glutamax supplemented with 10% foetal bovine serum (FBS) and 1% antibiotic solution (10 000 U/mL penicillin G, 10 000 U/mL streptomycin sulphate) at 37°C and 5% CO₂, as described previously.⁶ The cell culture medium was changed every 48 hours with fresh ACEi. Six different veins/patients were included in this study.

Human VSMCs were prepared and cultured from human saphenous vein segments as described previously.^{6,19} The study protocols for organ collection and use were reviewed and approved by CHUV and the Cantonal Human Research Ethics Committee (<http://www.cer-vd.ch/>, no Institutional Review Board number, protocol number 170/02), and were in accordance with the principles outlined in the Declaration of Helsinki of 1975, as revised in 1983 for the use of human tissues. Six different veins/patients were used in this study to generate VSMCs.

Histomorphometry

Ligated left carotids were isolated and embedded in paraffin. Six 6 µm cross sections were collected every 100 µm and up to 2 mm from the ligature and stained with Van Gieson Elastic Lamina (VGEL) staining. For intimal and medial thickness, 72 (12 measurements/cross section on six cross sections) measurements were performed.¹⁹ To account for the gradient of IH in relation to the distance from the ligature, the intima thickness was plotted against the distance to calculate the area under the curve of intima thickness. Mean intima and media thickness over the 2 mm distance were also calculated.

For human vein segments, after seven days in culture, or immediately upon vein isolation (D0), segments were fixed in buffered formalin, embedded in paraffin and cut into 6 µm sections, and stained with VGEL as described previously.⁶ For intimal and medial thickness, 96 (four measurements/photos and four photos per cross section on six cross sections) measurements were performed.¹⁹ Two independent researchers blinded to the conditions did the morphometric measurements using the Olympus Stream Start 2.3 software (Olympus, Wallisellen, Switzerland).^{6,19}

Immunohistochemistry

Proliferating cell nuclear antigen (PCNA) immunohistochemistry was performed on paraffin sections as described previously after antigen retrieval using TRIS–ethylenediaminetetraacetic acid (EDTA) buffer (pH 9) for 17 minutes in a microwave at 500 watts.⁶ Immunostaining was performed using the EnVision +/HRP, DAB+ system, according to manufacturer's instructions (Dako, Lausanne, Switzerland), and counterstained with haematoxylin. One slide per series was assessed and three images per section were taken. Two independent observers unaware of the conditions manually counted the PCNA and haematoxylin positive nuclei.

Live cell hydrogen sulphide measurement

Free sulphide was measured in cells using a 5 µM SF₇-AM fluorescent probe as described previously.⁶ Fluorescence intensity ($\lambda_{\text{ex}} = 495 \text{ nm}$; $\lambda_{\text{em}} = 520 \text{ nm}$) was measured continuously in a Synergy Mx fluorescent plate reader (Biotek, Basel, Switzerland) at 37°C before and after addition of various compounds, as indicated.

Persulfidation protocol

A persulfidation protocol was performed using a dimedone based probe, as described previously.²³ Flash frozen liver was ground into powder and 20 mg powder was homogenised in 300 µL HEN buffer (i.e., 100 mM HEPES, 1 mM EDTA, 100 µM neocuproin, 1 vol. % NP-40, 1 wt. % sodium dodecyl sulphate [SDS], and proteases inhibitors) supplemented with 5 mM 4-chloro-7-nitrobenzofurazan. Proteins were extracted by methanol/chloroform/water protein precipitation and the pellet was resuspended in 200 µL 50 mM HEPES-2 wt. % SDS. Protein content was measured using a Pierce BCA protein assay kit (Pierce, Rockford, IL, USA), and 75 µg proteins were incubated with 25 µM final Daz-2-biotin for one hour in the dark at 37°C. Daz-2-biotin was prepared with 1 mM Daz-2, 1 mM alkynyl biotin, 2 mM copper(II)-tris(benzyltriazolylmethyl)amine, and 4 mM ascorbic acid with overnight incubation at room temperature, followed by quenching with 20 mM EDTA. Proteins were then extracted by methanol/chloroform/water protein precipitation and the pellets resuspended in 150 µL SDS lysis buffer. Protein concentration was measured using the detergent compatible (DC) protein assay, 10 µg was loaded onto SDS polyacrylamide gel electrophoresis (SDS-PAGE) and the biotin signal was measured by Western blot analyses using a streptavidin–horseradish peroxidase antibody. Protein abundance was normalised to total protein staining using a Pierce Reversible Protein Stain Kit for polyvinylidene fluoride (PVDF) membranes.

BrdU (bromodeoxyuridine/5-bromo-2'-deoxyuridine) staining for vascular smooth muscle cell proliferation

VSMCs were grown at 80% confluence on glass coverslips in a 24 well plate and starved overnight in serum free medium. Then, VSMCs were either treated or not (ctrl) with the ACEi of choice for 24 hours in full medium (RPMI 10% FBS) in presence of 10 µM BrdU. All conditions were tested in parallel. All cells were fixed in 100% ice cold methanol after 24 hours of incubation and immunostained for BrdU. Images were acquired using a Nikon Eclipse 90i microscope. BrdU positive nuclei and total 4',6-diamidino-2-phenylindole (DAPI) positive nuclei were automatically detected using ImageJ software.⁶

Wound healing assay vascular smooth muscle cell migration

VSMCs were grown at confluence in a 12 well plate and starved overnight in serum free medium. Then, a scratch

wound was created using a sterile p200 pipette tip and medium was changed to full medium (RPMI 10% FBS). Repopulation of the wounded areas was recorded by phase contrast microscopy over 24 hours in a Nikon Ti2-E live cell microscope. The area of the denuded area was measured at 0 hours and 10 hours after the wound, using ImageJ software, by two independent observers blind to the conditions.

Western blotting

Human vein segments were washed twice in ice cold PBS, flash frozen in liquid nitrogen, ground to powder, and resuspended in SDS lysis buffer (62.5 mM TRIS pH 6.8, 5% SDS, 10 mM EDTA).

VSMCs were kept in serum free media overnight. The next morning, complete media was added with the ACEi. Five hours post-treatment, cells were washed once with ice

cold PBS and directly lysed with Laemmli buffer. Lysates were resolved by SDS-PAGE and transferred to a PVDF membrane (Immobilon-P; Millipore, Schaffhausen, Switzerland). Immunoblot analyses were performed as described previously,⁶ using the antibodies described in the [Supplementary Table S1](#). Blots were revealed by enhanced chemiluminescence (Immobilon; Millipore) using the ChemiDoc XRS+ System and analysed using Image Lab (BETA2) software, version 3.0.01 (Bio-Rad Laboratories, Fribourg, Switzerland).

Statistical analyses

All experiments were analysed quantitatively using GraphPad Prism 8 (GraphPad Inc., La Jolla, CA, USA), and results are shown as mean ± standard error of the mean. Statistical test details are indicated in the figure legends.

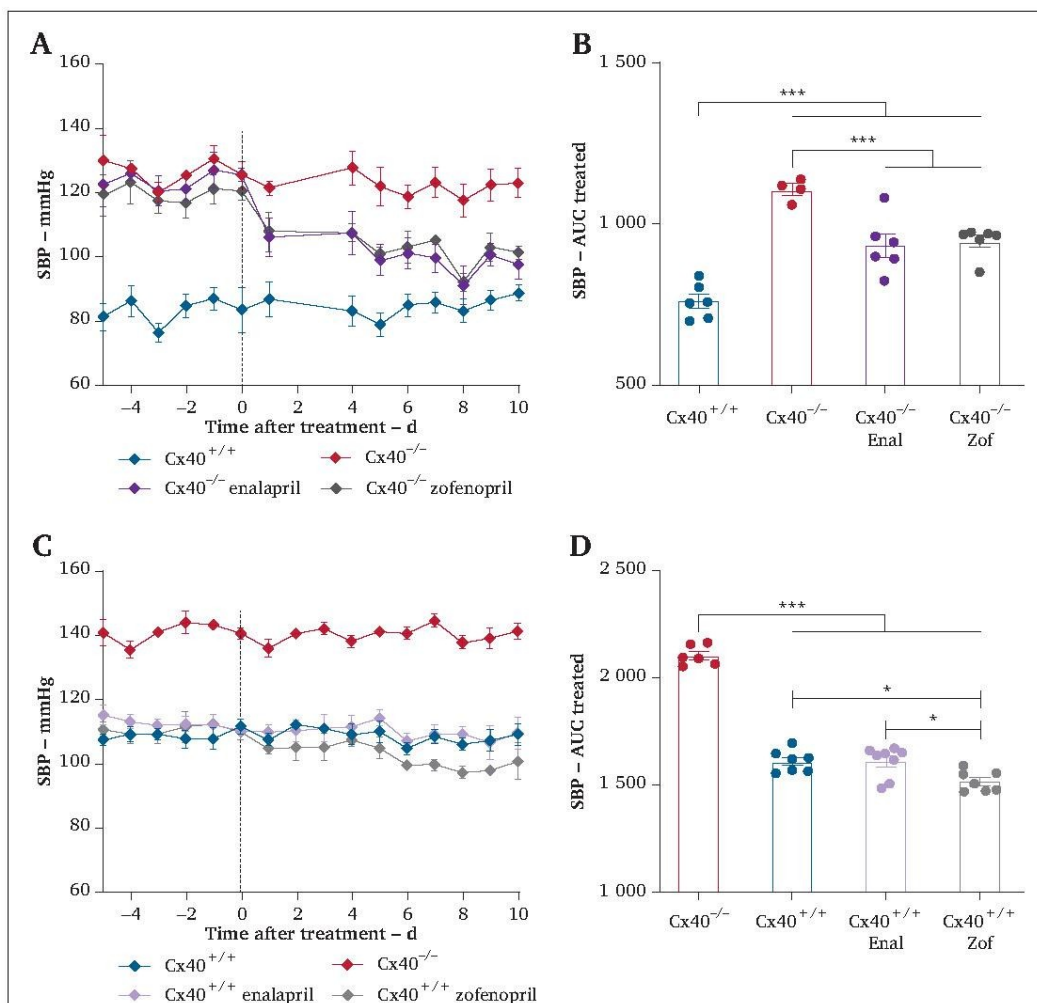
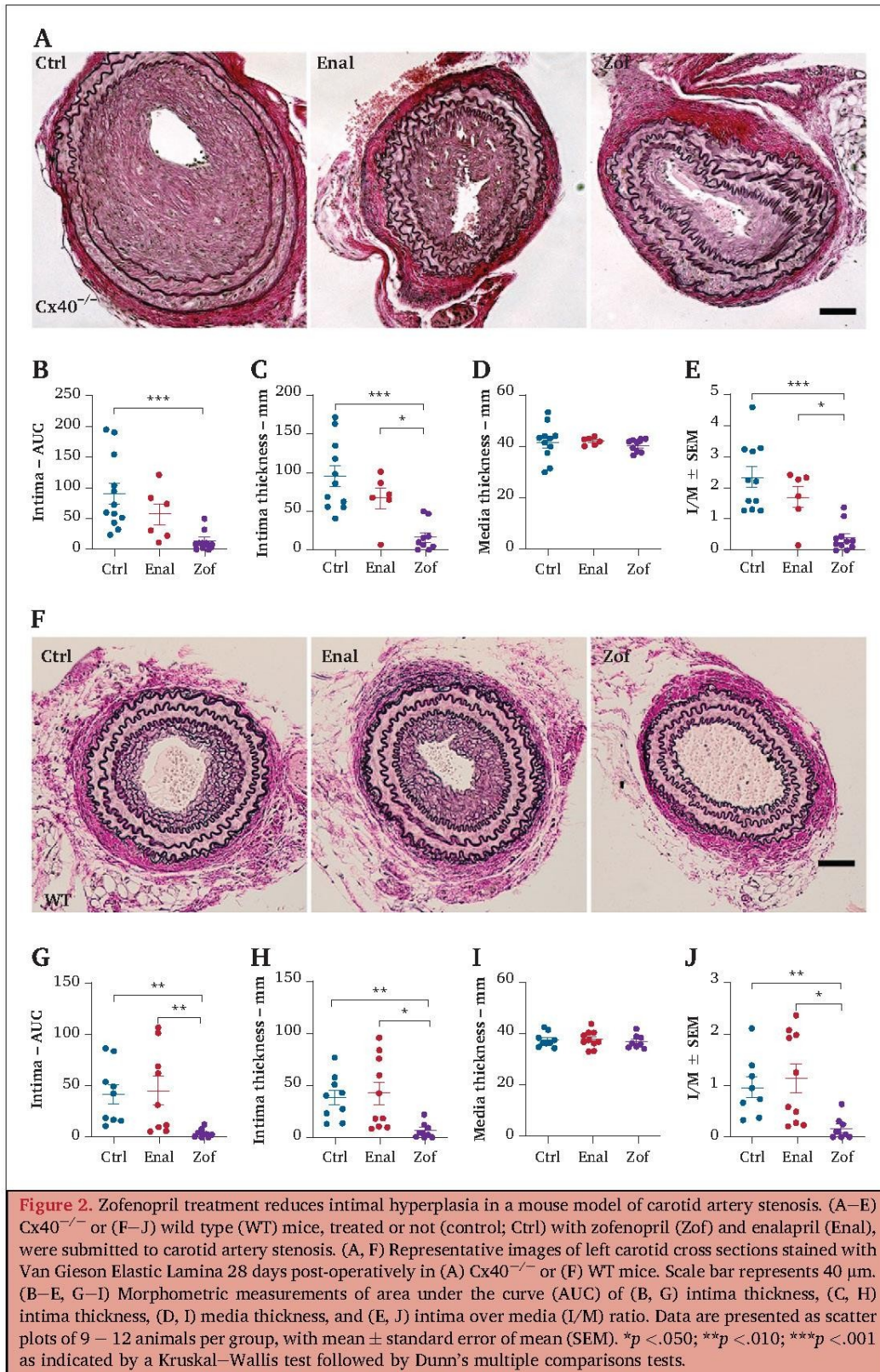


Figure 1. Zofenopril and enalapril similarly lower systolic blood pressure (SBP) in hypertensive Cx40^{-/-} mice. (A) Daily SBP values (mean ± standard error of mean [SEM]) in wild type (WT; Cx40^{+/+}) (n = 6) vs. Cx40^{-/-} mice treated or not (n = 5) with 10 mg/kg zofenopril (n = 6) and 10 mg/kg enalapril (n = 6) for the indicated time. (B) Area under the curve (AUC) of SBP from day 0 to 10. (C) Daily SBP values (mean ± SEM) in Cx40^{-/-} (n = 5) vs. WT mice treated or not (n = 6) with zofenopril (n = 8) and enalapril (n = 8) for the indicated time. (D) AUC of SBP between day 0 to 10. *p < .050; **p < .010; ***p < .001 as indicated by one way analysis of variance with Tukey's correction of multiple comparisons.



RESULTS

Zofenopril and enalapril similarly lower systolic blood pressure of hypertensive mice

Spontaneously hypertensive Cx40 deleted mice (Cx40^{-/-}) and WT littermates were given either 10 mg/kg zofenopril or 6 mg/kg enalapril in the drinking water to achieve similar blood lowering effects on hypertensive Cx40^{-/-} mice (Fig. 1A). Zofenopril also lowered SBP by 6 mmHg in normotensive WT mice (Fig. 1B). Enalapril (Fig. 1B), quinapril (10 mg/kg), and lisinopril (10 mg/kg) had no effect on SBP in WT mice (Supplementary Fig. S1).

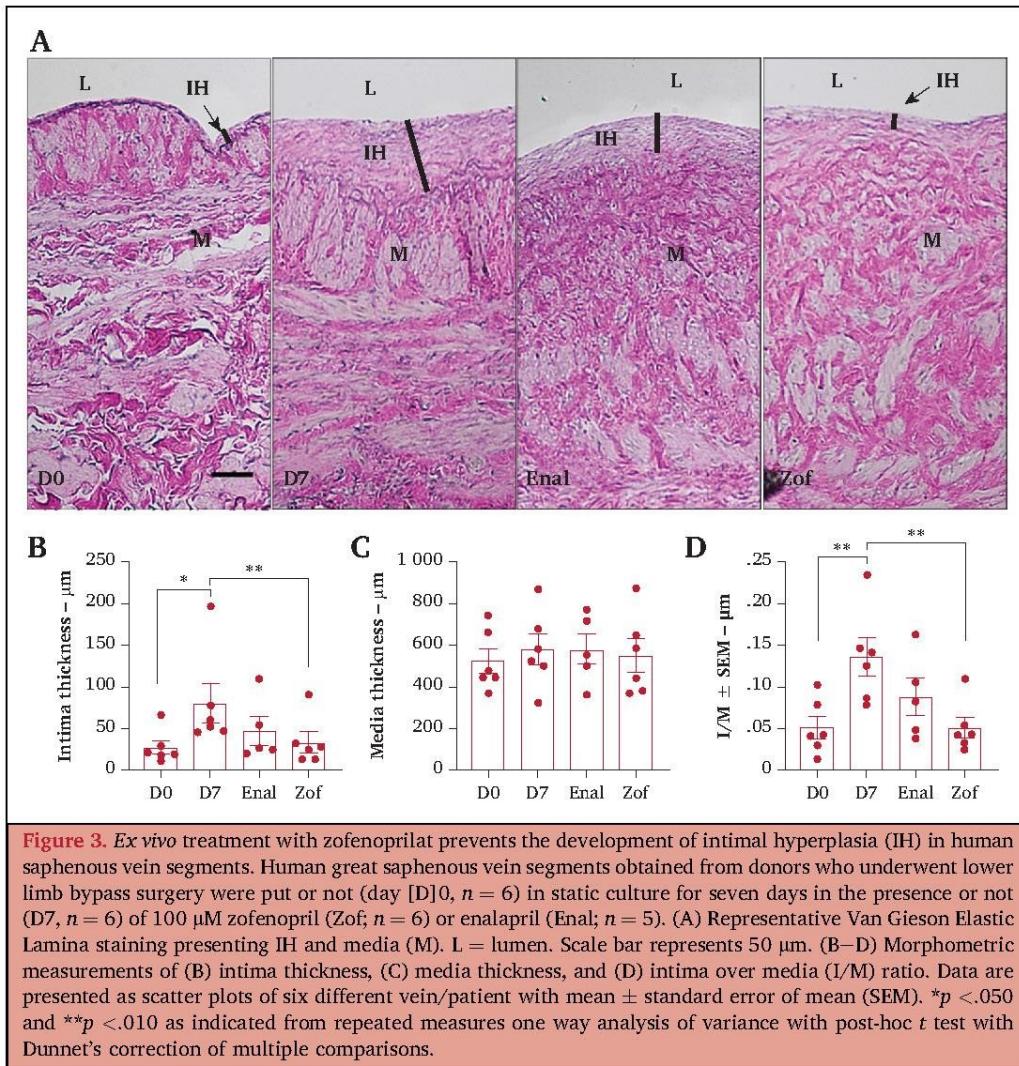
Zofenopril is superior to other angiotensin converting enzyme inhibitors in reducing intimal hyperplasia in a mouse model of carotid artery stenosis

As expected, the hypertensive mice developed twice as much IH as their normotensive littermates following the CAS model.²¹ Enalapril had a non-specific tendency to reduce IH in

Cx40^{-/-} mice (intima [I]/media [M] $p = 1.0$), while Zofenopril suppressed IH by 90% (I/M $p < .001$; Fig. 2, Supplementary Table S2). Enalapril had no effect in normotensive WT mice (I/M $p = 1.0$), whereas zofenopril also suppressed IH in those mice (I/M $p = .008$; Fig. 2, Supplementary Table S3). Quinapril and lisinopril did not affect IH in WT mice (Supplementary Fig. S2, Supplementary Table S4).

Zofenoprilat prevented the development of intimal hyperplasia in human saphenous vein segments

Next, the effect of zofenoprilat and enalaprilat, the active compounds derived from the prodrugs zofenopril and enalapril, respectively, were tested in the model of IH in *ex vivo* static vein culture.⁶ Continuous treatment with 100 μ M zofenoprilat, but not with enalaprilat, fully blocked the development of IH observed in veins maintained for seven days in culture in the absence of blood flow (D7), compared with initial values in freshly isolated veins (D0) (Fig. 3, Supplementary Table S5).



Zofenoprilat released H₂S

Besides its ACEi activity, zofenopril has been proposed to work as an H₂S donor.^{16–18} *In vitro* time lapse recording of the H₂S selective probe SF₇-AM revealed that zofenoprilat, but not enalaprilat, slowly released H₂S in RPMI medium, compared with the fast releasing sodium hydrosulphide salt (Fig. 4A). Similar experiments in the presence of live VSMCs (Fig. 4B) confirmed that zofenoprilat, but not enalaprilat, increased the SF₇-AM signal.

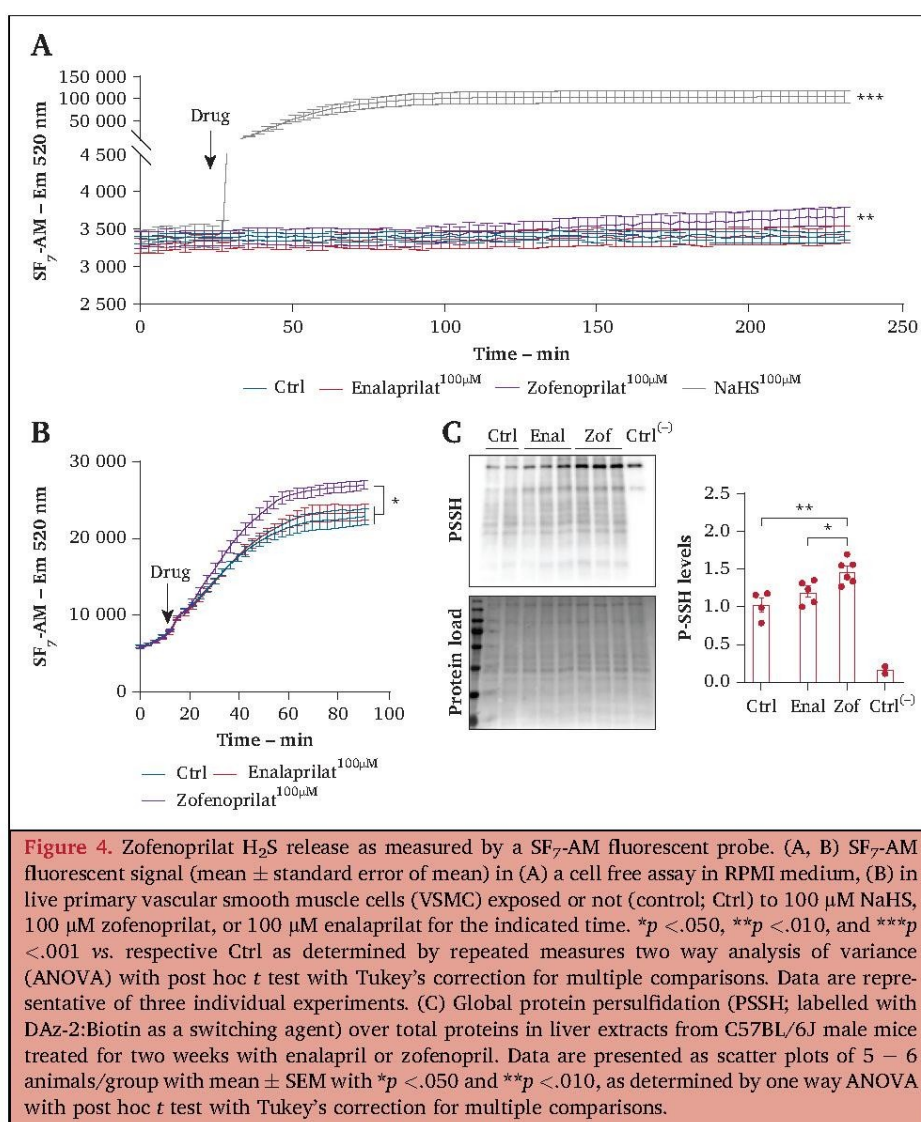
The biological activity of H₂S is mediated by post-translational modification of reactive cysteine residues by persulfidation, which modulates protein structure and/or function.^{9,23} Protein persulfidation was assessed using a dimedone based probe, as described previously.²³ Zofenopril significantly increased protein persulfidation in liver extracts from mice treated with enalapril or zofenopril for two weeks (Fig. 4C).

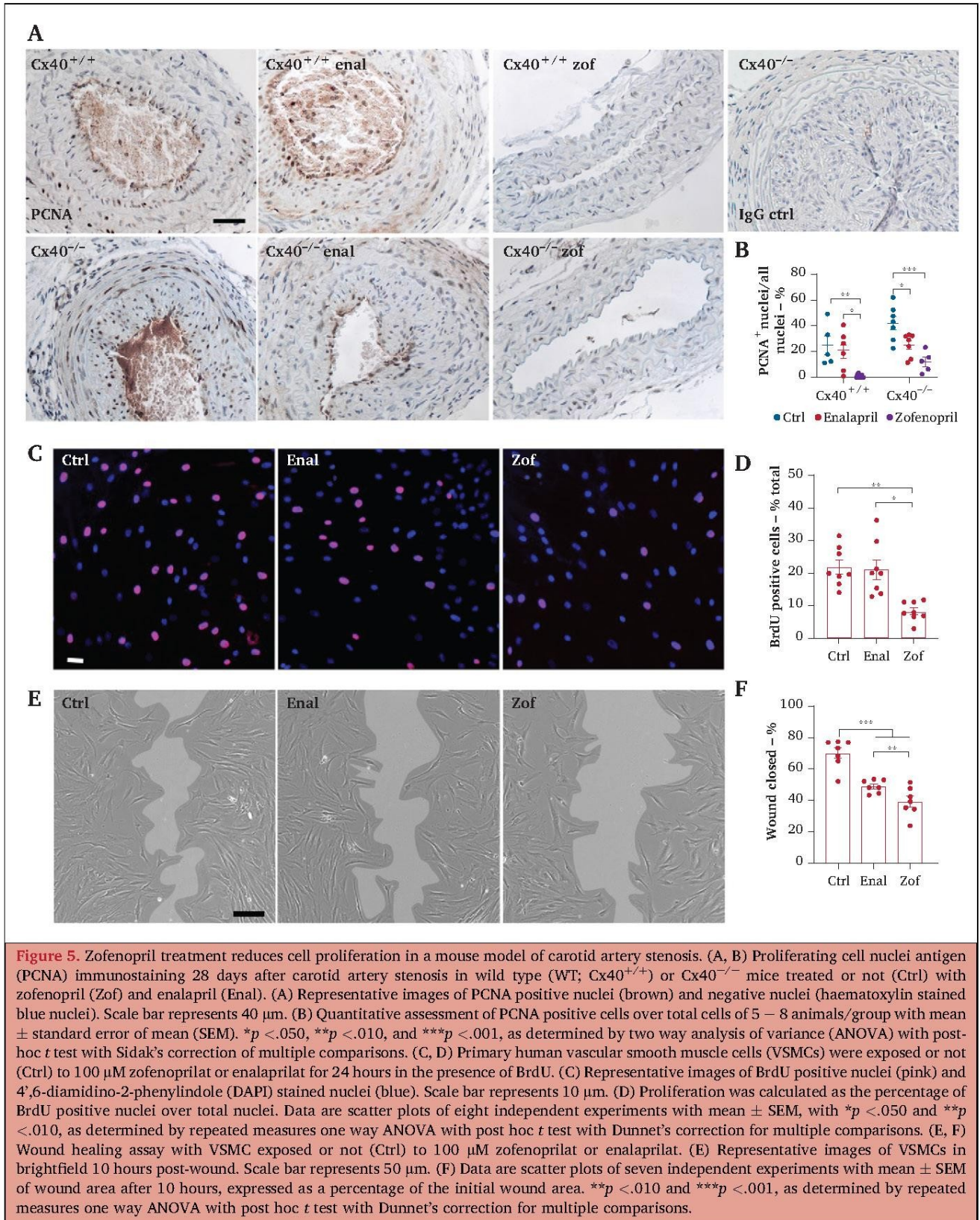
Zofenopril decreased vascular smooth muscle cell proliferation and migration

As various H₂S donors decrease VSMC proliferation in the context of IH,^{6,8} the effect of zofenopril on VSMCs was tested next. In the CAS model, zofenopril, but not enalapril, lowered cell proliferation in the carotid wall as assessed by PCNA staining (Fig. 5A, B). Zofenoprilat further inhibited the proliferation and primary human VSMC migration *in vitro*, while enalaprilat had no effect on proliferation (Fig. 5C, D) and reduced migration by 20% (Fig. 5E, F). Lisinopril and quinaprilat did not affect VSMC proliferation (Supplementary Fig. S3).

Zofenoprilat inhibited the mitogen activated protein kinase and mammalian target of rapamycin pathways

The mitogen activated protein kinase (MAPK) and mammalian target of rapamycin (mTOR) signalling pathways contribute to VSMC proliferation in the context of IH.²⁴





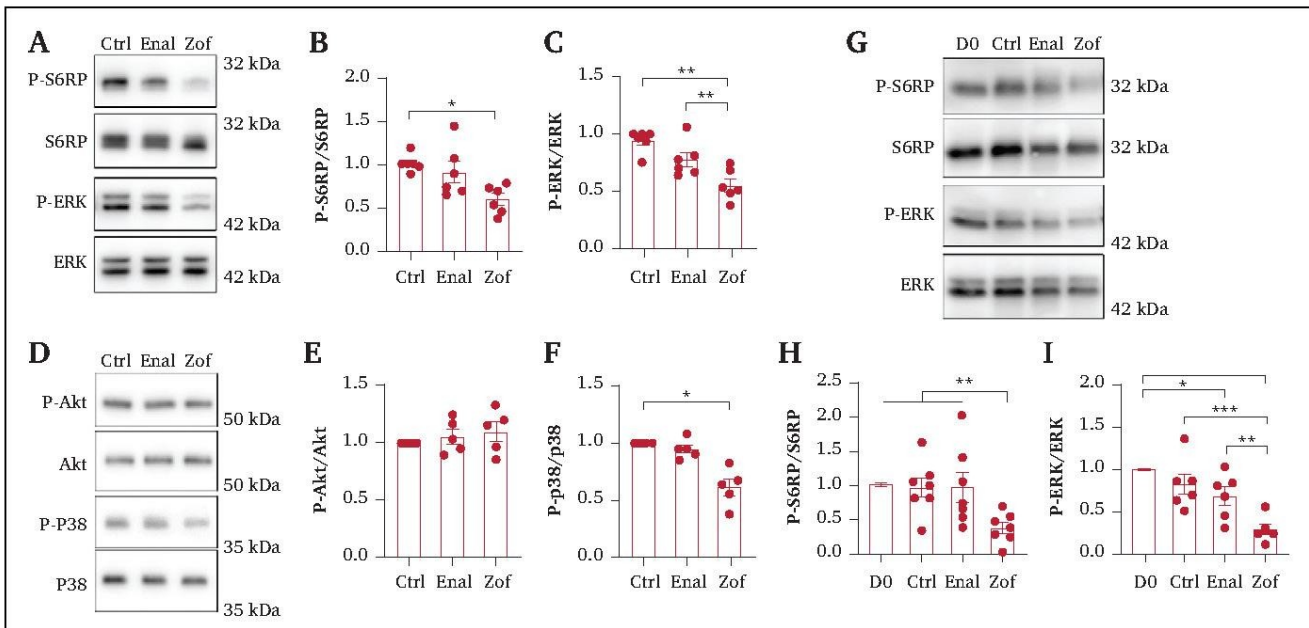


Figure 6. Zofenoprilat inhibits extracellular regulated kinase (ERK) and S6RP phosphorylation. (A–F) Western Blot analyses from vascular smooth muscle cells (VSMCs) exposed or not (Ctrl) to 100 μ M zofenoprilat or enalaprilat for five hours. (A, D) Representative Western blot for P-S6RP and total S6RP, P-ERK, and total ERK, P-Akt and total Akt, P-p38 and total p38. (B, C, E, F) Quantitative assessment of six independent experiments, normalised to their respective Ctrl condition, with mean \pm standard error of mean (SEM). * p < .050 and ** p < .010, as determined by repeated measures one way analysis of variance (ANOVA) with post hoc t test with Dunnett's correction for multiple comparisons. (G–I) Western blot analyses from human vein segments exposed or not (Ctrl) to 100 μ M zofenoprilat or enalaprilat for seven days. (G) Representative Western blot for P-S6RP and total S6RP, P-ERK, and total ERK. (H, I) Quantitative assessment of seven different veins, normalised to their respective control condition, with mean \pm SEM. * p < .050, ** p < .010, and *** p < .001, as determined by repeated measures one way ANOVA with post hoc t test with Dunnett's correction for multiple comparisons.

Western blot analyses revealed that zofenoprilat reduced by 50% the levels of P-ERK1,2, P-p38, and P-S6RP in cultured VSMCs, while enalaprilat had no effect (Fig. 6A–F). Moreover, P-S6RP and P-ERK1,2 levels were also decreased by zofenoprilat in human vein segments placed in culture for seven days (Fig. 6G–I).

DISCUSSION

In this study, it was hypothesised that zofenopril, an ACEi with a free thiol moiety acting as an H₂S donor, would be more efficient than other ACEi in the inhibition of IH in the context of hypertension. Zofenopril is not only more potent than enalapril in reducing IH in hypertensive Cx40^{-/-} mice, but it also suppresses IH in the normotensive condition, where other ACEi have no effect. Furthermore, zofenopril prevents IH in human saphenous vein segments in the absence of blood flow. The effect of zofenopril on IH correlates with reduced VSMC proliferation and migration, and decreased activity of the MAPK and mTOR pathways.

Several preclinical studies have shown that that SBP lowering medication such as ACEi reduce IH,¹² which prompted the large scale MERCATOR (Multicenter European Research Trial with Cilazapril after Angioplasty to prevent Transluminal Coronary Obstruction and Restenosis)/MARCATOR (Multicenter American Research Trial With Cilazapril After Angioplasty to Prevent Restenosis) and PARIS clinical trials.^{13–15} Here, it was also observed that lowering SBP with enalapril had a non-significant tendency

to protect from IH in hypertensive mice. However, enalapril, quinapril and lisinopril had no effect in normotensive WT mice. The fact that the sulfhydrated ACEi zofenopril almost abrogated IH in hypertensive and normotensive mice strongly supports the hypothesis that this ACEi provides additional effects independent of its ACEi activity, as suggested previously.^{16–18} Of interest, the SMILE (Survival of Myocardial Infarction Long-term Evaluation) clinical trials concluded that, compared with placebo or ramipril, zofenopril reduced the one year risk of cardiovascular events after acute myocardial infarction (MI).²⁵ These benefits might be related to H₂S release by zofenopril, as preclinical studies consistently show that H₂S supplementation promotes recovery after acute MI.⁴

Zofenopril has been proposed in several studies to work as a H₂S donor.^{16–18} Here, it was confirmed that zofenoprilat releases detectable amounts of H₂S. H₂S modifies proteins by post-translational persulfidation (S-sulfhydration) of reactive cysteine residues, which modulate protein structure and/or function.²³ Here, it was seen that zofenopril increases overall protein persulfidation *in vivo*, suggesting that zofenopril also generates H₂S *in vivo*.

It has previously been demonstrated that various H₂S donors inhibit VSMC proliferation.^{6,8,26} It was consistently confirmed that zofenopril inhibits VSMC proliferation and migration *in vitro* and reduces cell proliferation in the carotid wall *in vivo*. Although the exact mechanisms of action of Zofenoprilat and H₂S remain to be elucidated, it was

demonstrated that zofenoprilat inhibits the MAPK and mTOR signalling pathways, which contribute to VSMC proliferation and neointima formation.²⁴ Overall, the data strongly suggest that zofenopril acts similarly to other known H₂S donors to limit IH through inhibition of the MAPK and mTOR signalling pathways, leading to decreased VSMC proliferation and migration.

Overall, the data suggest that zofenopril, unlike other ACEi, might show benefits against re-stenosis in patients. These findings raise the question as to whether the scientific community was too quick to discard the whole class of ACEi as a treatment of re-stenosis based on the disappointing results of the MERCATOR/MARCATOR and PARIS trials.^{13–15} In the last decade, many efforts have been made in the development of a local drug delivery strategy well adapted to endovascular interventions. However, this strategy seems to bring great improvement in the mid term but not in the long term.² Thus, a more chronic approach, sustaining the early effect on cell proliferation and IH inhibition, should be encouraged. Such a strategy relies on oral medication, which is also better adapted to open surgery.

The present study had some limitations. Firstly, numerous oral drugs to limit re-stenosis have been tested clinically over the years, and in most trials the pharmacological treatment of re-stenosis failed to show positive results, despite promising results obtained in experimental models.²⁷ While there is no doubt that preclinical models have significantly advanced understanding of the mechanisms of re-stenosis formation, none fully mimics re-stenosis in humans. The genetic model of renin dependent hypertension used in that study is rarely observed in patients, which have complex multifactorial essential hypertension. Additional studies that better reflect comorbidities (dyslipidaemia, renal insufficiency, smoking, atherosclerosis, etc.) with a vein bypass model and larger animal models, or a small phase II clinical trial, are required before testing the benefits of zofenopril in a large, phase III clinical trials.

Secondly, although zofenopril was the only ACEi to provide benefits in the normotensive condition, it cannot be excluded that other ACEi not tested here could work as well. It is further acknowledged that pharmacokinetic and pharmacodynamic differences between zofenopril and other ACEi may contribute to the superiority of zofenopril. Zofenopril is more lipophilic and may have better tissue penetration than enalapril or ramipril, which may have an impact beyond the effect of H₂S liberated by zofenopril. However, it has been shown that vessel wall penetration of various ACEi is independent of lipophilia and that the endothelium constitutes no specific barrier for the passage of ACEi.²⁸

Finally, the working hypothesis is that zofenopril inhibits VSMC proliferation via direct release of H₂S at the level of the vessel media. However, it could not be ascertained that H₂S is released at the level of the VSMC. H₂S and zofenoprilat have been shown to promote endothelial cell function,^{9,17,18} including proliferation and migration. Thus, it cannot be excluded that zofenopril limits IH via a positive effect on endothelial cells. Further studies are required to

assess carefully the impact of zofenopril on the endothelium and quantify H₂S in vascular tissue.

Conclusion

Under the conditions of these experiments, zofenopril was superior to enalapril in reducing IH and providing a beneficial effect against IH in mice and in a model of IH in human vein segments *ex vivo*. The data strongly support the suggestion that zofenopril limits the development of IH via H₂S release, independently of its ACEi activity. The effects of zofenopril correlate with reduced MAPK and mTOR pathway activity, leading to decreased VSMC proliferation and migration.

Given the number of patients treated with ACEi worldwide, these findings may have broad implications for the treatment of patients suffering from peripheral atherosclerotic disease undergoing revascularisation, and beyond. These results warrant further research to evaluate the benefits of zofenopril in limiting re-stenosis and, eventually, prospective clinical trials to test the superiority of sulfhydrylated ACEi on re-stenosis over other ACEi.

FUNDING

This work was supported by the Swiss National Science Foundation (grant FN-310030_176158 to FA and SD, and PZ00P3-185927 to AL), the Union des Sociétés Suisses des Maladies Vasculaires (to SD), and the Novartis Foundation (to FA). The funders had no involvement in study design; in the collection, analysis, and interpretation of data; in the writing of the report; or in the decision to submit the article for publication.

CONFLICT OF INTEREST

None.

ACKNOWLEDGEMENTS

The authors thank Professor Jacques-Antoine Haefliger for providing the Cx40^{-/-} mice. The authors also thank the mouse pathology facility for their histology services (<https://www.unil.ch/mpf>).

APPENDIX A. SUPPLEMENTARY DATA

Supplementary data to this article can be found online at <https://doi.org/10.1016/j.ejvs.2021.09.032>.

REFERENCES

- 1 Davies MG, Hagen PO. Reprinted article “Pathophysiology of vein graft failure: a review”. *Eur J Vasc Endovasc Surg* 2011;42(Suppl. 1):S19–29.
- 2 Phillips J. Drug-eluting stents for PAD: what does (all) the data tell us? *J Cardiovasc Surg (Torino)* 2019;60:433–8.
- 3 Islam KN, Polhemus DJ, Donnarumma E, Brewster LP, Lefer DJ. Hydrogen sulfide levels and nuclear factor-erythroid 2-related factor 2 (NRF2) activity are attenuated in the setting of critical limb ischemia (CLI). *J Am Heart Assoc* 2015;4:e001986.
- 4 Zhang L, Wang Y, Li Y, Li L, Xu S, Feng X, et al. Hydrogen sulfide (H₂S)-releasing compounds: therapeutic potential in cardiovascular diseases. *Front Pharmacol* 2018;9:1066.

- 5 Ma B, Liang G, Zhang F, Chen Y, Zhang H. Effect of hydrogen sulfide on restenosis of peripheral arteries after angioplasty. *Mol Med Rep* 2012;**5**:1497–502.
- 6 Longchamp A, Kaur K, Macabrey D, Dubuis C, Corpataux JM, Deglise S, et al. Hydrogen sulfide-releasing peptide hydrogel limits the development of intimal hyperplasia in human vein segments. *Acta Biomater* 2019;**97**:347–84.
- 7 Yang G, Li H, Tang G, Wu L, Zhao K, Cao Q, et al. Increased neointimal formation in cystathionine gamma-lyase deficient mice: role of hydrogen sulfide in alpha5beta1-integrin and matrix metalloproteinase-2 expression in smooth muscle cells. *J Mol Cell Cardiol* 2012;**52**:677–88.
- 8 Yang G, Wu L, Bryan S, Khaper N, Mani S, Wang R. Cystathionine gamma-lyase deficiency and overproliferation of smooth muscle cells. *Cardiovasc Res* 2010;**86**:487–95.
- 9 Li Z, Polhemus DJ, Lefer DJ. Evolution of Hydrogen sulfide therapeutics to treat cardiovascular disease. *Circ Res* 2018;**123**:590–600.
- 10 Venermo M, Sprynger M, Desormais I, Bjorck M, Brodmann M, Cohnert T, et al. Editor's Choice – Follow-up of patients after revascularisation for peripheral arterial diseases: a consensus document from the European Society of Cardiology Working Group on Aorta and Peripheral Vascular Diseases and the European Society for Vascular Surgery. *Eur J Vasc Endovasc Surg* 2019;**58**:641–53.
- 11 Flu HC, Tamsma JT, Lindeman JH, Hamming JF, Lardenoye JH. A systematic review of implementation of established recommended secondary prevention measures in patients with PAOD. *Eur J Vasc Endovasc Surg* 2010;**39**:70–86.
- 12 Osgood MJ, Harrison DG, Sexton KW, Hocking KM, Voskresensky IV, Komalavilas P, et al. Role of the renin-angiotensin system in the pathogenesis of intimal hyperplasia: therapeutic potential for prevention of vein graft failure? *Ann Vasc Surg* 2012;**26**:1130–44.
- 13 Meurice T, Bauters C, Hermant X, Codron V, VanBelle E, Mc Fadden EP, et al. Effect of ACE inhibitors on angiographic restenosis after coronary stenting (PARIS): a randomised, double-blind, placebo-controlled trial. *Lancet* 2001;**357**:1321–4.
- 14 Does the new angiotensin converting enzyme inhibitor cilazapril prevent restenosis after percutaneous transluminal coronary angioplasty? Results of the MERCATOR study: a multicenter, randomized, double-blind placebo-controlled trial. Multicenter European Research Trial with Cilazapril after Angioplasty to Prevent Transluminal Coronary Obstruction and Restenosis (MERCATOR) Study Group. *Circulation* 1992;**86**:100–10.
- 15 Faxon DP. Effect of high dose angiotensin-converting enzyme inhibition on restenosis: final results of the MARCATOR Study, a multicenter, double-blind, placebo-controlled trial of cilazapril. The Multicenter American Research Trial With Cilazapril After Angioplasty to Prevent Transluminal Coronary Obstruction and Restenosis (MARCATOR) Study Group. *J Am Coll Cardiol* 1995;**25**:362–9.
- 16 Bucci M, Vellecco V, Cantalupo A, Brancaleone V, Zhou Z, Evangelista S, et al. Hydrogen sulfide accounts for the peripheral vascular effects of zofenopril independently of ACE inhibition. *Cardiovasc Res* 2014;**102**:138–47.
- 17 Monti M, Terzuoli E, Ziche M, Morbidelli L. H₂S dependent and independent anti-inflammatory activity of zofenoprilat in cells of the vascular wall. *Pharmacol Res* 2016;**113**:426–37.
- 18 Terzuoli E, Monti M, Vellecco V, Bucci M, Cirino G, Ziche M, et al. Characterization of zofenoprilat as an inducer of functional angiogenesis through increased H₂ S availability. *Br J Pharmacol* 2015;**172**:2961–73.
- 19 Allagnat F, Haefliger JA, Lambelet M, Longchamp A, Berard X, Mazzolai L, et al. Nitric oxide deficit drives intimal hyperplasia in mouse models of hypertension. *Eur J Vasc Endovasc Surg* 2016;**51**:733–42.
- 20 Le Gal L, Alonso F, Wagner C, Germain S, Nardelli Haefliger D, Meda P, et al. Restoration of connexin 40 (Cx40) in renin-producing cells reduces the hypertension of Cx40 null mice. *Hypertension* 2014;**63**:1198–204.
- 21 Tao M, Mauro CR, Yu P, Favreau JT, Nguyen B, Gaudette GR, et al. A simplified murine intimal hyperplasia model founded on a focal carotid stenosis. *Am J Pathol* 2013;**182**:277–87.
- 22 National Research Council (U.S.). *Guide for the Care and Use of Laboratory Animals*. 8th edn. Washington, DC: National Academies Press; 2011.
- 23 Zivanovic J, Kouroussis E, Kohl JB, Adhikari B, Bursac B, Schott-Roux S, et al. Selective persulfide detection reveals evolutionarily conserved antiaging effects of S-sulfhydration. *Cell Metab* 2019;**30**:1152–70.
- 24 Owens GK, Kumar MS, Wamhoff BR. Molecular regulation of vascular smooth muscle cell differentiation in development and disease. *Physiol Rev* 2004;**84**:767–801.
- 25 Borghi C, Omboni S, Novo S, Vinereanu D, Ambrosio G, Ambrosioni E. Efficacy and safety of zofenopril versus ramipril in the treatment of myocardial infarction and heart failure: a review of the published and unpublished data of the randomized double-blind SMILE-4 study. *Adv Ther* 2018;**35**:604–18.
- 26 Wang Y, Wang X, Liang X, Wu J, Dong S, Li H, et al. Inhibition of hydrogen sulfide on the proliferation of vascular smooth muscle cells involved in the modulation of calcium sensing receptor in high homocysteine. *Exp Cell Res* 2016;**347**:184–91.
- 27 Seedial SM, Ghosh S, Saunders RS, Suwanabol PA, Shi X, Liu B, et al. Local drug delivery to prevent restenosis. *J Vasc Surg* 2013;**57**:1403–14.
- 28 Raasch W, Dendorfer A, Ball B, Dominiak P. The lipophilic properties of angiotensin I-converting enzyme inhibitors do not influence their diffusion through cultured endothelium. *Jpn J Pharmacol* 1999;**81**:346–52.

Supplemental Table S1: Materials

product	Vendor	Catalog #	Working concentration
Zofenopril 30mg	Mylan SA		10mg/kg/day
Enalapril 20mg	Mepha Pharma		6mg/kg/day
Accupro "Quinaprilum" 20mg (Quinapril)	Pfizer		10mg/kg/day
Lisinopril 10mg	Mepha Pharma		10mg/kg/day
Zofenoprilat	Santa Cruz Biotech	Sc-220412	100µM
Enalaprilat	Sigma-Aldrich	e9858	100µM
Quinaprilat	Santa Cruz Biotech	sc-208193A	100µM
Lisinopril (pure active compound)	Santa Cruz Biotech	sc-205378	100µM
P-S6RP (Ser 236)	Cell Signaling Technology	#4858	1/1000
S6RP	Cell Signaling Technology	#2217	1/2000
P-ERK1,2 (Tyr 202-204)	Cell Signaling Technology	#4370	1/2000
ERK1,2	Cell Signaling Technology	#4695	1/5000
P-p38 (Thr 180/182)	Cell Signaling Technology	#9211	1/1000
p38	Cell Signaling Technology	#9212	1/1000
P-AKT (Ser 473)	Cell Signaling Technology	#4051	1/1000
AKT	Cell Signaling Technology	#9272	1/1000
HRP-Streptavidin	Sigma-Aldrich	RABHRP3	1/5000
Anti-Rabbit HRP	Invitrogen	#31460	1/20000
Anti-mouse HRP	Jackson ImmunoResearch	115-035-146	1/15000
BrdU	BD Biosciences	555627	1/200
PCNA	Dako, Baar, Switzerland	M0879	1/100
SF ₇ -AM fluorescent probe	Sigma-Aldrich	748110	
Daz-2	Cayman Chemicals	13382	
alkynyl biotin	Cayman Chemicals	13038	
copper(II)-TBTA	Lumiprobe	21050	
4-Chloro-7-nitrobenzofurazan	Sigma-Aldrich	163260	
Pierce™ BCA Protein Assay Kit	ThermoFisher Scientific	23225	
Pierce™ Reversible Protein Stain Kit for PVDF Membranes	Thermo Fisher Scientific	24585	
DC™ Protein Assay Kit I	Bio-Rad	5000111	
Dako EnVision® + Dual Link System-HRP (DAB+)	Agilent	K4065	
EGM™-2 (Endothelial Cell Growth Medium-2 BulletKit™)	Lonza	CC-3162	
RPMI 1640 Medium, GlutaMAX™ Supplement	Thermo Fisher Scientific	61870036	
Ketasol-100 (Ketamine)	Gräub E.Dr.AG, Switzerland	QN01AX03	
Rompun® 2% (Xylazine)	Provet AG, Switzerland	QN05CM92	
Temgesic® (Buprenorphin)	Reckitt Benckiser	N02AE01	

Supplemental Table S2: Detailed results table for Cx40^{-/-} mice

Cx40^{-/-} mice

	Ctrl	Enalapril	Zofenopril
Intima Thickness	96.1±13.7 (n=11)	67.1±13.3 (n=6)	16.8±6.3 (n=9)
Media Thickness	41.7±2.1 (n=11)	42.1±0.6 (n=6)	40.4±0.8 (n=9)
I/M	2.34±0.33 (n=11)	1.7±0.35 (n=6)	0.39±0.13 (n=9)

Supplemental Table S3: Detailed results table for WT mice

Wild type mice

	Ctrl	Enalapril	Zofenopril
Intima Thickness	38.3±7.2 (n=9)	42.1±10.9 (n=10)	6±2.8 (n=8)
Media Thickness	37.7±0.9 (n=9)	37.9±1.2 (n=10)	36.9±0.9 (n=8)
I/M	0.96±0.21 (n=9)	1.14±0.28 (n=10)	0.16±0.07 (n=8)

Supplemental Table S4: Detailed results table for WT mice

Wild type mice

	Ctrl	Quinapril	Lisinopril
Intima Thickness	33.4±7.1 (n=6)	40.5±9.1 (n=6)	37.7±12.4 (n=5)
Media Thickness	34.8±1.2 (n=6)	34.5±1.4 (n=6)	36.6±1.4 (n=5)
I/M	1.06±0.25 (n=6)	1.27±0.38 (n=6)	1.08±0.37 (n=5)

Supplemental Table S5: Detailed results table for human vein segments

Human vein segments

	D0	D7	D7-Enalapril	D7-Zofenopril
Intima Thickness	27.6±8.1 (n=6)	80.1±23.9 (n=6)	47.1±16.7 (n=5)	33.4±11.9 (n=6)
Media Thickness	522.3±59.7 (n=6)	578.9±74.6 (n=6)	578.4±73.5 (n=5)	548.7±79.1 (n=6)
I/M	0.05±0.01 (n=6)	0.13±0.02 (n=6)	0.08±0.02 (n=5)	0.05±0.01 (n=6)

SUPPLEMENTAL FIGURES

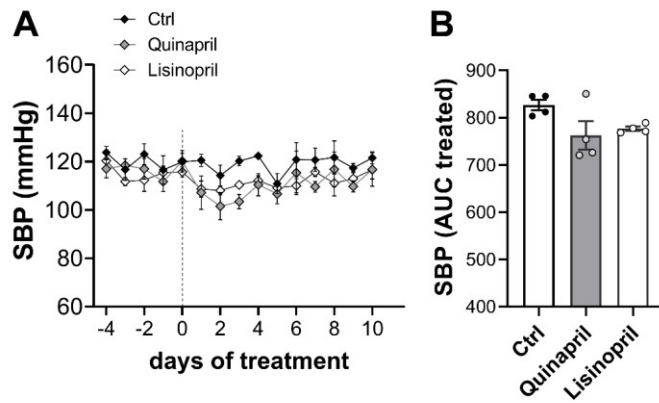


Figure S1. Quinapril and Lisinopril do not reduce SBP in WT mice

A) Daily systolic blood pressure (SBP) values (mean±SEM) in WT mice treated or not (Ctrl) with Quinapril (10 mg/kg) or Lisinopril (10 mg/kg) in 4 animals per group with mean±SEM. **B)** area under the curve (AUC) of SBP from day 0 to 10.

No statistical difference as determined by one-way ANOVA with Tukey's correction for multiple comparisons.

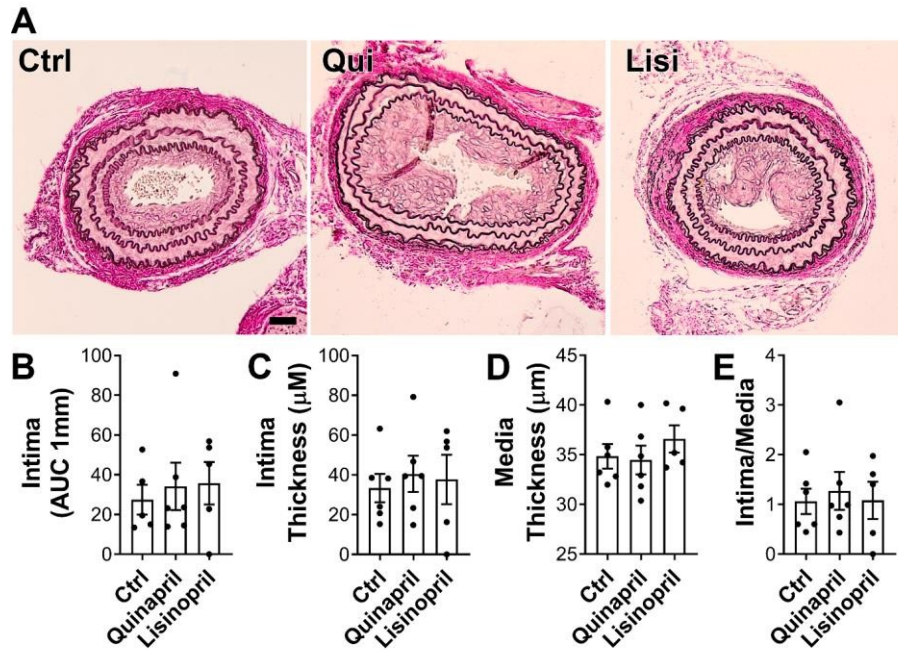


Figure S2. Quinapril and Lisinopril do not reduce IH in a mouse model of carotid artery stenosis

WT mice treated or not (Ctrl) with Quinapril (Qui) or Lisinopril (Lisi), were submitted to carotid artery stenosis. **A)** Representative left carotid cross sections stained with VGEL 28 days post-surgery. Scale bar represents 30 μm . **B-D)** Data are morphometric measurements of area under the curve (AUC) of intima thickness (**B**) intima thickness (**C**), media thickness (**D**) and intima over media ratio (**E**). Data are scatter plots of 5 to 6 animals per group with mean \pm SEM. No statistical difference as calculated by two-way ANOVA with Tukey's correction of multiple comparisons.

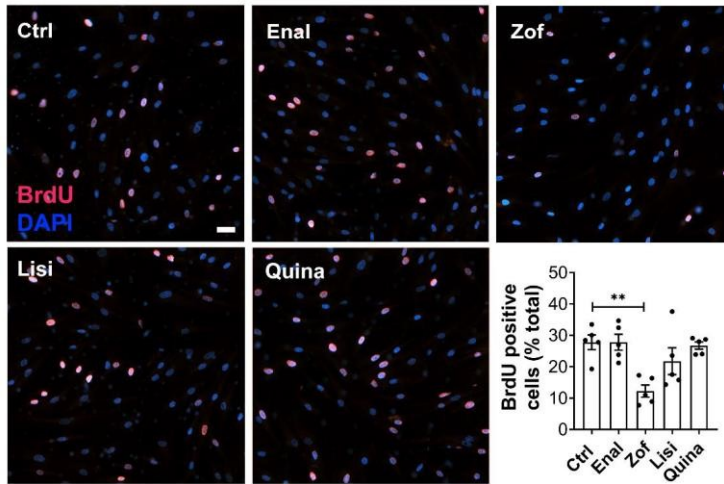


Figure S3. Quinaprilat and Lisinopril do not reduce VSMC proliferation.

Primary human vascular smooth muscle cells (VSMC) were exposed or not (Ctrl) to 100 μ M Zofenoprilat, Enalaprilat, Lisinopril or Quinaprilat for 24 h in presence of BrdU. Bar scale represents 20 μ m. Proliferation was calculated as the percentage of BrdU-positive nuclei (pink) over total DAPI-stained nuclei (blue). Data are shown as scatter plots of 5 independent experiments with mean \pm SEM. ** p <.01 as determined by paired one-way ANOVA with post-hoc t-test with Dunnet's correction for multiple comparisons.

7.3 Sodium thiosulfate, a source of hydrogen sulfide, promotes endothelial cells proliferation, angiogenesis and reperfusion following hind-limb ischemia in the mouse.

In this study, we tested the therapeutic potential of STS to promote reperfusion and angiogenesis *in vivo* in various models and investigated STS effects on cultured EC. We showed that STS promotes reperfusion following hindlimb ischemia. STS also promotes angiogenesis in matrigel plug implants and in the CAM model. STS stimulated EC proliferation and migration *in vitro* via metabolic reprogramming towards a more glycolytic state.

This study is almost ready for submission in the journal Frontiers and is therefore presented as already formatted according to Frontiers guidelines.

Sodium thiosulfate, a source of hydrogen sulfide, promotes endothelial cells proliferation, angiogenesis and reperfusion following hind-limb ischemia in the mouse.

1 **Diane Macabrey¹, Jaroslava Joniová², Quentin Gasser¹, Clémence Bechelli¹, Alban**
2 **Longchamp¹, Severine Urfer¹, Martine Lambelet¹, Georges Wagnieres², Sébastien Déglise¹, †**
3 **and Florent Allagnat¹†***

4 ¹Department of Vascular Surgery, Lausanne University Hospital, Lausanne, Switzerland

5 ²Laboratory for functional and metabolic imaging, LIFMET, Swiss Federal Institute of Technology
6 (EPFL), Lausanne, Switzerland.

7 †These authors have contributed equally to this work and share senior authorship

8

9 *** Correspondence:**

10 Florent Allagnat
11 CHUV-Service de chirurgie vasculaire
12 Département des Sciences Biomédicales
13 Bugnon 7A, 1005 Lausanne, Suisse
14 Florent.allagnat@chuv.ch

15 Article Type: Original Research

16 **Keywords: arteriogenesis¹, angiogenesis², peripheral arterial disease³, hydrogen sulfide (H₂S)⁴,**
17 **endothelial cells⁵, ischemia⁶.**

18

20 **Abstract**

21 Therapies to accelerate vascular repair are currently lacking. Pre-clinical studies suggest that
22 hydrogen sulfide (H₂S), an endogenous gasotransmitter, promotes angiogenesis. Here, we
23 hypothesized that sodium thiosulfate (STS), a clinically relevant H₂S donor substance, would
24 stimulate angiogenesis and vascular repair.

25 STS stimulated arteriogenesis and revascularization following hindlimb ischemia as evidenced by
26 increased laser Doppler imaging leg perfusion and vascular density in the gastrocnemius muscle in
27 wild type and LDL receptor knock-out C57BL/6J mice. STS also promoted angiogenesis in a
28 matrigel plug assay *in vivo* and *in ovo* in a chick chorioallantoic membrane angiogenesis assay. *In*
29 *vitro*, STS and NaHS stimulated HUVEC migration and proliferation. Seahorse experiments further
30 revealed that STS, as well as NaHS, inhibited mitochondrial respiration and promoted glycolysis in
31 HUVECs. The effect of STS on migration and proliferation was glycolysis-dependent.

32 STS, a clinically pertinent source of H₂S, promotes angiogenesis and revascularization in a model of
33 hindlimb ischemia. STS probably acts through metabolic reprogramming of endothelial cells toward
34 a more proliferative glycolytic state. These findings may hold broad clinical implications for patients
35 suffering from vascular occlusive diseases.

36

37 **1 Introduction**

38 Prevalence of peripheral artery disease (PAD) continues to rise worldwide, largely because of the
39 combination of aging, smoking, hypertension, and diabetes mellitus (1-3). PAD is due to
40 atherosclerosis, which leads to progressive obstruction of peripheral arteries. In severe
41 manifestations, PAD can progress to critical limb ischemia (CLI), which can lead to amputation if
42 not for surgical revascularization.

43 Hydrogen sulfide (H₂S) is an endogenous gasotransmitter derived from the cysteine metabolism.
44 Although environmental exposure to high H₂S is toxic, endogenous H₂S is now recognized as having
45 important vaso-relaxant, cyto-protective and anti-inflammatory properties (4). More specifically,
46 several *in vivo* studies investigated the effect of H₂S on recovery in models of PAD/CLI after skeletal
47 limb ischemia. Thus, NaHS or GYY4137 supplementation significantly increased revascularization in
48 mice after femoral artery ligation (HLI) (5, 6). Rushing et al. further showed that SG1002, a H₂S
49 releasing pro-drug, increases leg revascularization and collateral vessel number after occlusion of the
50 external iliac artery in miniswine (7). In these studies, H₂S effectively increased angiogenesis and
51 arteriogenesis, two processes central for ischemic skeletal muscle repair (8, 9).

52 On a cellular level, H₂S stimulates EC proliferation, migration and angiogenesis (10-13) through
53 several mechanisms. Thus, H₂S stimulates the VEGF pathway in EC, through sulfhydration of the
54 VEGF receptor VEGFR2, increasing its dimerization, autophosphorylation and activation (14). H₂S
55 may also promote eNOS activity and NO production, which is instrumental to EC function and
56 angiogenesis. In addition, H₂S promotes angiogenesis by inhibiting mitochondrial electron transport
57 and oxidative phosphorylation, resulting in increased glucose uptake and glycolytic ATP production
58 necessary to provide rapid energy for EC migration (15). However, despite these potent
59 cardiovascular benefits in pre-clinical studies, H₂S-based therapeutics are not available yet.

60 Sodium thiosulfate (Na₂S₂O₃) is a FDA-approved drug used in gram-quantity doses for the treatment
61 of cyanide poisoning (16) and calciphylaxis, a rare condition of vascular calcification affecting
62 patients with end-stage renal disease (17). Sodium thiosulfate (STS) participates in sulfur metabolism
63 within cells, releasing H₂S through non-enzymatic and enzymatic mechanisms (18, 19). STS protects
64 rat hearts from ischemia reperfusion injury (20), and we recently demonstrated that STS reduce
65 intimal hyperplasia in a mouse model and in human vein segments (21).

66 The aim of the present study was to test whether STS, similarly to other H₂S donors, stimulates
67 arteriogenesis and revascularization in a mouse model of PAD following hindlimb ischemia. STS
68 promoted vascular recovery following ischemia in WT and hypercholesterolemic LDLR^{-/-} mice. STS
69 also promoted angiogenesis in a matrigel plug assay and *in ovo* in the Chick Chorioallantoic
70 Membrane (CAM) angiogenesis assay. As expected, STS promoted HUVEC proliferation and
71 migration, similarly to other H₂S donors. Finally, STS inhibited mitochondrial respiration and
72 promoted glycolysis in EC, and inhibition of glycolysis abrogated the effect of STS in HUVEC.

73 **2 Materials and methods**

74 **2.1 Mice**

75 WT mice C57BL/6JRj (RRID:MGI:5752053) mice were purchased from Janvier Labs (Le Genest-
76 Saint-Isle, France). LDL receptor knock out (LDLR^{-/-}) mice (Ldlrtm1Her, JAX stock #002207 (22);
77 MGI Cat# 3611043, RRID:MGI:3611043), kindly provided by Prof. Caroline Pot (Lausanne
78 university Hospital, Switzerland), were bred and housed in our animal facility and genotyped as

Sodium thiosulfate promotes angiogenesis

79 previously described (22). All mice were housed at standard housing conditions (22 °C, 12 h
80 light/dark cycle), with ad libitum access to water and regular diet (SAFE®150 SP-25 vegetal diet,
81 SAFE diets, Augy, France). LDLR^{-/-} mice were put on a cholesterol rich diet (Western 1635, 0.2%
82 Cholesterol, 21% Butter, U8958 Version 35, SAFE® Complete Care Competence) for 3 weeks prior
83 to surgery. Mice were randomly treated with sodium thiosulfate (STS) or NaHS. Sodium Thiosulfate
84 (Hänseler AG, Herisau, Switzerland) was given in mice water bottle at 2 or 4g/L, changed 3 times a
85 week.

86 2.2 Hindlimb ischemia surgery

87 Hindlimb ischemia surgery was performed under isoflurane anesthesia (2.5% under 2.5 L O₂). Local
88 anesthesia was ensured by subcutaneous injection with a mix of lidocaine (6mg/kg) and bupivacaine
89 (2.5mg/kg) along the incision line. The femoral artery was exposed through a small incision in the
90 upper part of the leg. Two sutures (7-0 silk) were placed above the bifurcation with the epigastric
91 artery. The femoral artery was then cut between the two sutures and the incision was closed with 5-0
92 prolene. Buprenorphine (0.1 mg/kg Temgesic, Reckitt Benckiser AG, Switzerland) was provided
93 before surgery, as well as a post-operative analgesic every 12h for 36 hours. Perfusion of both
94 operated and non-operated contralateral leg was monitored using a High Resolution Laser Doppler
95 Imager (moorLDI2-HIR ; Moor Instruments) under isoflurane anesthesia on a heating pad. Muscles
96 were either put on OCT and frozen in liquid nitrogen, or flash frozen directly in liquid nitrogen. EdU
97 (A10044, ThermoFischer scientific) was diluted in NaCl at a concentration of 2mg/ml and 1 mg was
98 injected via i.p. injection 16 hours before euthanasia. Mice were euthanized at day 4 post HLI,
99 ischemic muscles were placed in OCT and frozen in liquid nitrogen vapor. Mice were euthanized
100 under general anesthesia by cervical dislocation and exsanguination. Surgeries were performed in a
101 random order, alternating mice from different cages to minimise potential confounders such as the
102 order of treatments and measurements, or animal/cage location. All series of surgeries included all
103 the groups to be compared to minimise batch effects. Surgeons were blind to the group during
104 surgeries.

105 2.3 Matrigel plug assay

106 Matrigel plug assay was conducted using Growth factor reduced Matrigel (BD Biosciences)
107 supplemented with 20U/ml heparin (L6510, Seromed) and 200ng/ml human VEGF 165 (100-20,
108 Peprotech), supplemented or not with 15mM STS. 400-500µl of Matrigel was injected
109 subcutaneously under isoflurane anesthesia (2.5% under 2.5 L O₂) on the back of the mouse with a
110 25G needle. Matrigel plugs were isolated seven days after implantation, dissolved overnight in 0.1%
111 Brij L23 (Sigma-aldrich). Haemoglobin content was measured in a 96 well plate via colorimetric
112 assay using 20µl of samples and 180 µl Drabkin's reagent (D5941, Sigma-aldrich). Absorbance was
113 measured after 20 min incubation at RT in the dark at 540nm using a Synergy Mx plate reader
114 (BioTek Instruments AG, Switzerland). Data were plotted against a standard curve of ferrous
115 stabilized human Hemoglobin A0 (H0267, Sigma-aldrich).

116 2.4 Bioethics

117 All animal experimentations conformed to the National Research Council: Guide for the Care and
118 Use of Laboratory Animals (23). All animal care, surgery, and euthanasia procedures were approved
119 by the CHUV and the Cantonal Veterinary Office (SCAV-EXPANIM, authorization number 3504).

120 2.5 Cell culture

Sodium thiosulfate promotes angiogenesis

121 Pooled HUVECs (Lonza) were maintained in EGMTM-2 (Endothelial Cell Growth Medium-2
122 BulletKitTM;Lonza) at 37°C, 5% CO₂ and 5% O₂ as previously described (24). Passages 1 to 8 were
123 used for the experiments.

124 2.6 Chicken chorioallantoic membrane (CAM)

125 Fertilized brown chicken eggs were purchased from Animalco AG, Switzerland. Eggs were
126 incubated for three days at 37 °C in an automatically rotating and humidified incubator with the blunt
127 end up. Then, at embryo development day (EDD) 3, at the pointed end of the shell, a small hole was
128 made (diameter: 3 mm) and covered with a tape. Until a further use, eggs were placed back to the
129 incubator in a stationary position. On EDD 11, the hole was enlarged to a diameter of 25 mm
130 enabling topical administration of 20 µl of a fresh STS solution (500 µM – 20 mM in sodium
131 chloride solution (NaCl; BioConcept, Swizerland)). 20 µl of 0.9 % NaCl was topically administered
132 on the CAM for all the control eggs. The concentrations of STS are relative to the weight of the
133 embryo at EDD 11. After STS administration, the hole was covered with a parafilm and eggs were
134 returned to the incubator. The fluorescent angiograms were recorded at EDD 13, 2 days after STS
135 administration. 20 µl of fluorescein isothiocyanate – dextran (25 kD, 25 mg/ml; Sigma – Aldrich,
136 Switzerland) dissolved in NaCl was intravenously injected to the CAM's vascular network. At the
137 same time, 100 µl of India ink (Parker) was injected under the CAM in order to improve the contrast
138 between the blood vessels and extravascular space of the CAM. An epifluorescent microscope
139 (Eclipse E 600 FN Nikon) was used for the acquisition of the angiograms using a 10x objective
140 (Nikon, Plan Fluor, NA: 0.30, WD 16.0). Effect of STS on the vascular network of the CAM was
141 quantified utilizing the quantitative analysis of the fluorescent angiograms in ImageJ Macro (NIH,
142 Bethesda, Maryland) that was developed in our laboratory (25). 5 eggs were dedicated to one
143 condition with 3 images taken per one egg (altogether, 15 images per condition were analyzed).

144 2.7 H₂S and persulfidation measurement

145 Free H₂S was measured in cells using the SF₇-AM fluorescent probe(26) (Sigma-Aldrich). The probe
146 was dissolved in anhydrous DMF at 5 mM and used at 5 µM in serum-free EBM-2. Persulfidation
147 staining was performed on HUVEC grown on glass coverslips. Briefly, 1mM 4-Chloro-7-
148 nitrobenzofurazan (NBF-Cl, Sigma) was diluted in PBS and added to live cells for 20 minutes. Cells
149 were washed with PBS then fixed for 10 minutes in ice-cold methanol. Coverslips were rehydrated in
150 PBS, and incubated with 1mM NBF-Cl for 1h at 37°C. Daz2-Cy5.5 (prepared with 1mM Daz-2,
151 1mM alkyne Cy5.5, 2mM copper(II)-TBTA, 4mM ascorbic acid with overnight incubation at RT,
152 followed by quenching for 1h with 20mM EDTA) was added to the coverslips and incubated at 37°C
153 for 1h. After washing with methanol and PBS, coverslips were mounted in vectashield mounting
154 medium with DAPI and visualized with a 90i Nikon fluorescence microscope.

155 2.8 Wound healing assay

156 HUVEC were grown to confluence in a 12-well plate and a scratch wound was created using a sterile
157 p200 pipette tip. Repopulation of the wound in presence of Mitomycin C was recorded by phase-
158 contrast microscopy over 16 hours in a Nikon Ti2-E live-cell microscope. The denuded area was
159 measured at t=0h and t=10h after the wound using the ImageJ software. Data were expressed as a
160 ratio of the healed area over the initial wound area.

161 2.9 BrdU assay

Sodium thiosulfate promotes angiogenesis

162 HUVEC were grown at 80% confluence ($5 \cdot 10^3$ cells per well) on glass coverslips in a 24-well plate
163 and starved overnight in serum-free medium (EBM-2, Lonza).. Then, HUVEC were either treated or
164 not (ctrl) with the drug of choice for 24 hours in full medium (EGM-2, Lonza) in presence of $10 \mu\text{M}$
165 BrdU. All conditions were tested in parallel. All cells were fixed in ice-cold methanol 100% after 24
166 hours of incubation and immunostained for BrdU. Images were acquired using a Nikon Eclipse 90i
167 microscope. BrdU-positive nuclei and total DAPI-positive nuclei were automatically detected using
168 the ImageJ software (24).

169 **2.10 Seahorse**

170 Glycolysis and Mitochondrial stress tests were performed on confluent HUVECs according to the
171 manufacturer's kit and protocol (Agilent Seahorse XF glycolysis stress test kit, Agilent Technologies,
172 IncAgilent technologies). $1 \mu\text{M}$ Oligomycin was used for HUVEC. Cells were pretreated for 4 or 24
173 hours with NaHS or STS before the seahorse experiments. Data were analyzed using the Seahorse
174 Wave Desktop Software (Agilent Technologies, Inc. Seahorse Bioscience).

175 **2.11 ATP Assay**

176 HUVEC were grown at 80% confluence ($10 \cdot 10^3$ cells per well) in a 12-well plate and starved
177 overnight in serum-free medium (EBM-2, Lonza). Then, HUVEC were either treated or not (ctrl)
178 with 3mM STS for 24 hours in full medium (EGM-2, Lonza), washed in ice-cold PBS and
179 resuspended according to the ATP Assay Kit (Colorimetric/Fluorometric) (ab83355, Abcam).

180 **2.12 Immunohistochemistry**

181 Ischemic and contralateral gastrocnemius muscle were collected and flash frozen in OCT 2 weeks
182 post-op. OCT blocks were cut into $10 \mu\text{M}$ slides for immunostaining. Muscle sections were
183 permeabilized in PBS supplemented with 2 wt. % BSA and 0.1 vol. % Triton X-100 for 30 min,
184 blocked in PBS supplemented with 2 wt. % BSA and 0.1 vol. % Tween 20 for another 30 min, and
185 incubated overnight using the antibodies described in **Supplemental Table 1** diluted in the same
186 buffer. The slides were then washed 3 times for 5 min in PBS supplemented with 0.1 vol. % Tween
187 20, and incubated for 1 h at room temperature with a mix of fluorescent-labelled secondary
188 antibodies (anti-rabbit AlexaFluor 488 and anti-mouse AlexaFluor 568; 1/1000). EdU
189 immunostaining was performed according to the manufacturer's instructions (Click-iT™ Plus EdU
190 Cell Proliferation Kit for Imaging, Alexa Fluor™ 594 dye, ThermoFisher). Slides were visualized
191 with a Nikon 90i fluorescence microscope and scanned using an Zeiss AxioScan.

192 **2.13 Western blotting**

193 Ischemic and contralateral gastrocnemius muscles were collected and flash-frozen in liquid nitrogen,
194 grinded to power and resuspended in SDS lysis buffer (62.5mM TRIS pH6,8, 5% SDS, 10 mM
195 EDTA). Protein concentration was determined by DC protein assay (Bio-Rad Laboratories, Reinach,
196 Switzerland). 10 to 20 μg of protein were loaded per well. Primary cells were washed once with ice-
197 cold PBS and directly lysed with Laemmli buffer as previously described (24, 27). Lysates were
198 resolved by SDS-PAGE and transferred to a PVDF membrane (Immobilon-P, Millipore AG,
199 Switzerland). Immunoblot analyses were performed as previously described (27) using the antibodies
200 described in Supplemental Table 1. Membranes were revealed by enhanced chemiluminescence
201 (Immobilon, Millipore) using the Azure 280 device (Azure Biosystems) and analysed using Fiji
202 (ImageJ 1.53c). Protein abundance was normalised to total protein using Pierce™ Reversible Protein
203 Stain Kit for PVDF Membranes (cat 24585; Thermo Fisher Scientific).

204 **2.14 Reverse transcription and quantitative polymerase chain reaction (RT-qPCR)**

205 HUVEC or grinded frozen gastrocnemius muscles were homogenised in Tripure Isolation Reagent
206 (Roche, Switzerland), and total RNA was extracted according to the manufacturer's instructions.
207 After RNA Reverse transcription (Prime Script RT reagent, Takara), cDNA levels were measured by
208 qPCR Fast SYBR™ Green Master Mix (Ref: 4385618, Applied Biosystems, ThermoFischer
209 Scientific AG, Switzerland) in a Quant Studio 5 Real-Time PCR System (Applied Biosystems,
210 ThermoFischer Scientific AG, Switzerland), using the primers given in the **Supplemental Table 2.**

211 **2.15 Statistical analyses**

212 All experiments adhered to the ARRIVE guidelines and followed strict randomisation. All
213 experiments and data analysis were conducted in a blind manner using coded tags rather than actual
214 group name. A power analysis was performed prior to the study to estimate sample-size. We
215 hypothesized that STS would increase reperfusion by 30%. Using an SD at +/- 20% for the surgery
216 and considering a power at 0.8, we calculated that n= 8 animals/group was necessary to validate a
217 significant effect of the STS. Animals with pre-existing conditions (malocclusion, injury, abnormal
218 weight) were not operated or excluded from the experiments upon discovery during dissection. A few
219 animals died during surgery or did not recover from surgery and had to be euthanized before the end
220 of the experiment. All experiments were analysed using GraphPad Prism 9. Normal distribution of
221 the data was assessed using Shapiro-Wilk test and Kolmogorov-Smirnov test. All data had a normal
222 distribution. Bilateral unpaired t-tests or one or two-ways ANOVA were performed followed by
223 multiple comparisons using post-hoc t-tests with the appropriate correction for multiple comparisons.

224 **3 Results**

225 **3.1 STS promotes revascularization and muscle recovery in a mouse model of hindlimb**
226 **ischemia**

227 To test the benefits of STS on vascular recovery, hindlimb ischemia (HLI) was induced by
228 transection of the femoral artery, which leads to ischemia-induced muscle damage. Laser Doppler
229 imaging showed that HLI reduced blood flow by >80% both in Ctrl and mice treated with 2 or 4g/L
230 of STS. Doppler imaging further revealed that 2g/L STS improved revascularization (**Figure 1A**),
231 while 4g/L tended to increase blood flow compared to Ctrl mice (**Figure 1C**). Morphological
232 analysis of the gastrocnemius muscle 14 days post-surgery further showed that STS reduced muscle
233 damaged as assessed by the muscle fiber cross-sectional area (**Figure 1B, D**). To model the
234 hyperlipidemia state of patients with PAD, we also performed the HLI on hypercholesterolemic
235 LDLR^{-/-} mice fed for 3 weeks with a cholesterol-rich diet. 2g/L STS also increased revascularization
236 (**Figure 1E**) and reduced muscle damage (**Figure 1F**) in this diseased model.

237 **3.2 STS leads to enzymatic production of H₂S and increases protein persulfidation**

238 We previously demonstrated that STS behaves as a H₂S donor (21, 28), which is known to promote
239 EC proliferation and angiogenesis (13, 24, 29). To test whether STS releases detectable amounts of
240 H₂S in HUVECs, we used the H₂S specific probe SF₇-AM (26). SF₇-AM signal was monitored in
241 HUVECs 90 min post addition of 15mM STS, and showed a 50% increase in SF₇-AM signal (**Figure**
242 **2A**). Thiosulfate is an intermediate of sulfur metabolism metabolized by the H₂S biosynthetic
243 pathway and sulfide-oxidizing unit (30, 31). A 4h treatment with STS, but not NaHS, increased the
244 mRNA expression of sulfite oxidase (SUOX), thiosulfate sulfurtransferase-like domain containing 1
245 (TSTD1), mercaptopyruvate sulfurtransferase (MPST), but not thiosulfate sulfurtransferase (TST) in

246 HUVECs (**Figure 2B**). However, neither STS nor NaHS influenced the mRNA expression of H₂S-
 247 generating enzymes CBS and CSE (**Figure S1**). Of note, both NaHS and STS increased the
 248 expression of the main mitochondrial H₂S-detoxifying enzymes sulfide quinone oxidoreductase
 249 (SQOR) and persulfide dioxygenase ETHE1 (**Figure 2B**). In gastrocnemius muscles from mice
 250 treated with 4g STS for 1 week, STS treatment significantly increased mRNA expression of Tstd2
 251 and Sqor, whereas the expression of Tst was decreased. The mRNA expression of Suox, Mpst and
 252 Ethe1 were not modulated by the STS treatment (**Figure 2C**). The biological activity of H₂S is
 253 mediated by post-translational modification of reactive cysteine residues by persulfidation (32, 33).
 254 As expected, both STS and NaHS increased global protein persulfidation as measured by DAZ-2-
 255 Cy5.5 labelling of persulfide residues in HUVEC treated for 4 hours with 100 μ M NaHS or 15mM
 256 STS (**Figure 2D**).

257 3.3 STS promotes arteriogenesis and angiogenesis in vivo

258 To test whether STS increased blood perfusion via improved micro-vessel regeneration, we
 259 determined the micro-vessel density in the gastrocnemius muscle using VE-Cadherin
 260 immunofluorescent staining of WT mice. Both 2 and 4g/L STS treatment increased the micro-vessel
 261 density as compared to Ctrl mice 14 days after HLI (**Figure 3A-B**). STS treatment also increased the
 262 micro-vessel density in LDLR^{-/-} mice (**Figure 3C**). EdU/Erg immunofluorescent staining on ischemic
 263 muscles 4 days after ischemia showed that STS increased the percentage of EC (**Figure 3D,E**) and
 264 proliferating EC (**Figure 3D,F**). Then, we also assessed the effect of STS on angiogenesis *in vivo*
 265 using the Chicken chorioallantoic membrane (CAM) assay and the Matrigel plug assay. STS was
 266 applied topically to achieve 0.5 or 5mM at embryonic development day 11 (EDD7), when the
 267 vasculature in the developing CAM is still immature. Observations at EDD13 revealed that STS
 268 promoted the capillary formation measured as the relative number of branching points/mm², relative
 269 mean mesh size and Q3 mesh area of the vessel network (**Figure 3G**). The addition of 15mM STS in
 270 Matrigel plugs also promoted VEGF-induced angiogenesis as assessed by hemoglobin content 7 days
 271 after subcutaneous injection in the mouse (**Figure 3H**). To investigate the effect of STS on EC
 272 directly, we assessed the proliferation and migration of primary human umbilical veins endothelial
 273 cells (HUVECs). STS 3mM increased HUVEC proliferation (**Figure 3I**), similarly to the H₂S donor
 274 salt NaHS and the slow-releasing H₂S donor GYY4137 (**Figure S2**). 3mM STS also promoted
 275 HUVEC migration in a wound healing assay (**Figure 3J**). To further study endothelial function, we
 276 investigated known markers of endothelial function (34). A 4h treatment with 3mM STS increased
 277 eNOS and VEGFR2 mRNA expression in HUVEC (**Figure S3A**). Western blot analysis from mice
 278 who underwent hindlimb ischemia treated with STS for 2 weeks revealed that 2 g/L STS increased
 279 the ratio of P-eNOS over eNOS and increased the ratio of P-VEGFR2/VEGFR2 levels in the
 280 ischemic gastrocnemius muscle (**Figure S3B**). Of note, total eNOS and VEGFR2 levels were
 281 decreased following this chronic long-term treatment.

282 3.4 STS limits inflammation and muscle damage 4 days after ischemia

283 After ischemia, inflammation plays a major role in muscle function and repair and the M2 anti-
 284 inflammatory macrophages are instrumental in arteriogenesis following ischemia (35). STS limited
 285 muscle damage in the gastrocnemius muscle of mice 4 days after HLI, as assessed by laminin
 286 staining (**Figure 4A**). Decreased muscle damage was accompanied by a significant reduction in
 287 macrophage infiltration, as assessed by CD68 staining. Furthermore, STS increased the percentage of
 288 HO1⁺ macrophages, a marker of M2 pro-resolving macrophages (**Figure 4B**). Of note, there is no
 289 correlation between muscle damage and percentage of ischemia at day 0.

290 **3.5 STS inhibits mitochondrial respiration and increases glycolysis and ATP production in**
291 **HUVECs**

292 ECs are glycolytic, thus favoring glycolysis for ATP production. This key feature allows EC to
293 proliferate and migrate in hypoxic conditions in the context of angiogenesis (36, 37). H₂S is known to
294 block mitochondrial respiration through inhibition of the complex IV of the mitochondria (38), which
295 increases compensatory glycolysis in EC and promotes angiogenesis (15). To test the effect of STS
296 on mitochondrial respiration, we performed a mitochondrial stress test in a Seahorse apparatus. A 4-
297 hour pre-treatment with STS dose-dependently inhibited oxygen consumption rate (OCR) in
298 HUVECs, leading to reduced basal and max respiration and ATP production in that assay (**Figure**
299 **5A**). To measure the cell's glycolytic reserve, i.e. the ability to increase glycolysis upon inhibition of
300 respiration, we then performed a glycolysis stress test on HUVEC pre-treated for 4 hours with STS or
301 NaHS. Inhibition of mitochondrial respiration using oligomycin promoted glycolysis in the control
302 condition in HUVEC. The donors increased basal glycolysis in HUVEC, thereby reducing the
303 glycolytic reserve (**Figure 5B**). We further confirmed that an 8-hour treatment with 3mM STS
304 increased ATP production in HUVECs (**Figure 5C**). In EC, the enzyme PFKFB3 tightly regulates
305 glycolysis (35). In gastrocnemius muscles treated for one week, 4g/L of STS significantly increased
306 the mRNA expression of PFKFB3, whereas the mRNA of PKM was not affected (**Figure 5D**). Of
307 note, CPT1 mRNA expression was significantly increased in HUVEC with STS and NaHS treatment
308 but not in the muscle. FASN mRNA expression was significantly increased in HUVEC only by STS
309 (**Figure S4**).

310 **3.6 STS-induced HUVEC proliferation requires glycolysis**

311 To confirm that the effect of STS on angiogenesis is glycolysis-dependent, we assessed the
312 proliferation of primary human umbilical vein endothelial cells (HUVECs), in presence or not of the
313 glycolysis inhibitor 3PO or the glucose competitor 2-deoxy-glucose (2-DG). Both 3PO (**Figure 6A**)
314 and 2-DG (**Figure 6B**) treatment reduced basal HUVEC proliferation and fully abolished the positive
315 effect of STS or NaHS on proliferation.

316 **3.7 Endothelial cell identity is tightly regulated by the KLF2 and FOXO1 pathway**

317 Endothelial cell phenotype is tightly regulated by the transcription factors KLF2 and FOXO1. KLF2
318 inhibits EC activation by diverse pro-inflammatory stimuli, regulates key factors involved in
319 maintaining an anti-thrombotic surface, and has potent antiangiogenic effects (39). KLF2 is mostly
320 induced by laminar flow. FOXO1 limits cell cycle progression, metabolic activity and vascular
321 expansion (40). In HUVECs, KLF2 and FOXO1 mRNA expression were both upregulated by 4
322 hours STS treatment, whereas 1 week of 4g/L STS only tended to increase KLF2 in the
323 gastrocnemius muscle (**Figure S5**).

324 **4 Discussion**

325 PAD prevalence continues to rise worldwide due to the combination of aging, smoking, hypertension
326 and diabetes mellitus. In severe manifestations, PAD leads to critical limb ischemia, which can cause
327 amputations if not for surgical revascularization. Unfortunately, treatment options for PAD patients
328 are limited and surgery is not always possible, nor effective. The gasotransmitter H₂S possesses
329 interesting pro-angiogenic and anti-inflammatory properties to develop new treatment for PAD
330 patients. H₂S is very reactive and rapidly transformed into byproducts such as thiols, sulfenic acid,
331 polysulfides and sulfites (41, 42), and there is no clinically-approved H₂S-releasing molecule. STS
332 does not directly release H₂S, but provides thiosulfate, which can be further processed into H₂S (18).

Sodium thiosulfate promotes angiogenesis

333 Our study supports that STS treatment promotes the enzymatic metabolism of thiosulfate through
334 both the H₂S biosynthetic pathway and sulfide oxidizing unit (30, 31), yielding minutes amounts of
335 H₂S with measurable effects on global protein persulfidation. The fact that STS increased protein
336 persulfidation suggests that STS works similarly to a H₂S donor (43). This is in line with previous
337 studies showing that thiosulfate can be metabolized to H₂S through sulfite formation or bound
338 sulfane sulfur release (18, 21, 28, 44-46).

339 In line with previous studies using other sources of H₂S (5-7, 47), STS increases revascularization *in*
340 *vivo* following hindlimb ischemia. Reminiscent of other studies performed with NaHS (10, 48, 49),
341 STS also promotes angiogenesis in the CAM model and in matrigel plug implants. At the cellular
342 levels, STS directly stimulates EC proliferation and migration *in vitro* in cultured endothelial cells,
343 and *in vivo* in the ischemic muscle, leading to increased capillary density and blood flow. H₂S
344 promotes angiogenesis via stimulation of the VEGFR2 and NO pathway (14, 50-53). In this study,
345 STS also stimulates the VEGFR2 and eNOS pathway.

346 The endothelial cells (ECs) covering the inner wall of blood vessels fine-tune oxygen and nutrient
347 delivery to match the metabolic needs of tissues. Quiescent ECs rely mostly on glycolysis for energy
348 production and further upregulate glycolysis to fuel migration and proliferation during angiogenesis
349 (36, 37). We previously showed that H₂S promotes the metabolic switch in EC to favor glycolysis,
350 and this mechanism promotes VEGF-induced EC migration (15). Here, STS acted similarly to the
351 classical H₂S donor salt NaHS, inhibiting mitochondrial respiration and inducing a compensatory
352 increase in glycolysis. Although further mechanistic studies remain to be performed, STS-induced
353 glycolysis seems instrumental to observe STS-induced EC proliferation. Whether mitochondrial
354 respiration inhibition/glycolysis activation and activation of the VEGFR2 pathway are linked remains
355 to be tested.

356 Inflammation and pro-resolving M2 macrophages are important for arteriogenesis/revascularization
357 and muscle repair following skeletal ischemia (54). Interestingly, H₂S possesses anti-inflammatory
358 properties (55) and was suggested to promote the M2 phenotype (56). Our data indicate an anti-
359 inflammatory effect of STS, and suggest a shift toward HO-1⁺ M2 anti-inflammatory macrophages
360 (57). However, the implication of HO1 expressing macrophages in muscle repair is controversial
361 (58). Given that the increase in HO1⁺ macrophages is accompanied by a decrease in total
362 macrophages and an increase in muscle repair, our data support a beneficial role of HO1⁺ cells in this
363 context, but additional experiments are required.

364 Endothelial cell function and quiescence are tightly linked to laminar shear stress, through the
365 activation of transcription factors such as KLF2 and FOXO1. Both ensure that EC remain quiescent,
366 and that the endothelium acts as an anti-inflammatory and anti-thrombotic surface (39, 40).
367 Surprisingly, both KLF2 and FOXO1 mRNA expression were increased in HUVEC after 4 hours of
368 treatment, suggesting that STS promotes EC quiescence. These findings are interesting but additional
369 experiments are required to determine whether mRNA overexpression translates into increased
370 pathway activation.

371 Importantly, STS is clinically approved and safe in gram quantities in humans. We recently
372 confirmed (21) that oral STS at 4g/L has no toxicity on mice but additional experiments are required
373 to assess STS distribution in tissues as well as finding the most efficient delivery route.

374 In conclusion, STS, a molecule with high translational potential since already approved clinically,
375 promotes EC proliferation and recovery after hindlimb ischemia, both in WT and

376 hypercholesterolemic LDLR^{-/-} mice. STS promotes EC proliferation in a glycolysis-dependent
377 manner. These findings suggest that STS holds strong potential to promote vascular repair in PAD
378 patients and calls for further pre-clinical studies in the large animal, and prospective clinical trials in
379 patients.

380 **4.1 Resource Identification Initiative**

381 To take part in the Resource Identification Initiative, please use the corresponding catalog number
382 and RRID in your current manuscript. For more information about the project and for steps on how to
383 search for an RRID, please click [here](#).

384 **4.2 Life Science Identifiers**

385 Life Science Identifiers (LSIDs) for ZOOBANK registered names or nomenclatural acts should be
386 listed in the manuscript before the keywords with the following format:

387 urn:lsid:<Authority>:<Namespace>:<ObjectID>[:<Version>]

388 For more information on LSIDs please see [Inclusion of Zoological Nomenclature](#) section of the
389 guidelines.

390 **5 Conflict of Interest**

391 The authors declare that the research was conducted in the absence of any commercial or financial
392 relationships that could be construed as a potential conflict of interest.

393 **6 Author Contributions**

394 FA, AL and SD designed the study. FA, JJ, QG, DM and ML performed the experiments. FA, JJ,
395 DM, ML, GW and SD analyzed the data. FA, DM, AL and SD wrote the manuscript. FA and DM
396 finalized the manuscript.

397 **7 Funding**

398 This work was supported by the following: The Swiss National Science Foundation (grant FN-
399 310030_176158 to FA and SD); the Novartis Foundation to FA; the Union des Sociétés Suisses des
400 Maladies Vasculaires to SD, and the Fondation pour la recherche en chirurgie thoracique et vasculaire.
401 The funding sources had no involvement in study design; in the collection, analysis and interpretation
402 of data; in the writing of the report; and in the decision to submit the article for publication.

403 **8 Acknowledgments**

404 We thank the mouse pathology facility for their services in histomorphology
405 (<https://www.unil.ch/mpf>).

406 **9 Data Availability Statement**

407 The datasets [GENERATED/ANALYZED] for this study can be found in the [NAME OF
408 REPOSITORY] [LINK]. Please see the [Data Availability section of the Author guidelines](#) for more
409 details.

410 **10 References**

- 411 1. Eraso LH, Fukaya E, Mohler ER, 3rd, Xie D, Sha D, Berger JS. Peripheral arterial disease,
412 prevalence and cumulative risk factor profile analysis. *European journal of preventive cardiology*.
413 2014;21(6):704-11.
- 414 2. Fowkes FG, Rudan D, Rudan I, Aboyans V, Denenberg JO, McDermott MM, et al.
415 Comparison of global estimates of prevalence and risk factors for peripheral artery disease in 2000
416 and 2010: a systematic review and analysis. *Lancet*. 2013;382(9901):1329-40.
- 417 3. Song P, Rudan D, Zhu Y, Fowkes FJI, Rahimi K, Fowkes FGR, et al. Global, regional, and
418 national prevalence and risk factors for peripheral artery disease in 2015: an updated systematic
419 review and analysis. *Lancet Glob Health*. 2019;7(8):e1020-e30.
- 420 4. Szabo C. A timeline of hydrogen sulfide (H₂S) research: From environmental toxin to
421 biological mediator. *Biochem Pharmacol*. 2018;149:5-19.
- 422 5. Majumder A, Singh M, George AK, Behera J, Tyagi N, Tyagi SC. Hydrogen sulfide
423 improves postischemic neoangiogenesis in the hind limb of cystathionine-beta-synthase mutant mice
424 via PPAR-gamma/VEGF axis. *Physiol Rep*. 2018;6(17):e13858.
- 425 6. Wang MJ, Cai WJ, Li N, Ding YJ, Chen Y, Zhu YC. The hydrogen sulfide donor NaHS
426 promotes angiogenesis in a rat model of hind limb ischemia. *Antioxid Redox Signal*.
427 2010;12(9):1065-77.
- 428 7. Rushing AM, Donnarumma E, Polhemus DJ, Au KR, Victoria SE, Schumacher JD, et al.
429 Effects of a novel hydrogen sulfide prodrug in a porcine model of acute limb ischemia. *J Vasc Surg*.
430 2019;69(6):1924-35.
- 431 8. Annex BH, Cooke JP. New Directions in Therapeutic Angiogenesis and Arteriogenesis in
432 Peripheral Arterial Disease. *Circ Res*. 2021;128(12):1944-57.
- 433 9. Yuan S, Kevil CG. Nitric Oxide and Hydrogen Sulfide Regulation of Ischemic Vascular
434 Remodeling. *Microcirculation*. 2016;23(2):134-45.
- 435 10. Papapetropoulos A, Pyriochou A, Altaany Z, Yang G, Marazioti A, Zhou Z, et al. Hydrogen
436 sulfide is an endogenous stimulator of angiogenesis. *Proc Natl Acad Sci U S A*. 2009;106(51):21972-
437 7.
- 438 11. Polhemus DJ, Kondo K, Bhushan S, Bir SC, Kevil CG, Murohara T, et al. Hydrogen sulfide
439 attenuates cardiac dysfunction after heart failure via induction of angiogenesis. *Circ Heart Fail*.
440 2013;6(5):1077-86.
- 441 12. Jang H, Oh MY, Kim YJ, Choi IY, Yang HS, Ryu WS, et al. Hydrogen sulfide treatment
442 induces angiogenesis after cerebral ischemia. *J Neurosci Res*. 2014;92(11):1520-8.
- 443 13. Altaany Z, Yang G, Wang R. Crosstalk between hydrogen sulfide and nitric oxide in
444 endothelial cells. *J Cell Mol Med*. 2013;17(7):879-88.
- 445 14. Tao BB, Liu SY, Zhang CC, Fu W, Cai WJ, Wang Y, et al. VEGFR2 functions as an H₂S-
446 targeting receptor protein kinase with its novel Cys1045-Cys1024 disulfide bond serving as a specific
447 molecular switch for hydrogen sulfide actions in vascular endothelial cells. *Antioxid Redox Signal*.
448 2013;19(5):448-64.
- 449 15. Longchamp A, Mirabella T, Arduini A, MacArthur MR, Das A, Trevino-Villarreal JH, et al.
450 Amino Acid Restriction Triggers Angiogenesis via GCN2/ATF4 Regulation of VEGF and H₂S
451 Production. *Cell*. 2018;173(1):117-29 e14.

Sodium thiosulfate promotes angiogenesis

- 452 16. Bebarta VS, Brittain M, Chan A, Garrett N, Yoon D, Burney T, et al. Sodium Nitrite and
453 Sodium Thiosulfate Are Effective Against Acute Cyanide Poisoning When Administered by
454 Intramuscular Injection. *Ann Emerg Med.* 2017;69(6):718-25 e4.
- 455 17. Nigwekar SU, Thadhani R, Brandenburg VM. Calciphylaxis. *N Engl J Med.*
456 2018;378(18):1704-14.
- 457 18. Olson KR, Deleon ER, Gao Y, Hurley K, Sadauskas V, Batz C, et al. Thiosulfate: a readily
458 accessible source of hydrogen sulfide in oxygen sensing. *Am J Physiol Regul Integr Comp Physiol.*
459 2013;305(6):R592-603.
- 460 19. Snijder PM, Frenay AR, de Boer RA, Pasch A, Hillebrands JL, Leuvenink HG, et al.
461 Exogenous administration of thiosulfate, a donor of hydrogen sulfide, attenuates angiotensin II-
462 induced hypertensive heart disease in rats. *Br J Pharmacol.* 2015;172(6):1494-504.
- 463 20. Ravindran S, Kurian GA. Effect of Sodium Thiosulfate Postconditioning on Ischemia-
464 Reperfusion Injury Induced Mitochondrial Dysfunction in Rat Heart. *J Cardiovasc Transl Res.*
465 2018;11(3):246-58.
- 466 21. Macabrey D, Longchamp A, MacArthur MR, Lambelet M, Urfer S, Deglise S, et al. Sodium
467 thiosulfate acts as a hydrogen sulfide mimetic to prevent intimal hyperplasia via inhibition of tubulin
468 polymerisation. *EBioMedicine.* 2022;78:103954.
- 469 22. Ishibashi S, Brown MS, Goldstein JL, Gerard RD, Hammer RE, Herz J.
470 Hypercholesterolemia in low density lipoprotein receptor knockout mice and its reversal by
471 adenovirus-mediated gene delivery. *J Clin Invest.* 1993;92(2):883-93.
- 472 23. National Research Council (U.S.). Committee for the Update of the Guide for the Care and
473 Use of Laboratory Animals., Institute for Laboratory Animal Research (U.S.), National Academies
474 Press (U.S.). Guide for the care and use of laboratory animals. 8th ed. Washington, D.C.: National
475 Academies Press; 2011. xxv, 220 p. p.
- 476 24. Longchamp A, Kaur K, Macabrey D, Dubuis C, Corpataux JM, Deglise S, et al. Hydrogen
477 sulfide-releasing peptide hydrogel limits the development of intimal hyperplasia in human vein
478 segments. *Acta Biomater.* 2019.
- 479 25. Nowak-Sliwinska P, Ballini JP, Wagnieres G, van den Bergh H. Processing of fluorescence
480 angiograms for the quantification of vascular effects induced by anti-angiogenic agents in the CAM
481 model. *Microvasc Res.* 2010;79(1):21-8.
- 482 26. Lin VS, Lippert AR, Chang CJ. Cell-trappable fluorescent probes for endogenous hydrogen
483 sulfide signaling and imaging H₂O₂-dependent H₂S production. *Proc Natl Acad Sci U S A.*
484 2013;110(18):7131-5.
- 485 27. Allagnat F, Dubuis C, Lambelet M, Le Gal L, Alonso F, Corpataux JM, et al. Connexin37
486 reduces smooth muscle cell proliferation and intimal hyperplasia in a mouse model of carotid artery
487 ligation. *Cardiovasc Res.* 2017;113(7):805-16.
- 488 28. Macabrey D, Longchamp A, MacArthur MR, Lambelet M, Urfer S, Corpataux J-M, et al.
489 Sodium Thiosulfate acts as an H₂S mimetic to prevent intimal hyperplasia via inhibition
490 of tubulin polymerization. *bioRxiv.* 2021.
- 491 29. Coletta C, Papapetropoulos A, Erdelyi K, Olah G, Modis K, Panopoulos P, et al. Hydrogen
492 sulfide and nitric oxide are mutually dependent in the regulation of angiogenesis and endothelium-
493 dependent vasorelaxation. *Proc Natl Acad Sci U S A.* 2012;109(23):9161-6.

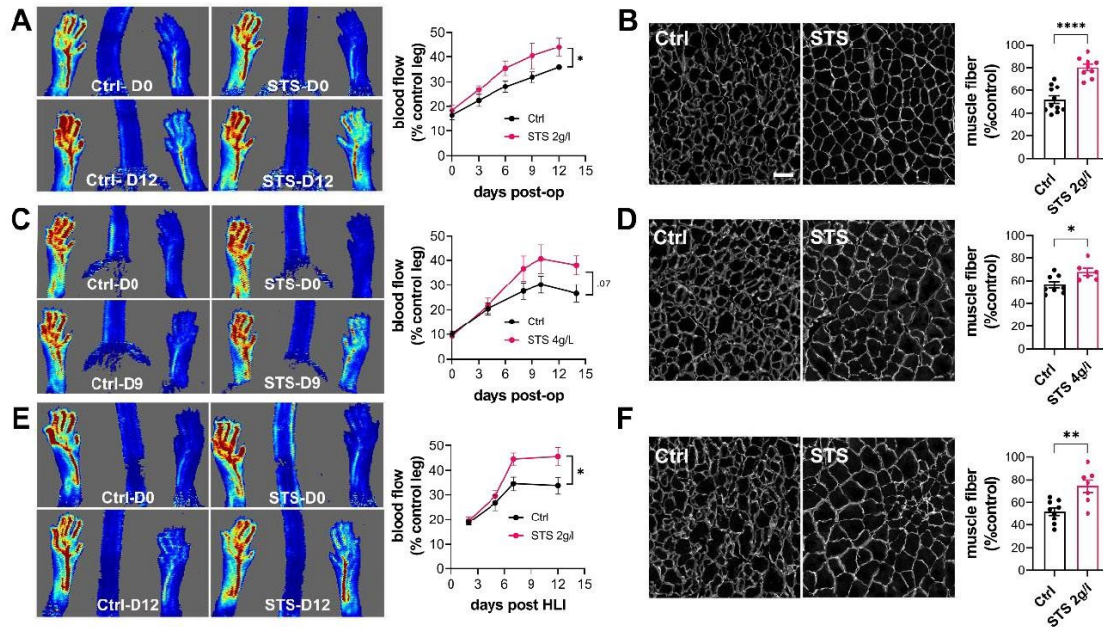
Sodium thiosulfate promotes angiogenesis

- 494 30. Paul BD, Snyder SH, Kashfi K. Effects of hydrogen sulfide on mitochondrial function and
495 cellular bioenergetics. *Redox Biol.* 2021;38:101772.
- 496 31. Olson KR. H₂S and polysulfide metabolism: Conventional and unconventional pathways.
497 *Biochem Pharmacol.* 2018;149:77-90.
- 498 32. Li Z, Polhemus DJ, Lefer DJ. Evolution of Hydrogen Sulfide Therapeutics to Treat
499 Cardiovascular Disease. *Circ Res.* 2018;123(5):590-600.
- 500 33. Zivanovic J, Kouroussis E, Kohl JB, Adhikari B, Bursac B, Schott-Roux S, et al. Selective
501 Persulfide Detection Reveals Evolutionarily Conserved Antiaging Effects of S-Sulphydration. *Cell*
502 *Metab.* 2019;30(6):1152-70 e13.
- 503 34. Heiss C, Rodriguez-Mateos A, Kelm M. Central role of eNOS in the maintenance of
504 endothelial homeostasis. *Antioxid Redox Signal.* 2015;22(14):1230-42.
- 505 35. De Bock K, Georgiadou M, Schoors S, Kuchnio A, Wong BW, Cantelmo AR, et al. Role of
506 PFKFB3-driven glycolysis in vessel sprouting. *Cell.* 2013;154(3):651-63.
- 507 36. Zecchin A, Kalucka J, Dubois C, Carmeliet P. How Endothelial Cells Adapt Their
508 Metabolism to Form Vessels in Tumors. *Front Immunol.* 2017;8:1750.
- 509 37. Eelen G, de Zeeuw P, Treps L, Harjes U, Wong BW, Carmeliet P. Endothelial Cell
510 Metabolism. *Physiol Rev.* 2018;98(1):3-58.
- 511 38. Szabo C, Ransy C, Modis K, Andriamihaja M, Murghes B, Coletta C, et al. Regulation of
512 mitochondrial bioenergetic function by hydrogen sulfide. Part I. Biochemical and physiological
513 mechanisms. *Br J Pharmacol.* 2014;171(8):2099-122.
- 514 39. Atkins GB, Jain MK. Role of Kruppel-like transcription factors in endothelial biology. *Circ*
515 *Res.* 2007;100(12):1686-95.
- 516 40. Andrade J, Shi C, Costa ASH, Choi J, Kim J, Doddaballapur A, et al. Control of endothelial
517 quiescence by FOXO-regulated metabolites. *Nat Cell Biol.* 2021;23(4):413-23.
- 518 41. Mishanina TV, Libiad M, Banerjee R. Biogenesis of reactive sulfur species for signaling by
519 hydrogen sulfide oxidation pathways. *Nat Chem Biol.* 2015;11(7):457-64.
- 520 42. Yuan S, Shen X, Kevil CG. Beyond a Gasotransmitter: Hydrogen Sulfide and Polysulfide in
521 Cardiovascular Health and Immune Response. *Antioxid Redox Signal.* 2017;27(10):634-53.
- 522 43. Fu L, Liu K, He J, Tian C, Yu X, Yang J. Direct Proteomic Mapping of Cysteine
523 Persulfidation. *Antioxid Redox Signal.* 2019.
- 524 44. Marutani E, Yamada M, Ida T, Tokuda K, Ikeda K, Kai S, et al. Thiosulfate Mediates
525 Cytoprotective Effects of Hydrogen Sulfide Against Neuronal Ischemia. *J Am Heart Assoc.*
526 2015;4(11).
- 527 45. Lee M, McGeer EG, McGeer PL. Sodium thiosulfate attenuates glial-mediated
528 neuroinflammation in degenerative neurological diseases. *J Neuroinflammation.* 2016;13:32.
- 529 46. Kolluru GK, Shen X, Bir SC, Kevil CG. Hydrogen sulfide chemical biology:
530 pathophysiological roles and detection. *Nitric Oxide.* 2013;35:5-20.
- 531 47. Bir SC, Kolluru GK, McCarthy P, Shen X, Pardue S, Pattillo CB, et al. Hydrogen sulfide
532 stimulates ischemic vascular remodeling through nitric oxide synthase and nitrite reduction activity
533 regulating hypoxia-inducible factor-1alpha and vascular endothelial growth factor-dependent
534 angiogenesis. *J Am Heart Assoc.* 2012;1(5):e004093.

Sodium thiosulfate promotes angiogenesis

- 535 48. Katsouda A, Bibli SI, Pyriochou A, Szabo C, Papapetropoulos A. Regulation and role of
536 endogenously produced hydrogen sulfide in angiogenesis. *Pharmacol Res.* 2016;113(Pt A):175-85.
- 537 49. Cai WJ, Wang MJ, Moore PK, Jin HM, Yao T, Zhu YC. The novel proangiogenic effect of
538 hydrogen sulfide is dependent on Akt phosphorylation. *Cardiovasc Res.* 2007;76(1):29-40.
- 539 50. Saha S, Chakraborty PK, Xiong X, Dwivedi SK, Mustafi SB, Leigh NR, et al. Cystathionine
540 beta-synthase regulates endothelial function via protein S-sulfhydration. *FASEB J.* 2016;30(1):441-
541 56.
- 542 51. Kolluru GK, Bir SC, Yuan S, Shen X, Pardue S, Wang R, et al. Cystathionine gamma-lyase
543 regulates arteriogenesis through NO-dependent monocyte recruitment. *Cardiovasc Res.*
544 2015;107(4):590-600.
- 545 52. Zheng Y, Ji X, Ji K, Wang B. Hydrogen sulfide prodrugs-a review. *Acta Pharm Sin B.*
546 2015;5(5):367-77.
- 547 53. Potenza DM, Guerra G, Avanzato D, Poletto V, Pareek S, Guido D, et al. Hydrogen sulphide
548 triggers VEGF-induced intracellular Ca(2)(+) signals in human endothelial cells but not in their
549 immature progenitors. *Cell Calcium.* 2014;56(3):225-34.
- 550 54. Zhang J, Muri J, Fitzgerald G, Gorski T, Gianni-Barrera R, Masschelein E, et al. Endothelial
551 Lactate Controls Muscle Regeneration from Ischemia by Inducing M2-like Macrophage Polarization.
552 *Cell Metab.* 2020;31(6):1136-53 e7.
- 553 55. Pan LL, Qin M, Liu XH, Zhu YZ. The Role of Hydrogen Sulfide on Cardiovascular
554 Homeostasis: An Overview with Update on Immunomodulation. *Front Pharmacol.* 2017;8:686.
- 555 56. Wu J, Chen A, Zhou Y, Zheng S, Yang Y, An Y, et al. Novel H₂S-Releasing hydrogel for
556 wound repair via in situ polarization of M2 macrophages. *Biomaterials.* 2019;222:119398.
- 557 57. Naito Y, Takagi T, Higashimura Y. Heme oxygenase-1 and anti-inflammatory M2
558 macrophages. *Arch Biochem Biophys.* 2014;564:83-8.
- 559 58. Ma Y, Jia L, Wang Y, Ji Y, Chen J, Ma H, et al. Heme Oxygenase-1 in Macrophages Impairs
560 the Perfusion Recovery After Hindlimb Ischemia by Suppressing Autolysosome-Dependent
561 Degradation of NLRP3. *Arterioscler Thromb Vasc Biol.* 2021;41(5):1710-23.
- 562
- 563

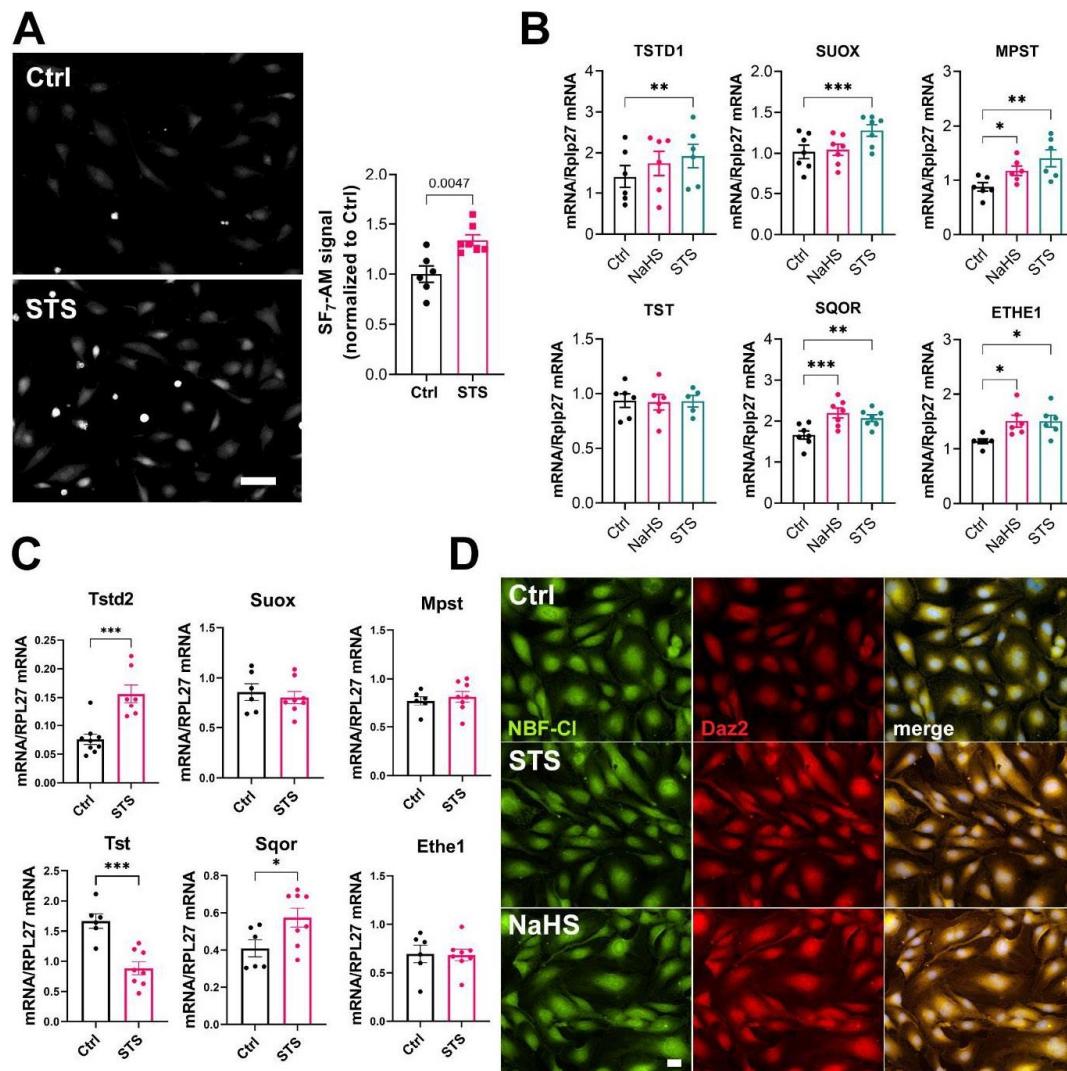
564 11 Figure Legends.



565

566 **Figure 1. STS promotes revascularization and muscle recovery in a mouse model of hindlimb**
 567 **ischemia.**

568 Doppler imaging (A, C, E) and laminin immunostaining in gastrocnemius muscle (B, D, F) in WT
 569 male mice submitted to HLI and treated or not (Ctrl) with 2g/L STS (A-B) or 4g/L STS (C-D), or
 570 LDLR^{-/-} mice treated with 2g/L STS (E-F). (A, C, E) Data are mean ± SEM of 8 to 12 animals per
 571 group. *p<.05 as determined by repeated measures Mixed-effects model (REML). (B, D, F) Data are
 572 mean ± SEM of 6 to 12 animals per group. *p<.05, **p<.01; ****p<.0001 as determined by bilateral
 573 unpaired t-test. Scale bar 100 μm.



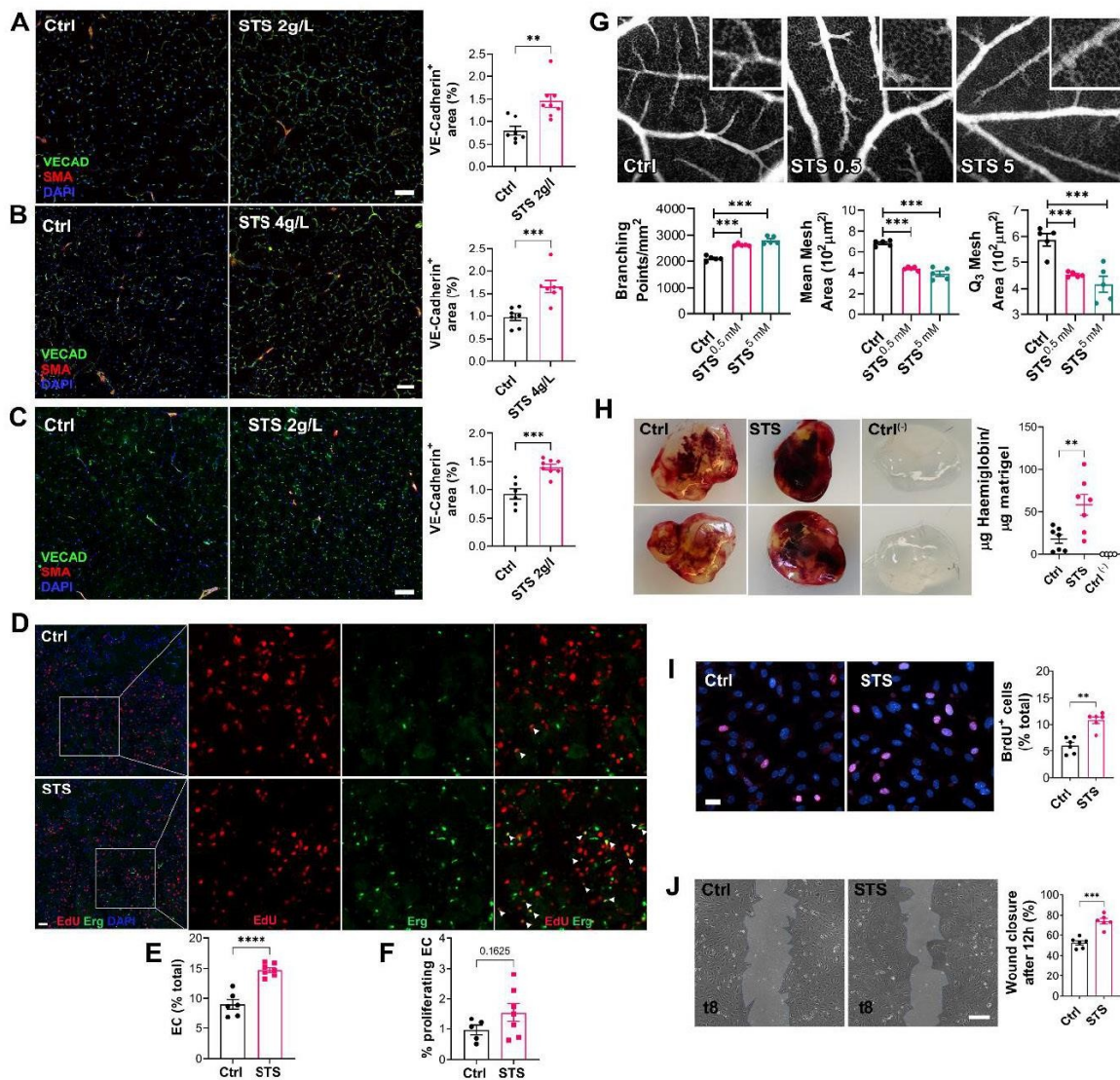
574

575 **Figure 2. STS leads to enzymatic production of H₂S and increases protein persulfidation.**

576 **A)** H₂S release measured by the SF₇-AM probe in HUVEC exposed for 90 min to STS. Data are
 577 mean ± SEM of 6 independent experiments. *p<.05 as determined by bilateral unpaired t-test. Scale
 578 bar 20 μm. **B)** mRNA expression in HUVEC exposed for 4h to 100μM NaHS or 3mM STS. Data are
 579 mean ± SEM of 6 independent experiments. *p<.05, **p<.01; ***p<.001 as determined by repeated
 580 measures one-way ANOVA with Dunnett's post-hoc test. **C)** mRNA expression in gastrocnemius
 581 muscle of mice treated for 1 week with 4g/L STS. Data are mean ± SEM of 6 to 8 animals per group.
 582 *p<.05, **p<.01; ***p<.001 as determined by bilateral- unpaired t-test **D)** *In situ* labeling of
 583 intracellular protein persulfidation assessed by Daz-2:Biotin-Streptavidin-584 (red), normalized to
 584 NBF-adducts fluorescence (green), in HUVEC exposed for 4 hours to NaHS (100 μM) or STS
 585 (20mM).

586

Sodium thiosulfate promotes angiogenesis



587

588 **Figure 3. STS promotes angiogenesis in vivo in several models**

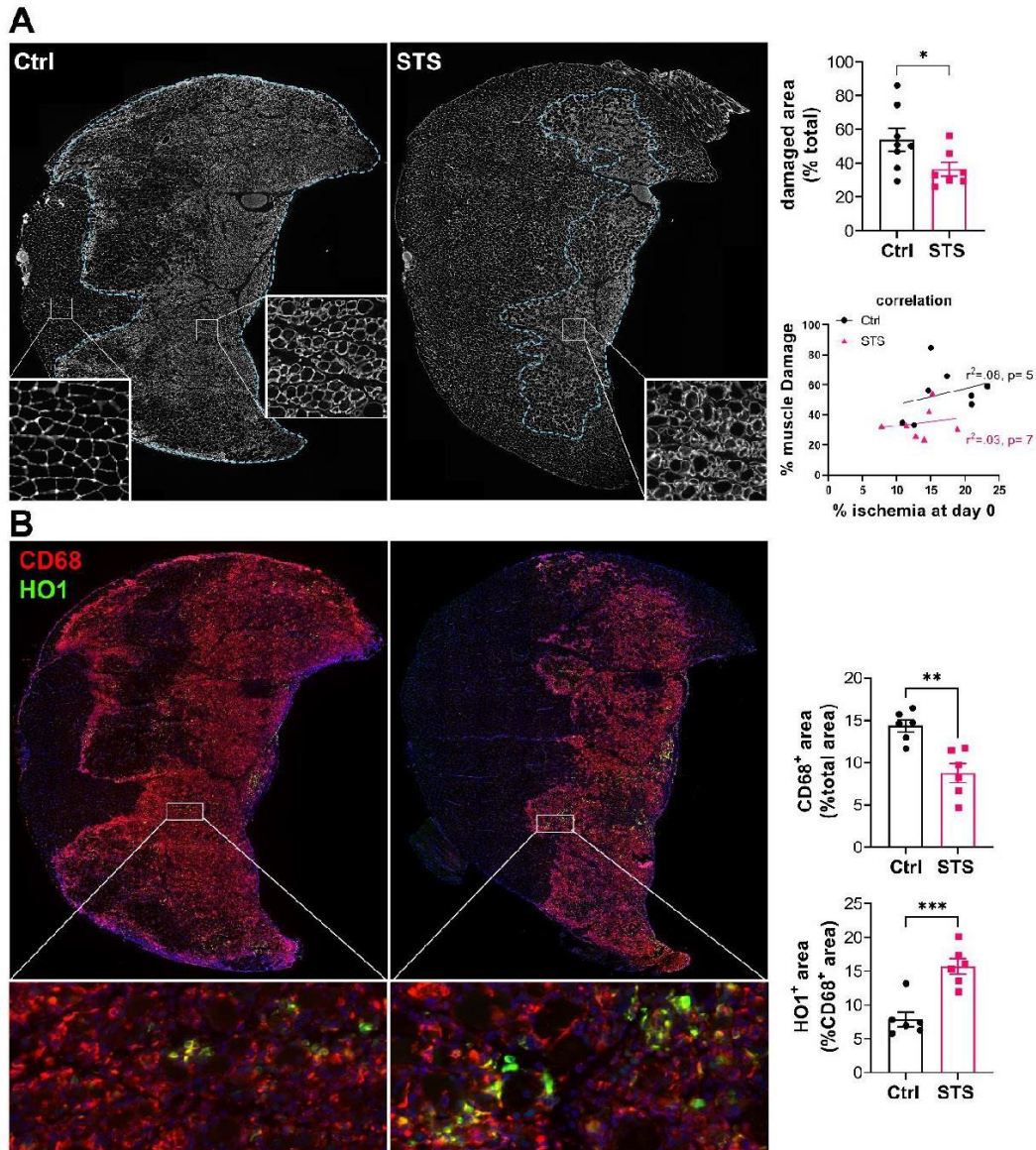
589 **A-C)** VE-cadherin (VECAD; green), smooth muscle actin (SMA; red) and nuclei (DAPI; blue)
 590 immunostaining in gastrocnemius muscle from WT male mice submitted to HLI and treated or not
 591 (Ctrl) with 2g/L STS (**A**) or 4g/L STS (**B**), or LDLR^{-/-} mice treated with 2g/L STS (**C**).
 592 Representative images and quantification of the VECAD staining in 6 to 9 animals per group. Data
 593 are mean ± SEM. **p<.01; ***p<.001 as determined by bilateral unpaired t-test. **D)** EdU (red), ERG
 594 (green) and nuclei (blue) immunostaining in ischemic muscle of WT mice treated with 2g/L STS 4
 595 days after HLI. Scale bar represent 100 µm. insets are 3-fold magnification of left images. **E)**
 596 Percentage of endothelial cells (ERG⁺/total nuclei count). **F)** Percentage of proliferating endothelial
 597 cells (EdU⁺/ERG⁺). Data are mean ± SEM. *p<.05, ****p<.0001 as determined by bilateral unpaired
 598 t-test. **G)** Representative fluorescein-dextran fluorescence angiographies at EDD13, 48 h after topical
 599 treatment with 0.9% NaCl (Ctrl), or STS (0.5 or 5mM final). Representative images and
 600 quantification of the vascular network from 5 eggs per group. Data are mean ± SEM. ***p<.001 as

18

Sodium thiosulfate promotes angiogenesis

601 determined by one-way ANOVA with Tukey's post-hoc test. **H)** Matrigel plugs supplemented or not
602 (ctrl) with VEGF₁₃₅ +/- STS 1 week post implantation. Representative plugs and hemoglobin content
603 normalized to plug weight. Quantification of 4 to 8 animals per group. Data are mean ± SEM.
604 **p<.01 as determined by one-way ANOVA with Tukey's post-hoc test. **I)** HUVEC proliferation
605 assessed by BrdU incorporation and expressed as BrdU positive cells (pink) over DAPI positive
606 nuclei. Data shown as mean ± SEM of 6 independent experiments. **p<.01 as determined by bilateral
607 unpaired t-test. **J)** HUVEC migration was assessed by wound healing assay in presence of Mitomycin
608 C and expressed as the percentage of wound closure after 10 hours. Data shown as mean ± SEM of 6
609 independent experiments. **p<.01, ***p<.001 as determined by bilateral unpaired t-test.

610



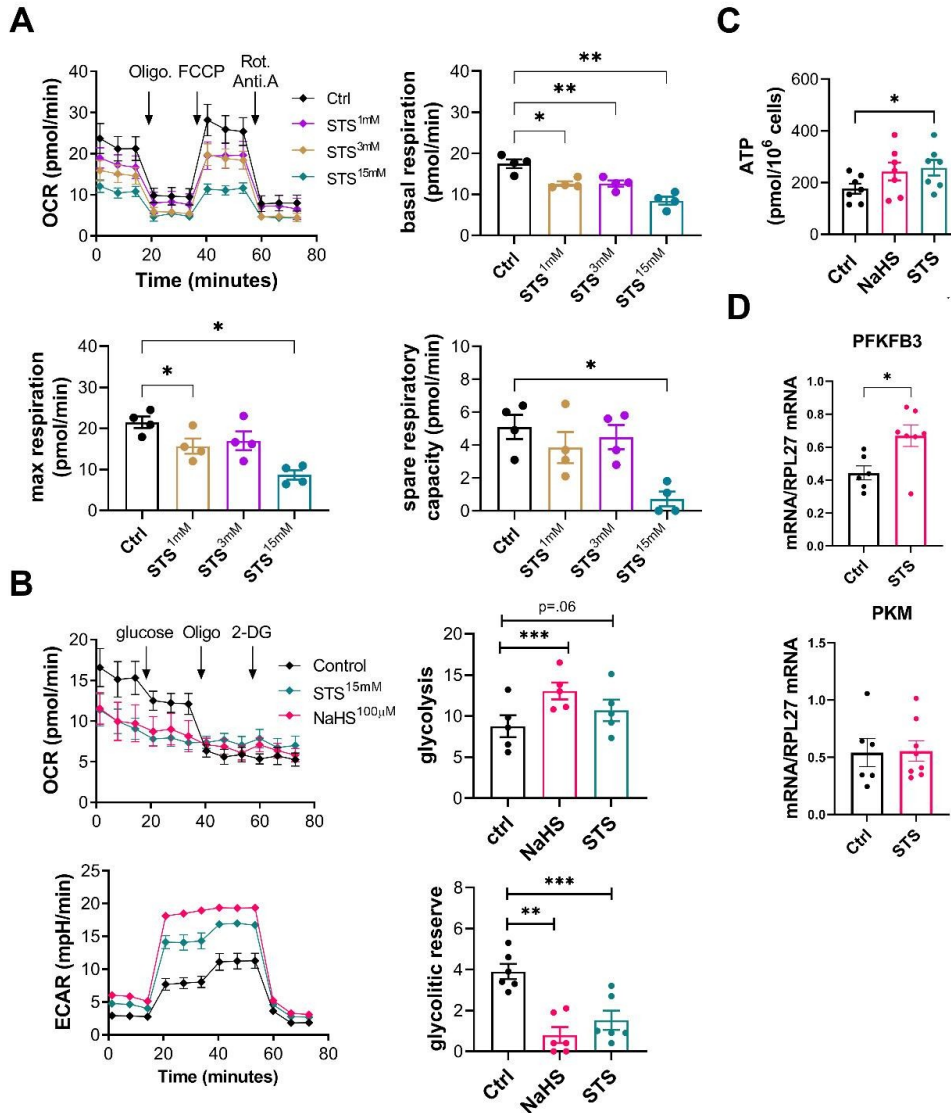
611

612 **Figure 4. STS limits inflammation and muscle damage 4 days after ischemia**

613 **A)** Left panel: Representative images of gastrocnemius and soleus muscle of WT mice treated or not
 614 (Ctrl) with 4g/L STS, stained for laminin (white). Damaged area delimited by the blue dotted line.
 615 Right upper panel: Quantification of the damaged area, expressed as a percentage of the total muscle
 616 area. Data are mean \pm SEM. * $p < 0.05$ as determined by unpaired t-test. Right lower panel: correlation
 617 between muscle damage and ischemia after the surgery. Data analyzed by Pearson correlation. **B)**
 618 *Left panel:* Representative images of gastrocnemius and soleus muscle of WT mice treated or not
 619 (Ctrl) with 2g/L STS, stained for CD68 (red) and HO1 (green). *Right panel:* CD68 and HO1 positive
 620 area quantification.. Data are mean \pm SEM. ** $p < .01$ *** $p < .001$ as determined by bilateral unpaired t-
 621 test.

20

622



623

624 **Figure 5. STS inhibits mitochondrial respiration and increases glycolysis and ATP production**
 625 **in HUVECs.**

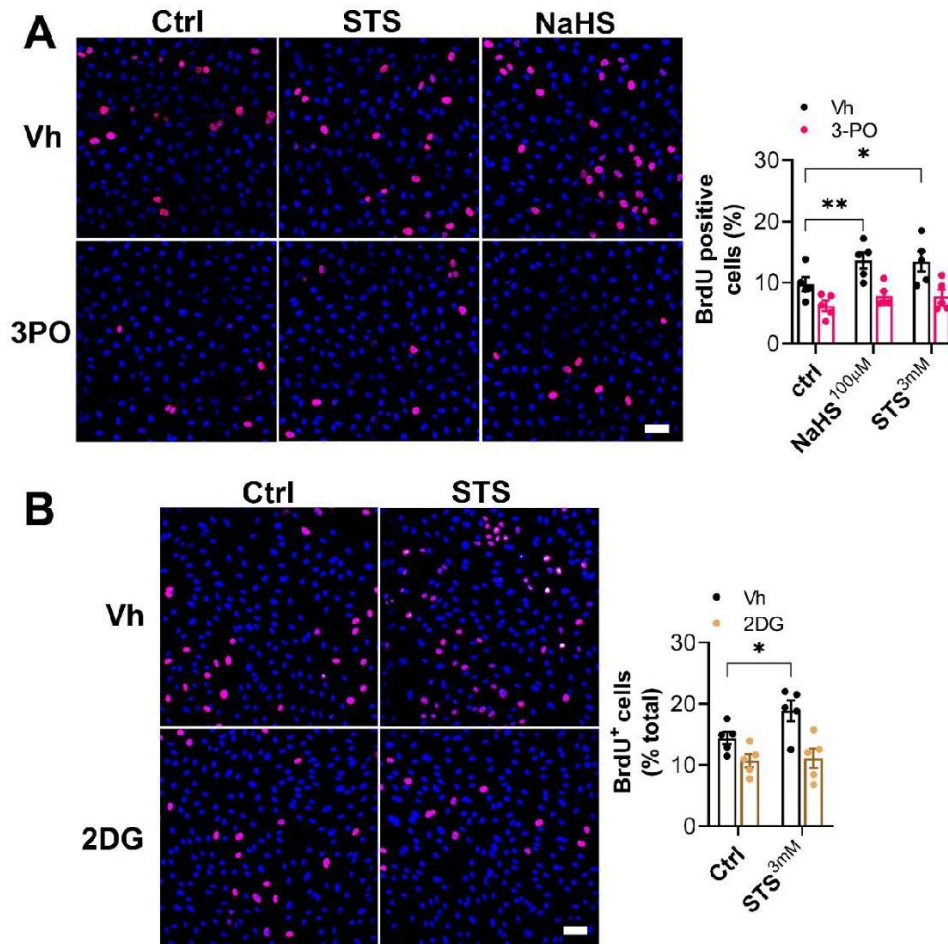
626 **A)** Mitochondrial stress test in HUVEC pre-treated for 4h with increasing concentration of STS. **B)**
 627 Glycolysis stress test performed on HUVECs treated for 4h with 15mM STS or 100μM NaHS.
 628 Mitochondrial respiration is expressed as oxygen consumption rate (OCR), glycolysis by
 629 extracellular acidification rate (ECAR). Data expressed as mean±SEM of 4 to 5 independent
 630 experiments. *p<0.05, **p<0.01, ***p<0.001 as determined by one-way ANOVA with Tukey's
 631 corrections for multiple comparisons. **C)** ATP production in HUVEC treated for 24h with 100μM
 632 NaHS or 3mM STS. **D)** mRNA levels in gastrocnemius muscle treated or not with 4g/L STS for 1

21

Sodium thiosulfate promotes angiogenesis

633 week. Data are mean \pm SEM of 7 independent experiments. * $p < .05$, ** $p < .01$; *** $p < .001$ as
 634 determined by bilateral unpaired t-test.

635



636

637 **Figure 6. STS-induced HUVEC proliferation requires glycolysis**

638 **A-B)** HUVEC proliferation in cells treated for 8h with 100µM NaHS, 3mM STS +/- 15µM PFKFB3
 639 inhibitor (3-PO) or 6mM 2 deoxy-glucose (2DG), or their respective vehicle (Vh). Data are mean \pm
 640 SEM of ratio of BrdU positive cells (pink) over DAPI positive nuclei (blue) in 5 independent
 641 experiments. * $p < 0.05$ as determined by repeated measures two-way ANOVA with Dunnett's post-
 642 hoc test.

643

Supplementary Material

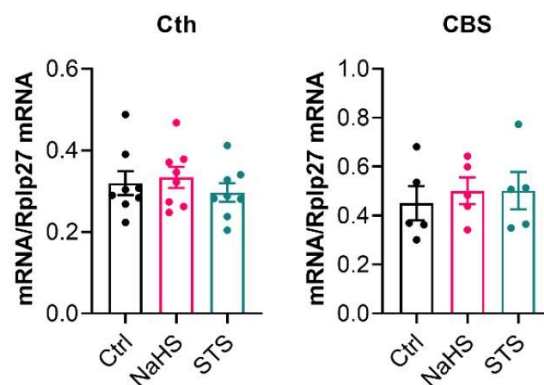
1 Supplementary Data

Supplementary Material should be uploaded separately on submission. Please include any supplementary data, figures and/or tables. All supplementary files are deposited to FigShare for permanent storage and receive a DOI.

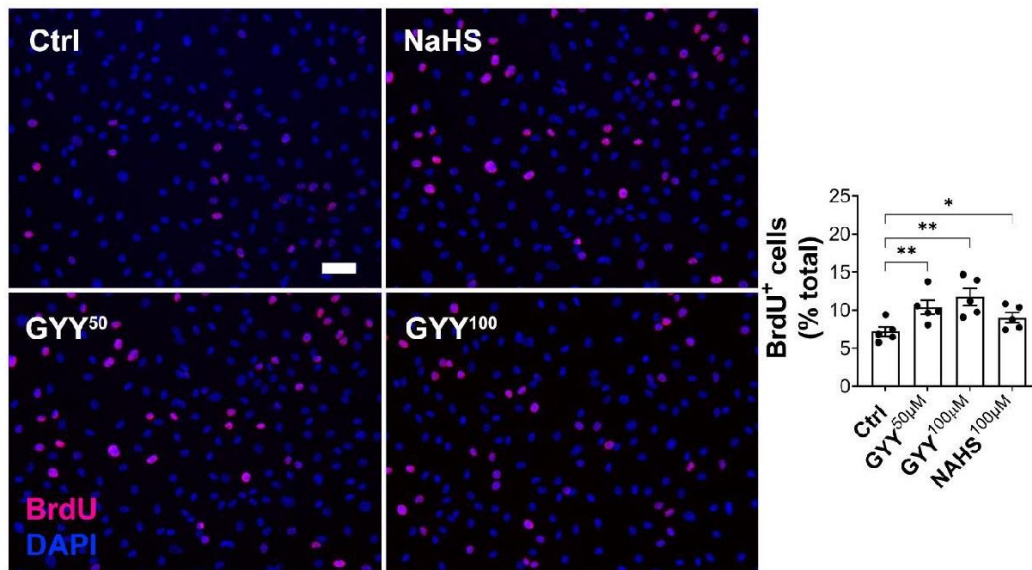
Supplementary material is not typeset so please ensure that all information is clearly presented, the appropriate caption is included in the file and not in the manuscript, and that the style conforms to the rest of the article. To avoid discrepancies between the published article and the supplementary material, please do not add the title, author list, affiliations or correspondence in the supplementary files.

2 Supplementary Figures and Tables

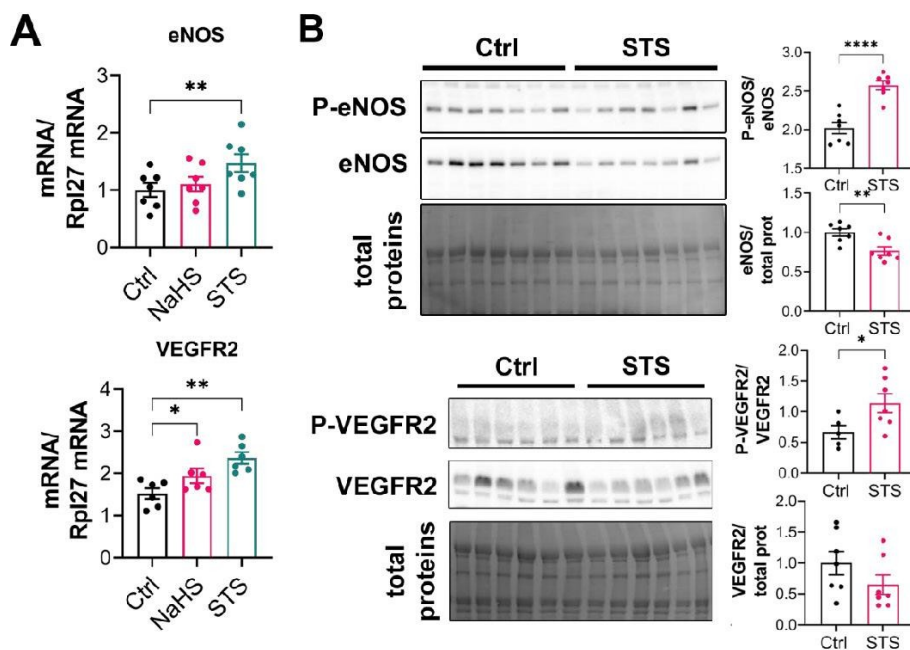
2.1 Supplementary Figures



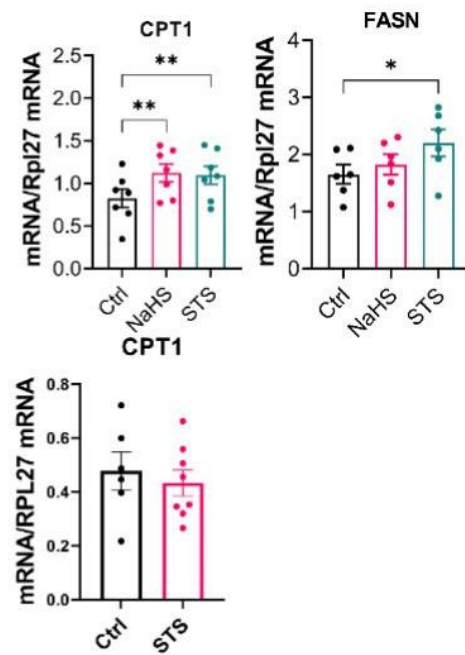
Supplementary Figure 1. Cth and Cbs mRNA expression in HUVEC exposed for 4h to 100 μ M NaHS or 3mM STS. Data are mean \pm SEM. No statistical differences as assessed by paired One-way ANOVA with DUNNET's correction for multiple comparisons.



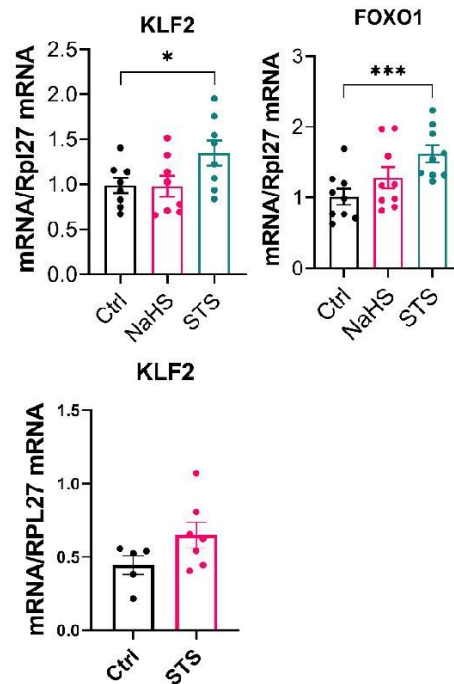
Supplementary Figure 2. HUVEC proliferation was assessed by BrdU incorporation and expressed as BrdU positive cells (pink) over DAPI positive nuclei. Data shown as mean \pm SEM of 5 independent experiments. * $p < .05$ ** $p < .01$ *** $p < .001$ as determined by paired one-way ANOVA with Dunnett's post-hoc test.



Supplementary Figure 3. A) Normalized eNOS and VEGFR2 mRNA levels in HUVEC treated or not (Ctrl) with 100 μ M NaHS or 15mM STS for 4h. * p <.05, *** p <.01 as determined by paired one-way ANOVA with Dunnett's post-hoc tests. B) Western blot on ischemic muscles after 14 days of STS treatment, P-eNOS levels normalized with total eNOS levels, VEGFR2 levels normalized to total proteins. * p <.05, ** p <.01, **** p <.0001 as determined by bilateral unpaired t-test. All proteins normalized to total protein stain.



Supplementary Figure 4. CPT1 and FASN mRNA expression in HUVECs treated for 4 hours with 3mM STS or 100 μ M NaHS (upper panel) and of CPT1 in gastrocnemius muscle of mice treated with 4g/L STS for 1 week (lower panel). Data are mean \pm SEM. * p <.05 ** p <.01 **** p <.0001 as determined one-way ANOVA with Dunnett's post-hoc test for HUVECs and unpaired t-test for muscle.



Supplementary Figure 5. KLF2 and FOXO1 mRNA expression in HUVECs treated for 4 hours with 3mM STS or 100 μ M NaHS (upper panel) and of KLF2 in gastrocnemius muscle of mice treated with 4g/L STS for 1 week (lower panel). Data are mean \pm SEM. * p <.05 ** p <.01 *** p <.001 as determined one-way ANOVA with Dunnett's post-hoc test for HUVECs and unpaired t-test for muscle.

2.2 Supplementary Tables

Supplementary Table 1: Antibodies

Target antigen	Vendor	Catalog #	Working concentration	RRID
Laminin	Sigma	L9393	1/200	
Ve-Cadherin	Abcam	AB33168	1/100	
CD68	Biorad	MCA1957T	1/500	
HO-1	Abcam	13243	1/200	
ERG	CST	#4695	1/100	
Anti-Rabbit HRPO	Thermo Fisher Scientific	31460A21109	1/20000 (WB)1/250 (ICC)	

Anti-mouse HRPO	Jackson ImmunoResearch Labs	115-035-146	1/15000 (WB)	
Anti-Rabbit HRPO	Thermo Fisher Scientific	31460	1/20000 (WB)	
BrdU	BD Biosciences	555627	1/200 (ICC)	
eNOS	BD Biosciences	610297	1/1000	
peNOS	CST	#9571	1/500	
VEGFR2	CST	#2479	1/1000	
pVEGFR2	CST	#2478	1/500	
SMA	CST	#19245		
Goat anti-Rabbit IgG Secondary Antibody, Alexa Fluor 680	Thermo Fisher Scientific	A21109	1/500	
Goat anti-Rabbit IgG Secondary Antibody, Alexa Fluor 405	Thermo Fisher Scientific	A31556	1/500	
Goat anti-Rat IgG Secondary Antibody, Alexa Fluor 488	Thermo Fisher Scientific	A11006	1/500	
Donkey anti-Rabbit IgG Secondary Antibody, Alexa Fluor 488	Thermo Fisher Scientific	A21206	1/500	

Supplemental table 2: DNA oligo primers

Primer Name	Sequence
hTSTD1	Fw: TCAACATCCCGGTGTCCGAG Rv: TCCAGCTTTGGCTTCTCAGC
hSUOX	Fw: GGTGCAGTGTTGGCCTATCA Rv: ACCCAGATCCCAGTCTCAGG
hMPST	Fw: CCGAGACGGCATTGAACCT Rv: CCTGGCTCAGGAAGTCTGTG
hTST	Fw: GGAGCCGGATATAGTAGGACT Rv: AATATGGCACGCAGCTCCTC
hSQOR	TBD
hETHE1	Fw: Rv:

Supplementary Material

mTstd2	Fw: CCTAGGGTTTGC GGATACTTG Rv: TCGTCTGGTGAAGTGAAGAAG
mSuox	Fw: CATCGGTGTAGGGCTTCTCA Rv: AGGGTTGTTGTGAGAACGCA
mMpst	Fw:GGCCACCACTCTGTGCATT Rv:GGAGCTGATTGGCAGGTTCT
mTst	Fw: GGAGCCGGATATAGTAGGACT Rv: AATATGGCACGCAGCTCCTC
mSqor	Fw:TGGAATATGATGCTCAGAGGCT Rv:AAAGCAAGCTGTGAGCCATC
mEthe1	Fw; ACAGACTTCCAACAAGGCTGT Rv:TGGTAATCGTGAGCCGGT
mPFKFB3	Fw: AAATGTCCGCTCCACACTGT Rv: GGTGTGTGCTCACCGATTCT
mPKM	Fw: TCGCATGCAGCACCTGATAG Rv: TCCATGAGGTCTGTGGAGTGA
hCth	Fw: CCAGCACTCGGGTTTTGAAT Rv: TACTTAGCCCCATCCAGTGC
hCbs	Fw: ATGGTGACGCTTGGGAACAT Rv: GGCGGATCTGTTTGAAGTGC
heNOS	Fw:GCCGGAACAGCACAAAGAGTTA Rv:CCCTGCACTGTCTGTGTTACT
hVEGFR2	Fw: Rv:
hCPT1	Fw:TTCCAAGTTCTTTGCCCTGAG Rv:GGCCTTGTTTCCATATGCTGAG
hFASN	Fw: AACTCCAAGGACACAGTCACCAT Rv: CAGCTGCTCCACGAACTCAA
mCPT1	Fw: CACTGCAGCTCGCACATTAC Rv: CCAGCACAAAGTTGCAGGAC
hKLF2	Fw:TGGGCATTTTTGGGCTACCT Rv:TCCAAGCAACCAGACCAAGT
hFOXO1	Fw:AGTGGATGGTCAAGAGCGTG Rv:GCACACGAATGAAGTGTGCTGT
mKLF2	Fw: TATCTTGCCGTCCTTTGCCA Rv: CGTTGTTTAGGTCCTCATCCG

8 Conclusion

In summary, in the present thesis we demonstrated that STS, a FDA-approved source of sulfur, and Zofenopril, a sulfhydrated ACE inhibitor, hold promising therapeutic potential against PAD and post-surgical complications (IH).

8.1 STS inhibits IH

In **chapter 7.1**, we demonstrated that STS limits IH development *in vivo* in a model of arterial restenosis and *ex vivo* in a model of human vein segments. Mechanistically, STS increases H₂S bioavailability, which leads to inhibition of cell apoptosis and matrix deposition, as well as VSMC proliferation and migration via microtubules depolymerisation.

In this study, we hypothesized that STS inhibits VSMC proliferation by persulfidation of the tubulin protein, thereby interfering with its polymerization. This hypothesis is supported by various studies that showed the persulfidation of cytoskeletal proteins (55, 56). However, in our study, direct evidence that STS persulfidates the tubulin protein is lacking. Mass spectrometry should be undertaken to confirm persulfidation of the tubulin protein. Specific inhibition of protein persulfidation by blocking/modifying cysteine residues on target proteins is necessary to prove that tubulin persulfidation accounts for the effect of STS on VSMC proliferation and migration.

A major issue with the use of STS is thiosulfate detection. Farese et al. showed that oral STS has low and variable bioavailability and only iv injections should be used in humans (130). Working on mice, we had to select oral administration because 28 days iv injection cannot be done, and repeated ip injection is frowned upon. To assess the amount of STS that accumulates in tissues and organs after oral administration, we tested a colorimetric technique (131) but failed to detect thiosulfate. We are currently working with the Central Environmental Laboratory

(EPFL) that uses ion-chromatography couple with mass spectrometry to detect circulating thiosulfate levels in plasma.

8.2 Zofenopril inhibits IH

In **chapter 7.2**, we demonstrated that the sulfhydrated ACEi Zofenopril is superior than non-sulfhydrated ACEi Enalapril in limiting IH development *in vivo* in a mouse model of hypertension and in normotensive conditions as well as in an *ex vivo* model of human vein segments. Mechanistically, Zofenopril increases H₂S bioavailability, leading to inhibition of VSMC proliferation and migration by targeting the MAPK and mTOR pathway.

Our study demonstrating superiority of Zofenopril over Enalapril goes in line with previous studies (132, 133). Given the beneficial actions of H₂S in the vascular system, Zofenopril superiority is most likely due to its ability to release H₂S, as evidenced by increase overall protein persulfidation in our experimental settings and by others before us (132, 133).

The present work holds important therapeutic potential as it is estimated that 32% (women) and 34% (men) of the population between the age of 30 and 79 is hypertensive (134). Anti-hypertensive drugs are therefore one of the most used medication in the world. Further studies in bigger animal models as well as in large patients cohort are of course required by these data suggest that Zofenopril should be the ACEi of choice for patients suffering from hypertension.

Considering the widespread use of anti-hypertensive medication in PAD patients (135), we believe it might be use not only to limit vascular surgery complications but also to promote reperfusion, which remains to be tested.

8.3 STS promotes reperfusion in a HLI model in mice

In **chapter 7.3**, we showed that STS promotes reperfusion following hind limb ischemia in healthy and hypercholesterolemic mice. H₂S also promoted angiogenesis *in vivo* in the CAM model

and in matrigel plug implants. Our data suggest that STS directly stimulates EC proliferation and migration *in vitro* and following hind limb ischemia *in vivo*. Mechanistically, STS most likely acts by increasing H₂S bioavailability. H₂S induces a metabolic reprogramming towards increased glycolysis, leading to increased proliferation and migration. STS also promotes the activation of the VEGFR2 pathway.

The HLI model lacks the complexity of the disease that we see in humans. To replicate some of the comorbidities that PAD patients have, we tested STS on hypercholesterolemic mice but we remain far from the patient's actual situation. Furthermore, the HLI model induces an acute ischemia, with limited impairment in limb function and fast reperfusion to asymptomatic levels. Recently, Krishna et al. developed a two stages HLI model, which leads to more severe and sustained ischemia than the conventionally used model. In the new model, 2 ameroid constrictors are placed on the femoral artery to induce a gradual occlusion and the femoral artery is finally excised 14 days after constrictors placement. This new model may be more relevant to evaluate novel PAD therapies (136).

The exact mechanisms leading to revascularization following skeletal ischemia in PAD patients are controversial. Both arteriogenesis and angiogenesis probably co-exist (137). In our study, we showed that STS promotes arteriogenesis in the hindlimb ischemia model. Arteriogenesis, or the growth of collateral arteries, is mainly stimulated by shear stress and requires macrophages to achieve proper vessel remodeling (138, 139). In line with arteriogenesis in our experimental settings, we showed huge macrophages infiltration 4 days after HLI. We also showed activation of the VEGFR2 pathway 14 days after surgery, suggested to take part in arteriogenesis (140).

In addition to arteriogenesis in the HLI model, STS promotes angiogenesis *in vivo* in matrigel plug implants and in the CAM model, suggesting that STS may promote different types of neovessel formation. *In vitro*, STS promotes EC proliferation and migration. In our study, STS induces a metabolic reprogramming towards glycolysis, which seems instrumental to increase proliferation and migration. Interestingly, during sprouting angiogenesis, EC differentiate into

migratory tip-cells versus proliferative stalk cells. On the one hand, tip-cells rely solely on glycolysis for cytoskeletal remodeling during migration. On the other hand, proliferative stalk cells rely on glycolysis for energy production, but require also fatty acid oxidation and amino acid metabolism to support proliferation (141). Here, STS promotes both HUVECs proliferation and migration, suggesting a potential effect both on tip cells and stalk cells. Furthermore, STS increased the mRNA expression of fatty acid metabolism enzymes CPT1 and FASN in HUVEC. Further studies will be performed to assess the effect of STS on beta-oxidation, although *in vivo* data did not suggest an impact of STS on beta-oxidation in the whole muscle.

Our data further suggest that STS also stimulates the VEGF/VEGFR2 pathway, which plays a pivotal role in sprouting angiogenesis and in arteriogenesis (137). Downstream the VEGF/VEGFR2 pathway are the Akt and MAPK pathways responsible for proliferation and migration. Further studies are ongoing to characterize the effect of STS on those pathways. VEGF can also stimulate eNOS downstream of Akt, which will support EC function. AKT also phosphorylate FOXO1, leading to activation of the transcriptional factor MYC, promoting glycolysis (141). Whether VEGFR2 activation is necessary to observe STS-induced glycolysis and EC proliferation and migration remains to be tested. Experiments using VEGFR2 inhibitors are under way in HUVEC to test this hypothesis.

Our study supports that STS promotes VEGF-dependent sprouting angiogenesis and arteriogenesis. However, a recent report suggests that skeletal muscle revascularization following HLI in the mouse happens mainly via intussusception (142). Intussusception, or vessel splitting, (143) is a dynamic intravascular process capable of dramatically modifying the structure of the microcirculation, that relies on the separation of a “mother” vessel into two “daughter” vessels, by endothelial cell projection into the luminal space. Mechanisms regulating this process are not well understood and the implication of VEGFR2 is controversial (142). In our experimental settings, we did not examined the VEGFR2 pathway at early time points, nor did we carefully checked the

appearance of the early vascular network. However, vessel immunostaining at day 4 highlights structures reminiscent of intussusceptive vessel formation. Further experiments are required to test if intussusception really plays a part in early muscle revascularization and if STS somehow modifies this process.

Overall, the effects of STS on ECs may be multifactorial. Furthermore, *in vivo*, STS likely affects other cell types, such as macrophages and smooth muscle cells, implicated in angiogenesis and arteriogenesis.

Additional studies in larger animal models with surgeries similar to what is done in patients are required before testing the benefits of STS in a large, phase II-III clinical trials. The next step is to test STS in a porcine model. We will simultaneously generate a model of IH through balloon angioplasty of the carotid artery (144), and a model of limb ischemia via intravascular placement of an occluder into the left external iliac artery (145). A pharmacological grade injectable STS solution (25g STS) will be given intravenously three times per week. Blood samples will be taken weekly and organs will be collected 4 weeks after the surgeries. Primary outcome for the carotid angioplasty is intimal hyperplasia thickness assessed by histomorphology. Primary outcome for external iliac artery occlusion is reperfusion index as assessed by angiography and capillary density in the leg muscles. Secondary outcome will include toxicology and pharmacology studies to assess STS accumulation and elimination in the minipig organism. Thiosulfate and sulfate levels will be evaluated by ion-chromatography couple with mass spectrometry in plasma samples (146) by the Central Environmental Laboratory (EPFL). Plasma samples will also be used to assess inflammation (CRP), kidney (electrolytes, creatinine, urea), liver (ASAT, ALAT) and cardiac (CK-MB, troponin) function.

8.4 Further perspectives: Clinical potential of STS in a mouse model of AAA

Both of our studies showed that STS limits IH formation and promotes revascularization. Based on these results, we believe that STS may hold therapeutic potential in other cardiovascular disease.

Abdominal Aortic Aneurysm (AAA) is a degenerative disease in the aortic wall that affects 5% of men aged ≥ 65 years (147, 148). AAA is defined as a local expansion of the abdominal aorta wall, with at least a 50% increase over its normal diameter. AAA is often asymptomatic and 80% of AAA rupture is fatal. AAA is the 13th leading cause of death in the United States (149). Open surgical repair or minimally invasive endovascular aortic repair (EVAR) are the only treatments (150, 151). Although the risk factors for AAA are well recognized (atherosclerosis, age, male sex, hypertension, genetic predispositions, and smoking), the cellular and molecular mechanisms of AAA remain poorly understood. Basic and clinical studies have revealed that the key pathological features of AAA include i) infiltration of innate and adaptive immune cells in the aortic wall, ii) loss of vascular smooth muscle cells (VSMCs), and iii) proteolysis of the extracellular matrix leading to degradation (ECM). The absence of resolution of those processes leads to progressive AAA growth and culminates in AAA rupture. However, the exact sequence of events leading to rupture remains incompletely understood (152-154).

Although pre-clinical studies have shown that H₂S has potent cardiovascular benefits (reviewed in (155)), only a couple of studies investigated the potential protective effect of H₂S against AAA. Gomez et al., demonstrated that endogenous HS level and CTH expression were lower in AAA samples obtained from patients (14 males and 3 females, aged 67 ± 2 years) undergoing aortic repair surgery, as compared to healthy aorta (156). It was also recently shown that NaHS attenuates inflammation and aortic remodeling in a model of aortic dissection induced by β -aminopropionitrile fumarate (BAPN) and angiotensin II (Ang-II) in WT mice (157).

Interestingly, as mentioned in the introduction, many studies report anti-inflammatory and anti-oxidant properties of H₂S in the context of atherosclerosis and cardiac failure (for full review

see (97)). Whether or not H₂S-based strategies may reduce oxidative stress and inflammation in the context of AAA remains to be tested.

Various models to replicate AAA development have been developed over the years (reviewed in (158)). Intravascular injection of elastase has been shown to induce significant AAA but is challenging technically. An adapted model commonly used consists in perivascular application of elastase (159, 160), which can be further aggravated by BAPN systemic administration (161). Elastase will degrade the elastin, the main component of the elastic lamina (162). BAPN is a lysyl oxidase inhibitor (163) that will prevent the crosslinking of collagen with elastin. In the lab, we slightly modified the protocol for elastase perivascular application. The following preliminary experiments were performed on 10 weeks-old male WT mice without the use of BAPN to setup the peri-aortic elastase application. Surgery was performed under isoflurane anesthesia. While deeply anesthetized, a midline incision was made and the aorta separated from the surrounding fascia below the kidneys. A Whatmann paper impregnated with 8 μ L of Elastase solution (Sigma-Aldrich) was applied on the surface of the aorta for 10 minutes. Following Whatmann removal, the peritoneum cavity was rinsed with warm saline and the abdomen closed with sutures. Aortas were collected 14 days post-op, fixed in buffered formalin and included in paraffin for histology studies. As compared to sham-operated mice with a normal aorta, the mice exposed to peri-aortic elastase application had an enlarged lumen, as quantified by the lumen area along the length of the sub-renal aorta and max diameter of the aorta (**Fig. 1**). The aortic wall also displayed proteolysis of the elastic laminae as assessed by VGEL staining and matrix deposition (newly formed collagen deposit in blue) as observed by Herovici staining. Operated aortas also displayed increased inflammation as measured by T-cell (CD3⁺ cells), macrophages (CD86⁺ cells) and neutrophils (MPO⁺ cells) infiltration in the aortic wall. Finally, Calponin staining of VSMC revealed a major remodeling of the media layer upon elastase application (**Fig. 1**). Preliminary experiments show that STS tends to reduce the severity of the elastase-induced AAA, as well as elastin degradation and a composite inflammation grades (**Fig. 1; STS vs. Ctrl**). However, further

surgeries and staining are required to evaluate the therapeutic potential of STS against AAA formation in this model.

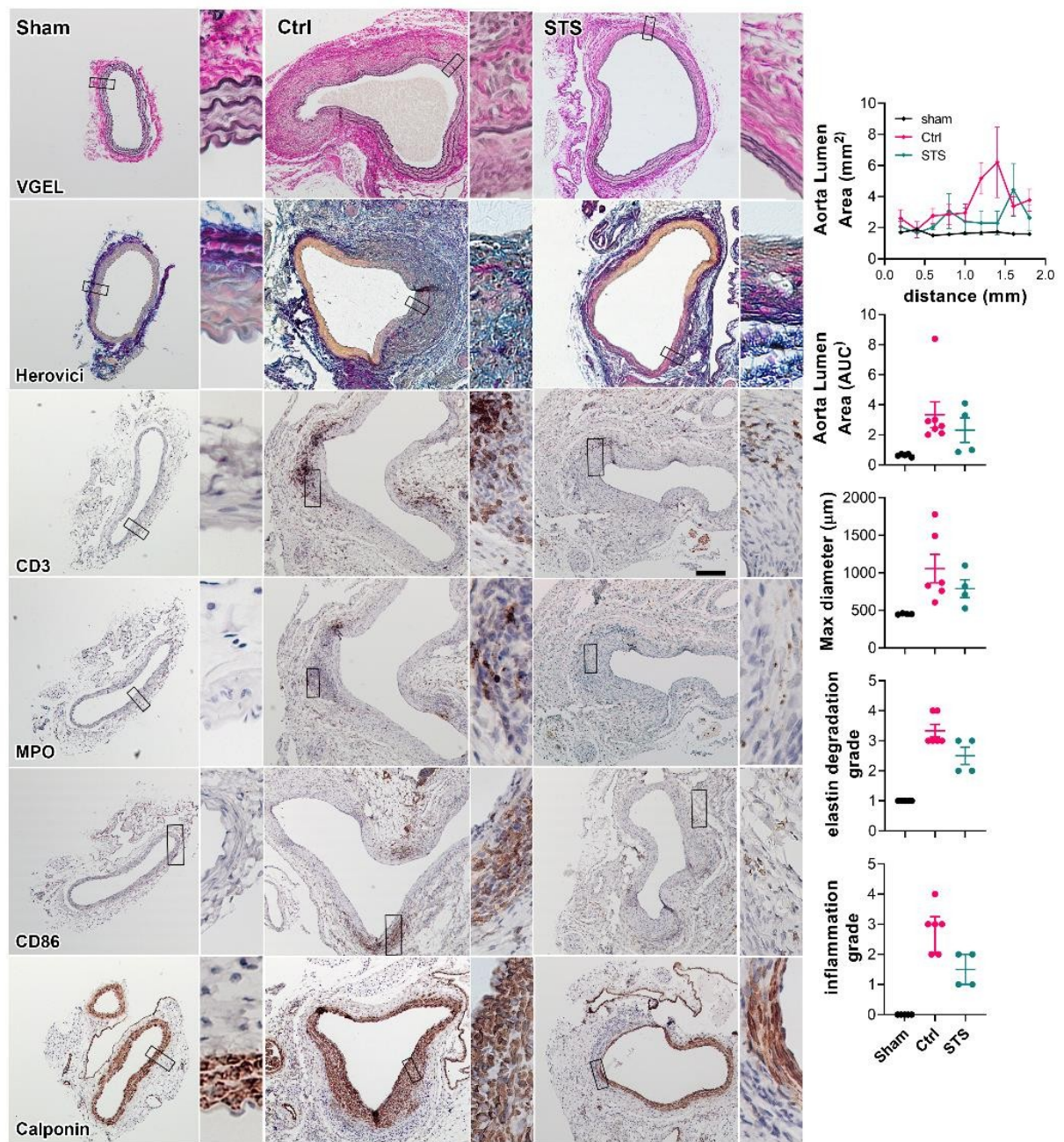


Figure 1 STS reduces AAA formation in a mouse model of topical application of elastase

Representative VGEL and Herovici staining, and CD3, CD86, MPO or calponin immunostaining in sub-renal mouse aorta in sham-operated WT mice (Sham) or in mice with topical elastase application, treated or not (Ctrl) with 4g/L STS (STS). Quantitative assessment of aorta lumen, aorta max diameter, elastin degradation grade (1 to 4), or inflammation grade (1 to 4). Data are mean±SEM of 4 to 6 animals per group. Grades were determined by two independent observers blind to the experimental condition.

9 References

1. Eraso LH, Fukaya E, Mohler ER, 3rd, Xie D, Sha D, Berger JS. Peripheral arterial disease, prevalence and cumulative risk factor profile analysis. *European journal of preventive cardiology*. 2014;21(6):704-11.
2. Fowkes FG, Rudan D, Rudan I, Aboyans V, Denenberg JO, McDermott MM, et al. Comparison of global estimates of prevalence and risk factors for peripheral artery disease in 2000 and 2010: a systematic review and analysis. *Lancet*. 2013;382(9901):1329-40.
3. Song P, Rudan D, Zhu Y, Fowkes FJL, Rahimi K, Fowkes FGR, et al. Global, regional, and national prevalence and risk factors for peripheral artery disease in 2015: an updated systematic review and analysis. *Lancet Glob Health*. 2019;7(8):e1020-e30.
4. Aboyans V, Ricco JB, Bartelink MEL, Bjorck M, Brodmann M, Cohnert T, et al. 2017 ESC Guidelines on the Diagnosis and Treatment of Peripheral Arterial Diseases, in collaboration with the European Society for Vascular Surgery (ESVS): Document covering atherosclerotic disease of extracranial carotid and vertebral, mesenteric, renal, upper and lower extremity arteries Endorsed by: the European Stroke Organization (ESO) The Task Force for the Diagnosis and Treatment of Peripheral Arterial Diseases of the European Society of Cardiology (ESC) and of the European Society for Vascular Surgery (ESVS). *Eur Heart J*. 2018;39(9):763-816.
5. Shu J, Santulli G. Update on peripheral artery disease: Epidemiology and evidence-based facts. *Atherosclerosis*. 2018;275:379-81.
6. Libby P, Buring JE, Badimon L, Hansson GK, Deanfield J, Bittencourt MS, et al. *Atherosclerosis*. *Nat Rev Dis Primers*. 2019;5(1):56.
7. Gimbrone MA, Jr., Garcia-Cardena G. Endothelial Cell Dysfunction and the Pathobiology of Atherosclerosis. *Circ Res*. 2016;118(4):620-36.
8. Hamburg NM, Creager MA. Pathophysiology of Intermittent Claudication in Peripheral Artery Disease. *Circ J*. 2017;81(3):281-9.
9. Hiatt WR, Armstrong EJ, Larson CJ, Brass EP. Pathogenesis of the limb manifestations and exercise limitations in peripheral artery disease. *Circ Res*. 2015;116(9):1527-39.
10. Fowkes FG, Aboyans V, Fowkes FJ, McDermott MM, Sampson UK, Criqui MH. Peripheral artery disease: epidemiology and global perspectives. *Nat Rev Cardiol*. 2017;14(3):156-70.
11. Lane R, Ellis B, Watson L, Leng GC. Exercise for intermittent claudication. *Cochrane Database Syst Rev*. 2014(7):CD000990.
12. Arao K, Yasu T, Endo Y, Funazaki T, Ota Y, Shimada K, et al. Effects of pitavastatin on walking capacity and CD34(+)/133(+) cell number in patients with peripheral artery disease. *Heart Vessels*. 2017;32(10):1186-94.
13. Shahin Y, Barnes R, Barakat H, Chetter IC. Meta-analysis of angiotensin converting enzyme inhibitors effect on walking ability and ankle brachial pressure index in patients with intermittent claudication. *Atherosclerosis*. 2013;231(2):283-90.
14. Iyer SR, Annex BH. Therapeutic Angiogenesis for Peripheral Artery Disease: Lessons Learned in Translational Science. *JACC Basic Transl Sci*. 2017;2(5):503-12.
15. Simpson EL, Kearns B, Stevenson MD, Cantrell AJ, Littlewood C, Michaels JA. Enhancements to angioplasty for peripheral arterial occlusive disease: systematic review, cost-effectiveness assessment and expected value of information analysis. *Health Technol Assess*. 2014;18(10):1-252.

16. Buccheri D, Piraino D, Andolina G, Cortese B. Understanding and managing in-stent restenosis: a review of clinical data, from pathogenesis to treatment. *J Thorac Dis.* 2016;8(10):E1150-E62.
17. Nakano M, Otsuka F, Yahagi K, Sakakura K, Kutys R, Ladich ER, et al. Human autopsy study of drug-eluting stents restenosis: histomorphological predictors and neointimal characteristics. *Eur Heart J.* 2013;34(42):3304-13.
18. Liu R, Leslie KL, Martin KA. Epigenetic regulation of smooth muscle cell plasticity. *Biochim Biophys Acta.* 2015;1849(4):448-53.
19. Sterpetti AV, Cucina A, Lepidi S, Randone B, Stipa F, Aromatario C, et al. Progression and regression of myointimal hyperplasia in experimental vein grafts depends on platelet-derived growth factor and basic fibroblastic growth factor production. *J Vasc Surg.* 1996;23(4):568-75.
20. Abdoli S, Mert M, Lee WM, Ochoa CJ, Katz SG. Network meta-analysis of drug-coated balloon angioplasty versus primary nitinol stenting for femoropopliteal atherosclerotic disease. *J Vasc Surg.* 2021;73(5):1802-10 e4.
21. Teichgraber U, Lehmann T, Aschenbach R, Scheinert D, Zeller T, Brechtel K, et al. Efficacy and safety of a novel paclitaxel-nano-coated balloon for femoropopliteal angioplasty: one-year results of the EffPac trial. *EuroIntervention.* 2020;15(18):e1633-e40.
22. Caradu C, Lakhlifi E, Colacchio EC, Midy D, Berard X, Poirier M, et al. Systematic review and updated meta-analysis of the use of drug-coated balloon angioplasty versus plain old balloon angioplasty for femoropopliteal arterial disease. *J Vasc Surg.* 2019;70(3):981-95 e10.
23. Ding Y, Zhou M, Wang Y, Cai L, Shi Z. Comparison of Drug-Eluting Stent with Bare-Metal Stent Implantation in Femoropopliteal Artery Disease: A Systematic Review and Meta-Analysis. *Ann Vasc Surg.* 2018;50:96-105.
24. Fattori R, Piva T. Drug-eluting stents in vascular intervention. *Lancet.* 2003;361(9353):247-9.
25. Jukema JW, Verschuren JJ, Ahmed TA, Quax PH. Restenosis after PCI. Part 1: pathophysiology and risk factors. *Nat Rev Cardiol.* 2011;9(1):53-62.
26. Bjorck M, Earnshaw JJ, Acosta S, Bastos Goncalves F, Cochennec F, Debus ES, et al. Editor's Choice - European Society for Vascular Surgery (ESVS) 2020 Clinical Practice Guidelines on the Management of Acute Limb Ischaemia. *Eur J Vasc Endovasc Surg.* 2020;59(2):173-218.
27. Katsanos K, Spiliopoulos S, Kitrou P, Krokidis M, Karnabatidis D. Risk of Death Following Application of Paclitaxel-Coated Balloons and Stents in the Femoropopliteal Artery of the Leg: A Systematic Review and Meta-Analysis of Randomized Controlled Trials. *J Am Heart Assoc.* 2018;7(24):e011245.
28. Rocha-Singh KJ, Duval S, Jaff MR, Schneider PA, Ansel GM, Lyden SP, et al. Mortality and Paclitaxel-Coated Devices: An Individual Patient Data Meta-Analysis. *Circulation.* 2020;141(23):1859-69.
29. Royce S, Chakraborty A, Zhao Y. US Food and Drug Administration Perspective on "Mortality and Paclitaxel-Coated Devices: An Individual Patient Data Meta-Analysis". *Circulation.* 2020;141(23):1870-1.
30. Dinh K, Gomes ML, Thomas SD, Paravastu SCV, Holden A, Schneider PA, et al. Mortality After Paclitaxel-Coated Device Use in Patients With Chronic Limb-Threatening Ischemia: A Systematic Review and Meta-Analysis of Randomized Controlled Trials. *J Endovasc Ther.* 2020;27(2):175-85.

31. Ipema J, Huizing E, Schreve MA, de Vries JPM, Unlu C. Editor's Choice - Drug Coated Balloon Angioplasty vs. Standard Percutaneous Transluminal Angioplasty in Below the Knee Peripheral Arterial Disease: A Systematic Review and Meta-Analysis. *Eur J Vasc Endovasc Surg.* 2020;59(2):265-75.
32. Katsanos K, Spiliopoulos S, Kitrou P, Krokidis M, Paraskevopoulos I, Karnabatidis D. Risk of Death and Amputation with Use of Paclitaxel-Coated Balloons in the Infrapopliteal Arteries for Treatment of Critical Limb Ischemia: A Systematic Review and Meta-Analysis of Randomized Controlled Trials. *J Vasc Interv Radiol.* 2020;31(2):202-12.
33. Nordanstig J, James S, Andersson M, Andersson M, Danielsson P, Gillgren P, et al. Mortality with Paclitaxel-Coated Devices in Peripheral Artery Disease. *N Engl J Med.* 2020;383(26):2538-46.
34. Secemsky EA, Kundi H, Weinberg I, Jaff MR, Krawisz A, Parikh SA, et al. Association of Survival With Femoropopliteal Artery Revascularization With Drug-Coated Devices. *JAMA Cardiol.* 2019;4(4):332-40.
35. Beckman JA, White CJ. Paclitaxel-Coated Balloons and Eluting Stents: Is There a Mortality Risk in Patients with Peripheral Artery Disease? *Circulation.* 2019.
36. Byrne RA, Stone GW, Ormiston J, Kastrati A. Coronary balloon angioplasty, stents, and scaffolds. *Lancet.* 2017;390(10096):781-92.
37. Teichgraber U, Ingwersen M, Platzer S, Lehmann T, Zeller T, Aschenbach R, et al. Head-to-head comparison of sirolimus- versus paclitaxel-coated balloon angioplasty in the femoropopliteal artery: study protocol for the randomized controlled SIRONA trial. *Trials.* 2021;22(1):665.
38. Zhu P, Zhou X, Zhang C, Li H, Zhang Z, Song Z. Safety and efficacy of ultrathin strut biodegradable polymer sirolimus-eluting stent versus durable polymer drug-eluting stents: a meta-analysis of randomized trials. *BMC Cardiovasc Disord.* 2018;18(1):170.
39. El-Hayek G, Bangalore S, Casso Dominguez A, Devireddy C, Jaber W, Kumar G, et al. Meta-Analysis of Randomized Clinical Trials Comparing Biodegradable Polymer Drug-Eluting Stent to Second-Generation Durable Polymer Drug-Eluting Stents. *JACC Cardiovasc Interv.* 2017;10(5):462-73.
40. Nakashima Y, Wight TN, Sueishi K. Early atherosclerosis in humans: role of diffuse intimal thickening and extracellular matrix proteoglycans. *Cardiovasc Res.* 2008;79(1):14-23.
41. Sur S, Sugimoto JT, Agrawal DK. Coronary artery bypass graft: why is the saphenous vein prone to intimal hyperplasia? *Can J Physiol Pharmacol.* 2014;92(7):531-45.
42. Szabo C, Ransy C, Modis K, Andriamihaja M, Murghez B, Coletta C, et al. Regulation of mitochondrial bioenergetic function by hydrogen sulfide. Part I. Biochemical and physiological mechanisms. *Br J Pharmacol.* 2014;171(8):2099-122.
43. Yang G, Wu L, Jiang B, Yang W, Qi J, Cao K, et al. H₂S as a physiologic vasorelaxant: hypertension in mice with deletion of cystathionine gamma-lyase. *Science.* 2008;322(5901):587-90.
44. Cheng Y, Ndisang JF, Tang G, Cao K, Wang R. Hydrogen sulfide-induced relaxation of resistance mesenteric artery beds of rats. *Am J Physiol Heart Circ Physiol.* 2004;287(5):H2316-23.
45. Mustafa AK, Sikka G, Gazi SK, Steppan J, Jung SM, Bhunia AK, et al. Hydrogen sulfide as endothelium-derived hyperpolarizing factor sulfhydrates potassium channels. *Circ Res.* 2011;109(11):1259-68.

46. Shibuya N, Mikami Y, Kimura Y, Nagahara N, Kimura H. Vascular endothelium expresses 3-mercaptopyruvate sulfurtransferase and produces hydrogen sulfide. *J Biochem.* 2009;146(5):623-6.
47. Ishii I, Akahoshi N, Yamada H, Nakano S, Izumi T, Suematsu M. Cystathionine gamma-Lyase-deficient mice require dietary cysteine to protect against acute lethal myopathy and oxidative injury. *J Biol Chem.* 2010;285(34):26358-68.
48. Szijarto IA, Marko L, Filipovic MR, Miljkovic JL, Tabeling C, Tsvetkov D, et al. Cystathionine gamma-Lyase-Produced Hydrogen Sulfide Controls Endothelial NO Bioavailability and Blood Pressure. *Hypertension.* 2018;71(6):1210-7.
49. Bibli SI, Hu J, Sigala F, Wittig I, Heidler J, Zukunft S, et al. Cystathionine gamma Lyase Sulfhydrates the RNA Binding Protein Human Antigen R to Preserve Endothelial Cell Function and Delay Atherogenesis. *Circulation.* 2019;139(1):101-14.
50. Bibli SI, Hu J, Leisegang MS, Wittig J, Zukunft S, Kapasakalidi A, et al. Shear stress regulates cystathionine gamma lyase expression to preserve endothelial redox balance and reduce membrane lipid peroxidation. *Redox Biol.* 2020;28:101379.
51. Yuan S, Yurdagul A, Jr., Peretik JM, Alfaidi M, Al Yafeai Z, Pardue S, et al. Cystathionine gamma-Lyase Modulates Flow-Dependent Vascular Remodeling. *Arterioscler Thromb Vasc Biol.* 2018;38(9):2126-36.
52. Filipovic MR, Zivanovic J, Alvarez B, Banerjee R. Chemical Biology of H₂S Signaling through Persulfidation. *Chem Rev.* 2018;118(3):1253-337.
53. Sen N. Functional and Molecular Insights of Hydrogen Sulfide Signaling and Protein Sulfhydration. *J Mol Biol.* 2017;429(4):543-61.
54. Mustafa AK, Gadalla MM, Sen N, Kim S, Mu W, Gazi SK, et al. H₂S signals through protein S-sulfhydration. *Sci Signal.* 2009;2(96):ra72.
55. Bibli SI, Hu J, Looso M, Weigert A, Ratiu C, Wittig J, et al. Mapping the Endothelial Cell S-Sulfhydrone Highlights the Crucial Role of Integrin Sulfhydration in Vascular Function. *Circulation.* 2021;143(9):935-48.
56. Fu L, Liu K, He J, Tian C, Yu X, Yang J. Direct Proteomic Mapping of Cysteine Persulfidation. *Antioxid Redox Signal.* 2020;33(15):1061-76.
57. Zivanovic J, Kouroussis E, Kohl JB, Adhikari B, Bursac B, Schott-Roux S, et al. Selective Persulfide Detection Reveals Evolutionarily Conserved Antiaging Effects of S-Sulfhydration. *Cell Metab.* 2019;30(6):1152-70 e13.
58. Roy A, Khan AH, Islam MT, Prieto MC, Majid DS. Interdependency of cystathione gamma-lyase and cystathione beta-synthase in hydrogen sulfide-induced blood pressure regulation in rats. *Am J Hypertens.* 2012;25(1):74-81.
59. Jackson-Weaver O, Osmond JM, Riddle MA, Naik JS, Gonzalez Bosc LV, Walker BR, et al. Hydrogen sulfide dilates rat mesenteric arteries by activating endothelial large-conductance Ca(2)(+)-activated K(+) channels and smooth muscle Ca(2)(+) sparks. *Am J Physiol Heart Circ Physiol.* 2013;304(11):H1446-54.
60. Coletta C, Papapetropoulos A, Erdelyi K, Olah G, Modis K, Panopoulos P, et al. Hydrogen sulfide and nitric oxide are mutually dependent in the regulation of angiogenesis and endothelium-dependent vasorelaxation. *Proc Natl Acad Sci U S A.* 2012;109(23):9161-6.
61. Altaany Z, Ju Y, Yang G, Wang R. The coordination of S-sulfhydration, S-nitrosylation, and phosphorylation of endothelial nitric oxide synthase by hydrogen sulfide. *Sci Signal.* 2014;7(342):ra87.
62. Kanagy NL, Szabo C, Papapetropoulos A. Vascular biology of hydrogen sulfide. *Am J Physiol Cell Physiol.* 2017;312(5):C537-C49.

63. Wang MJ, Cai WJ, Li N, Ding YJ, Chen Y, Zhu YC. The hydrogen sulfide donor NaHS promotes angiogenesis in a rat model of hind limb ischemia. *Antioxid Redox Signal*. 2010;12(9):1065-77.
64. Majumder A, Singh M, George AK, Behera J, Tyagi N, Tyagi SC. Hydrogen sulfide improves postischemic neoangiogenesis in the hind limb of cystathionine-beta-synthase mutant mice via PPAR-gamma/VEGF axis. *Physiol Rep*. 2018;6(17):e13858.
65. Xiong Y, Chang LL, Tran B, Dai T, Zhong R, Mao YC, et al. ZYZ-803, a novel hydrogen sulfide-nitric oxide conjugated donor, promotes angiogenesis via cross-talk between STAT3 and CaMKII. *Acta Pharmacol Sin*. 2020;41(2):218-28.
66. Annex BH, Cooke JP. New Directions in Therapeutic Angiogenesis and Arteriogenesis in Peripheral Arterial Disease. *Circ Res*. 2021;128(12):1944-57.
67. Yuan S, Kevil CG. Nitric Oxide and Hydrogen Sulfide Regulation of Ischemic Vascular Remodeling. *Microcirculation*. 2016;23(2):134-45.
68. Altaany Z, Yang G, Wang R. Crosstalk between hydrogen sulfide and nitric oxide in endothelial cells. *J Cell Mol Med*. 2013;17(7):879-88.
69. Papapetropoulos A, Pyriochou A, Altaany Z, Yang G, Marazioti A, Zhou Z, et al. Hydrogen sulfide is an endogenous stimulator of angiogenesis. *Proc Natl Acad Sci U S A*. 2009;106(51):21972-7.
70. Katsouda A, Bibli SI, Pyriochou A, Szabo C, Papapetropoulos A. Regulation and role of endogenously produced hydrogen sulfide in angiogenesis. *Pharmacol Res*. 2016;113(Pt A):175-85.
71. Cai WJ, Wang MJ, Moore PK, Jin HM, Yao T, Zhu YC. The novel proangiogenic effect of hydrogen sulfide is dependent on Akt phosphorylation. *Cardiovasc Res*. 2007;76(1):29-40.
72. Tao BB, Liu SY, Zhang CC, Fu W, Cai WJ, Wang Y, et al. VEGFR2 functions as an H₂S-targeting receptor protein kinase with its novel Cys1045-Cys1024 disulfide bond serving as a specific molecular switch for hydrogen sulfide actions in vascular endothelial cells. *Antioxid Redox Signal*. 2013;19(5):448-64.
73. Longchamp A, Mirabella T, Arduini A, MacArthur MR, Das A, Trevino-Villarreal JH, et al. Amino Acid Restriction Triggers Angiogenesis via GCN2/ATF4 Regulation of VEGF and H₂S Production. *Cell*. 2018;173(1):117-29 e14.
74. Eelen G, de Zeeuw P, Treps L, Harjes U, Wong BW, Carmeliet P. Endothelial Cell Metabolism. *Physiol Rev*. 2018;98(1):3-58.
75. Schoors S, De Bock K, Cantelmo AR, Georgiadou M, Ghesquiere B, Cauwenberghs S, et al. Partial and transient reduction of glycolysis by PFKFB3 blockade reduces pathological angiogenesis. *Cell Metab*. 2014;19(1):37-48.
76. De Bock K, Georgiadou M, Schoors S, Kuchnio A, Wong BW, Cantelmo AR, et al. Role of PFKFB3-driven glycolysis in vessel sprouting. *Cell*. 2013;154(3):651-63.
77. Szabo C, Papapetropoulos A. Hydrogen sulphide and angiogenesis: mechanisms and applications. *Br J Pharmacol*. 2011;164(3):853-65.
78. Moccia F, Bertoni G, Pla AF, Dragoni S, Pupo E, Merlino A, et al. Hydrogen sulfide regulates intracellular Ca²⁺ concentration in endothelial cells from excised rat aorta. *Curr Pharm Biotechnol*. 2011;12(9):1416-26.
79. Jang H, Oh MY, Kim YJ, Choi IY, Yang HS, Ryu WS, et al. Hydrogen sulfide treatment induces angiogenesis after cerebral ischemia. *J Neurosci Res*. 2014;92(11):1520-8.
80. Szabo C. Hydrogen sulfide, an enhancer of vascular nitric oxide signaling: mechanisms and implications. *Am J Physiol Cell Physiol*. 2017;312(1):C3-C15.

81. Meng QH, Yang G, Yang W, Jiang B, Wu L, Wang R. Protective effect of hydrogen sulfide on balloon injury-induced neointima hyperplasia in rat carotid arteries. *Am J Pathol.* 2007;170(4):1406-14.
82. Islam KN, Polhemus DJ, Donnarumma E, Brewster LP, Lefer DJ. Hydrogen Sulfide Levels and Nuclear Factor-Erythroid 2-Related Factor 2 (NRF2) Activity Are Attenuated in the Setting of Critical Limb Ischemia (CLI). *J Am Heart Assoc.* 2015;4(5).
83. Beard RS, Jr., Bearden SE. Vascular complications of cystathionine beta-synthase deficiency: future directions for homocysteine-to-hydrogen sulfide research. *Am J Physiol Heart Circ Physiol.* 2011;300(1):H13-26.
84. Longchamp A, MacArthur MR, Trocha K, Ganahl J, Mann CG, Kip P, et al. Plasma Hydrogen Sulfide Is Positively Associated With Post-operative Survival in Patients Undergoing Surgical Revascularization. *Front Cardiovasc Med.* 2021;8:750926.
85. Yang G, Li H, Tang G, Wu L, Zhao K, Cao Q, et al. Increased neointimal formation in cystathionine gamma-lyase deficient mice: role of hydrogen sulfide in alpha5beta1-integrin and matrix metalloproteinase-2 expression in smooth muscle cells. *J Mol Cell Cardiol.* 2012;52(3):677-88.
86. Macabrey D, Longchamp A, MacArthur MR, Lambelet M, Urfer S, Corpataux J-M, et al. Sodium Thiosulfate acts as an H₂S mimetic to prevent intimal hyperplasia via inhibition of tubulin polymerization. *bioRxiv.* 2021.
87. Trocha KM, Kip P, Tao M, MacArthur MR, Trevino-Villarreal H, Longchamp A, et al. Short-Term Preoperative Protein Restriction Attenuates Vein Graft Disease via Induction of Cystathionine Upsilon-Lyase. *Cardiovasc Res.* 2019.
88. Ma B, Liang G, Zhang F, Chen Y, Zhang H. Effect of hydrogen sulfide on restenosis of peripheral arteries after angioplasty. *Mol Med Rep.* 2012;5(6):1497-502.
89. Longchamp A, Kaur K, Macabrey D, Dubuis C, Corpataux JM, Deglise S, et al. Hydrogen sulfide-releasing peptide hydrogel limits the development of intimal hyperplasia in human vein segments. *Acta Biomater.* 2019.
90. Yang G, Wu L, Wang R. Pro-apoptotic effect of endogenous H₂S on human aorta smooth muscle cells. *FASEB J.* 2006;20(3):553-5.
91. Yang G, Wu L, Bryan S, Khaper N, Mani S, Wang R. Cystathionine gamma-lyase deficiency and overproliferation of smooth muscle cells. *Cardiovasc Res.* 2010;86(3):487-95.
92. Tong X, Khandelwal AR, Qin Z, Wu X, Chen L, Ago T, et al. Role of smooth muscle Nox4-based NADPH oxidase in neointimal hyperplasia. *J Mol Cell Cardiol.* 2015;89(Pt B):185-94.
93. Wang Y, Wang X, Liang X, Wu J, Dong S, Li H, et al. Inhibition of hydrogen sulfide on the proliferation of vascular smooth muscle cells involved in the modulation of calcium sensing receptor in high homocysteine. *Exp Cell Res.* 2016;347(1):184-91.
94. Zhong X, Wang Y, Wu J, Sun A, Yang F, Zheng D, et al. Calcium sensing receptor regulating smooth muscle cells proliferation through initiating cystathionine-gamma-lyase/hydrogen sulfide pathway in diabetic rat. *Cell Physiol Biochem.* 2015;35(4):1582-98.
95. Macabrey D, Deslarzes-Dubuis C, Longchamp A, Lambelet M, Ozaki CK, Corpataux J-M, et al. Hydrogen sulfide release via the ACE inhibitor Zofenopril prevents intimal hyperplasia in human vein segments and in a mouse model of carotid artery stenosis. *bioRxiv.* 2021.
96. Lee KY, Kim JR, Choi HC. Gliclazide, a KATP channel blocker, inhibits vascular smooth muscle cell proliferation through the CaMKKbeta-AMPK pathway. *Vascul Pharmacol.* 2018;102:21-8.

97. Pan LL, Qin M, Liu XH, Zhu YZ. The Role of Hydrogen Sulfide on Cardiovascular Homeostasis: An Overview with Update on Immunomodulation. *Front Pharmacol.* 2017;8:686.
98. Liu Z, Han Y, Li L, Lu H, Meng G, Li X, et al. The hydrogen sulfide donor, GYY4137, exhibits anti-atherosclerotic activity in high fat fed apolipoprotein E(-/-) mice. *Br J Pharmacol.* 2013;169(8):1795-809.
99. Fan J, Zheng F, Li S, Cui C, Jiang S, Zhang J, et al. Hydrogen sulfide lowers hyperhomocysteinemia dependent on cystathionine gamma lyase S-sulfhydration in ApoE-knockout atherosclerotic mice. *Br J Pharmacol.* 2019;176(17):3180-92.
100. Elrod JW, Calvert JW, Morrison J, Doeller JE, Kraus DW, Tao L, et al. Hydrogen sulfide attenuates myocardial ischemia-reperfusion injury by preservation of mitochondrial function. *Proc Natl Acad Sci U S A.* 2007;104(39):15560-5.
101. Zhang Y, Li H, Zhao G, Sun A, Zong NC, Li Z, et al. Hydrogen sulfide attenuates the recruitment of CD11b(+)Gr-1(+) myeloid cells and regulates Bax/Bcl-2 signaling in myocardial ischemia injury. *Sci Rep.* 2014;4:4774.
102. Qipshidze N, Metreveli N, Mishra PK, Lominadze D, Tyagi SC. Hydrogen sulfide mitigates cardiac remodeling during myocardial infarction via improvement of angiogenesis. *Int J Biol Sci.* 2012;8(4):430-41.
103. Wu T, Li H, Wu B, Zhang L, Wu SW, Wang JN, et al. Hydrogen Sulfide Reduces Recruitment of CD11b(+)Gr-1(+) Cells in Mice With Myocardial Infarction. *Cell Transplant.* 2017;26(5):753-64.
104. Predmore BL, Kondo K, Bhushan S, Zlatopolsky MA, King AL, Aragon JP, et al. The polysulfide diallyl trisulfide protects the ischemic myocardium by preservation of endogenous hydrogen sulfide and increasing nitric oxide bioavailability. *Am J Physiol Heart Circ Physiol.* 2012;302(11):H2410-8.
105. Ravindran S, Jahir Hussain S, Boovarahan SR, Kurian GA. Sodium thiosulfate post-conditioning protects rat hearts against ischemia reperfusion injury via reduction of apoptosis and oxidative stress. *Chem Biol Interact.* 2017;274:24-34.
106. Wang Y, Zhao X, Jin H, Wei H, Li W, Bu D, et al. Role of hydrogen sulfide in the development of atherosclerotic lesions in apolipoprotein E knockout mice. *Arterioscler Thromb Vasc Biol.* 2009;29(2):173-9.
107. Du J, Huang Y, Yan H, Zhang Q, Zhao M, Zhu M, et al. Hydrogen sulfide suppresses oxidized low-density lipoprotein (ox-LDL)-stimulated monocyte chemoattractant protein 1 generation from macrophages via the nuclear factor kappaB (NF-kappaB) pathway. *J Biol Chem.* 2014;289(14):9741-53.
108. Wang XH, Wang F, You SJ, Cao YJ, Cao LD, Han Q, et al. Dysregulation of cystathionine gamma-lyase (CSE)/hydrogen sulfide pathway contributes to ox-LDL-induced inflammation in macrophage. *Cell Signal.* 2013;25(11):2255-62.
109. Sen N, Paul BD, Gadalla MM, Mustafa AK, Sen T, Xu R, et al. Hydrogen sulfide-linked sulfhydration of NF-kappaB mediates its antiapoptotic actions. *Mol Cell.* 2012;45(1):13-24.
110. Dufton N, Natividad J, Verdu EF, Wallace JL. Hydrogen sulfide and resolution of acute inflammation: A comparative study utilizing a novel fluorescent probe. *Sci Rep.* 2012;2:499.
111. Lin Y, Chen Y, Zhu N, Zhao S, Fan J, Liu E. Hydrogen sulfide inhibits development of atherosclerosis through up-regulating protein S-nitrosylation. *Biomed Pharmacother.* 2016;83:466-76.

112. Nicholson CK, Lambert JP, Molckentin JD, Sadoshima J, Calvert JW. Thioredoxin 1 is essential for sodium sulfide-mediated cardioprotection in the setting of heart failure. *Arterioscler Thromb Vasc Biol.* 2013;33(4):744-51.
113. Murphy B, Bhattacharya R, Mukherjee P. Hydrogen sulfide signaling in mitochondria and disease. *FASEB J.* 2019;33(12):13098-125.
114. Peake BF, Nicholson CK, Lambert JP, Hood RL, Amin H, Amin S, et al. Hydrogen sulfide preconditions the db/db diabetic mouse heart against ischemia-reperfusion injury by activating Nrf2 signaling in an Erk-dependent manner. *Am J Physiol Heart Circ Physiol.* 2013;304(9):H1215-24.
115. Polhemus DJ, Lefer DJ. Emergence of hydrogen sulfide as an endogenous gaseous signaling molecule in cardiovascular disease. *Circ Res.* 2014;114(4):730-7.
116. Calvert JW, Jha S, Gundewar S, Elrod JW, Ramachandran A, Pattillo CB, et al. Hydrogen sulfide mediates cardioprotection through Nrf2 signaling. *Circ Res.* 2009;105(4):365-74.
117. Corsello T, Komaravelli N, Casola A. Role of Hydrogen Sulfide in NRF2- and Sirtuin-Dependent Maintenance of Cellular Redox Balance. *Antioxidants (Basel).* 2018;7(10).
118. Ono K, Akaike T, Sawa T, Kumagai Y, Wink DA, Tantillo DJ, et al. Redox chemistry and chemical biology of H₂S, hydropersulfides, and derived species: implications of their possible biological activity and utility. *Free Radic Biol Med.* 2014;77:82-94.
119. Xie ZZ, Liu Y, Bian JS. Hydrogen Sulfide and Cellular Redox Homeostasis. *Oxid Med Cell Longev.* 2016;2016:6043038.
120. Cheung SH, Lau JYW. Hydrogen sulfide mediates athero-protection against oxidative stress via S-sulfhydration. *PLoS One.* 2018;13(3):e0194176.
121. Xie L, Gu Y, Wen M, Zhao S, Wang W, Ma Y, et al. Hydrogen Sulfide Induces Keap1 S-sulfhydration and Suppresses Diabetes-Accelerated Atherosclerosis via Nrf2 Activation. *Diabetes.* 2016;65(10):3171-84.
122. Shefa U, Kim MS, Jeong NY, Jung J. Antioxidant and Cell-Signaling Functions of Hydrogen Sulfide in the Central Nervous System. *Oxid Med Cell Longev.* 2018;2018:1873962.
123. Tian D, Dong J, Jin S, Teng X, Wu Y. Endogenous hydrogen sulfide-mediated MAPK inhibition preserves endothelial function through TXNIP signaling. *Free Radic Biol Med.* 2017;110:291-9.
124. Balaban RS, Nemoto S, Finkel T. Mitochondria, oxidants, and aging. *Cell.* 2005;120(4):483-95.
125. Turrens JF. Mitochondrial formation of reactive oxygen species. *J Physiol.* 2003;552(Pt 2):335-44.
126. Paul BD, Snyder SH, Kashfi K. Effects of hydrogen sulfide on mitochondrial function and cellular bioenergetics. *Redox Biol.* 2021;38:101772.
127. Sun HJ, Zhao MX, Ren XS, Liu TY, Chen Q, Li YH, et al. Salusin-beta Promotes Vascular Smooth Muscle Cell Migration and Intimal Hyperplasia After Vascular Injury via ROS/NFkappaB/MMP-9 Pathway. *Antioxid Redox Signal.* 2016;24(18):1045-57.
128. Wang Y, Ji L, Jiang R, Zheng L, Liu D. Oxidized high-density lipoprotein induces the proliferation and migration of vascular smooth muscle cells by promoting the production of ROS. *J Atheroscler Thromb.* 2014;21(3):204-16.
129. Benavides GA, Squadrito GL, Mills RW, Patel HD, Isbell TS, Patel RP, et al. Hydrogen sulfide mediates the vasoactivity of garlic. *Proc Natl Acad Sci U S A.* 2007;104(46):17977-82.

130. Farese S, Stauffer E, Kalicki R, Hildebrandt T, Frey BM, Frey FJ, et al. Sodium thiosulfate pharmacokinetics in hemodialysis patients and healthy volunteers. *Clin J Am Soc Nephrol*. 2011;6(6):1447-55.
131. Sharma R. Estimation of thiosulfate using sodium nitroprusside by a newer photochemical method. *Journal of Chemical and Pharmaceutical Research*. 2009;1:321-8.
132. Bucci M, Vellecco V, Cantalupo A, Brancaleone V, Zhou Z, Evangelista S, et al. Hydrogen sulfide accounts for the peripheral vascular effects of zofenopril independently of ACE inhibition. *Cardiovasc Res*. 2014;102(1):138-47.
133. Monti M, Terzuoli E, Ziche M, Morbidelli L. H₂S dependent and independent anti-inflammatory activity of zofenoprilat in cells of the vascular wall. *Pharmacol Res*. 2016;113(Pt A):426-37.
134. Collaboration NCDRF. Worldwide trends in hypertension prevalence and progress in treatment and control from 1990 to 2019: a pooled analysis of 1201 population-representative studies with 104 million participants. *Lancet*. 2021;398(10304):957-80.
135. Clement DL, De Buyzere ML, Duprez DA. Hypertension in peripheral arterial disease. *Curr Pharm Des*. 2004;10(29):3615-20.
136. Krishna SM, Omer SM, Li J, Morton SK, Jose RJ, Golledge J. Development of a two-stage limb ischemia model to better simulate human peripheral artery disease. *Sci Rep*. 2020;10(1):3449.
137. Rajendran S, Shen X, Glawe J, Kolluru GK, Kevil CG. Nitric Oxide and Hydrogen Sulfide Regulation of Ischemic Vascular Growth and Remodeling. *Compr Physiol*. 2019;9(3):1213-47.
138. Fung E, Helisch A. Macrophages in collateral arteriogenesis. *Front Physiol*. 2012;3:353.
139. Grundmann S, Piek JJ, Pasterkamp G, Hoefer IE. Arteriogenesis: basic mechanisms and therapeutic stimulation. *Eur J Clin Invest*. 2007;37(10):755-66.
140. Babiak A, Schumm AM, Wangler C, Loukas M, Wu J, Dombrowski S, et al. Coordinated activation of VEGFR-1 and VEGFR-2 is a potent arteriogenic stimulus leading to enhancement of regional perfusion. *Cardiovasc Res*. 2004;61(4):789-95.
141. Fitzgerald G, Soro-Arnaiz I, De Bock K. The Warburg Effect in Endothelial Cells and its Potential as an Anti-angiogenic Target in Cancer. *Front Cell Dev Biol*. 2018;6:100.
142. Arpino JM, Yin H, Prescott EK, Staples SCR, Nong Z, Li F, et al. Low-flow intussusception and metastable VEGFR2 signaling launch angiogenesis in ischemic muscle. *Sci Adv*. 2021;7(48):eabg9509.
143. Mentzer SJ, Konerding MA. Intussusceptive angiogenesis: expansion and remodeling of microvascular networks. *Angiogenesis*. 2014;17(3):499-509.
144. Burke SE, Lubbers NL, Chen Y-W, Hsieh GC, Mollison KW, Luly JR, et al. Neointimal Formation After Balloon-Induced Vascular Injury in Yucatan Minipigs is Reduced by Oral Rapamycin. 1999;33(6):829-35.
145. Rushing AM, Donnarumma E, Polhemus DJ, Au KR, Victoria SE, Schumacher JD, et al. Effects of a novel hydrogen sulfide prodrug in a porcine model of acute limb ischemia. *J Vasc Surg*. 2019;69(6):1924-35.
146. Terstappen F, Clarke SM, Joles JA, Ross CA, Garrett MR, Minnion M, et al. Sodium Thiosulfate in the Pregnant Dahl Salt-Sensitive Rat, a Model of Preeclampsia. *Biomolecules*. 2020;10(2).

147. Beck AW, Sedrakyan A, Mao J, Venermo M, Faizer R, Debus S, et al. Variations in Abdominal Aortic Aneurysm Care: A Report From the International Consortium of Vascular Registries. *Circulation*. 2016;134(24):1948–58.
148. Wanhainen A, Verzini F, Van Herzele I, Allaire E, Bown M, Cohnert T, et al. Editor's Choice - European Society for Vascular Surgery (ESVS) 2019 Clinical Practice Guidelines on the Management of Abdominal Aorto-iliac Artery Aneurysms. *European Journal of Vascular and Endovascular Surgery: The Official Journal of the European Society for Vascular Surgery*. 2019;57(1):8–93.
149. Chaikof EL, Dalman RL, Eskandari MK, Jackson BM, Lee WA, Mansour MA, et al. The Society for Vascular Surgery practice guidelines on the care of patients with an abdominal aortic aneurysm. *J Vasc Surg*. 2018;67(1):2-77 e2.
150. Kandail H, Hamady M, Xu XY. Patient-specific analysis of displacement forces acting on fenestrated stent grafts for endovascular aneurysm repair. *Journal of Biomechanics*. 2014;47(14):3546–54.
151. Kurosawa K, Matsumura JS, Yamanouchi D. Current status of medical treatment for abdominal aortic aneurysm. *Circ J*. 2013;77(12):2860-6.
152. Gurung R, Choong AM, Woo CC, Foo R, Sorokin V. Genetic and Epigenetic Mechanisms Underlying Vascular Smooth Muscle Cell Phenotypic Modulation in Abdominal Aortic Aneurysm. *Int J Mol Sci*. 2020;21(17).
153. Petsophonsakul P, Furmanik M, Forsythe R, Dweck M, Schurink GW, Natour E, et al. Role of Vascular Smooth Muscle Cell Phenotypic Switching and Calcification in Aortic Aneurysm Formation. *Arterioscler Thromb Vasc Biol*. 2019;39(7):1351-68.
154. Ouyang M, Wang M, Yu B. Aberrant Mitochondrial Dynamics: An Emerging Pathogenic Driver of Abdominal Aortic Aneurysm. *Cardiovasc Ther*. 2021;2021:6615400.
155. Wallace JL, Wang R. Hydrogen sulfide-based therapeutics: exploiting a unique but ubiquitous gasotransmitter. *Nat Rev Drug Discov*. 2015;14(5):329-45.
156. Gomez I, Ozen G, Deschildre C, Amgoud Y, Boubaya L, Gorenne I, et al. Reverse Regulatory Pathway (H₂S / PGE₂ / MMP) in Human Aortic Aneurysm and Saphenous Vein Varicosity. *PLoS One*. 2016;11(6):e0158421.
157. Lu HY, Hsu HL, Li CH, Li SJ, Lin SJ, Shih CM, et al. Hydrogen Sulfide Attenuates Aortic Remodeling in Aortic Dissection Associating with Moderated Inflammation and Oxidative Stress through a NO-Dependent Pathway. *Antioxidants (Basel)*. 2021;10(5).
158. Golledge J. Abdominal aortic aneurysm: update on pathogenesis and medical treatments. *Nat Rev Cardiol*. 2019;16(4):225-42.
159. Xue C, Zhao G, Zhao Y, Chen YE, Zhang J. Mouse Abdominal Aortic Aneurysm Model Induced by Perivascular Application of Elastase. *J Vis Exp*. 2022(180).
160. Spinoso M, Su G, Salmon MD, Lu G, Cullen JM, Fashandi AZ, et al. Resolvin D1 decreases abdominal aortic aneurysm formation by inhibiting NETosis in a mouse model. *J Vasc Surg*. 2018;68(6S):93S-103S.
161. Senemaud J, Caligiuri G, Etienne H, Delbosc S, Michel JB, Coscas R. Translational Relevance and Recent Advances of Animal Models of Abdominal Aortic Aneurysm. *Arterioscler Thromb Vasc Biol*. 2017;37(3):401-10.
162. Heinz A. Elastases and elastokines: elastin degradation and its significance in health and disease. *Crit Rev Biochem Mol Biol*. 2020;55(3):252-73.
163. Chen T, Jiang N, Zhang S, Chen Q, Guo Z. BAPN-induced rodent model of aortic dissecting aneurysm and related complications. *J Thorac Dis*. 2021;13(6):3643-51.

10 Annex: Clinical use of hydrogen sulfide to protect against intimal hyperplasia

The present paper has been accepted by Frontiers for publication and is currently under final formatting by the journal and the online version is not available yet. The version presented here in an intermediate version provided by the journal pending final formatting.



Clinical Use of Hydrogen Sulfide to Protect Against Intimal Hyperplasia

Diane Macabrey^{1,2†}, Alban Longchamp^{1,2†}, Sebastien Deglise^{1,2†} and Florent Allagnat^{1,2*‡}

¹ Department of Vascular Surgery, Lausanne University Hospital, Lausanne, Switzerland, ² Department of Biomedical Sciences, University of Lausanne, Lausanne, Switzerland

OPEN ACCESS

Edited by:

Jinwei Tian,
The Second Affiliated Hospital
of Harbin Medical University, China

Reviewed by:

Ming Tao,
Brigham and Women's Hospital
and Harvard Medical School,
United States

Hong Li,
Harbin Medical University (Daqing),
China

Hiroaki Neki,
Hamamatsu University School
of Medicine, Japan

Daniele Mancardi,
University of Turin, Italy

*Correspondence:

Florent Allagnat
Florent.allagnat@chuv.ch

[†]These authors have contributed
equally to this work and share first
authorship

[‡]These authors have contributed
equally to this work and share senior
authorship

Specialty section:

This article was submitted to
General Cardiovascular Medicine,
a section of the journal
Frontiers in Cardiovascular Medicine

Received: 15 February 2022

Accepted: 18 March 2022

Published: xx xx 2022

Citation:

Macabrey D, Longchamp A,
Deglise S and Allagnat F (2022)
Clinical Use of Hydrogen Sulfide
to Protect Against Intimal Hyperplasia.
Front. Cardiovasc. Med. 9:876639.
doi: 10.3389/fcvm.2022.876639

Arterial occlusive disease is the narrowing of the arteries *via* atherosclerotic plaque buildup. The major risk factors for arterial occlusive disease are age, high levels of cholesterol and triglycerides, diabetes, high blood pressure, and smoking. Arterial occlusive disease is the leading cause of death in Western countries. Patients who suffer from arterial occlusive disease develop peripheral arterial disease (PAD) when the narrowing affects limbs, stroke when the narrowing affects carotid arteries, and heart disease when the narrowing affects coronary arteries. When lifestyle interventions (exercise, diet...) fail, the only solution remains surgical endovascular and open revascularization. Unfortunately, these surgeries still suffer from high failure rates due to re-occlusive vascular wall adaptations, which is largely due to intimal hyperplasia (IH). IH develops in response to vessel injury, leading to inflammation, vascular smooth muscle cells dedifferentiation, migration, proliferation and secretion of extra-cellular matrix into the vessel's innermost layer or intima. Re-occlusive IH lesions result in costly and complex recurrent end-organ ischemia, and often lead to loss of limb, brain function, or life. Despite decades of IH research, limited therapies are currently available. Hydrogen sulfide (H₂S) is an endogenous gasotransmitter derived from cysteine metabolism. Although environmental exposure to exogenous high H₂S is toxic, endogenous H₂S has important vasorelaxant, cytoprotective and anti-inflammatory properties. Its vasculo-protective properties have attracted a remarkable amount of attention, especially its ability to inhibit IH. This review summarizes IH pathophysiology and treatment, and provides an overview of the potential clinical role of H₂S to prevent IH and restenosis.

Keywords: restenosis, Hydrogen sulfide (H₂S), intimal and medial thickening, H₂S (hydrogen sulfide), vascular SMCs

Abbreviations: 3-MST, 3-mercaptopyruvate sulfurtransferase; AKT, Serine/Threonine Kinase 1; AOOA, aminoxyacetic acid; bFGF, Basic Fibroblast Growth Factor; CAT, cysteine aminotransferase; CBS, cystathionine β synthase; COX, cytochrome c oxidase; CSE, cystathionine γ lyase; DATS, Diacyltrisulfite; DES, Drug-Eluting Stents; DCB, Drug-Coated Balloons; EC, Endothelial Cells; ECM, Extracellular Matrix; EEL, external elastic lamina; Enos, Endothelial Nitric Oxide Synthase; ER, endoplasmic reticulum; ERK, Extracellular Signal-Regulated Kinase; ETHE1, ethylmalonic encephalopathy 1 protein; GSH, Reduced Glutathione; GSSG, oxidized GSH; ICAM1, Intercellular Adhesion Molecule 1; IEL, internal elastic lamina; IH, Intimal Hyperplasia; IL-1β, Interleukin 1 beta; JNK, C-Jun N Terminal Kinase; KATP, ATP-sensitive K⁺; Keap1, kelch-like ECH-associated protein 1; LDH, lactate dehydrogenase; LDL, Low-Density Lipoprotein; MAPK, Mitogen-Activated Protein Kinase; MCP-1 (CCL-2), Monocyte Chemoattractant Protein-1; MMP, Matrix Metalloproteinase; NaHS, Sodium Hydrogen Sulfur; NF-Kb, Nuclear Factor Kappa b; NO, Nitric Oxide; Nrf2, nuclear factor (erythroid-derived 2)-like 2; PCI, percutaneous coronary intervention; PCNA, Proliferating Cell Nuclear Antigen; PDGF, Platelet-Derived Growth Factor; Pdgfr-B, Beta-Type Platelet-Derived Growth Factor Receptor; PLP, pyridoxal 5'-phosphate; POBA, plain old balloon angioplasty; ROS, Reactive Oxygen Specie; SDF-1α, Stromal Cell-Derived Factor 1; SM22α (Tagln), Smooth Muscle 22 Alpha/Transgelin; SMA (ACTA2), Smooth Muscle Actin Alpha; SQR, sulfide quinone oxidoreductase; STEMI, ST-segment elevation myocardial infarction; STS, Sodium Thiosulfate; TNF-α, Tumor Necrosis Factor Alpha; TIMP, Tissue Inhibitors Of Metalloproteinase; Trx, thioredoxin; TXNIP, Trx-interacting protein; VCAM1, Vascular Cell Adhesion Protein 1; VSMC, Vascular Smooth Muscle Cells; WT, wild type.

INTRODUCTION

Prevalence of arterial occlusive disease continues to rise worldwide, largely due to the combination of aging, smoking, hypertension, and mostly diabetes mellitus (1–3).

Vascular surgery, open or endovascular, remains the only treatment for advanced arterial occlusive disease. However, the vascular trauma associated with the intervention eventually lead to secondary occlusion of the injured vessel, usually referred to as restenosis.

The overall incidence of restenosis varies greatly depending on the initial clinical presentation and the anatomic pattern of disease (e.g., coronary vs. femoro-popliteal vs. infra popliteal etc.). Overall, for open surgeries such as bypass and endarterectomy, the rate of restenosis after 1 year ranges between 20 and 30% (4). For endovascular approaches, the rate of restenosis following plain old balloon angioplasty (POBA) ranges from 30 to 60%, depending on location (5). In coronary arteries, the use of bare metal stents (BMS) lowered the rate of restenosis to 17–41% (5). In stented peripheral arteries, restenosis occurs in up to 51% of the patients 1 year after the surgery (6).

The most recent advances in the treatment of restenosis rely on the use of drug-coated balloons (DCB) and drug-eluting stents (DES), which nowadays represent a first line therapy in many endovascular approaches to treat short lesions in coronary or femoral arteries. The most used drug is the anti-tumor chemotherapy Paclitaxel (Taxol™). Several paclitaxel-coated balloons and eluting stents with various formulations and different dose of paclitaxel demonstrated superiority to POBA (7–9) or BMS (7, 10). Overall, the arrival of DES and DCB reduced the incidence of restenosis below 10% in coronary arteries (11), although restenosis has been delayed rather than suppressed (12). DES also require prolonged antiplatelet therapy and hinder future surgical revascularization. In peripheral *below the knee* small arteries, the use of DCB is controversial, and stents are not recommended due to the risk of thrombosis (13). In December 2018, Katsanos and colleagues reported, in a systematic review and meta-analysis, an increased risk of all-cause mortality following application of paclitaxel-coated balloons and stents in the femoropopliteal artery (14). Other groups recently confirmed these findings using the same data (15, 16). However, other meta-analyses did not find any association between paclitaxel devices and long-term survival, despite similar target populations and vessel segments (17–21). These reports questioned the widespread use of paclitaxel for the treatment of restenosis (22), and supports the need to develop other approaches or use other molecules. In coronary intervention Sirolimus is increasingly used (23), and new devices are under evaluation to validate the use of sirolimus-coated devices in *below the knee* peripheral arteries (24). Recent studies even report the safety and efficacy of biodegradable polymer sirolimus-eluting stent (25, 26).

Restenosis has various origins, such as secondary growth of atherosclerotic lesions or inward remodeling. However, it is due mostly to intimal hyperplasia (IH), a process whereby a “neointima” layer is formed between the internal elastic lamina (IEL) and the endothelium (Figure 1). IH is a known

complication of all types of vascular procedures, including arterial bypass, angioplasty, stenting, and endarterectomy. Stenosis due to IH is also a major limitation of arteriovenous fistulas for hemodialysis patients, arteriovenous grafts, and other vascular accesses. The progressive growth of the neointima layer causes both an outward and an inward remodeling of the vessel wall, leading to a narrowing of the lumen, and eventually leads to impaired perfusion of downstream organs.

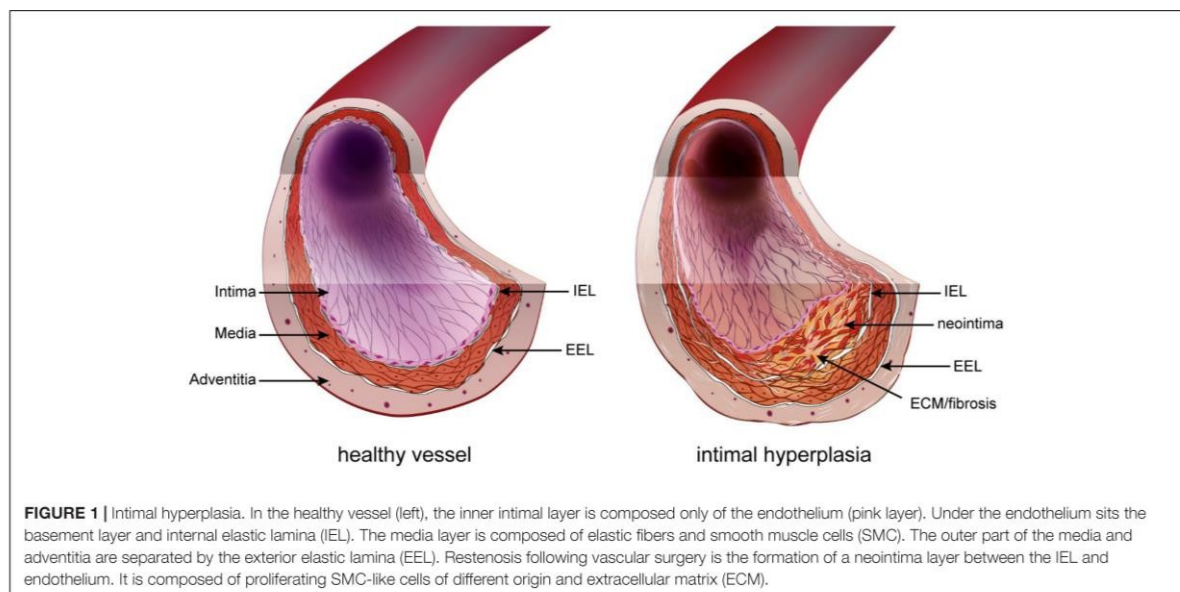
All current strategies to limit IH such as Paclitaxel and Sirolimus target cell proliferation. Paclitaxel is a chemotherapeutic agent that stabilizes microtubules, thereby preventing cell division (mitosis). High dose or prolonged exposure to paclitaxel may also lead to apoptotic cell death (27). Sirolimus inhibits the mammalian target of rapamycin (mTOR), a master regulator of cell growth and metabolism (28). However, targeting cell proliferation to reduce IH also impairs re-endothelization. Endothelium repair is crucial to limit inflammation, remodeling and IH. Poor endothelial repair also prolongs the need for anti-thrombotic therapies. Therefore, there is a need for new strategies to inhibit IH while promoting endothelium recovery. In that regard, the gasotransmitter hydrogen sulfide (H₂S) possesses interesting properties.

H₂S is a gasotransmitter derived from cysteine metabolism (29). Circulating H₂S levels are reduced in humans suffering from vascular occlusive disease (30, 31) and pre-clinical studies using water-soluble sulfide salts such as Na₂S and NaHS have shown that H₂S has cardiovascular protective properties [reviewed in Zhang et al. (29)], including reduction of IH in various models (32–35).

In this review, we present the pathophysiology of IH and the clinical potential of H₂S against IH. The pleiotropic benefits of H₂S on the cardiovascular system are described, and the interesting possibilities to target the multifactorial process leading to IH using H₂S are discussed.

THE PATHOPHYSIOLOGY OF INTIMAL HYPERPLASIA

The basic structure of large vessels (vein and artery) include three concentric layers: intima, media, and adventitia. The intima layer, also called endothelium, is the inner section of the vessel and is made of a single layer of endothelial cells (EC). The media is composed primarily of vascular smooth muscle cells (VSMC) and connective tissue made of collagen, elastin, and proteoglycans. The outermost adventitial layer is composed primarily of collagen and fibroblasts. In arteries, the intima and media layers are separated by a layer of elastic fibers called the internal elastic lamina (IEL), while the media and adventitia layers are separated by a second layer of elastic fibers called the external elastic lamina (EEL) (36). IH, also called neointima, develops between the intima and the IEL. The IH process is triggered in response to the injury to the blood vessel during surgery (37). This new layer is made of SMC-like cells and proteoglycan-rich extracellular matrix (ECM) (Figure 1).



Endothelial Dysfunction or Lesion

Located at the contact between the blood and the vessel wall, the EC maintain a non-thrombogenic surface and regulate the vasomotor activity (vasodilation and vasoconstriction) of vessels. In arteries, EC require high laminar shear stress to maintain proper function, i.e., secrete anti-coagulation and vasodilation agents, mainly nitric oxide (NO) and prostacyclins (36). However, the hemodynamic forces are not uniform throughout the vascular system. In straight segments of arteries, blood flow is laminar and shear stress is high. However, at bifurcations, curvatures, or other regions with complex geometry, blood flow is disturbed and turbulent. These abnormal patterns of “low” shear stress induce “endothelial dysfunction” or “endothelium activation.” Because of these disturbed arterial flow patterns, nearly all humans develop benign IH, also referred to as diffuse intimal thickening, around vessel bifurcations or in curved sections of arteries. This type of lesion serves as a precursor for the development of atherosclerosis by facilitating local inflammatory reaction and entrapment of LDL in the vessel wall (38). Inevitably, these “weak” spots of the vascular system are the sites of primary occlusion by atherosclerotic plaques that require vascular interventions. Any vascular surgery destroys the endothelial layer, furthering endothelium damage on those existing weak spots. This is the case for balloon angioplasty, stenting, or endarterectomy, which directly target the site of the atherosclerotic plaques. In the case of bypass surgery and arteriovenous fistulas, the surgery damages the endothelium while creating new regions of disturbed arterial flow patterns, which will foster IH lesions (Figure 2).

Endothelial dysfunction or injury following surgery results in loss of eNOS, the enzyme producing nitric oxide (NO), a gasotransmitter maintaining healthy vessel function. Reduced NO production promotes vasoconstriction, platelet aggregation

and recruitment/activation of resident and circulating inflammatory cells (mostly macrophages). The activated EC, recruited platelets and immune cells secrete cytokines and chemokines, which trigger a pro-inflammatory response (Figure 2). In addition, these cells secrete growth factors, including platelet-derived growth factor (PDGF), basic fibroblast growth factor (bFGF), transforming growth factor beta 1 (TGF- β) and thromboxane A₂. Downstream of those multiple growth factors, cytokines and chemokines, the Mitogen-activated protein kinase (MAPK) pathway, including extracellular signal-regulated kinase (ERK), c-Jun-N-terminal kinase (JNK) and p38 mitogen-activated protein kinases, plays a major role in VSMC migration and proliferation in SMCs and fibroblasts. Other signals derived from oxidative stress also regulate the p38 MAPK and JNK pathways (39, 40).

Together, the secretion of these factors and the loss of NO promote vessel remodeling and reprogramming of cells composing the media and adventitia layers, leading to the formation of a neointima between the endothelium and the IEL (41) (Figures 1, 2).

The Origin of Neointimal Cells

IH is mostly formed by proliferating VSMC originating from dedifferentiated contractile medial VSMC. Unlike other terminally differentiated cells of the myogenic lineage, such as cardiac and skeletal muscle cells, adult VSMC are highly plastic and capable of phenotypic alterations in response to their environment. Modulation of VSMC from a quiescent “contractile” phenotype to a proliferative “synthetic” phenotype is important for vascular injury repair, but is also a key factor in the pathogenesis of IH (42).

Upon vascular injury, the growth factors (PDGF-BB, bFGF), chemokines (SDF-1 α , MCP-1) and cytokines (TNF- α , IL-1 β)

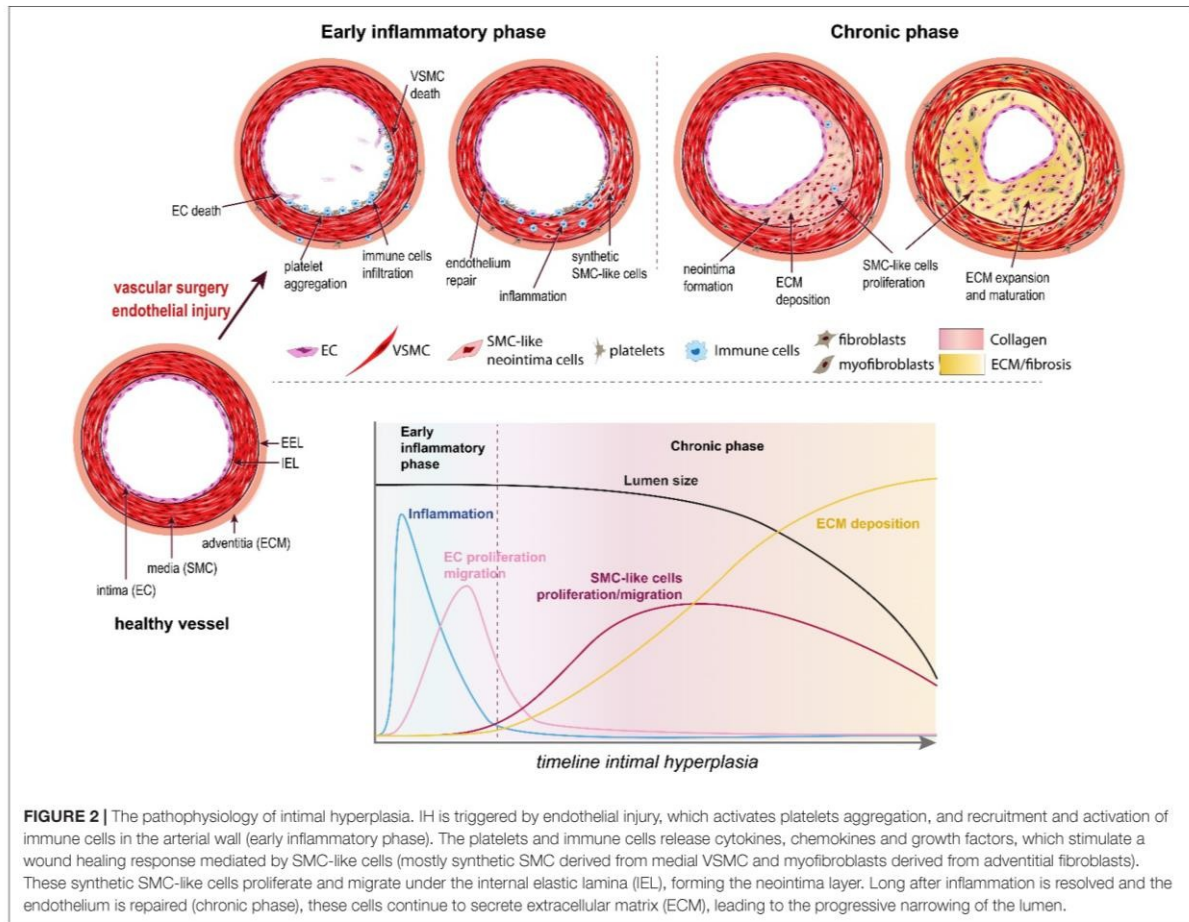


FIGURE 2 | The pathophysiology of intimal hyperplasia. IH is triggered by endothelial injury, which activates platelets aggregation, and recruitment and activation of immune cells in the arterial wall (early inflammatory phase). The platelets and immune cells release cytokines, chemokines and growth factors, which stimulate a wound healing response mediated by SMC-like cells (mostly synthetic SMC derived from medial VSMC and myofibroblasts derived from adventitial fibroblasts). These synthetic SMC-like cells proliferate and migrate under the internal elastic lamina (IEL), forming the neointima layer. Long after inflammation is resolved and the endothelium is repaired (chronic phase), these cells continue to secrete extracellular matrix (ECM), leading to the progressive narrowing of the lumen.

secreted by activated EC, platelets and immune cells stimulate ECM production and secretion, and reduce the expression of the contractile VSMC markers smooth muscle alpha-actin (α -SMA), smooth muscle myosin heavy chain (SM-MHC), calponin, and smooth muscle 22 alpha (SM22 α) (42–44). In addition, the “activated” VSMC themselves produce cytokines such as TNF α and MCP-1, leading to positive feedback cascades of enhanced VSMC migration and proliferation (42). The main signaling pathway consistently shown to play a major role in SMC-like cells reprogramming and proliferation/migration is the MAPK pathway, mainly ERK1,2, JNK, and p38 (39, 40).

However, it is now accepted that neointimal VSMCs are phenotypically heterogeneous and that their origin and identity is diverse (45). After medial VSMC, the most abundant cell involved in neointima formation are probably myofibroblasts. Myofibroblasts originate from quiescent fibroblasts in the adventitia, which have converted into proliferating cells expressing several SMC markers such as α -SMA, SM-22 α and calponin (46, 47) (Figure 2). Studies also support the existence of populations of mesenchymal stem cells or multipotent progenitor cells within the vessel wall, especially the adventitia layer, which

could give rise to the fibroblasts and SMC-like cells found in the neointima layer (48, 49). Further studies identified similar progenitor cells in human arterial and venous tissue (50–52), suggesting a role for these cells in arterial remodeling and IH.

Neointimal cells may also arise from circulating progenitor cells or from the bone marrow (48, 53). However, the contribution of circulating progenitor cells to IH seems to depend upon the model and the type of injury (54). Similarly, studies in the atherosclerosis field yield conflicting results as to whether neointimal SMC-like cells originate from the bone marrow [reviewed in details in Albiero et al. (55)]. Of note, in human, it has been impossible to evaluate the role of circulating progenitors and *ex vivo* studies using human vessels clearly demonstrated that IH forms in a vessel self-sufficient manner, independently of circulating factors (56, 57). Drawing conclusion from these studies remains challenging given the small number of studies and the variety of experimental models and methodology, especially the methods and markers employed to isolate and identify “progenitor cells.” Recent studies of VSMC lineage in the context of atherosclerosis suggest that up to 80% of SMC-derived cells in the plaques do not express the classic SMC markers

α -SMA, but express macrophage markers (CD68, LGALS3), mesenchymal stem cell marker (Sca 1) or myofibroblasts markers (PDGFR- β). These cells all express KLF4, a major stem cell and differentiation mediator [reviewed in Allahverdian et al. (45)]. These new evidences underscore how little is known about the identity and origin of the cells responsible for the formation of IH. Advanced techniques of single cell lineage may shed new lights on key questions in the field. Clearly, further work is required to better characterize the cells composing the neointima layer in patients.

Once the neointima starts to form, the arrival and proliferation of SMC-like cells secreting important amount of ECM progressively expand the neointima layer. At first, this expansion is compensated by an outward remodeling of the vessel under the pressure of the blood flow to maintain the lumen area. The vessel gradually thickens as fibrosis sets in. Eventually, the resistance of the arterial wall exceeds the parietal pressure and the neointima extends inward, leading to a narrowing of the lumen and impaired blood flow (Figure 2).

HYDROGEN SULFIDE

Endogenous Hydrogen Sulfide Production

The discovery of an endogenous pathway releasing H₂S in mammalian tissues came long after the discovery of NO, in 1960 with the work of Du Vigneaud, who investigated the oxidation of sulfur-containing amino acids in tissues. He discovered a new metabolic pathway involving the inter-conversion of cysteine and homocysteine and termed this pathway “transsulfuration.” Specifically, H₂S is produced by two pyridoxal 5'-phosphate (PLP) dependent enzymes, cystathionine γ -lyase (CSE) and cystathionine β -synthase (CBS). Two additional PLP-independent enzymes, 3-mercaptopyruvate sulfurtransferase (3-MST) and cysteine aminotransferase (CAT) generate sulfane sulfur that can be further processed into H₂S. 3-MST and CAT are expressed ubiquitously, whereas CBS and CSE display more tissue-specific patterns of expression. Thus, CBS is the only PLP-dependent enzyme expressed in the brain, while CSE is more prominent in the cardiovascular system. In the kidney and liver, both CSE and CBS are highly expressed. Although the enzymes and pathways responsible for endogenous H₂S production are well defined, little is known about their regulation and their relative contributions to H₂S and sulfane sulfur levels (e.g., polysulfides, persulfides, thiosulfate) in the circulation and in tissues under normal and disease conditions.

All H₂S-synthesizing enzymes have been reported to be expressed by cardiovascular cells. The study of CSE^{-/-} mice demonstrated impaired endothelium-dependent vasorelaxation, with no apparent dysfunction at the level of VSMC (58). Furthermore, CSE seems sufficient to observe H₂S-mediated vasodilation (59, 60). These observations strongly promoted the idea that CSE is the main H₂S-producing enzyme in the cardiovascular system at the level of EC. However, other reports suggest a key role of 3-MST, along with CAT, in H₂S production in the vascular endothelium (61). In contradiction

to this early report, studies performed using CSE^{-/-} mice generated on a pure C57BL/6J genetic background by the group of Prof. Isao Ishii failed to show impaired endothelial function and hypertension (62, 63). In addition, most studies of endogenous H₂S inhibition rely of the use of high concentrations of propargylglycine (PAG) to inhibit CSE. At these concentrations, PAG may also inhibit CBS, as well as other non-specific targets. Bibli et al. recently demonstrated that CSE expression is negatively regulated by shear stress, as opposed to eNOS in the mouse aorta (64, 65). This is in line with a previous study showing that only disturbed flow regions show discernable CSE protein expression after carotid artery ligation in the mouse (66).

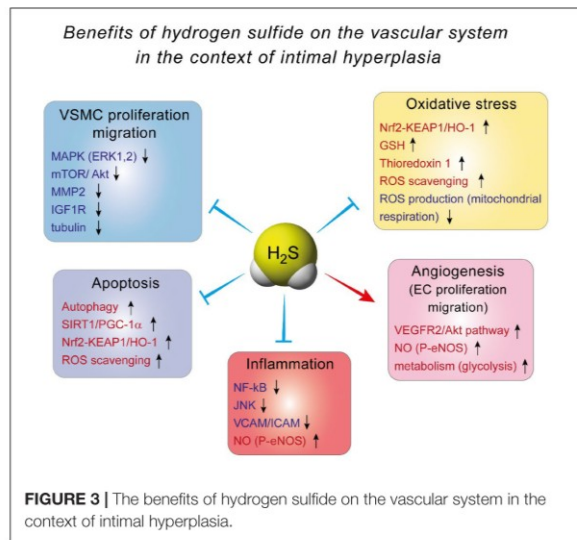
Cellular Effects of Hydrogen Sulfide

H₂S contributes to the homeostasis of numerous systems, including the cardiovascular, neuronal, gastrointestinal, respiratory, renal, liver and reproductive systems (67).

The chemical nature of the molecules responsible for the biological activity of H₂S remains elusive. HS⁻, polysulfides and sulfates have all been shown to affect a variety of signaling pathways and biological responses. The sulfur atom is a very potent electron acceptor/donor and H₂S can undergo complex oxidation, yielding thiosulfate, sulfenic acids, persulfides, polysulfides and sulfate (68). These oxidative products are likely mediating the principal mechanism through which H₂S exerts its biological actions: post-translational modification of proteins, known as persulfidation. Persulfidation is a chemical reaction whereby a persulfide group (RSSH) is formed on reactive cysteine residues of target proteins (68, 69). Since H₂S has the same oxidation state as cysteine residues, a redox reaction cannot occur. Cysteine residues or H₂S have to be oxidized first (for instance in the form of polysulfides H₂S_n). In 2009, Mustafa et al. performed LC/MS/MS analysis on liver lysates after NaHS treatment and identified 39 proteins that were persulfidated. Amongst them, they identified GAPDH, β -tubulin, and actin. Interestingly, these proteins were not persulfidated in the liver of mice lacking CSE (CSE KO) (70). Furthermore, new high throughput techniques allowing global assessment of post-translational modification of cysteinyl thiols (-SH) to persulfides (-SSH) demonstrated extensive cysteine residues persulfidation in response to various H₂S donors across various experimental designs (71–73).

Hydrogen Sulfide in Intimal Hyperplasia

Few studies directly assessed the effects of endogenous or exogenous H₂S on IH. CSE expression and activity are reduced after balloon-injury in a rat model of IH (32). CSE expression and activity, as well as free circulating H₂S, are also reduced in human suffering from vascular occlusive diseases (30, 74). We recently demonstrated that, in patient undergoing vascular surgery, circulating H₂S levels were associated with long-term survival (75), suggesting low H₂S production as a risk-factor for cardiovascular diseases. Mice lacking CSE show a significant increase in IH formation as compared to WT mice in a model of carotid artery ligation (34, 76). On the contrary, CSE overexpression decreases IH formation in a murine model of



vein graft by carotid-interposition cuff technique (77). Similarly, NaHS administration limits the development of IH in *in vivo* models in rats (32), rabbits (33), and mice (34), and in human great saphenous vein segments *ex vivo* (35).

The effect of H₂S against IH is probably mediated by inhibition of VSMC proliferation and migration. Indeed, it was demonstrated, using BrdU and TUNEL assays, that H₂S supplementation or CSE overexpression decreases VSMCs proliferation and increases VSMCs apoptosis, respectively (33, 35, 78). VSMCs isolated from Cse^{-/-} mice exhibit more motility than their WT counterpart, and blocking CSE activity using PAG in WT VSMCs increases cell migration (34, 79). The mechanisms whereby H₂S affect VSMCs are not fully understood. In mouse VSMC, H₂S has been shown to modulate the MAPK pathway, especially ERK1, 2 (32), and calcium-sensing receptors (80, 81). In addition, H₂S may limit MMP2 expression and ECMs degradation, preventing migration of VSMCs from the media to the intima (34, 79). In human VSMC, we recently reported that the H₂S donor Zofenopril decreases the activity of the MAPK and mTOR pathways, which correlates with reduced VSMC proliferation and migration (82). We also showed that the H₂S donor salt NaHS, as well the thiol source sodium thiosulfate, inhibit microtubule polymerization, which results in cell cycle arrest and inhibition of proliferation and migration in primary human VSMC (76) (Figure 3).

Other studies also inform on potential mechanism of action of H₂S on VSMC. The first evidence of H₂S being a gasotransmitter comes from the consistent observation across species and vascular beds that H₂S and other derived products induce vasodilation. H₂S triggers vasodilation mostly *via* persulfidation of several ion channels such as K_{ATP}, voltage and Ca²⁺-activated K⁺ channels (59, 60, 83). By reducing extracellular Ca²⁺ entry, H₂S improves VSMC relaxation. Despite the obvious fact that improved vasorelaxation may be beneficial in the context of IH, these channels may also directly regulate cell proliferation in

VSMC. For instance, the anti-diabetic and K_{ATP} channel blocker glibenclamide has been shown to reduce VSMC proliferation in a recent study (84).

Other Benefits of Hydrogen Sulfide in the Cardiovascular System

Hydrogen Sulfide Stimulates Endothelial Cell Proliferation and Migration

Vascular surgery invariably leads to injury of the operated vessels. The single-cell endothelial barrier is very vulnerable and severely injured during surgery, which promotes inflammation and reprogramming of the adventitial and medial cells. The ability of endothelial cells to proliferate and migrate to restore the endothelial layer of the vessel is a key step in the resolution of post-operative inflammation to limit IH and restenosis. Unfortunately, EC are often neglected in strategies to reduce the formation of IH.

Although it has never been demonstrated in the context of IH, a large amount of studies established that H₂S and polysulfides stimulate EC function and angiogenesis. Exogenous H₂S treatment stimulates EC growth, motility and organization into vessel-like structure *in vitro*. On the contrary, inhibition of H₂S biosynthesis, either *via* pharmacological inhibitors or *via* silencing of CSE, CBS or 3MST, reduces EC growth, migration and vessel-like structure formation (85, 86). Further *in vivo* studies of chicken chorioallantoic membranes (CAM) treated with the CSE inhibitor PAG suggest that CSE is important for vessel branching and elongation (87). Matrigel plug angiogenesis assay also confirmed the importance of CSE and H₂S in vascular endothelial growth factor (VEGF)-induced angiogenesis (88, 89).

Several mechanisms have been proposed to explain H₂S-induced angiogenesis. First and probably foremost, H₂S stimulates the VEGF pathway in EC, through sulfhydration of the VEGF receptor VEGFR2, increasing its dimerization, autophosphorylation and activation (90). Interestingly, short term exposure of human EC to VEGF increases H₂S production (87), suggesting a positive feedback loop of VEGF signaling through H₂S. In addition, H₂S promotes angiogenesis by inhibiting mitochondrial electron transport and oxidative phosphorylation, resulting in increased glucose uptake and glycolytic ATP production necessary to provide rapid energy for EC migration (91) (Figure 3).

H₂S also promotes angiogenesis through its extensive interaction with the NO pathway. In endothelial cells, H₂S may induce eNOS persulfidation at Cys433, which increases the phosphorylation of its activator site and stabilizes eNOS in its dimeric form (86, 92). H₂S may also increase intracellular calcium levels, leading to increase eNOS activity and NO production (93, 94). Exogenous H₂S donors have also been shown to stimulate the growth pathways Akt, p38 and ERK1/2, which all promote EC proliferation and migration (87, 89, 95). Finally, both H₂S- and NO-induced angiogenesis require the other gasotransmitter (86, 92). Thus, the vascular effects of NO and H₂S are interdependent and closely intertwined, with both gasotransmitter having direct and indirect effects on each other [for full review see Szabo et al. (96)]. Overall, the effect of

H₂S on EC may facilitate re-endothelialization following vascular trauma, accelerating healing of the intima layer and limiting IH (Figure 3).

Hydrogen Sulfide Inhibits Inflammation

The surgical trauma and injury to the endothelial layer triggers inflammation, which contributes to IH. Many studies report anti-inflammatory properties of H₂S, in particular in the context of atherosclerosis and cardiac failure [for full review see Pan et al. (97)]. Thus, H₂S reduces adhesion and infiltration of pro-inflammatory cells and circulating levels of pro-inflammatory chemokines and cytokines in the ApoE^{-/-} mouse model of atherosclerosis (98, 99). Similarly, several reports document that H₂S donors (NaHS, DATS, SG1002, STS) or CSE overexpression decrease leukocyte and neutrophil infiltration and cytokine production following ischemic injury in various models of myocardial infarction (100–105).

Mechanistically, evidence from EC and macrophages indicate that Nuclear factor kappa B (NFκB) inhibition seems to be the key to H₂S anti-inflammatory effects (98, 106–108). NF-κB is a transcription factor and a master regulator of pro-inflammatory genes, including cytokines and cell adhesion molecules. NaHS inhibits NF-κB activity probably *via* persulfidation/stabilization of IκB (109), which controls NF-κB (p65) translocation to the nucleus. In EC, this leads to decreased expression of adhesion molecule VCAM and ICAM, thereby limiting recruitment of leukocyte to the aortic wall (98, 106, 108). NaHS also promotes a shift in macrophages to the M2, pro-resolution state (110). Moreover, NaHS and GYY increase eNOS phosphorylation, thereby improving NO production, which reduces inflammation (106, 111). Whether or not H₂S-based strategies may reduce inflammation in the context of IH remains to be tested (Figure 3).

Hydrogen Sulfide Has Anti-oxidant Properties

Several studies in various models also consistently showed that H₂S holds anti-oxidant properties. First, H₂S can directly scavenge reactive oxygen species (ROS), such as superoxide anions O₂⁻, at higher rates than other classic antioxidants such as GSH. However, since H₂S physiologic concentration is in the nanomolar range whereas GSH is present in millimolar quantity, it is debatable whether H₂S direct contribution to anti-oxidation is significant.

Actually, the effect of H₂S probably arises from stimulation of anti-oxidant pathways, rather than *via* direct scavenging of ROS. First, H₂S increases GSH production *via* modulation of the transsulfuration pathway. H₂S interaction with GSH has been studied in details in the central nervous system, where GSH plays a major role in maintaining the homeostasis between anti-oxidant and ROS production [reviewed in details in Shefa et al. (112)]. In the vascular system, H₂S persulfidates the glutathione peroxidase 1, which promotes glutathione synthesis and results in decreased lipid peroxidation in the aortic wall in the context of atherosclerosis (113). Second, numerous studies document that H₂S promotes the Nrf2 pathway [reviewed in Corsello et al. (114)]. H₂S promotes the Nrf2 anti-oxidant response *via* persulfidation of Kelch-like ECH-associated protein 1 (Keap1), which sequesters Nrf-2 in the cytosol. Keap1 persulfidation

prompts dissociation from Nrf2, which induces the expression of several proteins, among which the major antioxidant protein heme oxygenase 1 (HO-1). This mechanism reduces oxidative stress, leading to reduced atherosclerosis in diabetic low density lipoprotein receptor (LDLR) knock-out mice (115), and cardioprotection in a model of ischemia-reperfusion injury (116, 117). Finally, H₂S also stimulates thioredoxin 1 (Trx) expression, *via* silencing the expression of inhibitory protein Trx-interacting protein (TXNIP) (118, 119). Increased Trx is instrumental in the cardioprotective effects of H₂S against ischemia-induced heart failure (118) (Figure 3).

Mitochondrial respiration is a major source of ROS (120, 121). H₂S has a bell-shaped effect on mitochondrial respiration. At low nanomolar concentrations, sulfide quinone oxidoreductase (SQR) transfers electrons from H₂S to the coenzyme Q in the Complex II of the electron transport chain, thereby promoting mitochondrial respiration. At higher concentrations, H₂S binds the copper center of cytochrome c oxidase (complex IV), thereby inhibiting respiration and limiting ROS production (122).

These anti-oxidant properties of H₂S may have a beneficial impact on IH, as ROS contribute to endothelial dysfunction and VSMC dedifferentiation (123, 124).

DISCUSSION: NEW PERSPECTIVES FOR THE TREATMENT OF Intimal Hyperplasia USING HYDROGEN SULFIDE-BASED THERAPIES

There is currently no clinically approved molecule exploiting the clinical potential of H₂S. Most compounds available for research have poor translational potential due to their pharmacokinetic properties. Thus, the highly soluble unstable salts sodium hydrogen sulfide (NaHS) and disodium sulfide (Na₂S) release H₂S instantly in an uncontrollable manner, and thus have narrow clinical ranges. Other H₂S-releasing molecules extracted from garlic such as DATS (Diallyl trisulfide) and DADS (Diallyl disulfide), which have both been shown to possess vasoactive properties (125), are also very short lived and hard to stabilize (125). In the past years, several H₂S-releasing compounds have been studied and developed for clinical purposes (Table 1).

Hydrogen Sulfide-Based Therapies: Current Strategies

S-allylcysteine (SAC), an organosulfur compound present in abundance in garlic, has been shown to lower the mortality and reduce the infarct size in a rat model of acute myocardial infarction (126) and improves blood flow recovery after hindlimb ischemic injury in the mouse (127). S-propyl-L-cysteine and S-propargyl-L-cysteine, structural analogs of SAC found in garlic, have also been shown to slowly release H₂S (128). Interestingly, S-propargyl-L-cysteine has been demonstrated to have both cardio protective (129, 130) and pro-angiogenic properties in preclinical models (131). However, despite the well-known cardiovascular-protective properties of garlic, these active compounds are not currently used for clinical studies.

TABLE 1 | Clinical development of H₂S-releasing compound.

Name	Description	Indications	Development phase	References
Zofenopril	ACE inhibitor combined to an H ₂ S donor	Hypertension	Approved	(136, 137)
ATB-340	H ₂ S-releasing derivative of low dose aspirin	Anti-thrombotic for chronic prevention of cardiovascular diseases and cancer chemoprevention	Dropped	(139)
ATB-352	H ₂ S-releasing derivative of ketoprofen	NSAID	Pre-clinical	(153)
ATB-346 Otenaproxesul	H ₂ S-releasing derivative of naproxen	NSAID; Gastric Ulcer, Osteoarthritis	Phase II NCT03978208 NCT03291418	(140)
S-Diclofenac	Derivative of Diclofenac combined to an H ₂ S donor	NSAID	Pre-clinical; Dropped?	(141–143)
IK-1001	Injectable stable form of Na ₂ S	Reduction of heart complications during coronary artery bypass graft	Stopped during phase 2 trial NCT00858936	(144)
SG1002	H ₂ S-releasing prodrug	Heart failure	Phase 1 NCT02278276	(146)
Sodium thiosulfate	Inorganic sodium salt with thiosulfate ions	Calciophylaxis (ESRD) and cyanide poisoning	Approved NCT00568399 NCT01008631 NCT03150420 NCT02899364	(149, 154)

NSAID, Non-steroidal anti-inflammatory drug; ESRD, End Stage Renal disease.

Another strategy used by pharmaceutical companies to harness the benefits of H₂S has been to combine a H₂S-releasing moiety with well-established parent compounds.

Zofenopril is one such product. Zofenopril is an ACE Inhibitors (ACEi) and a H₂S donor combined (132). ACEi constitute one of the first-line class of antihypertensive drugs (133). Several clinical studies have shown that sulfhydrylated ACEi zofenopril has additional beneficial actions compared to non-sulfhydrylated ACEi such as enalapril or ramipril. Thus, zofenopril improves the clinical outcome of patients with different cardiovascular diseases such as acute myocardial infarction and congestive heart failure (134–137). We recently demonstrated that Zofenopril is more potent than Enalapril in reducing IH in a genetic model of hypertensive mice. In addition, it suppresses IH in normotensive condition, where other non-sulfhydrylated ACEi (Enalapril, Lisinopril and Quinapril) have no effect. Furthermore, Zofenopril prevents IH in an *ex vivo* model of IH in human saphenous vein. The effect of Zofenopril on IH correlates with reduced VSMC proliferation and migration and decreased activity of the MAPK and mTOR pathways (138).

Antibe Clinicals, a startup created around H₂S-releasing compounds, synthesizes several H₂S-releasing derivatives conjugated to NSAID for the treatments of pain and inflammation.¹ ATB-340 is a H₂S-releasing derivative of low-dose aspirin without the serious risk of gastrointestinal bleeding. Pre-clinical studies have demonstrated that ATB-340 caused negligible GI damage compared to low-dose aspirin

¹<http://www.antibetheras.com>

(139). ATB 346, which is derived from the NSAID naproxen, was recently shown in a Phase 2B study to reduce GI toxicity compared to naproxen alone, with equivalent suppression of COX activity (140). The H₂S-releasing diclofenac *S-Diclofenac* (ATB-337 or ACS-15), where H₂S is linked to diclofenac *via* an ester bond, may also present advantages compared to classical Diclofenac (141, 142). *S-Diclofenac* has been shown to inhibit smooth muscle cell proliferation, and may play a role in restenosis in vascular injury (143). However, there was no further development of this compound

The compound IK-1001, from the company Mallinckrodt, is an injectable stable form of Na₂S (144). Despite a first phase I safety trial showing no adverse events, the development of IK-1001 was stopped by the company during a phase II efficacy trial in patients undergoing surgery for a coronary artery bypass graft (ClinicalTrials.gov ID: NCT00858936).

SG1002, initially developed by Kondo et al. (145), and further developed by the startup company Sulfagenix, is a prodrug releasing H₂S. It has been tested on humans in the setting of congestive heart failure during one of the first phase I trial using a sulfide-based therapy to treat cardiovascular diseases. The results of this study were promising as SG1002 was able to restore sulfide and NO levels in patients with heart failure (146). However, additional studies are obviously required.

Sodium thiosulfate (STS; Na₂S₂O₃) is an inorganic sodium salt containing thiosulfate ions in a 2:1 ratio. Pharmaceutical-grade STS is available and has been suggested to release H₂S through non-enzymatic and enzymatic mechanisms (147, 148). STS is the treatment of choice for cyanide poisoning as

thiosulfate is used by Rhodanese to convert cyanide to less toxic thiocyanate. Intravenous STS is also used to increase the solubility of calcium for the treatment of acute calciphylaxis, a rare vascular complication of patients with end-stage renal disease (149). Sodium thiosulfate is also under test in a number of clinical trials for the treatment of ectopic calcification (NCT03639779; NCT04251832; NCT02538939); to reduce ototoxicity in patients receiving cisplatin chemotherapy for standard risk hepatoblastoma (NCT05129748); in combination with chemotherapy to prevent low platelet count in patients with malignant brain tumors (NCT00075387). We also recently demonstrated that STS limits IH development *in vivo* in a model of arterial restenosis and in our *ex vivo* model of IH in human veins. STS treatment increases H₂S bioavailability, which inhibits cell apoptosis and fibrosis, as well as VSMC proliferation and migration *via* microtubules depolymerization (76). Interestingly, an ongoing clinical study aims to evaluate the efficacy and safety of STS compared to placebo on myocardial infarct size in ST-segment elevation myocardial infarction (STEMI) patients treated with percutaneous coronary intervention (PCI) (NCT02899364).

The focal nature of IH lesions provide a window of opportunities for the use of local drug delivery using vascular medical devices. A number of approaches have been tested to apply treatment locally, including DCB and DES, as well as periadventitial drug delivery and targeted systemic therapies (150). Unlike current non-specific cytostatic drugs, local H₂S delivery might provide a unique clinical opportunity to inhibit VSMCs proliferation while promoting ECs proliferation and endothelial repair. We recently developed and evaluated the clinical potential of an H₂S-releasing biodegradable hydrogel to limit the development of IH in human veins. The thiol-triggered, controlled H₂S release from peptide hydrogels provided sustained H₂S concentrations over the period of hours, which inhibited VSMC proliferation and IH in human vein models more effectively than the sulfide salts (NaHS). The H₂S-releasing peptide hydrogel also facilitated HUVEC proliferation and transmigration *in vitro*, which may promote re-endothelization, thereby supporting vascular repair (35). Recently, it was shown that a locally applicable gel containing the hydrogen sulfide releasing prodrug (GYY4137) mitigates graft failure and improve arterial remodeling in a model of vein graft surgery in the mouse (151).

Hydrogen Sulfide-Based Therapies: Advantages and Limitations

IH is a complex process, involving multiple cell types and developing over the course of several years. IH is triggered by an acute endothelial dysfunction and associated pro-inflammatory response, which triggers a cascade of event leading to the formation of the neointima layer. The neointima slowly grows over the course of months to years, long after the acute inflammation is resolved and the endothelium repaired (Figure 2). H₂S is unique in the context of IH because it can have beneficial impact on both the acute pro-inflammatory response and the chronic neointima growth. Thus, on the one hand, H₂S

limits inflammation and oxidative damages, while promoting EC proliferation and endothelium repair. On the other hand, H₂S limits the proliferation and migration of synthetic SMC-like cells forming the neointima layer. In contrast, current strategies to reduce IH aggressively target cell proliferation, which also affect re-endothelization, prolonging inflammation and the need for anti-thrombotic therapies. Moreover, recent reports suggest that paclitaxel-releasing balloons and stents may have deleterious long-term effects, which is not surprising given that it is a cytotoxic chemotherapeutic agent.

Numerous drugs have been tested over the years to limit IH, demonstrating outstanding potential in pre-clinical studies in the small animal. Yet, in most trials, the pharmacologic treatment of restenosis failed to have a positive impact (150, 152). It is probable that the lack of efficacy in humans is, at least partly, due to insufficient drug delivery at the site of injury, as much higher dosages of drugs were generally used in animal models. It will be interesting to see whether H₂S-based solutions can bridge the gap between benchtop and bedside. The first challenge will be to develop stable H₂S-donor molecules allowing slow and sustained H₂S release over the course of months/years. Such molecules are yet to be developed and will be hard to design given the instability and short half-life of H₂S. Another challenge for either systemic or local release of H₂S reside in the delivery system. The development of DCB and DES releasing paclitaxel or sirolimus led to innovative delivery systems. Gels, nanoparticles, multiple-layer coatings and biodegradable scaffolds have been invented to allow sustained drug release. It will be interesting to apply this knowledge to H₂S-donor molecules. Eventually, the development of H₂S-releasing balloons and stents could provide much-needed device to limit VSMC proliferation while promoting EC recovery. However, combining local delivery and systemic oral drug administration will probably be necessary to prevent IH successfully.

CONCLUSION

Restenosis due to IH is recurrent and there is no efficient therapy. The neointima layer has a muscular and fibrotic rigid structure, which is hard to treat. Additional interventions to re-open the vessel invariably results in trauma, leading to further IH. DCB and DES improved the primary patency of vessels following endovascular surgeries but in-stent restenosis poses new challenges. Current strategies target cell proliferation to reduce IH, which also affect re-endothelization, prolonging the need for anti-thrombotic agents. Moreover, recent reports suggests that paclitaxel-releasing balloons and stents may have deleterious long-term effects.

These limitations warrant further research to better understand the molecular mechanisms of IH and develop new molecules limiting VSMC proliferation while stimulating EC proliferation and re-endothelization. Although H₂S research is still in its infancy, ample evidence point to a protective role for this gaseous transmitter in the development of cardiovascular diseases. However, further animal studies are required to test the potential and safety of new H₂S-based therapies.

Understanding these questions will provide insightful knowledge about the biology of H₂S and help design successful H₂S-based therapies in the future.

AUTHOR CONTRIBUTIONS

FA and SD made the backbone. DM, FA, AL, and SD wrote and revised the manuscript. FA made the figures. All authors contributed to the article and approved the submitted version.

REFERENCES

- Eraso LH, Fukaya E, Mohler ER III, Xie D, Sha D, Berger JS. Peripheral arterial disease, prevalence and cumulative risk factor profile analysis. *Eur J Prev Cardiol.* (2014) 21:704–11. doi: 10.1177/2047487312452968
- Fowkes FG, Rudan D, Rudan I, Aboyans V, Denenberg JO, McDermott MM, et al. Comparison of global estimates of prevalence and risk factors for peripheral artery disease in 2000 and 2010: a systematic review and analysis. *Lancet.* (2013) 382:1329–40. doi: 10.1016/S0140-6736(13)61249-0
- Song P, Rudan D, Zhu Y, Fowkes FJL, Rahimi K, Fowkes FGR, et al. Global, regional, and national prevalence and risk factors for peripheral artery disease in 2015: an updated systematic review and analysis. *Lancet Glob Health.* (2019) 7:e1020–30. doi: 10.1016/S2214-109X(19)30255-4
- Simpson EL, Kearns B, Stevenson MD, Cantrell AJ, Littlewood C, Michaels JA. Enhancements to angioplasty for peripheral arterial occlusive disease: systematic review, cost-effectiveness assessment and expected value of information analysis. *Health Technol Assess.* (2014) 18:1–252. doi: 10.3310/hta18100
- Buccheri D, Piraino D, Andolina G, Cortese B. Understanding and managing in-stent restenosis: a review of clinical data, from pathogenesis to treatment. *J Thorac Dis.* (2016) 8:E1150–62. doi: 10.21037/jtd.2016.10.93
- Zen K, Takahara M, Iida O, Soga Y, Kawasaki D, Nanto S, et al. Drug-eluting stenting for femoropopliteal lesions, followed by cilostazol treatment, reduces stent restenosis in patients with symptomatic peripheral artery disease. *J Vasc Surg.* (2017) 65:720–5. doi: 10.1016/j.jvs.2016.10.098
- Abdoli S, Mert M, Lee WM, Ochoa CJ, Katz SG. Network meta-analysis of drug-coated balloon angioplasty versus primary nitinol stenting for femoropopliteal atherosclerotic disease. *J Vasc Surg.* (2021) 73:1802–10.e4. doi: 10.1016/j.jvs.2020.10.075
- Teichgraber U, Lehmann T, Aschenbach R, Scheinert D, Zeller T, Brechtel K, et al. Efficacy and safety of a novel paclitaxel-nano-coated balloon for femoropopliteal angioplasty: one-year results of the effpac trial. *EuroIntervention.* (2020) 15:e1633–40. doi: 10.4244/EIJ-D-19-00292
- Caradu C, Lakhilfi E, Colacchio EC, Midy D, Berard X, Poirier M, et al. Systematic review and updated meta-analysis of the use of drug-coated balloon angioplasty versus plain old balloon angioplasty for femoropopliteal arterial disease. *J Vasc Surg.* (2019) 70:981–95.e10. doi: 10.1016/j.jvs.2019.01.080
- Ding Y, Zhou M, Wang Y, Cai L, Shi Z. Comparison of drug-eluting stent with bare-metal stent implantation in femoropopliteal artery disease: a systematic review and meta-analysis. *Ann Vasc Surg.* (2018) 50:96–105. doi: 10.1016/j.avsg.2017.12.003
- Fattori R, Piva T. Drug-eluting stents in vascular intervention. *Lancet.* (2003) 361:247–9. doi: 10.1016/S0140-6736(03)12275-1
- Jukema JW, Verschuren JJ, Ahmed TA, Quax PH. Restenosis after PCI. Part 1: pathophysiology and risk factors. *Nat Rev Cardiol.* (2011) 9:53–62. doi: 10.1038/nrcardio.2011.132
- Bjorck M, Earnshaw JJ, Acosta S, Bastos Goncalves F, Cochenne F, Debus ES, et al. Editor's Choice – European society for vascular surgery (ESVS) 2020 clinical practice guidelines on the management of acute limb ischaemia. *Eur J Vasc Endovasc Surg.* (2020) 59:173–218. doi: 10.1016/j.ejvs.2019.09.006
- Katsanos K, Spiliopoulos S, Kitrou P, Krokidis M, Karnabatidis D. Risk of death following application of paclitaxel-coated balloons and stents in the femoropopliteal artery of the leg: a systematic review and meta-analysis of randomized controlled trials. *J Am Heart Assoc.* (2018) 7:e011245. doi: 10.1161/JAHA.118.011245
- Rocha-Singh KJ, Duval S, Jaff MR, Schneider PA, Ansel GM, Lyden SP, et al. Mortality and paclitaxel-coated devices: an individual patient data meta-analysis. *Circulation.* (2020) 141:1859–69. doi: 10.1161/CIRCULATIONAHA.119.044697
- Royce S, Chakraborty A, Zhao Y. Us food and drug administration perspective on “mortality and paclitaxel-coated devices: an individual patient data meta-analysis”. *Circulation.* (2020) 141:1870–1. doi: 10.1161/CIRCULATIONAHA.120.047376
- Dinh K, Gomes ML, Thomas SD, Paravastu SCV, Holden A, Schneider PA, et al. Mortality after paclitaxel-coated device use in patients with chronic limb-threatening ischemia: a systematic review and meta-analysis of randomized controlled trials. *J Endovasc Ther.* (2020) 27:175–85. doi: 10.1177/1526602820904783
- Ipema J, Huizing E, Schreve MA, de Vries JPM, Unlu C. Editor's choice – drug coated balloon angioplasty vs. standard percutaneous transluminal angioplasty in below the knee peripheral arterial disease: a systematic review and meta-analysis. *Eur J Vasc Endovasc Surg.* (2020) 59:265–75. doi: 10.1016/j.ejvs.2019.10.002
- Katsanos K, Spiliopoulos S, Kitrou P, Krokidis M, Paraskevopoulos I, Karnabatidis D. Risk of death and amputation with use of paclitaxel-coated balloons in the infrapopliteal arteries for treatment of critical limb ischemia: a systematic review and meta-analysis of randomized controlled trials. *J Vasc Interv Radiol.* (2020) 31:202–12. doi: 10.1016/j.jvir.2019.11.015
- Nordanstig J, James S, Andersson M, Andersson M, Danielsson P, Gillgren P, et al. Mortality with paclitaxel-coated devices in peripheral artery disease. *N Engl J Med.* (2020) 383:2538–46. doi: 10.1056/NEJMoa2005206
- Secemsky EA, Kundi H, Weinberg I, Jaff MR, Krawisz A, Parikh SA, et al. Association of survival with femoropopliteal artery revascularization with drug-coated devices. *JAMA Cardiol.* (2019) 4:332–40. doi: 10.1001/jamacardio.2019.0325
- Beckman JA, White CJ. Paclitaxel-coated balloons and eluting stents: is there a mortality risk in patients with peripheral artery disease? *Circulation.* (2019) 140:1342–51. doi: 10.1161/CIRCULATIONAHA.119.041099
- Byrne RA, Stone GW, Ormiston J, Kastrati A. Coronary balloon angioplasty, stents, and scaffolds. *Lancet.* (2017) 390:781–92. doi: 10.1016/S0140-6736(17)31927-X
- Teichgraber U, Ingwersen M, Platzer S, Lehmann T, Zeller T, Aschenbach R, et al. Head-to-head comparison of sirolimus- versus paclitaxel-coated balloon angioplasty in the femoropopliteal artery: study protocol for the randomized controlled sirona trial. *Trials.* (2021) 22:665. doi: 10.1186/s13063-021-05631-9
- Zhu P, Zhou X, Zhang C, Li H, Zhang Z, Song Z. Safety and efficacy of ultrathin strut biodegradable polymer sirolimus-eluting stent versus durable polymer drug-eluting stents: a meta-analysis of randomized trials. *BMC Cardiovasc Disord.* (2018) 18:170. doi: 10.1186/s12872-018-0902-5
- El-Hayek G, Bangalore S, Casso Dominguez A, Devireddy C, Jaber W, Kumar G, et al. Meta-analysis of randomized clinical trials comparing biodegradable polymer drug-eluting stent to second-generation durable polymer drug-eluting stents. *JACC Cardiovasc Interv.* (2017) 10:462–73. doi: 10.1016/j.jcin.2016.12.002
- Yu-Wei D, Li ZS, Xiong SM, Huang G, Luo YF, Huo TY, et al. Paclitaxel induces apoptosis through the TAK1-JNK activation

- pathway. *FEBS Open Bio*. (2020) 10:1655–67. doi: 10.1002/2211-5463.12917
28. Chakraborty R, Chatterjee P, Dave JM, Ostriker AC, Greif DM, Rzuclido EM, et al. Targeting smooth muscle cell phenotypic switching in vascular disease. *JVS Vasc Sci*. (2021) 2:79–94. doi: 10.1016/j.jvssci.2021.04.001
 29. Zhang L, Wang Y, Li Y, Li L, Xu S, Feng X, et al. Hydrogen Sulfide (H₂S)-releasing compounds: therapeutic potential in cardiovascular diseases. *Front Pharmacol*. (2018) 9:1066. doi: 10.3389/fphar.2018.01066
 30. Islam KN, Polhemus DJ, Donnarumma E, Brewster LR, Lefer DJ. Hydrogen sulfide levels and Nuclear Factor-Erythroid 2-Related Factor 2 (NRF2) activity are attenuated in the setting of critical limb ischemia (CLI). *J Am Heart Assoc*. (2015) 4:e001986. doi: 10.1161/JAHA.115.001986
 31. Longchamp A, MacArthur MR, Trocha K, Ganahl J, Mann CG, Kip P, et al. Plasma hydrogen sulfide production capacity is positively associated with post-operative survival in patients undergoing surgical revascularization. *medRxiv*. [Preprint]. (2021). doi: 10.1101/2021.02.16.21251804
 32. Meng QH, Yang G, Yang W, Jiang B, Wu L, Wang R. Protective effect of hydrogen sulfide on balloon injury-induced neointima hyperplasia in rat carotid arteries. *Am J Pathol*. (2007) 170:1406–14. doi: 10.2353/ajpath.2007.060939
 33. Ma B, Liang G, Zhang F, Chen Y, Zhang H. Effect of hydrogen sulfide on restenosis of peripheral arteries after angioplasty. *Mol Med Rep*. (2012) 5:1497–502. doi: 10.3892/mmr.2012.853
 34. Yang G, Li H, Tang G, Wu L, Zhao K, Cao Q, et al. Increased neointimal formation in cystathionine gamma-lyase deficient mice: role of hydrogen sulfide in alpha5beta1-integrin and matrix metalloproteinase-2 expression in smooth muscle cells. *J Mol Cell Cardiol*. (2012) 52:677–88. doi: 10.1016/j.jmcc.2011.12.004
 35. Longchamp A, Kaur K, Macabrey D, Dubuis C, Corpataux JM, Deglise S, et al. Hydrogen sulfide-releasing peptide hydrogel limits the development of intimal hyperplasia in human vein segments. *Acta Biomater*. (2019) 97:374–84. doi: 10.1016/j.actbio.2019.07.042
 36. Stone JR. Diseases of small and medium-sized blood vessels. In: Buja LM, Butany J editors. *Cardiovascular Pathology*. Cambridge: Academic Press (2016). p. 125–68. doi: 10.1016/b978-0-12-420219-1.00004-5
 37. Nakano M, Otsuka F, Yahagi K, Sakakura K, Kutys R, Ladich ER, et al. Human autopsy study of drug-eluting stents restenosis: histomorphological predictors and neointimal characteristics. *Eur Heart J*. (2013) 34:3304–13. doi: 10.1093/eurheartj/ehs241
 38. Nakashima Y, Wight TN, Sueishi K. Early atherosclerosis in humans: role of diffuse intimal thickening and extracellular matrix proteoglycans. *Cardiovasc Res*. (2008) 79:14–23. doi: 10.1093/cvr/cvn099
 39. Tong X, Khandelwal AR, Qin Z, Wu X, Chen L, Ago T, et al. Role of smooth muscle Nox4-Based NADPH oxidase in neointimal hyperplasia. *J Mol Cell Cardiol*. (2015) 89:185–94. doi: 10.1016/j.jmcc.2015.11.013
 40. Sterpetti AV, Cucina A, Lepidi S, Randone B, Sùpa F, Aromatario C, et al. Progression and regression of myointimal hyperplasia in experimental vein grafts depends on platelet-derived growth factor and basic fibroblastic growth factor production. *J Vasc Surg*. (1996) 23:568–75. doi: 10.1016/s0741-5214(96)80034-6
 41. Owens GK, Kumar MS, Wamhoff BR. Molecular regulation of vascular smooth muscle cell differentiation in development and disease. *Physiol Rev*. (2004) 84:767–801. doi: 10.1152/physrev.00041.2003
 42. Liu R, Leslie KL, Martin KA. Epigenetic regulation of smooth muscle cell plasticity. *Biochim Biophys Acta*. (2015) 1849:448–53. doi: 10.1016/j.bbagr.2014.06.004
 43. Zhang QJ, Goddard M, Shanahan C, Shapiro L, Bennett M. Differential gene expression in vascular smooth muscle cells in primary atherosclerosis and in stent stenosis in humans. *Arterioscler Thromb Vasc Biol*. (2002) 22:2030–6. doi: 10.1161/01.atv.0000042206.98651.15
 44. Lynch M, Barallobre-Barreiro J, Jahangiri M, Mayr M. Vascular proteomics in metabolic and cardiovascular diseases. *J Intern Med*. (2016) 280:325–38. doi: 10.1111/joim.12486
 45. Allahverdian S, Chaabane C, Boukais K, Francis GA, Bochaton-Piallat ML. Smooth muscle cell fate and plasticity in atherosclerosis. *Cardiovasc Res*. (2018) 114:540–50. doi: 10.1093/cvr/cvy022
 46. Sartore S, Chiavegato A, Faggini E, Franch R, Puato M, Ausoni S, et al. Contribution of adventitial fibroblasts to neointima formation and vascular remodeling: from innocent bystander to active participant. *Circ Res*. (2001) 89:1111–21. doi: 10.1161/hh2401.100844
 47. Tinajero MG, Gottlieb AI. Recent developments in vascular adventitial pathobiology: the dynamic adventitia as a complex regulator of vascular disease. *Am J Pathol*. (2019) 190:520–34. doi: 10.1016/j.ajpath.2019.10.021
 48. Wang G, Jacquet L, Karamariti E, Xu Q. Origin and differentiation of vascular smooth muscle cells. *J Physiol*. (2015) 593:3013–30. doi: 10.1113/JP270033
 49. Hu Y, Zhang Z, Torsney E, Afzal AR, Davison F, Metzler B, et al. Abundant progenitor cells in the adventitia contribute to atherosclerosis of vein grafts in ApoE-deficient mice. *J Clin Invest*. (2004) 113:1258–65. doi: 10.1172/JCI19628
 50. Torsney E, Mandal K, Halliday A, Jahangiri M, Xu Q. Characterisation of progenitor cells in human atherosclerotic vessels. *Atherosclerosis*. (2007) 191:259–64. doi: 10.1016/j.atherosclerosis.2006.05.033
 51. Campagnolo P, Cesselli D, Al Haj Zen A, Beltrami AP, Krankel N, Katare R, et al. Human adult vena saphena contains perivascular progenitor cells endowed with clonogenic and proangiogenic potential. *Circulation*. (2010) 121:1735–45. doi: 10.1161/CIRCULATIONAHA.109.899252
 52. Klein D, Weisshardt B, Kleff V, Jastrow H, Jakob HG, Ergun S. Vascular wall-resident Cd44+ multipotent stem cells give rise to pericytes and smooth muscle cells and contribute to new vessel maturation. *PLoS One*. (2011) 6:e20540. doi: 10.1371/journal.pone.0020540
 53. Shimizu K, Sugiyama S, Aikawa M, Fukumoto Y, Rabkin E, Libby P, et al. Host bone-marrow cells are a source of donor intimal smooth-muscle-like cells in murine aortic transplant arteriopathy. *Nat Med*. (2001) 7:738–41. doi: 10.1038/89121
 54. Tanaka K, Sata M, Hirata Y, Nagai R. Diverse contribution of bone marrow cells to neointimal hyperplasia after mechanical vascular injuries. *Circ Res*. (2003) 93:783–90. doi: 10.1161/01.RES.0000096651.13001.B4
 55. Albiero M, Menegazzo L, Fadini GP. Circulating smooth muscle progenitors and atherosclerosis. *Trends Cardiovasc Med*. (2010) 20:133–40. doi: 10.1016/j.tcm.2010.12.001
 56. Prandi F, Piola M, Soncini M, Colussi C, D'Alessandra Y, Penza E, et al. Adventitial vessel growth and progenitor cells activation in an ex vivo culture system mimicking human saphenous vein wall strain after coronary artery bypass grafting. *PLoS One*. (2015) 10:e0117409. doi: 10.1371/journal.pone.0117409
 57. Longchamp A, Alonso F, Dubuis C, Allagnat F, Berard X, Meda P, et al. The use of external mesh reinforcement to reduce intimal hyperplasia and preserve the structure of human saphenous veins. *Biomaterials*. (2014) 35:2588–99. doi: 10.1016/j.biomaterials.2013.12.041
 58. Yang G, Wu L, Jiang B, Yang W, Qi J, Cao K, et al. H₂S as a physiologic vasorelaxant hypertension in mice with deletion of cystathionine gamma-lyase. *Science*. (2008) 322:587–90. doi: 10.1126/science.1162667
 59. Cheng Y, Ndisang JE, Tang G, Cao K, Wang R. Hydrogen sulfide-induced relaxation of resistance mesenteric artery beds of rats. *Am J Physiol Heart Circ Physiol*. (2004) 287:H2316–23. doi: 10.1152/ajpheart.00331.2004
 60. Mustafa AK, Sikka G, Gazi SK, Steppan J, Jung SM, Bhunia AK, et al. Hydrogen sulfide as endothelium-derived hyperpolarizing factor sulphydrates potassium channels. *Circ Res*. (2011) 109:1259–68. doi: 10.1161/CIRCRESAHA.111.240242
 61. Shibuya N, Mikami Y, Kimura Y, Nagahara N, Kimura H. Vascular endothelium expresses 3-mercaptopyruvate sulfurtransferase and produces hydrogen sulfide. *J Biochem*. (2009) 146:623–6. doi: 10.1093/jb/mvp111
 62. Ishii I, Akahoshi N, Yamada H, Nakano S, Izumi T, Suematsu M. Cystathionine gamma-lyase-deficient mice require dietary cysteine to protect against acute lethal myopathy and oxidative injury. *J Biol Chem*. (2010) 285:26358–68. doi: 10.1074/jbc.M110.147439
 63. Szjarto IA, Marko L, Filipovic MR, Miljkovic JL, Tabelaing C, Tsvetkov D, et al. Cystathionine gamma-lyase-produced hydrogen sulfide controls endothelial no bioavailability and blood pressure. *Hypertension*. (2018) 71:1210–7. doi: 10.1161/HYPERTENSIONAHA.117.10562
 64. Bibli SI, Hu J, Sigala F, Wittig I, Heidler J, Zukunf S, et al. Cystathionine γ lyase sulphydrates the RNA binding protein human antigen R to preserve endothelial cell function and delay atherogenesis. *Circulation*. (2019) 139:101–14. doi: 10.1161/CIRCULATIONAHA.118.034757
 65. Bibli SI, Hu J, Leisegang MS, Wittig J, Zukunf S, Kapasakalidi A, et al. Shear stress regulates cystathionine gamma lyase expression to preserve endothelial

- redox balance and reduce membrane lipid peroxidation. *Redox Biol.* (2020) 28:101379. doi: 10.1016/j.redox.2019.101379
66. Yuan S, Yurdagul A Jr, Peretik JM, Alfaidi M, Al Yafeai Z, Pardue S, et al. Cystathionine γ -lyase modulates flow-dependent vascular remodeling. *Arterioscler Thromb Vasc Biol.* (2018) 38:2126–36. doi: 10.1161/ATVBAHA.118.311402
 67. Szabo C. A timeline of hydrogen sulfide (H₂S) research: from environmental toxin to biological mediator. *Biochem Pharmacol.* (2018) 149:5–19. doi: 10.1016/j.bcp.2017.09.010
 68. Filipovic MR, Zivanovic J, Alvarez B, Banerjee R. Chemical biology of H₂S signaling through persulfidation. *Chem Rev.* (2018) 118:1253–337. doi: 10.1021/acs.chemrev.7b00205
 69. Sen N. Functional and molecular insights of hydrogen sulfide signaling and protein S-sulfhydration. *J Mol Biol.* (2017) 429:543–61. doi: 10.1016/j.jmb.2016.12.015
 70. Mustafa AK, Gadalla MM, Sen N, Kim S, Mu W, Gazi SK, et al. H₂S signals through protein S-sulfhydration. *Sci Signal.* (2009) 2:ra72. doi: 10.1126/scisignal.2000464
 71. Bibli SI, Hu J, Looso M, Weigert A, Ratiu C, Wittig J, et al. Mapping the endothelial cell S-sulfhydrylome highlights the crucial role of integrin sulfhydration in vascular function. *Circulation.* (2021) 143:935–48. doi: 10.1161/CIRCULATIONAHA.120.051877
 72. Fu L, Liu K, He J, Tian C, Yu X, Yang J. Direct proteomic mapping of cysteine persulfidation. *Antioxid Redox Signal.* (2020) 33:1061–76. doi: 10.1089/ars.2019.7777
 73. Zivanovic J, Kouroussis E, Kohl JB, Adhikari B, Bursac B, Schott-Roux S, et al. Selective persulfide detection reveals evolutionarily conserved antiangiogenic effects of S-sulfhydration. *Cell Metab.* (2019) 30:1152–70.e13. doi: 10.1016/j.cmet.2019.10.007
 74. Beard RS Jr, Bearden SE. Vascular complications of cystathionine beta-synthase deficiency: future directions for homocysteine-to-hydrogen sulfide research. *Am J Physiol Heart Circ Physiol.* (2011) 300:H13–26. doi: 10.1152/ajpheart.00598.2010
 75. Longchamp A, MacArthur MR, Trocha K, Ganahl J, Mann CG, Kip P, et al. Plasma hydrogen sulfide is positively associated with post-operative survival in patients undergoing surgical revascularization. *Front Cardiovasc Med.* (2021) 8:750926. doi: 10.3389/fcvm.2021.750926
 76. Macabrey D, Longchamp A, MacArthur MR, Lambelet M, Urfer S, Corpataux J-M, et al. Sodium thiosulfate acts as an H₂S mimetic to prevent intimal hyperplasia via inhibition of tubulin polymerization. *bioRxiv.* [Preprint]. (2021). doi: 10.1101/2021.09.09.459573
 77. Trocha KM, Kip P, Tao M, MacArthur MR, Trevino-Villarreal H, Longchamp A, et al. Short-term preoperative protein restriction attenuates vein graft disease via induction of cystathionine γ -lyase. *Cardiovasc Res.* (2019) 116:416–28. doi: 10.1093/cvr/cvz086
 78. Yang G, Wu L, Wang R. Pro-apoptotic effect of endogenous H₂S on human aorta smooth muscle cells. *FASEB J.* (2006) 20:553–5. doi: 10.1096/fj.05-4712.fj
 79. Yang G, Wu L, Bryan S, Khaper N, Mani S, Wang R. Cystathionine gamma-lyase deficiency and overproliferation of smooth muscle cells. *Cardiovasc Res.* (2010) 86:487–95. doi: 10.1093/cvr/cvp420
 80. Wang Y, Wang X, Liang X, Wu J, Dong S, Li H, et al. Inhibition of hydrogen sulfide on the proliferation of vascular smooth muscle cells involved in the modulation of calcium sensing receptor in high homocysteine. *Exp Cell Res.* (2016) 347:184–91. doi: 10.1016/j.yexcr.2016.08.004
 81. Zhong X, Wang Y, Wu J, Sun A, Yang F, Zheng D, et al. Calcium sensing receptor regulating smooth muscle cells proliferation through initiating cystathionine-gamma-lyase/hydrogen sulfide pathway in diabetic rat. *Cell Physiol Biochem.* (2015) 35:1582–98. doi: 10.1159/000373973
 82. Macabrey D, Deslarzes-Dubuis C, Longchamp A, Lambelet M, Ozaki CK, Corpataux J-M, et al. Hydrogen sulfide release via the ace inhibitor zofenopril prevents intimal hyperplasia in human vein segments and in a mouse model of carotid artery stenosis. *bioRxiv.* [Preprint]. (2021). doi: 10.1101/2021.09.13.460108
 83. Jackson-Weaver O, Osmond JM, Riddle MA, Naik JS, Gonzalez Bosc LV, Walker BR, et al. Hydrogen sulfide dilates rat mesenteric arteries by activating endothelial large-conductance Ca²⁺-Activated K⁺ channels and smooth muscle Ca²⁺ sparks. *Am J Physiol Heart Circ Physiol.* (2013) 304:H1446–54. doi: 10.1152/ajpheart.00506.2012
 84. Lee KY, Kim JR, Choi HC. Gliclazide, a K_{ATP} channel blocker, inhibits vascular smooth muscle cell proliferation through the CaMKK β -AMPK pathway. *Vascul Pharmacol.* (2018) 102:21–8. doi: 10.1016/j.vph.2018.01.001
 85. Altaany Z, Yang G, Wang R. Crosstalk between hydrogen sulfide and nitric oxide in endothelial cells. *J Cell Mol Med.* (2013) 17:879–88. doi: 10.1111/jcmm.12077
 86. Coletta C, Papapetropoulos A, Erdelyi K, Olah G, Modis K, Panopoulos P, et al. Hydrogen sulfide and nitric oxide are mutually dependent in the regulation of angiogenesis and endothelium-dependent vasorelaxation. *Proc Natl Acad Sci U S A.* (2012) 109:9161–6. doi: 10.1073/pnas.1202916109
 87. Papapetropoulos A, Pyriochou A, Altaany Z, Yang G, Marazioti A, Zhou Z, et al. Hydrogen sulfide is an endogenous stimulator of angiogenesis. *Proc Natl Acad Sci U S A.* (2009) 106:21972–7. doi: 10.1073/pnas.0908047106
 88. Katsouda A, Bibli SI, Pyriochou A, Szabo C, Papapetropoulos A. Regulation and role of endogenously produced hydrogen sulfide in angiogenesis. *Pharmacol Res.* (2016) 113:175–85. doi: 10.1016/j.phrs.2016.08.026
 89. Cai WJ, Wang MJ, Moore PK, Jin HM, Yao T, Zhu YC. The novel proangiogenic effect of hydrogen sulfide is dependent on Akt phosphorylation. *Cardiovasc Res.* (2007) 76:29–40. doi: 10.1016/j.cardiores.2007.05.026
 90. Tao BB, Liu SY, Zhang CC, Fu W, Cai WJ, Wang Y, et al. VEGFR2 functions as an H₂S-targeting receptor protein kinase with its novel Cys1045–Cys1024 disulfide bond serving as a specific molecular switch for hydrogen sulfide actions in vascular endothelial cells. *Antioxid Redox Signal.* (2013) 19:448–64. doi: 10.1089/ars.2012.4565
 91. Longchamp A, Mirabella T, Arduini A, MacArthur MR, Das A, Trevino-Villarreal JH, et al. Amino acid restriction triggers angiogenesis via GCN2/ATF4 regulation of VEGF and H₂S production. *Cell.* (2018) 173:117–29.e14. doi: 10.1016/j.cell.2018.03.001
 92. Altaany Z, Ju Y, Yang G, Wang R. The coordination of S-sulfhydration, S-nitrosylation, and phosphorylation of endothelial nitric oxide synthase by hydrogen sulfide. *Sci Signal.* (2014) 7:ra87. doi: 10.1126/scisignal.2005478
 93. Szabo C, Papapetropoulos A. Hydrogen sulphide and angiogenesis: mechanisms and applications. *Br J Pharmacol.* (2011) 164:853–65. doi: 10.1111/j.1476-5381.2010.01191.x
 94. Moccia F, Bertoni G, Pla AE, Dragoni S, Pupo E, Merlino A, et al. Hydrogen sulfide regulates intracellular Ca²⁺ concentration in endothelial cells from excised rat aorta. *Curr Pharm Biotechnol.* (2011) 12:1416–26. doi: 10.2174/138920111798281117
 95. Jang H, Oh MY, Kim YJ, Choi IY, Yang HS, Ryu WS, et al. Hydrogen sulfide treatment induces angiogenesis after cerebral ischemia. *J Neurosci Res.* (2014) 92:1520–8. doi: 10.1002/jnr.23427
 96. Szabo C. Hydrogen sulfide, an enhancer of vascular nitric oxide signaling: mechanisms and implications. *Am J Physiol Cell Physiol.* (2017) 312:C3–15. doi: 10.1152/ajpcell.00282.2016
 97. Pan LL, Qin M, Liu XH, Zhu YZ. The role of hydrogen sulfide on cardiovascular homeostasis: an overview with update on immunomodulation. *Front Pharmacol.* (2017) 8:686. doi: 10.3389/fphar.2017.00686
 98. Liu Z, Han Y, Li L, Lu H, Meng G, Li X, et al. The hydrogen sulfide donor, GYY4137, exhibits anti-atherosclerotic activity in high fat fed apolipoprotein E(-/-) mice. *Br J Pharmacol.* (2013) 169:1795–809. doi: 10.1111/bph.12246
 99. Fan J, Zheng F, Li S, Cui C, Jiang S, Zhang J, et al. Hydrogen sulfide lowers hyperhomocysteinemia dependent on cystathionine γ lyase S-sulfhydration in ApoE-knockout atherosclerotic mice. *Br J Pharmacol.* (2019) 176:3180–92. doi: 10.1111/bph.14719
 100. Elrod JW, Calvert JW, Morrison J, Doeller JE, Kraus DW, Tao L, et al. Hydrogen sulfide attenuates myocardial ischemia-reperfusion injury by preservation of mitochondrial function. *Proc Natl Acad Sci U S A.* (2007) 104:15560–5. doi: 10.1073/pnas.0705891104
 101. Zhang Y, Li H, Zhao G, Sun A, Zong NC, Li Z, et al. Hydrogen sulfide attenuates the recruitment of CD11b⁺Gr-1⁺ myeloid cells and regulates Bax/Bcl-2 signaling in myocardial ischemia injury. *Sci Rep.* (2014) 4:4774. doi: 10.1038/srep04774
 102. Qipshidze N, Metreveli N, Mishra PK, Lominadze D, Tyagi SC. Hydrogen sulfide mitigates cardiac remodeling during myocardial infarction via

- improvement of angiogenesis. *Int J Biol Sci.* (2012) 8:430–41. doi: 10.7150/ijbs.3632
103. Wu T, Li H, Wu B, Zhang L, Wu SW, Wang JN, et al. Hydrogen sulfide reduces recruitment of CD11b⁺Gr-1⁺ cells in mice with myocardial infarction. *Cell Transplant.* (2017) 26:753–64. doi: 10.3727/096368917X695029
 104. Predmore BL, Kondo K, Bhushan S, Zlatopolsky MA, King AL, Aragon JR, et al. The polysulfide diallyl trisulfide protects the ischemic myocardium by preservation of endogenous hydrogen sulfide and increasing nitric oxide bioavailability. *Am J Physiol Heart Circ Physiol.* (2012) 302:H2410–8. doi: 10.1152/ajpheart.00044.2012
 105. Ravindran S, Jahir Hussain S, Boovarahan SR, Kurian GA. Sodium thiosulfate post-conditioning protects rat hearts against ischemia reperfusion injury via reduction of apoptosis and oxidative stress. *Chem Biol Interact.* (2017) 274:24–34. doi: 10.1016/j.cbi.2017.07.002
 106. Wang Y, Zhao X, Jin H, Wei H, Li W, Bu D, et al. Role of hydrogen sulfide in the development of atherosclerotic lesions in apolipoprotein E knockout mice. *Arterioscler Thromb Vasc Biol.* (2009) 29:173–9. doi: 10.1161/ATVBAHA.108.179333
 107. Du J, Huang Y, Yan H, Zhang Q, Zhao M, Zhu M, et al. Hydrogen sulfide suppresses oxidized low-density lipoprotein (ox-LDL)-stimulated monocyte chemoattractant protein 1 generation from macrophages via the nuclear factor κB (NF-κB) pathway. *J Biol Chem.* (2014) 289:9741–53. doi: 10.1074/jbc.M113.517995
 108. Wang XH, Wang F, You SJ, Cao YI, Cao LD, Han Q, et al. Dysregulation of cystathionine gamma-lyase (CSE)/hydrogen sulfide pathway contributes to ox-LDL-induced inflammation in macrophage. *Cell Signal.* (2013) 25:2255–62. doi: 10.1016/j.cellsig.2013.07.010
 109. Sen N, Paul BD, Gadalla MM, Mustafa AK, Sen T, Xu R, et al. Hydrogen sulfide-linked sulphydration of NF-κB mediates its antiapoptotic actions. *Mol Cell.* (2012) 45:13–24. doi: 10.1016/j.molcel.2011.10.021
 110. Duffton N, Natividad J, Verdu EE, Wallace JL. Hydrogen sulfide and resolution of acute inflammation: a comparative study utilizing a novel fluorescent probe. *Sci Rep.* (2012) 2:499. doi: 10.1038/srep00499
 111. Lin Y, Chen Y, Zhu N, Zhao S, Fan J, Liu E. Hydrogen sulfide inhibits development of atherosclerosis through up-regulating protein S-nitrosylation. *Biomed Pharmacother.* (2016) 83:466–76. doi: 10.1016/j.biopha.2016.07.003
 112. Shefa U, Kim MS, Jeong NY, Jung J. Antioxidant and cell-signaling functions of hydrogen sulfide in the central nervous system. *Oxid Med Cell Longev.* (2018) 2018:1873962. doi: 10.1155/2018/1873962
 113. Cheung SH, Lau YW. Hydrogen sulfide mediates athero-protection against oxidative stress via S-sulphydration. *PLoS One.* (2018) 13:e0194176. doi: 10.1371/journal.pone.0194176
 114. Corsello T, Komaravelli N, Casola A. Role of hydrogen sulfide in NRF2- and sirtuin-dependent maintenance of cellular redox balance. *Antioxidants (Basel).* (2018) 7:129. doi: 10.3390/antiox7100129
 115. Xie L, Gu Y, Wen M, Zhao S, Wang W, Ma Y, et al. Hydrogen sulfide induces Keap1 S-sulphydration and suppresses diabetes-accelerated atherosclerosis via NRF2 activation. *Diabetes.* (2016) 65:3171–84. doi: 10.2337/db16-0020
 116. Calvert JW, Jha S, Gundewar S, Elrod JW, Ramachandran A, Pattillo CB, et al. Hydrogen sulfide mediates cardioprotection through NRF2 signaling. *Circ Res.* (2009) 105:365–74. doi: 10.1161/CIRCRESAHA.109.199919
 117. Peake BF, Nicholson CK, Lambert JP, Hood RL, Amin H, Amin S, et al. Hydrogen sulfide preconditions the db/db diabetic mouse heart against ischemia-reperfusion injury by activating Nrf2 signaling in an Erk-dependent manner. *Am J Physiol Heart Circ Physiol.* (2013) 304:H1215–24. doi: 10.1152/ajpheart.00796.2012
 118. Nicholson CK, Lambert JP, Molkentin JD, Sadoshima J, Calvert JW. Thioredoxin 1 is essential for sodium sulfide-mediated cardioprotection in the setting of heart failure. *Arterioscler Thromb Vasc Biol.* (2013) 33:744–51. doi: 10.1161/ATVBAHA.112.300484
 119. Tian D, Dong J, Jin S, Teng X, Wu Y. Endogenous hydrogen sulfide-mediated MAPK inhibition preserves endothelial function through TXNIP signaling. *Free Radic Biol Med.* (2017) 110:291–9. doi: 10.1016/j.freeradbiomed.2017.06.016
 120. Balaban RS, Nemoto S, Finkel T. Mitochondria, oxidants, and aging. *Cell.* (2005) 120:483–95. doi: 10.1016/j.cell.2005.02.001
 121. Turrens JF. Mitochondrial formation of reactive oxygen species. *J Physiol.* (2003) 552:335–44. doi: 10.1113/jphysiol.2003.049478
 122. Paul BD, Snyder SH, Kashfi K. Effects of hydrogen sulfide on mitochondrial function and cellular bioenergetics. *Redox Biol.* (2021) 38:101772. doi: 10.1016/j.redox.2020.101772
 123. Sun HJ, Zhao MX, Ren XS, Liu TY, Chen Q, Li YH, et al. Salusin-β promotes vascular smooth muscle cell migration and intimal hyperplasia after vascular injury via ROS/NFκB/MMP-9 Pathway. *Antioxid Redox Signal.* (2016) 24:1045–57. doi: 10.1089/ars.2015.6475
 124. Wang Y, Ji L, Jiang R, Zheng L, Liu D. Oxidized high-density lipoprotein induces the proliferation and migration of vascular smooth muscle cells by promoting the production of ROS. *J Atheroscler Thromb.* (2014) 21:204–16. doi: 10.5551/jat.19448
 125. Benavides GA, Squadrito GL, Mills RW, Patel HD, Isbell TS, Patel RP, et al. Hydrogen sulfide mediates the vasoactivity of garlic. *Proc Natl Acad Sci U S A.* (2007) 104:17977–82. doi: 10.1073/pnas.0705710104
 126. Chuah SC, Moore PK, Zhu YZ. S-allylcysteine mediates cardioprotection in an acute myocardial infarction rat model via a hydrogen sulfide-mediated pathway. *Am J Physiol Heart Circ Physiol.* (2007) 293:H2693–701. doi: 10.1152/ajpheart.00853.2007
 127. Syu JN, Yang MD, Tsai SY, Chiang EI, Chiu SC, Chao CY, et al. S-allylcysteine improves blood flow recovery and prevents ischemic injury by augmenting neovasculation. *Cell Transplant.* (2017) 26:1636–47. doi: 10.1177/0963689717724792
 128. Wen YD, Zhu YZ. The pharmacological effects of s-propargyl-cysteine, a novel endogenous H₂S-producing compound. *Handb Exp Pharmacol.* (2015) 230:325–36. doi: 10.1007/978-3-319-18144-8_16
 129. Wang Q, Liu HR, Mu Q, Rose P, Zhu YZ. S-Propargyl-cysteine protects both adult rat hearts and neonatal cardiomyocytes from ischemia/hypoxia injury: the contribution of the hydrogen sulfide-mediated pathway. *J Cardiovasc Pharmacol.* (2009) 54:139–46. doi: 10.1097/FJC.0b013e3181ac8e12
 130. Huang C, Kan J, Liu X, Ma F, Tran BH, Zou Y, et al. Cardioprotective effects of a novel hydrogen sulfide agent-controlled release formulation of S-Propargyl-Cysteine on heart failure rats and molecular mechanisms. *PLoS One.* (2013) 8:e69205. doi: 10.1371/journal.pone.0069205
 131. Kan J, Guo W, Huang C, Bao G, Zhu Y, Zhu YZ. S-propargyl-cysteine, a novel water-soluble modulator of endogenous hydrogen sulfide, promotes angiogenesis through activation of signal transducer and activator of transcription 3. *Antioxid Redox Signal.* (2014) 20:2303–16. doi: 10.1089/ars.2013.5449
 132. Bucci M, Vellecco V, Cantalupo A, Brancaleone V, Zhou Z, Evangelista S, et al. Hydrogen sulfide accounts for the peripheral vascular effects of zofenopril independently of ace inhibition. *Cardiovasc Res.* (2014) 102:138–47. doi: 10.1093/cvr/cvu026
 133. Christe V, Waerber G, Vollenweider R, Marques-Vidal P. Antihypertensive drug treatment changes in the general population: the colaus study. *BMC Pharmacol Toxicol.* (2014) 15:20. doi: 10.1186/2050-6511-15-20
 134. Julian DG. GISSI-3. *Lancet.* (1994) 344:203.
 135. Borghi C, Bacchelli S, Esposti DD, Bignamini A, Magnani B, Ambrosioni E. Effects of the administration of an angiotensin-converting enzyme inhibitor during the acute phase of myocardial infarction in patients with arterial hypertension. SMILE study investigators. Survival of myocardial infarction long-term evaluation. *Am J Hypertens.* (1999) 12:665–72. doi: 10.1016/s0895-7061(99)00042-4
 136. Borghi C, Omboni S, Novo S, Vinereanu D, Ambrosio G, Ambrosioni E. Efficacy and safety of zofenopril versus ramipril in the treatment of myocardial infarction and heart failure: a review of the published and unpublished data of the randomized double-blind smile-4 study. *Adv Ther.* (2018) 35:604–18. doi: 10.1007/s12325-018-0697-x
 137. Ambrosioni E, Borghi C, Magnani B. The effect of the angiotensin-converting-enzyme inhibitor zofenopril on mortality and morbidity after anterior myocardial infarction. The survival of myocardial infarction long-term evaluation (SMILE) study investigators. *N Engl J Med.* (1995) 332:80–5. doi: 10.1056/NEJM199501123320203
 138. Macabrey D, Deslarzes-Dubuis C, Longchamp A, Lamblet M, Ozaki CK, Corpataux JM, et al. Hydrogen sulphide release via the angiotensin converting enzyme inhibitor zofenopril prevents intimal hyperplasia in

- human vein segments and in a mouse model of carotid artery stenosis. *Eur J Vasc Endovasc Surg.* (2021) 63:336–46. doi: 10.1016/j.ejvs.2021.09.032
139. Pavlovskiy Y, Yashchenko A, Zayachkivska O. H₂S donors reverse age-related gastric malfunction impaired due to fructose-induced injury via CBS, CSE, and TST expression. *Front Pharmacol.* (2020) 11:1134. doi: 10.3389/fphar.2020.01134
140. Wallace JL, Nagy P, Feener TD, Allain T, Ditroi T, Vaughan DJ, et al. A proof-of-concept, phase 2 clinical trial of the gastrointestinal safety of a hydrogen sulfide-releasing anti-inflammatory drug. *Br J Pharmacol.* (2020) 177:769–77. doi: 10.1111/bph.14641
141. Li L, Rossoni G, Sparatore A, Lee LC, Del Soldato P, Moore PK. Anti-inflammatory and gastrointestinal effects of a novel diclofenac derivative. *Free Radic Biol Med.* (2007) 42:706–19. doi: 10.1016/j.freeradbiomed.2006.12.011
142. Wallace JL, Caliendo G, Santagada V, Cirino G, Fiorucci S. Gastrointestinal safety and anti-inflammatory effects of a hydrogen sulfide-releasing diclofenac derivative in the rat. *Gastroenterology.* (2007) 132:261–71. doi: 10.1053/j.gastro.2006.11.042
143. Baskar R, Sparatore A, Del Soldato P, Moore PK. Effect of S-diclofenac, a novel hydrogen sulfide releasing derivative inhibit rat vascular smooth muscle cell proliferation. *Eur J Pharmacol.* (2008) 594:1–8. doi: 10.1016/j.ejphar.2008.07.029
144. Jha S, Calvert JW, Duranski MR, Ramachandran A, Lefer DJ. Hydrogen sulfide attenuates hepatic ischemia-reperfusion injury: role of antioxidant and antiapoptotic signaling. *Am J Physiol Heart Circ Physiol.* (2008) 295:H801–6. doi: 10.1152/ajpheart.00377.2008
145. Kondo K, Bhushan S, King AL, Prabhu SD, Hamid T, Koenig S, et al. H₂S protects against pressure overload-induced heart failure via upregulation of endothelial nitric oxide synthase. *Circulation.* (2013) 127:1116–27. doi: 10.1161/CIRCULATIONAHA.112.000855
146. Polhemus DJ, Li Z, Pattillo CB, Gojon G Sr, Gojon G Jr, Giordano T, et al. A Novel hydrogen sulfide prodrug, Sg1002, promotes hydrogen sulfide and nitric oxide bioavailability in heart failure patients. *Cardiovasc Ther.* (2015) 33:216–26. doi: 10.1111/1755-5922.12128
147. Olson KR, Deleon ER, Gao Y, Hurley K, Sadauskas V, Batz C, et al. Thiosulfate: a readily accessible source of hydrogen sulfide in oxygen sensing. *Am J Physiol Regul Integr Comp Physiol.* (2013) 305:R592–603. doi: 10.1152/ajpregu.00421.2012
148. Snijder PM, Frenay AR, de Boer RA, Pasch A, Hillebrands JL, Leuvenink HG, et al. Exogenous administration of thiosulfate, a donor of hydrogen sulfide, attenuates angiotensin II-induced hypertensive heart disease in rats. *Br J Pharmacol.* (2015) 172:1494–504. doi: 10.1111/bph.12825
149. Peng T, Zhuo L, Wang Y, Jun M, Li G, Wang L, et al. Systematic review of sodium thiosulfate in treating calciphylaxis in chronic kidney disease patients. *Nephrology (Carlton).* (2018) 23:669–75. doi: 10.1111/nep.13081
150. Seedial SM, Ghosh S, Saunders RS, Suwanabol PA, Shi X, Liu B, et al. Local drug delivery to prevent restenosis. *J Vasc Surg.* (2013) 57:1403–14. doi: 10.1016/j.jvs.2012.12.069
151. Kip P, Tao M, Trocha KM, MacArthur MR, Peters HAB, Mitchell SJ, et al. Periprocedural hydrogen sulfide therapy improves vascular remodeling and attenuates vein graft disease. *J Am Heart Assoc.* (2020) 9:e016391. doi: 10.1161/JAHA.120.016391
152. Sharma S, Christopoulos C, Kukreja N, Gorog DA. Local drug delivery for percutaneous coronary intervention. *Pharmacol Ther.* (2011) 129:260–6. doi: 10.1016/j.pharmthera.2010.11.003
153. Costa S, Muscara MN, Allain T, Dallazen J, Gonzaga L, Buret AG, et al. Enhanced analgesic effects and gastrointestinal safety of a novel, hydrogen sulfide-releasing anti-inflammatory drug (ATB-352): a role for endogenous cannabinoids. *Antioxid Redox Signal.* (2020) 33:1003–9. doi: 10.1089/ars.2019.7884
154. Farese S, Stauffer E, Kalicki R, Hildebrandt T, Frey BM, Frey FJ, et al. Sodium thiosulfate pharmacokinetics in hemodialysis patients and healthy volunteers. *Clin J Am Soc Nephrol.* (2011) 6:1447–55. doi: 10.2215/CJN.10241110

Conflict of Interest: The authors declare that the research was conducted in the absence of any commercial or financial relationships that could be construed as a potential conflict of interest.

Publisher's Note: All claims expressed in this article are solely those of the authors and do not necessarily represent those of their affiliated organizations, or those of the publisher, the editors and the reviewers. Any product that may be evaluated in this article, or claim that may be made by its manufacturer, is not guaranteed or endorsed by the publisher.

Copyright © 2022 Macabrey, Longchamp, Deglise and Allagnat. This is an open-access article distributed under the terms of the Creative Commons Attribution License (CC BY). The use, distribution or reproduction in other forums is permitted, provided the original author(s) and the copyright owner(s) are credited and that the original publication in this journal is cited, in accordance with accepted academic practice. No use, distribution or reproduction is permitted which does not comply with these terms.